

Zinc(II)cyclen in Molecular Recognition

&

New Water-Soluble Cholesterol Derivatives

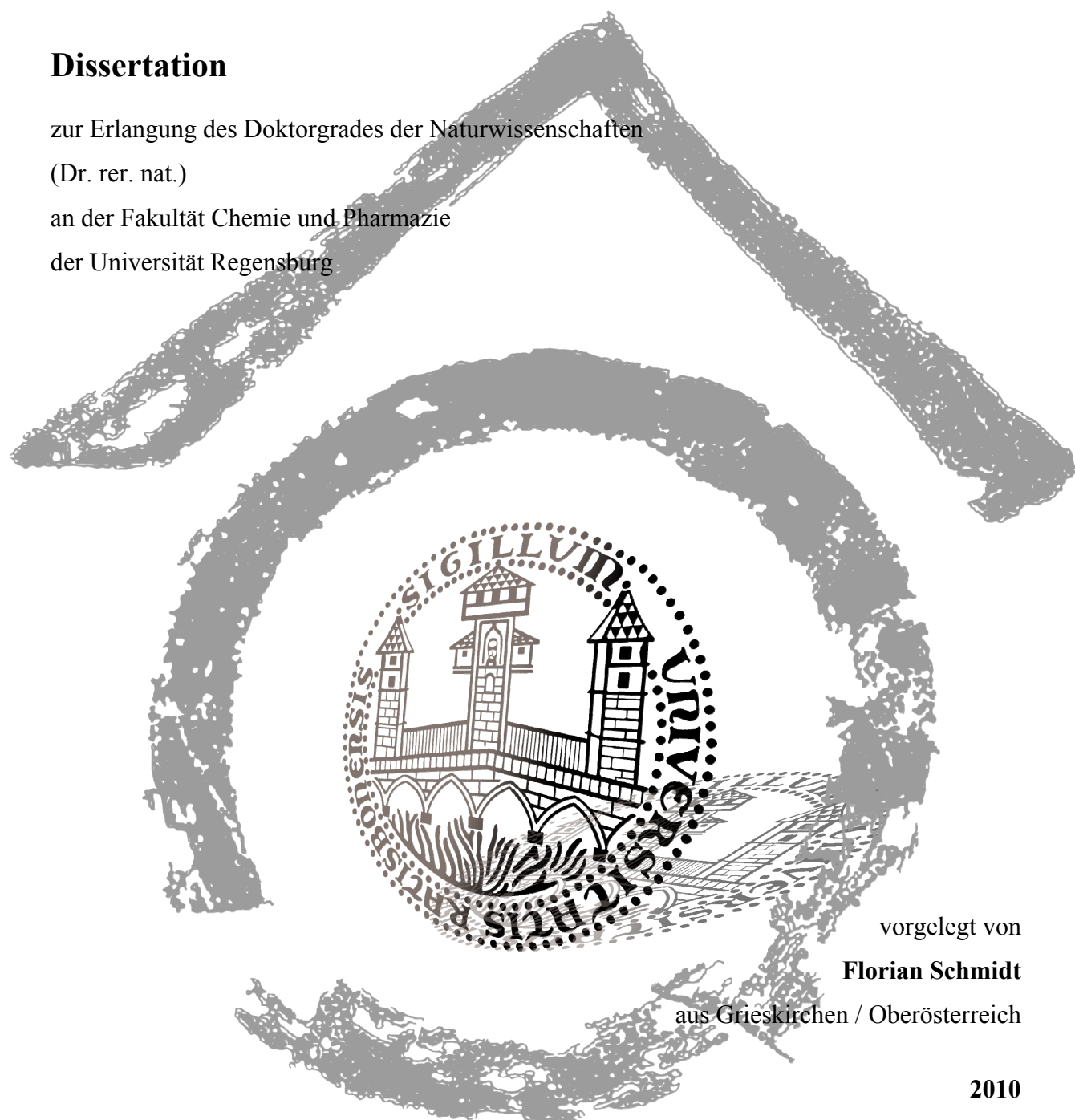
Dissertation

zur Erlangung des Doktorgrades der Naturwissenschaften

(Dr. rer. nat.)

an der Fakultät Chemie und Pharmazie

der Universität Regensburg



vorgelegt von

Florian Schmidt

aus Grieskirchen / Oberösterreich

2010

The experimental part of this work was carried out between January 2007 and April 2010 under the supervision of Prof. Dr. Burkhard König at the Institute for Organic Chemistry, University of Regensburg, Regensburg/Germany.

The PhD thesis was submitted on: 20.05.2010

The colloquium took place on: 18.06.2010

Board of Examiners:	Prof. Dr. Arno Pfitzner	(Chairman)
	Prof. Dr. Burkhard König	(1 st Referee)
	Prof. Dr. Hans-Achim Wagenknecht	(2 nd Referee)
	Prof. Dr. Joachim Wegener	(Examiner)

Danksagung

Meinen besonderen Dank möchte ich meinem Doktorvater Prof. Dr. B. König für die Möglichkeit, dieses interessante und vielseitige Thema zu bearbeiten, entgegenbringen. Seine Förderung und seine Unterstützung durch zahlreiche Anregungen und Diskussionen haben maßgeblichen Anteil an dieser Arbeit.

Den Mitarbeitern der Zentralen Analytik der Fakultät Chemie und Pharmazie danke ich für die schnelle und Gewissenhafte Durchführung der analytischen Messungen. Insbesondere gilt mein Dank Herrn Dr. T. Burgemeister, Herrn F. Kastner, Frau A. Schramm und Frau G. Stühler für die Aufnahme der NMR-Spektren, sowie Herrn J. Kiermaier und Herrn W. Söllner für die Messung und Auswertung der Massenspektren.

Dem Arbeitskreis von Prof. Dr. O. Reiser und seinen Mitarbeitern danke ich für die Möglichkeit der Nutzung des IR-Spektrometers und des Polarimeters.

Für die gute Zusammenarbeit im Rahmen gemeinsamer Forschungsprojekte danke ich Ina Rosnizeck, Dr. Michael Spörner und Prof. Dr. Dr. H. R. Kalbitzer (Universität Regensburg), sowie Daniel Filchtinski und Prof. Dr. C. Herrmann (Ruhr-Universität Bochum). Des Weiteren bedanke ich mich bei Susann Haase und Prof. Dr. J. Heilmann (Universität Regensburg) sowie Petra Unger und Prof. Dr. A.-K. Bosserhoff (Universitätsklinikum Regensburg). Besonderer Dank gilt hierbei auch meinen ehemaligen Kollegen Alexander Riechers und Dr. Stefan Stadlbauer, sowie meiner Frau Dr. Jennifer Schmidt.

Für ein besonders angenehmes Arbeitsklima, beste Stimmung und gute Zusammenarbeit möchte ich mich bei allen aktuellen und auch früheren Mitarbeitern des Arbeitskreises bedanken. Ganz besonders gilt hierbei mein Dank:

Meinen Laborkollegen Benjamin Gruber, für das in allen Belangen wirklich beste Jahr im Labor, und Alexander Riechers, für seine besonders verrückten Ideen, sowie dem „Neuen“ – Stefan Balk – für ein besonders amüsantes abschließendes Vierteljahr. Außerdem Jana („Claudia“) Aschenbrenner, die in ihrer halbjährigen Laborzugehörigkeit auch immer eine angenehme Schreibtischnachbarin war.

Robert Lechner für grandiose Liedtexte, seine Gelassenheit, die immerwährend gute Laune und gute, wohltuende Gespräche. Ohne Dich wäre die Zeit wohl nur halb so lustig und wertvoll gewesen!

Stefan Földner für gute Gespräche nach Feierabend und seine grandiosen Ideen, um die Zeit im Arbeitskreis noch abwechslungsreicher zu gestalten. (Földnerball, Königstriathlon, u.v.m.)

Den ehemaligen Kollegen Dr. Michael Egger, Dr. Daniel Engel und Dr. Stefan Stadlbauer für ihre Gabe, nahezu ausnahmslos Garanten guter Laune zu sein; nicht zu vergessen auch ihre fachliche Hilfestellung. Dr. Florian Ilgen für unzählige interessante Gespräche über unsere lieben Hobbies und Dr. Harald Schmaderer für sein beispielhaftes Engagement rund um den Arbeitskreis. Dr. Andreas Grauer für fachlich fundierte Diskussionen und Tipps, sowie die gemeinsame Pausengestaltung an den vernetzten PCs.

Dr. Claudia Wanninger-Weiß für ihre fröhliche und nette Art, und für fachliche Diskussionen rund ums Thema DNA.

Dr. Evgeny Katayev für lustige deutsch-englische Konversationen mit einigen unerwarteten und deswegen sehr witzigen Aussagen.

Des Weiteren Herrn Dr. R. Vasold und Frau S. Strauss für die Durchführung analytischer als auch präparativer HPLC-Läufe.

Frau Stephanie Graetz, Frau Anke-Susanne Schulze, Herrn Ernst Lautenschlager, Frau Britta Badziura, Frau Regina Hoheisl und Frau Elisabeth Liebl für Ihre organisatorische Unterstützung.

Und abschließend speziell all denjenigen Kollegen, die hier nicht namentlich erwähnt sind, sich aber ganz besonders um eine gute Atmosphäre am Arbeitskreis bemüht und somit dazu beigetragen haben, dass ich mich äußerst wohl gefühlt habe und mir diese Zeit immer in sehr guter Erinnerung bleiben wird.

Mein Dank gilt außerdem Dr. Michael Kruppa und Dr. Thorsten Graf für lehrreiche Erfahrungen und eine sehr angenehme Zeit bei Forschungspraktika.

Matthias Neumann, Michael Dobmeier, Dennis Kühbeck und Thimo Huber danke ich für ihre Unterstützung und sehr gute Mitarbeit bei meinen Projekten im Rahmen ihrer Forschungspraktika bzw. Bachelorarbeiten. Darüber hinaus möchte ich mich auch bei Ludwig Werny bedanken, der während seiner Ausbildung sehr engagiert an den Projekten mitgewirkt hatte.

Meinen ehemaligen Kommilitonen und guten Freunden Patrick Pohla und Doris Kruppa möchte ganz besonders für eine tolle Zeit und die gegenseitige Unterstützung während unseres Studiums, sowie für ihre Freundschaft danken.

Darüber hinaus bedanke ich mich bei Christoph Beyer für Freundschaft, interessante Gespräche über Musik, Gitarren, Verstärker, Effekte und Chemie, seine Bastelarbeiten, sowie die gemeinsamen Abfahrten durch Powder, Parks und über Pistengrenzen hinweg und hoffe, dass wir das weiter fortführen können.

Tobias Trottmann und Ralph Mild danke ich für eine schöne Zeit, die beide durch ihr Mitarbeiten am Lehrstuhl geprägt haben, interessante Gespräche und aufbauende Worte.

Meinem früheren Nachbarn und Schulkamerad Michael Erkens sowie meinem guten Freund Christian Peppe möchte ganz besonders für ihre langjährige Freundschaft und ihr großes Verständnis danken. Danke auch für die schöne Zeit bei gemeinsamen Unternehmungen und die Unterstützung in schwierigen Zeiten.

Ein ganz besonders wichtiger Dank gilt meinen Bandkollegen Daniel Czichran, Michael Sobieraj und Tobias Kirchberger für die gemeinsame Zeit beim Austoben im Proberaum, eine wichtige Energiequelle, um meinen Akku wieder aufzuladen. Auch den Ehemaligen Mitmusikern Michael Dürr, Markus Hilgart und Dr. Sebastian Karnatz möchte ich für 9 tolle Jahre danken, in denen wir gemeinsam viel erleben durften.

Aus tiefstem Herzen danke ich meiner Frau Jennifer für Ihre Liebe, ihr großes Verständnis und ihre großartige Unterstützung in all den Jahren seit wir uns kennen. Auch meinen Schwiegereltern, die mich so herzlich in ihre Familie aufgenommen haben, gebührt ein großes Dankeschön.

Zuletzt danke ich aber vor allem meinen Eltern für ihre großartige Unterstützung über all die Jahre hinweg und ihren bedingungslosen Rückhalt, die somit einen bedeutenden Anteil an der Entstehung dieser Arbeit haben. Auch bei meinen Geschwistern Sebastian und Magdalena möchte ich mich für unseren Zusammenhalt speziell in den letzten Jahren bedanken.

- DANKE -

Für meine JEN

§

meine Familie

“ *the answer to the
ultimate question
of life, the universe
and everything* ”

— DEEP THOUGHT —
(IN DOUGLAS ADAMS’ “THE HITCHHIKER’S GUIDE TO THE GALAXY”)

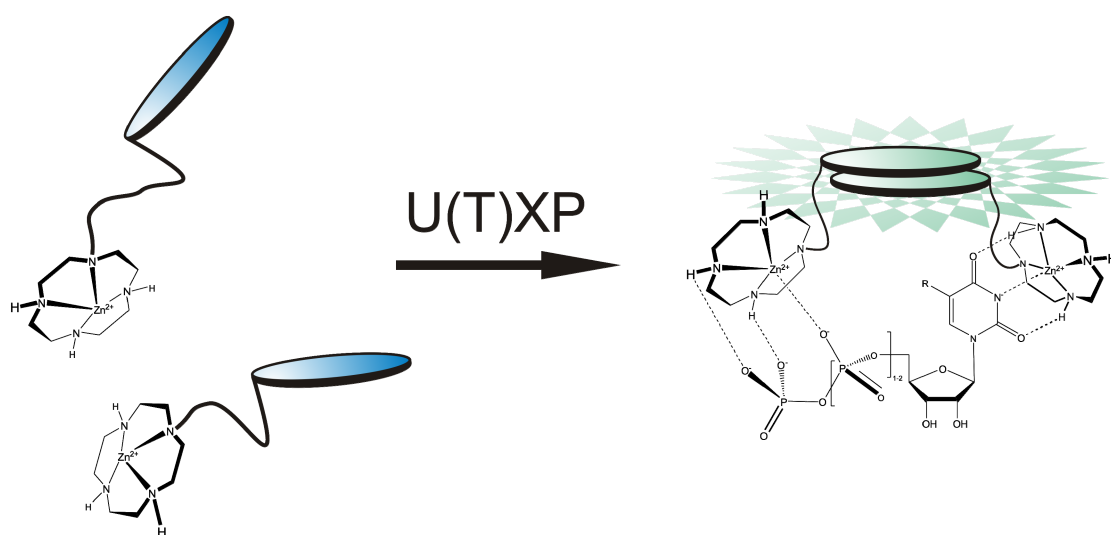
Table of Contents

1	ZINC(II)CYCLEN COORDINATION TO UTP, TTP OR PYROPHOSPHATE INDUCES PYRENE EXCIMER EMISSION	1
1.1	INTRODUCTION	2
1.2	RESULTS & DISCUSSION	3
1.2.1	Design and Synthesis of Pyrene Zn ²⁺ -cyclen Complexes	3
1.2.2	Fluorescence Screening of Nucleotides	6
1.2.3	Fluorescence Titrations	8
1.3	CONCLUSIONS	15
1.4	EXPERIMENTAL SECTION	16
1.4.1	General	16
1.4.2	Binding Studies	17
1.4.2.1	Fluorescence Screening of Analytes	17
1.4.2.2	Fluorescence Titrations of Representative Analytes	17
1.4.3	Investigation in Aqueous TRIS buffer	18
1.4.4	pH-Dependency of Excimer-Formation and Effect on Cross-Selectivity	18
1.4.5	Determination of Fluorescence Quantum Yields	18
1.4.6	Syntheses	19
1.5	SUPPORTING INFORMATION	26
1.6	REFERENCES	33
2	DNA STAINING IN AGAROSE GELS WITH ZINC(II)CYCLEN-PYRENE	37
2.1	INTRODUCTION	38
2.2	RESULTS & DISCUSSION	39
2.2.1	Staining of DNA with Zn ²⁺ -Cyclen-pyrene	39
2.2.2	Sensitivity Comparison of Zn ²⁺ -Cyclen-pyrene with Ethidium Bromide	41
2.2.3	Gel Extraction Experiments after Staining with Zn ²⁺ -Cyclen-pyrene	42
2.2.4	Staining of Short DNA Strands	42
2.2.5	Determination of Cytotoxicity	43
2.3	CONCLUDING REMARKS	45
2.4	ACKNOWLEDGEMENTS	46
2.5	CONFLICT OF INTEREST STATEMENT	46
2.6	MATERIALS & METHODS	46
2.6.1	General	46
2.6.2	Cytotoxicity Investigations	48
2.6.3	Synthesis	49
2.7	REFERENCES	53

3	DETECTION OF PROTEIN PHOSPHORYLATION ON SDS-PAGE USING PROBES WITH A PHOSPHATE-SENSITIVE EMISSION RESPONSE	55
3.1	INTRODUCTION	56
3.2	RESULTS & DISCUSSION	57
3.3	CONCLUSIONS	61
3.4	ACKNOWLEDGEMENTS	61
3.5	MATERIALS & METHODS	62
3.5.1	General	62
3.5.2	Synthesis of Probes 1 and 2	64
3.6	REFERENCES	72
4	ZINC(II)CYCLEN PEPTIDE CONJUGATES INTERACTING WITH THE WEAK EFFECTOR BINDING STATES OF RAS	75
4.1	INTRODUCTION	76
4.2	RESULTS & DISCUSSION	77
4.2.1	Ligand Design	77
4.2.2	Synthesis and Characterization of Zn ²⁺ -Cyclen-peptide Hybrid Ligands	79
4.2.3	PEG-linked bis(Zn ²⁺ -cyclen) Complexes	82
4.3	CONCLUSIONS	85
4.4	ACKNOWLEDGEMENTS	85
4.5	EXPERIMENTAL SECTION	86
4.5.1	General	86
4.5.2	Protein Preparation	87
4.5.3	STD NMR Spectroscopy	87
4.5.4	Syntheses	88
4.7	REFERENCES	103
5	SYNTHESIS OF NEW WATER-SOLUBLE CHOLESTEROL DERIVATIVES	107
5.1	INTRODUCTION	108
5.2	RESULTS & DISCUSSION	109
5.2.1	Design of Water-Soluble Cholesterol Derivatives & Synthesis Strategy	109
5.2.2	Determination of Water Solubility of Compounds 4, 5 and 9 by NMR	111
5.3	CONCLUSIONS	112
5.4	EXPERIMENTAL SECTION	113
5.4.1	General	113
5.4.2	NMR Studies in Aqueous Solution	113
5.4.3	Syntheses	114
5.5	SUPPORTING INFORMATION	119
5.6	REFERENCES	123

6	SUMMARY	126
7	ZUSAMMENFASSUNG	128
8	ABBREVIATIONS	131
9	APPENDIX	134
9.1	PUBLICATIONS	134
9.2	PATENT	134
9.3	POSTER PRESENTATION & CONFERENCES	135
9.4	CURRICULUM VITAE	135

1 ZINC(II)CYCLEN COORDINATION TO UTP, TTP OR PYROPHOSPHATE INDUCES PYRENE EXCIMER EMISSION



Pyrene labelled Zn^{2+} -cyclen **1** and bis- Zn^{2+} -bis-cyclen **2** complexes were synthesized. The reversible coordination at physiological pH of Zn^{2+} -cyclens to phosphate anions and to imide moieties, as present in thymine and uracil nucleotides, is well known. In the presence of analytes bearing a phosphate and an imide or two phosphate groups the formation of a ternary complex consisting of two pyrene-labelled metal complexes and the analyte molecule, is observed. The close proximity of the pyrene labels in the complex induces pyrene excimer emission, which is observable by the unarmred eye. By this, the presence of UMP, UDP, UTP and TTP in buffered aqueous solution is signalled, while other nucleotides are not able to induce excimer emission. In the same way, Zn^{2+} -Cyclen-pyrene acts as luminescent chemosensor for PP_i and Fructose-1,6-bisphosphate in aqueous buffer.

1.1 INTRODUCTION

Nucleotides are the building blocks of DNA- and RNA-biopolymers, which store the genetic information of an organism and provide the blueprint of protein biosynthesis.¹ The selective recognition of specific nucleotides is a prerequisite for all processes they are involved. Protein nucleotide receptors fulfil this important task in cell biology.²⁻¹² The nucleotide receptors P1- and P2 bind mainly ATP and UTP.⁶ By this, P1-type receptors are regulating specific ATP transporters that are responsible for the release of ATP into the extracellular space.⁶ Furthermore, P2X-type receptors are known as mainly ATP controlled Ca^{2+} -channels.⁶ Receptors of the P2Y-subtype are G-protein coupled and show mainly ATP selectivity.⁶ The endogenous Ras-like proteins A (RalA) and RalB, which are both GTPases, were identified to be specific GTP binders and are by this responsible for GTP-dependent exocytosis.¹² The membrane fusion protein Synexin (Annexin VII) was suggested to be a Ca^{2+} -conditional GTP binding protein whose fusion activity is substantially enhanced upon GTP binding and deactivated by GTP hydrolysis.¹¹

Inspired by the biological models artificial systems for nucleotide recognition and detection have been investigated, mainly targeting adenosine and guanidine nucleotides. Bioluminescence assays,¹³ enzyme-coupled electrochemical sensors,¹⁴⁻¹⁶ fluorimetric and colorimetric approaches¹⁷⁻²³ have been described for ATP detection. Recently, *Yoon et al.*²⁴ reported a pincer-like bis-pyrene ligand that binds to the phosphate moiety of NTPs, but only addition of ATP changed the excimer emission. Another colorimetric sensor for ATP was published by *Soto et al.*²⁵ based on 1,3,5-triarylpent-2-en-1,5-diones. The corresponding pyrylium dye changes color from yellow to red in the presence of PP_i and to magenta, when ATP is added. Only the response to GMP and ADP was reported. A selective GTP receptor was reported by *Chang et al.*²⁶ The emission of a benzyliimidazolium dye at 540 nm increases up to 80-fold when GTP is added, while all other nucleotides had little or no effect. *Kwon et al.*²⁷ presented a symmetrical, benzene-based tripodal imidazolium receptor coordinating the nucleotide. The addition of GTP quenches fluorescence intensity, while the addition of ATP, ADP or AMP enhances the fluorescence intensity.

The number of reported receptors which are selective for uracil- or thymine nucleotides is much smaller.²⁸⁻²⁹ *Zeng et al.*³⁰ published a 1,7-bis-pyrene- Zn^{2+} -cyclen complex coordinating to the imide unit of the nucleobase. A protonated amino group of the receptor is proposed to coordinate to the anionic phosphate unit bringing the pyrene units in close proximity which results in enhanced excimer emission. The authors report good selectivities

even in the presence of other nucleotides, but all investigations were performed in MeCN/HEPES (1:9) and MeCN/Tris-HCl (1:9) mixtures. Another TTP-sensor was described by *Kwon et al.*³¹ They use the FRET-pair FIrpic-Zn²⁺-DPA, an acceptor with preference for the triphosphate moiety and mCP-Zn²⁺-cyclen, a donor binding the imide-anion to signal the presence of TTP in a nucleotide-induced 1:1:1-ensemble. A drawback is the required excess of FIrpic-Zn²⁺-DPA (2 equiv.) for quantitative observation of FRET-based emission of the Ir(III)-complex, as otherwise 2:1- ensembles of only mCP-Zn²⁺-cyclen and TTP are also possible.

We report the differentiation of nucleotides using only one single sensor molecule: Zn²⁺-Cyclen-pyrene **1** or Bis-Zn²⁺-bis-cyclen-pyrene **2**. Both compounds are able to interact via reversible coordination with phosphate- and imide-moieties and therefore form ternary complexes with uracil- and thymine-based nucleotides in HEPES buffer at physiological conditions. Other analytes that induce the formation of 2:1 aggregates are PP_i and Fructose-1,6-bisphosphate. The ternary complexes are easily detected due to an increase in pyrene-excimer emission at 500 nm, while the monomer emission at 400 nm decreases.

1.2 RESULTS & DISCUSSION

1.2.1 Design and Synthesis of Pyrene Zn²⁺-cyclen Complexes

Zn²⁺-cyclen complexes are known for their affinity to phosphate anions³²⁻³⁵ and imides.^{32, 34-37} The pyrene functionalized Zn²⁺-cyclens **1** and **2** (Figure 1) were expected to coordinate to Pyrophosphate, Fructose-1,6-bisphosphate, uracil- and thymine-nucleotides with binding affinities for the mononuclear Zn²⁺-cyclen complexes at physiological conditions in the millimolar range.^{32, 36, 38} A stoichiometry of 2:1, Zn²⁺-cyclen complex to anion is foreseen for both complexes **1** and **2**.³⁹ Moreover, compound **2** is expected to show enhanced binding affinity for phosphate anions and imides resulting in increased sensitivity.³⁷ In such ternary complexes, e.g. **1**₂-UTP (Figure 1), the two pyrene fluorophors are in close proximity and thus enhanced excimer emission at about 500 nm is expected upon excitation at 360 nm.

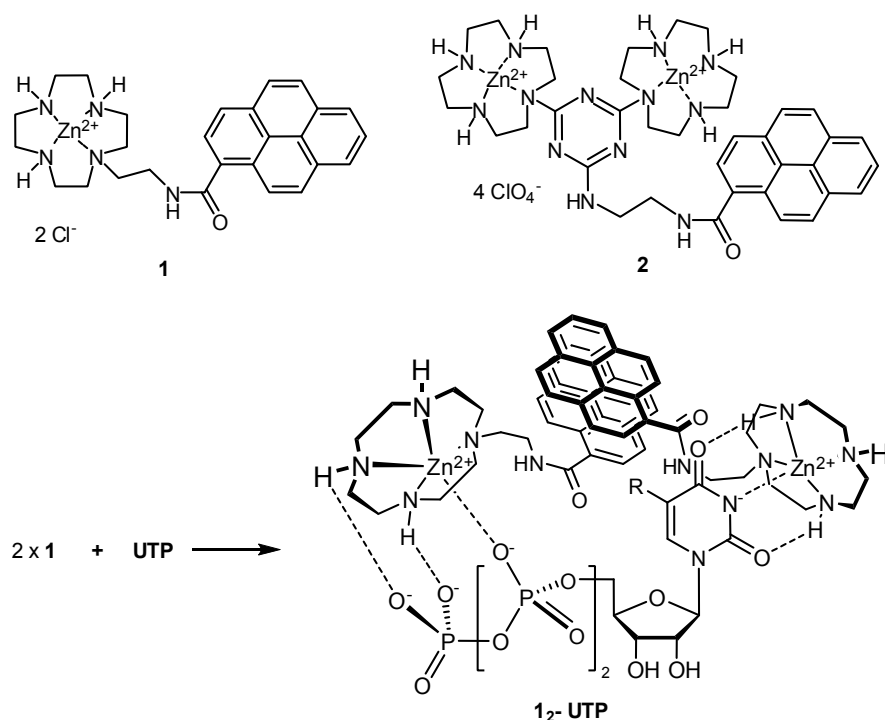
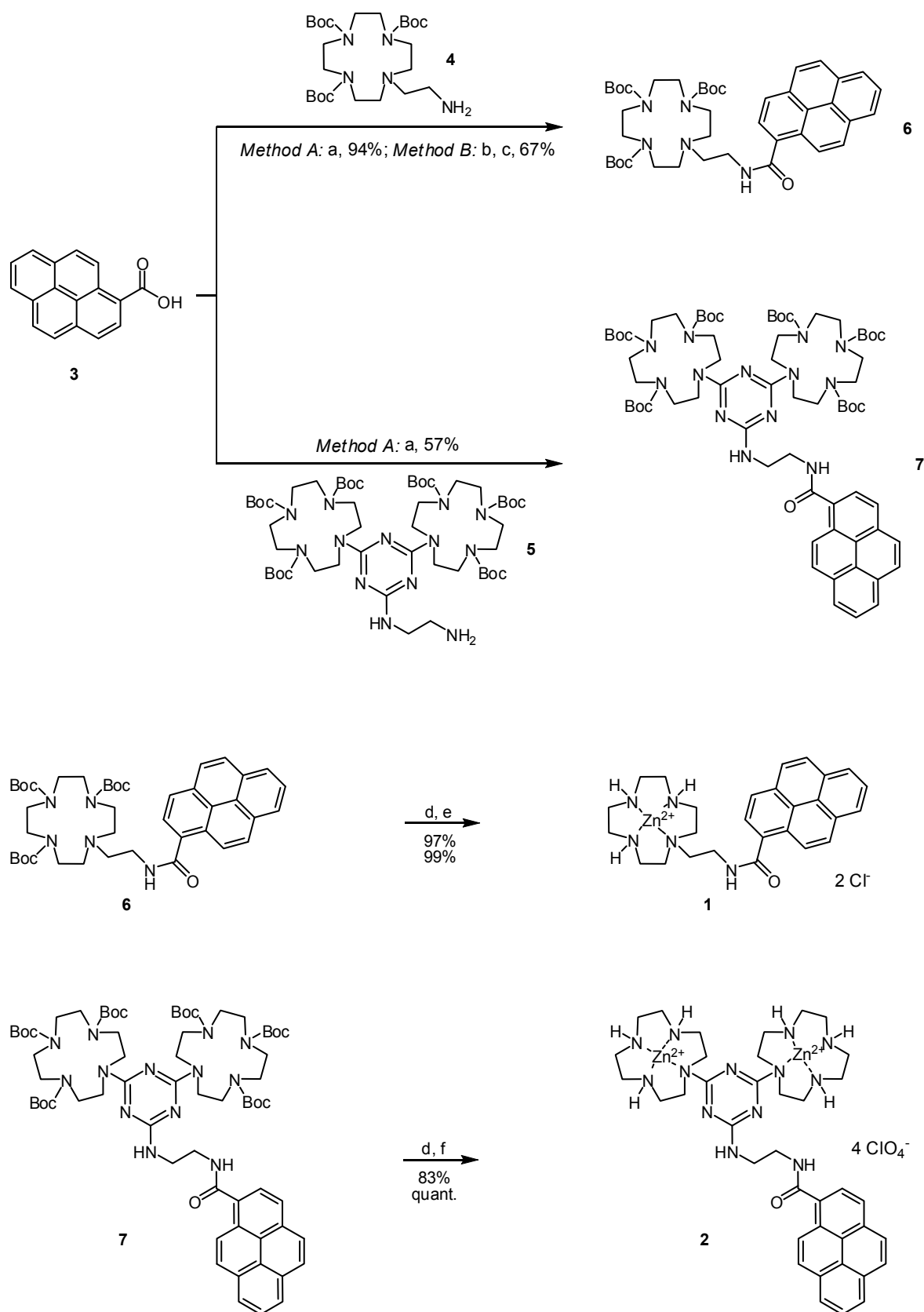


Figure 1: Receptors 1 and 2 and the proposed binding motif for 1₂-UTP

Amino-group bearing cyclen derivatives **4**⁴⁰⁻⁴¹ and **5**⁴² as well as Pyrene-1-carboxylic acid **3**⁴³⁻⁴⁴ were synthesized as precursors for the preparation of **1** and **2** according to literature known procedures.

As shown in Scheme 1, Zn²⁺-Cyclen-pyrene **1** was prepared from **3** and **4** by amide bond formation using standard peptide coupling conditions (TBTU and HOBT, *Method A*) or conversion of **3** into the acid chloride by treatment with Thionyl chloride (*Method B*).⁴⁵ For the coupling of **5** and **3** to **7** only *Method A* was used.

Boc protecting groups of the cyclen ligands were removed under acidic conditions. Deprotonation of the hydrochloride salts with a basic anion exchanger gave the free amine cyclen ligands, which were reacted with either 1 or 2 equiv. of Zn²⁺-salts, respectively.



Scheme 1: Synthesis of pyrene-metal-chelates. a) TBTU, HOBt, DIPEA, dry DMF/DCM (*Method A*); b) SOCl₂, DMF (*Method B*); c) DMAP, DIPEA, dry DMF/DCM (*Method B*); d) HCl-Et₂O, DCM, basic anion exchanger; e) ZnCl₂, MeOH, H₂O; f) Zn(ClO₄)₂, MeOH, H₂O

1.2.2 Fluorescence Screening of Nucleotides

The emission response of **1** and **2** to the presence of adenine, cytosine, guanine, hypoxanthine, thymine and uracil nucleotides, Ortho- and Pyrophosphate (P_i , PP_i), thymidine-dimer (TpT), a pentameric ssDNA sequence ($pTACCG$) and Fructose-1,6-bisphosphate was investigated in a well plate format assay in buffered solution (HEPES 50 mM, NaCl 154 mM, pH 7.4, 25°C). Solutions ($[analyte]_{well} = 0.17$ mM) of each analyte were mixed with solutions of compounds **1** and **2** ($[1]_{well} = [2]_{well} = 0.33$ mM) in a stoichiometric ratio of 1:2 and the emission spectra were recorded at an excitation wavelength of 360 nm. UDP, UTP and TTP containing solutions exhibit enhanced excimer emission at about 500 nm, while the monomer emission at 400 nm decreased in comparison to the other samples. The change in emission wavelength is observable by the naked eye as a color change from blue to turquoise (Figure 3). Compound **1** shows, in addition, enhanced excimer emission with added UMP, PP_i and Fructose-1,6-bisphosphate, while IDP and ITP induce pyrene excimer formation with compound **2**. To evaluate the screening results more quantitatively, we compared the excimer-to-monomer emission ratio of both pyrene-metal-chelates in the presence and in the absence of the analyte to obtain the enhancement factor F_{fe} .

$$F_{fe} = \left(\frac{F_{500nm}}{F_{404nm}} \right)_{+analyte} \bigg/ \left(\frac{F_{500nm}}{F_{404nm}} \right)_{blank} \quad \text{Equation 1}$$

As shown in Figure 2, an about 20-fold enhancement of excimer-to-monomer emission ratio for compound **1** is observed upon addition of TTP, UDP, UTP or PP_i . The largest change of about 25-fold is induced by PP_i . UMP is the only NMP enhancing the ratio (fourfold). Moreover, Fructose-1,6-bisphosphate results in a 5-fold enhancement of F_{fe} . All other tested compounds only lead to comparably small changes in the emission ratio of compound **1**.⁴⁶ Compound **2** turned out to be less selective in nucleotide binding as beside TTP, UDP and UTP, also IDP and ITP induced an increase of F_{fe} . However, the addition of PP_i , UMP or Fructose-1,6-bisphosphate did not affect the emission ratio.⁴⁷ The interaction of Zn^{2+} -Cyclen with the deprotonated amide N(3)-H of Inosine has been reported with a binding affinity of $\log K = 4.2$ at pH 8.6.³⁶ The data support the observed IDP and ITP induced excimer formation.⁴⁸ The interaction between Zn^{2+} -cyclen binding sites and nucleotides correlates to the overall negative charge of the anions: Triphosphates have a much higher affinity to the

metal complex binding sites and induce therefore much larger changes in the monomer-excimer emission ratio than monophosphates.

In addition, fluorescence quantum yields of compounds **1** ($\Phi_F = 0.11 \pm 0.02$) and **2** ($\Phi_F = 0.30 \pm 0.04$) alone and in combination with several analytes inducing either excimer emission or not were determined in a well plate format assay. Addition of not excimer inducing nucleotides to compound **1** generally increased the quantum yield: $\Phi_{F, AMP} = 0.22 \pm 0.03 > \Phi_{F, CMP} = 0.19 \pm 0.03 > \Phi_{F, GMP} = 0.13 \pm 0.02$; the same trend was reported in literature.⁴⁹ For compound **2**, a similar trend was observed: $\Phi_{F, AMP} = 0.30 \pm 0.04 > \Phi_{F, CMP} = 0.28 \pm 0.04 > \Phi_{F, GTP} = 0.20 \pm 0.03$; however, in general fluorescence quantum yield of **2** was not increased by addition of any analyte. For excimer inducing nucleotides, compound **1** did not show any significant change in quantum yield ($\Phi_{F, UMP} = 0.12 \pm 0.02$, $\Phi_{F, UTP} = 0.11 \pm 0.02$). A nucleobase dependent trend can not be derived, as only uridine and thymidine phosphates amongst all nucleotides induce excimer emission. In contrast, for compound **2** the fluorescence quantum yields were found to decrease by addition of excimer inducing nucleotides such as ITP and UDP: $\Phi_{F, ITP} = 0.18 \pm 0.03$, $\Phi_{F, UDP} = 0.19 \pm 0.03$. Also in this case, a nucleobase dependent trend is hardly observed. (For spectral data see Supporting Information)

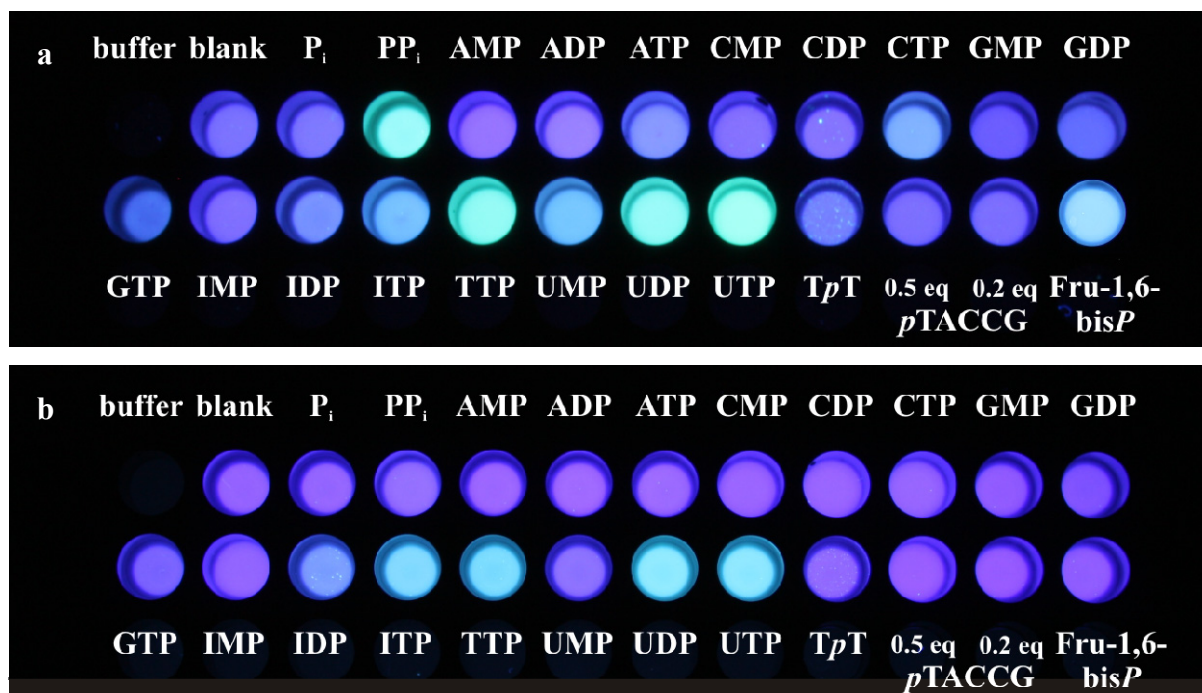


Figure 2: Visible emission changes of the screening experiment. (a) 0.33 mM Zn²⁺-Cyclen-pyrene **1** and (b) Bis-Zn²⁺-bis-cyclen-pyrene **2**, respectively, in the presence of 0.5 equiv. of analyte upon excitation at 316 nm; turquoise emission indicates excimer formation initiated by analyte (2:1 binding event), bluish emission indicates absence of excimer; photographs taken on a PeqLab Superbright UV table with a Canon EOS 450D

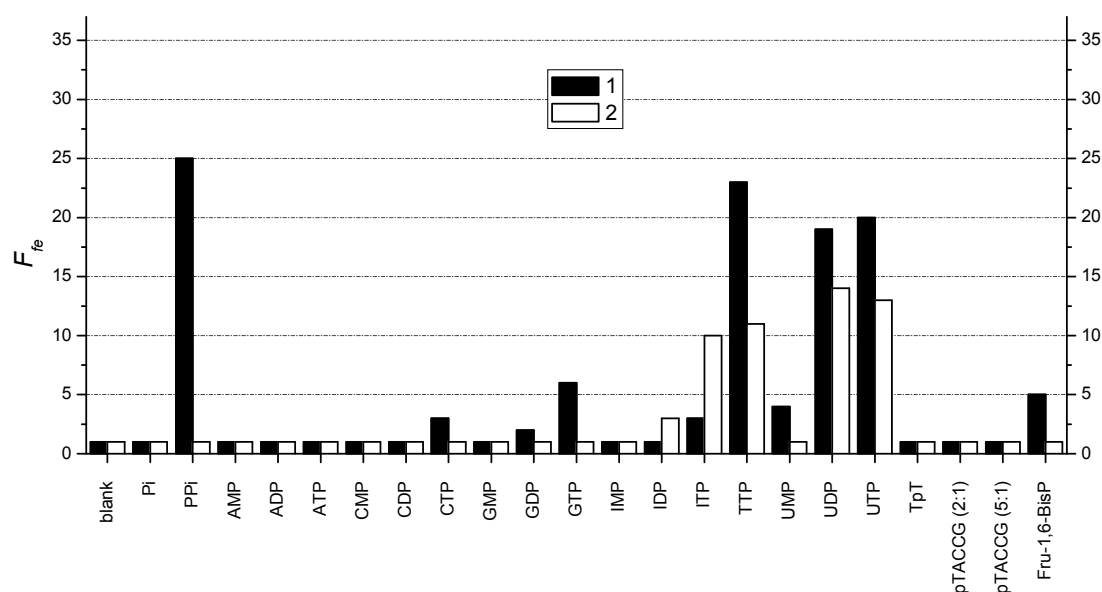


Figure 3: Change in fluorescence enhancement factor F_{fe} of compounds **1 and **2** upon addition of phosphate ions.** 0.5 equiv. of analyte was mixed with 1 equiv. of compound **1** (black) or compound **2** (white); all screening experiments were done in aqueous HEPES buffer at a concentration of $[1] = [2] = 0.33$ mM and 0.5 equiv. of each analyte

1.2.3 Fluorescence Titrations

Based on the screening results, fluorescence titration experiments were performed to investigate binding affinity, stoichiometry and possible cooperative effects of our system. Pyrene-metal-chelate **1** and **2** were titrated under identical conditions with the most representative analytes identified in the screening. Figure 4 shows a typical titration curve for compound **1** and PP_i initiating the excimer formation. The initial induction period of the titration curves indicates cooperative binding. Titration curves reach a maximum of emission change at 0.5 equiv. of added analyte. Addition of more than 0.5 equiv. of the analyte leads to decreasing values. This can be explained, as the addition of further analyte is disrupting the excimer-emitting ternary 2:1 complexes of pyrene-metal-chelate and analyte and successively changing them to monomer-emitting 1:1-aggregates. However, disruption of 2:1-aggregates is a less favorable process compared to their formation indicated by non-symmetric curve progression. Non-linear fitting methods (Hill-equation, Equation 2) were applied to extract binding affinities in the range of $10^{-4} - 10^{-5}$ M and Hill coefficients ($1.7 < n_{Hill} < 3.4$), indicating cooperative effects, from the titration curves (Table S1). Job's plot analyses confirm the expected stoichiometry of 2:1 for aggregates of PP_i , UMP, UDP, UTP, TTP and Fructose-1,6-bisphosphate with compound **1**. Again, the overall charge of the anion

determines the stability of the aggregate: Di- and triphosphates lead at a given concentration to a more complete formation of the ternary complex than monophosphates, which is seen by a more pronounced emission ratio change. (Figures 5, 6, S1-3)

$$\Delta I_{exc/mon} = \frac{\Delta I_{exc/mon, max} \cdot [analyte]^n}{K_{app}^n + [analyte]^n} \quad \text{Equation 2}$$

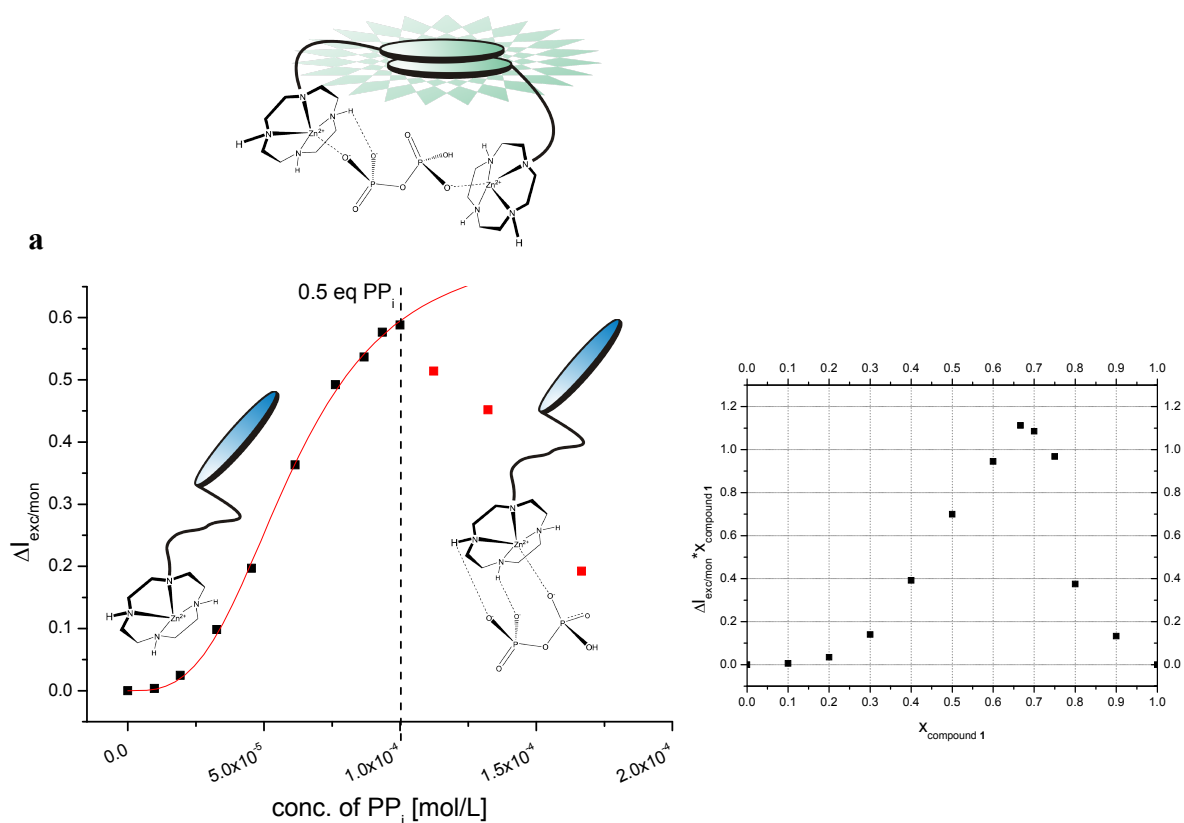


Figure 4: Fluorescence titration of compound 1 with PP_i in aqueous HEPES buffer (pH 7.4). [1] = 0.25 mM, [PP_i] = 0.5 mM; (a) titration curve (left) and Job's plot analysis (right); emission spectra for (b) 0.0-0.5 equiv. and (c) 0.5-1.4 equiv. of added PP_i , respectively; (d) successive excimer formation by addition of up to 0.5 equiv. of PP_i ; (e) disruption of the 2:1-aggregates by further addition of PP_i ; due to the finally formed 1:1-aggregate, pyrene monomer emission 1:1-(1- PP_i)-aggregate and 1 itself are not congruent as the bound anion also influences the emission of the fluorophor

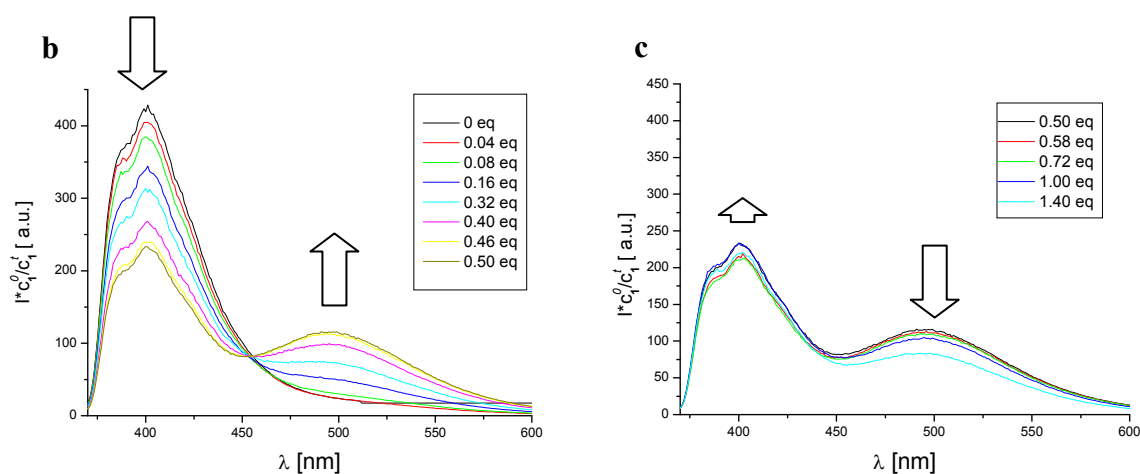


Figure 4 (cont.): Fluorescence titration of compound 1 with PPi in aqueous HEPES buffer (pH 7.4). $[1] = 0.25$ mM, $[\text{PPi}] = 0.5$ mM; (a) titration curve (left) and Job's plot analysis (right); emission spectra for (b) 0.0-0.5 equiv. and (c) 0.5-1.4 equiv. of added PPi , respectively; (b) successive excimer formation by addition of up to 0.5 equiv. of PPi ; (c) disruption of the 2:1-aggregates by further addition of PPi ; due to the finally formed 1:1-aggregate, pyrene monomer emission 1:1-(1- PPi)-aggregate and **1** itself are not congruent as the bound anion also influences the emission of the fluorophor

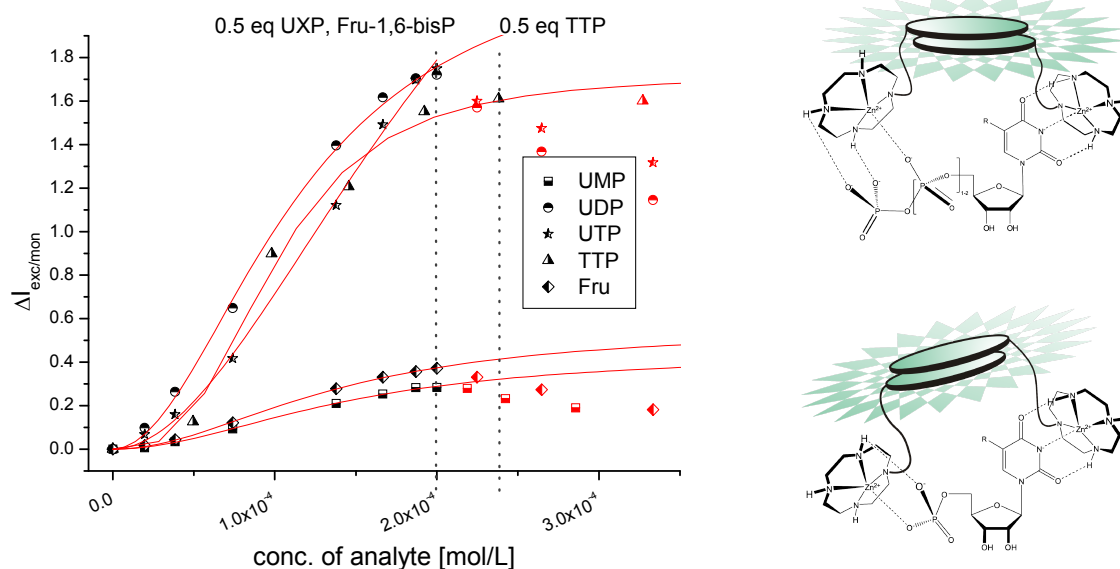


Figure 5: Fluorescence titration of compound 1 with nucleotides and Fructose-1,6-bisphosphate in aqueous HEPES buffer (pH 7.4). Titration curves (upper left) and Job's plot analyses (bottom, left) of compound 1 and UMP (R = H), UDP (R = H), UTP (R = H), TTP (R = Me) and Fru-1,6-bisP, respectively; $[1] = 0.5$ mM, $[\text{UMP}] = [\text{UDP}] = [\text{UTP}] = [\text{Fru-1,6-bisP}] = 1.0$ mM, $[\text{TTP}] = 5.0$ mM; on upper right side, suggested structures of the formed 2:1-aggregates leading to observable excimer emission

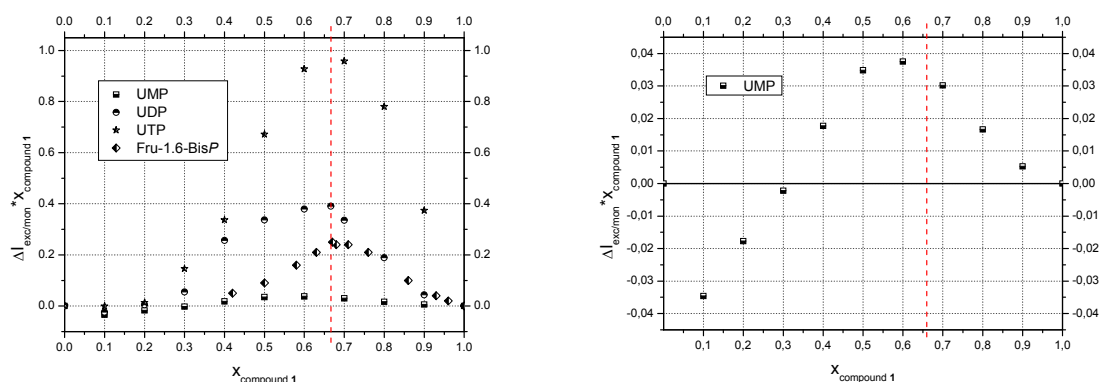


Figure 5 (cont.): Fluorescence titration of compound 1 with nucleotides and Fructose-1,6-bisphosphate in aqueous HEPES buffer (pH 7.4). Titration curves (upper left) and Job's plot analyses (bottom, left) of compound 1 and UMP (R = H), UDP (R = H), UTP (R = H), TTP (R = Me) and Fru-1,6-bisP, respectively; [1] = 0.5 mM, [UMP] = [UDP] = [UTP] = [Fru-1,6-bisP] = 1.0 mM, [TTP] = 5.0 mM; on upper right side, suggested structures of the formed 2:1-aggregates leading to observable excimer emission

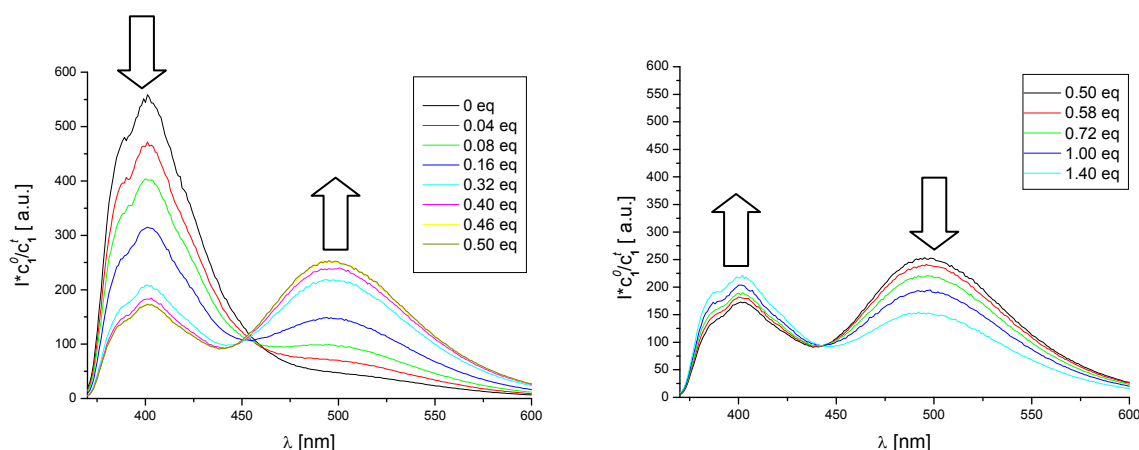


Figure 6: Emission spectra of compound 1 titrated with UTP. [1] = 0.5 mM, [UTP] = 1.0 mM; left side shows successively addition of up to 0.5 equiv. of nucleotide hence, formation of 2:1-aggregates indicated by arising excimer and decreasing monomer emission; right side displays disruption of 2:1 stoichiometry observable as increase in monomer emission, while excimer emission decreases

The assembly process of the 2:1 aggregate of the nucleotides and **1** is concentration sensitive: No induced excimer formation is observed at concentrations of **1** and UTP of 0.10 mM. The emission titration indicates the formation of a 1:1 aggregate (Figure 7). As the interaction of the charged phosphate moieties of the nucleotide with the Lewis-acidic Zn^{2+} -Cyclen is stronger than the imide – metal complex interaction at the pH of the experiments, the binding process is dominated by this interaction. The formation of the ternary 2:1 aggregates requires a concentration range where phosphate and imide interaction with Zn^{2+} -Cyclen are both possible.

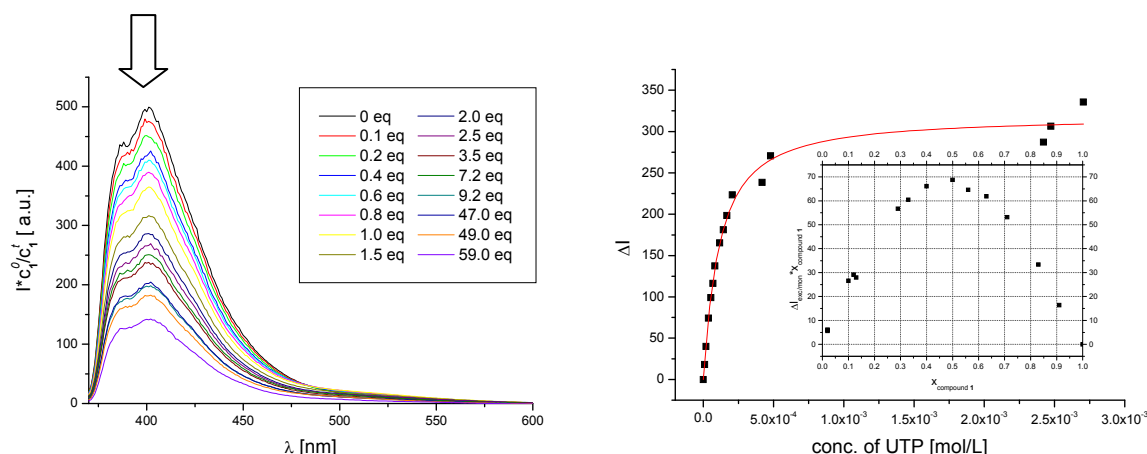


Figure 7: Fluorescence titration of compound 1 with UTP at lower concentration. Emission spectra (left), corresponding titration curve (right) and Job's plot of compound 1 (0.1 mM) titrated with UTP (0.5 mM, 1.0 mM, 5.0 mM) in aqueous HEPES buffer; no excimer is formed as can be derived from the emission spectra, which is furthermore confirmed by the shape of the resulting titration curve and the obtained Job's plot

Titration curves of compound 2 with UDP, UTP, IDP or ITP are analogous to the observations for compound 1 and binding constants were found to be about $10^{-3} - 10^{-4}$ M. Job's plot analysis confirms the expected 2:1 stoichiometry. Figure 8 shows the corresponding titration curves and Job's plot analyses. Emission titration spectra are provided in the Supporting Information. (Figure S4)

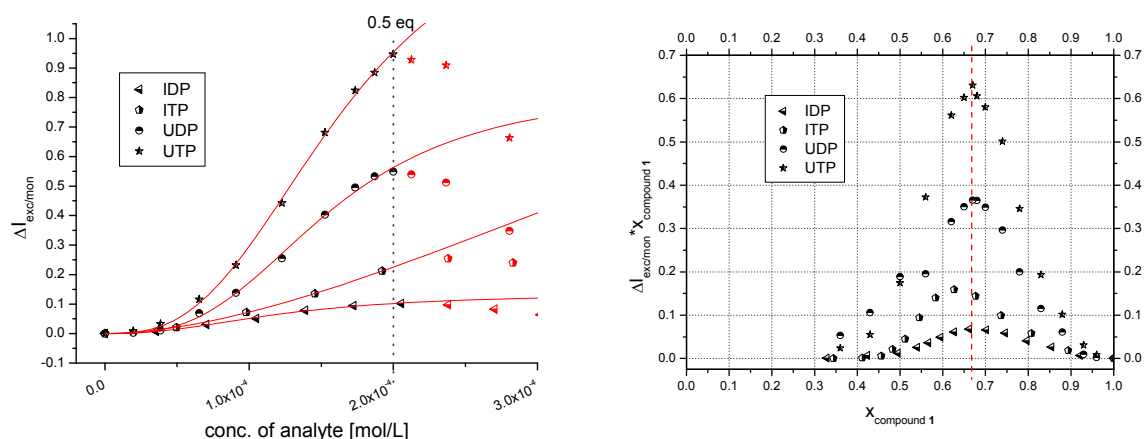


Figure 8: Titration of compound 2 with IDP, ITP, UDP and UTP. Fluorescence titration of compound 2 with IDP, ITP, UDP and UTP (left); Job's plot analyses of compound 2 (0.5 mM) titrated with IDP, ITP, UDP and UTP (1.0 mM) in aqueous HEPES buffer at pH 7.4 (right)

		PP _i	UMP	UDP	UTP	TTP	IDP	ITP	Fru-1,6-BisP
	log K_{app}	4.3±0.1*	3.8±0.0**	4.0±0.2**	3.9±0.5**	3.9±0.1***	4.0±0.1**	---	3.8±0.1**
1	n_{Hill}	3.4±0.5	2.0±0.1	2.0±0.3	1.7±0.5	1.1±0.1	3.0±0.3	---	1.9±0.1
	n	2:1	2:1	2:1	2:1	1:1	2:1	---	2:1
	log K_{app}	---	---	3.8±0.1**	3.7±0.1**	---	3.9±0.1**	3.5±0.5**	---
2	n_{Hill}	---	---	2.9±0.4	2.5±0.4	---	2.3±0.3	1.8±0.7	---
	n	---	---	2:1	2:1	---	2:1	2:1	---

Table 1: Apparent binding affinities derived from fluorescence titrations of compound 1 and 2 with selected anions. * [1] = 0.25 mM, ** [1] = 0.5 mM, *** [1] = 0.1 mM; for all ternary complexes means ± s.d. (range) of binding affinity $\log K_{app}$ given in L^2/mol^2 , for binary UTP-1-complex $\log K_{app}$ given in L/mol ; all titrations were repeated at least three times

Next, the emission response of a 1₂-UTP aggregate (1, 0.48 mM; UTP, 0.24 mM) upon addition of ATP was investigated. With increasing amounts of ATP a decrease in excimer emission occurred, but the addition of 0.5 equiv. of ATP is not sufficient to fully disrupt the 2:1-aggregates. The addition of 2 equiv. of ATP is necessary to annihilate the excimer emission. (Figure 9)

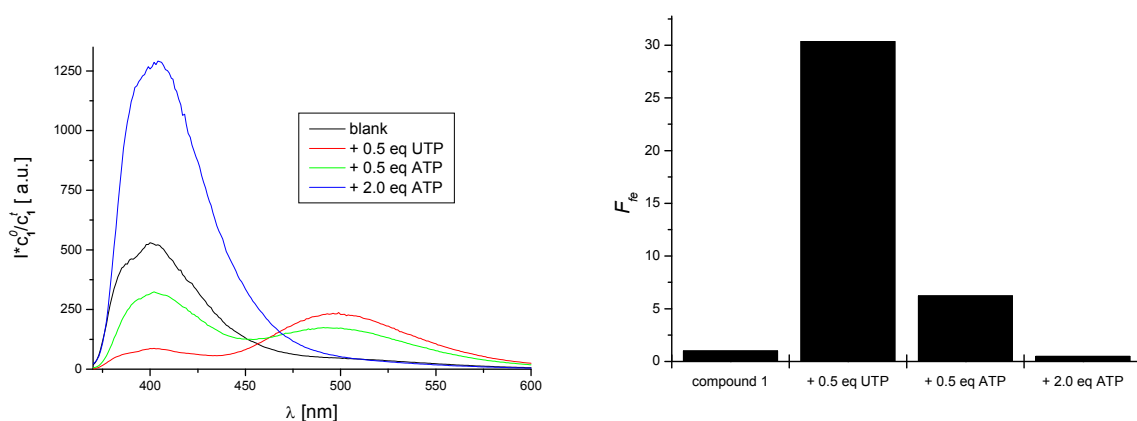


Figure 9: Disruption of 1₂-UTP by added ATP in aqueous HEPES buffer at pH 7.4. Emission spectra (left) of (black) compound 1 (blank; [1] = 0.5 mM), (red) 1 with 0.5 equiv. of UTP, (green) 1 with 0.5 equiv. of UTP and ATP, respectively, and (blue) 1 with 0.5 equiv. of UTP and 2.5 equiv. of ATP; changes in F_{fe} (right)

The influence of buffer and pH on the aggregate formation was tested. A titration of compound 1 with UTP in TRIS buffer at pH 7.4 gave under identical conditions same results as in aqueous HEPES buffered solution (Figure 10). Variation of the pH of the solution

between 6.5, 7.4 and 8.0 changes the emission response slightly. Monomer emission of compound **1** was found to decrease with increasing pH, while the excimer emission is not pH dependent within the investigated pH range (Figure 11).

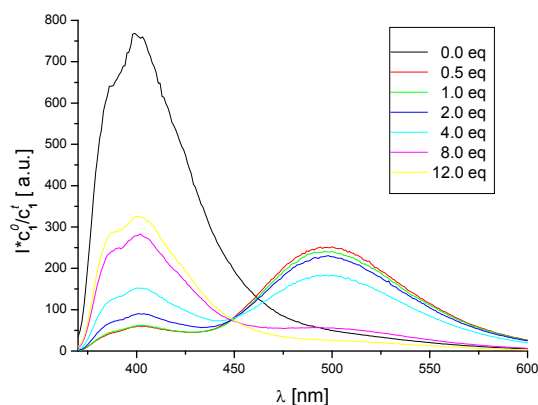


Figure 10: Titration of **1 with UTP in TRIS buffer.** Subsequent formation of **1**₂-UTP and disruption by further addition of UTP is observed in aqueous TRIS buffered solution. Conditions were identical to that previously used for investigations in HEPES buffer.

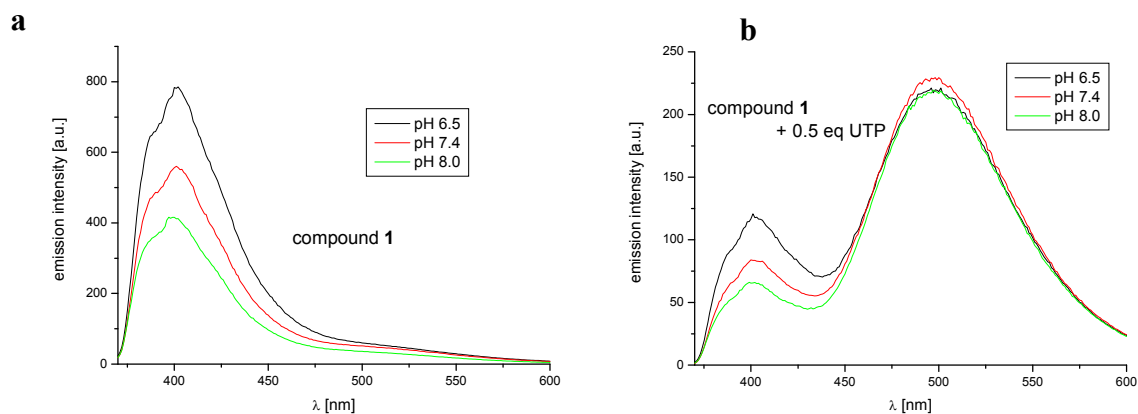


Figure 11: pH Dependence of pyrene monomer and excimer emission. (a) ($[1] = 0.5$ mM); (b) after addition of 0.5 equiv. of UTP, the spectra of 2:1-(**1**-UTP)-aggregate show only changes in the region of monomer emission by variation of pH

1.3 CONCLUSIONS

Titration of Zn^{2+} -Cyclen-pyrene **1** at specific concentrations in aqueous buffer with phosphate anions revealed that the addition of 0.5 equivalents of UTP, UDP, TTP or PP_i induced a strong increase in pyrene excimer emission observable with the unaided eye. The effect was less pronounced for UMP, GTP and Fructose-1,6-bisphosphate; all other tested nucleotides did not affect the excimer emission. We explain the observation by the formation of a 2:1 aggregate of **1** and the respective nucleotide or pyrophosphate; the stoichiometry was confirmed by Job's plot analyses. Zn^{2+} -cyclen complexes are known to interact with phosphate anions and with imide groups. Nucleotides, such as UTP or TTP, can act as a bidentate guest templating the assembly of two complexes **1**. This places their two pyrene moieties in close proximity, which results in an increased excimer emission intensity. Compound **2** shows a different selectivity pattern and increased excimer emission is observed in the presence of UTP, UDP, IDP and ITP. Addition of excess nucleotides restored for both complexes **1** and **2** the monomer emission by formation of the respective 1:1 complexes.

Compared to reported FRET-based nucleotide sensing methods that require a separate donor-acceptor pair for detection, single compounds like **1** or **2** are sufficient under our conditions to indicate the presence of a certain nucleotide. The selectivity among the different nucleotides is similar or even superior to previously reported fluorescence nucleotide sensors. The easy synthetic availability of the pyrene Zn^{2+} -cyclen complexes and the directly to observe excimer emission are advantages of the sensing method, while the restricted concentration range is a limitation. The induced excimer emission of pyrene-functionalized metal complexes by twofold coordination to a bidentate ligand is a simple concept to visualize the presence of analytes. Although practical applications of **1** or **2** in nucleotide sensing have restrictions, the examples illustrate and confirm the principle of the approach for the luminescent detection of complex analytes.

1.4 EXPERIMENTAL SECTION

1.4.1 General

Absorption spectroscopy. Absorption spectra were recorded on a Varian Cary BIO 50 UV/VIS/NIR Spectrometer by use of a 1 cm quartz cuvettes (Hellma) and Uvasol solvents (Merck or Baker).

Emission spectroscopy. Fluorescence spectra were recorded on a Varian Cary Eclipse fluorescence spectrophotometer either by use of a 3 mm quartz cuvettes (Hellma) or in wellplates (384 wells; provided by Greiner) and an appropriate wellplate reader. As solvent systems, HEPES or TRIS buffered aqueous solutions were used.

NMR spectroscopy. Bruker Avance 600 (Cryo) (^1H : 600.1 MHz, ^{13}C : 150.1 MHz, T = 300 K), Bruker Avance 400 (^1H : 400.1 MHz, ^{13}C : 100.6 MHz, T = 300 K), Bruker Avance 300 (^1H : 300.1 MHz, ^{13}C : 75.5 MHz, T = 300 K). The chemical shifts are reported in δ [ppm] relative to internal standards (solvent residual peak). The spectra were analyzed by first order, the coupling constants are given in Hertz [Hz]. Characterization of the signals: s = singlet, d = doublet, t = triplet, q = quartet, m = multiplet, bs = broad singlet, dd = double doublet, ddd = double double doublet. Integration is determined as the relative number of atoms. Assignment of signals in ^{13}C -spectra was determined with DEPT-technique (pulse angle: 135°) and given as (+) for CH_3 or CH , (–) for CH_2 and ($\text{C}_{\text{quat.}}$) for quaternary $\text{C}_{\text{quat.}}$. Error of reported values: chemical shift: 0.01 ppm for ^1H -NMR, 0.1 ppm for ^{13}C -NMR and 0.1 Hz for coupling constants. The solvent used is reported for each spectrum.

Mass spectrometry. Varian CH-5 (EI), Finnigan MAT 95 (CI), Finnigan MAT TSQ 7000 (ESI).

IR spectroscopy. Recorded with a Bio-Rad FTS 2000 MX FT-IR.

Melting point. Melting points were determined on Büchi SMP or a Lambda Photometrics OptiMelt MPA 100.

TLC analysis and column chromatography. Analytical TLC plates (silica gel 60 F254) and silica gel 60 (70-230 or 230-400 mesh) for column chromatography were purchased from Merck. Spots were visualized by UV light and/or staining with Ninhydrin in EtOH.

Dry DMF was purchased from Fluka, Dichloromethane (DCM) was dried by adsorption and stored over molecular sieves. Petrol ether (PE) had a boiling range of 70-90°C. All other solvents and chemicals were of reagent grade and used without further purification.

1.4.2 Binding Studies

1.4.2.1 Fluorescence Screening of Analytes

The interaction of Zn^{2+} -Cyclen-pyrene **1** or Bis- Zn^{2+} -bis-cyclen-pyrene **2** with P_i , PP_i , AMP, ADP, ATP, CMP, CDP, CTP, GMP, GDP, GTP, IMP, IDP, ITP, TTP, UMP, UDP, UTP, TpT, pTACCG, Fructose-1,6-bisphosphate was investigated in screening experiments in buffered aqueous solution (HEPES 50 mM, NaCl 154 mM, pH 7.4, 25°C) using a well plate with 384 wells. To a 0.5 mM solution of the metal-complex 0.5 equiv. of each analyte were added yielding a volume of 120 μL per well. The final concentrations were 0.33 mM for Zn^{2+} -Cyclen-pyrene and mM for Bis- Zn^{2+} -bis-cyclen-pyrene, respectively. The emission spectra were recorded at an excitation wavelength of 360 nm.

Screening conditions

Solvent:	HEPES buffer 50 mM, NaCl 154 mM, pH 7.4		
Volume/well:	120 μL ; $V_{\text{well}} = V_{\text{pyrene}} + V_{\text{analyte}}$		
	$c_{\text{pyrene}}^0 = 0.50 \text{ mM}$		$c_{\text{analyte}}^0 = 0.50 \text{ mM}$
Zn^{2+} -cyclen complexes:	$V_{\text{pyrene}}^{\text{well}} = 80 \mu\text{L}$	+	$V_{\text{analyte}}^{\text{well}} = 40 \mu\text{L}$
	$\Rightarrow c_{\text{pyrene}}^{\text{well}} = 0.33 \text{ mM}$		$c_{\text{analyte}}^{\text{well}} = 0.17 \text{ mM}$

1.4.2.2 Fluorescence Titrations of Representative Analytes

To a cuvette with 50 μL of a 0.50 mM solution of Zn^{2+} -Cyclen-pyrene **1** in HEPES buffer aliquots of an analyte solution were added (PP_i , ATP, GTP, IDP, ITP, TTP, UMP, UDP, UTP, TpT, pTACCG, Fructose-1,6-bisphosphate). After equilibration for 2 min, an emission spectrum was recorded at an excitation wavelength of 360 nm. For determination of the binding constants, the obtained fluorescence output was volume corrected, plotted against the concentration of added analyte and evaluated by non-linear fitting methods. The stoichiometry was investigated by Job's plot analysis from separate measurements. Therefore, for each molar fraction data point the corresponding mixing ratio was prepared anew from equimolar solutions of metal complex and analyte.

Titration conditions

Solvent:	HEPES buffer 50 mM, NaCl 154 mM, pH 7.4
Starting volume:	50 μ L
Conc. (Zn^{2+} -cyclen complexes):	0.10 mM (for 1:1-ensemble 1 and UTP) 0.25 mM (for PP_i) 0.50 mM (for all other analytes)
Conc. (analytes):	2 x [compound 1/2] in general; [TTP] = 5.0 mM

In a cuvette 50 μ L of a 0.50 mM solution of Zn^{2+} -Cyclen-pyrene **1** in HEPES buffer were propounded and 2.5 μ L of a 5.0 mM (0.5 equiv.) solution of UTP were added yielding a 2:1 ratio. Then, 2.5 μ L of a 5.0 mM (0.5 equiv.) solution of ATP and finally, a further 2.0 equiv. were added. Emission spectra were recorded at an excitation wavelength of 360 nm for each data point.

1.4.3 Investigation in Aqueous TRIS buffer

To a cuvette with 50 μ L of a 0.50 mM solution of Zn^{2+} -Cyclen-pyrene **1** in TRIS buffer (50 mM, NaCl 0.035 mM, pH 7.4) aliquots of an UTP solution (5.0 mM) were added. Then, emission spectra were recorded at an excitation wavelength of 360 nm. The obtained data was compared to the results obtained from measurements in HEPES buffered solution.

1.4.4 pH-Dependency of Excimer-Formation and Effect on Cross-Selectivity

Separate samples at three different pH values (6.5, 7.4 and 8.0) were prepared and emission spectra were recorded at an excitation wavelength of 360 nm. Therefore, 50 μ L of a 0.50 mM solution of Zn^{2+} -Cyclen-pyrene **1** in HEPES with appropriate pH were put into a cuvette. Then, 0.5 equiv. of UTP (2.5 μ L of a 5.00 mM solution) were added. The obtained spectra for different pH values were compared.

1.4.5 Determination of Fluorescence Quantum Yields

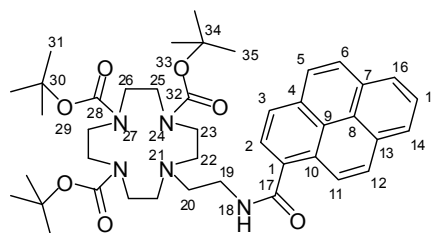
For evaluation of quantum yields of emission, compounds **1** and **2** (0.33 mM) either in combination with analytes (0.17 mM) or not were investigated in a well plate format assay at identical conditions as described for the screening experiments. Quinine sulfate dihydrate in 0.1 N H_2SO_4 ($\Phi_F = 0.55$, $\lambda_{\text{exc.}} = 345$ nm) was used for referencing. Emission spectra for each probe were recorded at three different combinations of emission and excitation slit widths (5/5, 5/10, 10/5 [nm/nm]), while PMT voltage was constant for each testing series

(compound **1**: 550 V, compound **2**: 500 V, Quinine sulfate dihydrate: 500 V and 550 V, respectively). Subsequently, integrals $\int F$ of solvent-baseline corrected spectra were determined. Additionally, UV spectra of each probe were recorded. According to Equation 3, the fluorescence quantum yields Φ_F for each probe at all slit width combinations were calculated and finally given as mean \pm s.d. of these three slit width combinations.

$$\Phi_{F, probe} = \frac{A_{ref.}^{345\text{ nm}}}{A_{probe}^{360\text{ nm}}} \cdot \frac{\int F_{probe}}{\int F_{ref.}} \cdot \left(\frac{n_{probe}}{n_{ref.}} \right)^2 \cdot \Phi_{F, ref.} \quad \text{Equation 3}$$

1.4.6 Syntheses

Following compounds were synthesized according to literature known procedures and determined to be consistent with analytical data derived from the corresponding published syntheses: Tri-*tert*-butyl 10-(2-aminoethyl)-1,4,7,10-tetraazacyclododecane-1,4,7-tricarboxylate **4**,⁴⁰⁻⁴¹ Bis(3-boc-cyclen)-triazene-ED **5**,^{42, 50} 1,8-dihydropyrene-1-carboxylic acid **3**.⁴³⁻⁴⁴



Tri-tert-butyl 10-[2-(pyrene-1-carboxamido)ethyl]-1,4,7,10-tetraazacyclododecane-1,4,7-tricarboxylate (6)

Method A

Pyrene-1-carboxylic acid **3** (0.12 g, 0.49 mmol) was dissolved in a nitrogen flushed round bottom flask in 2 mL of dry DCM. In the following, DIPEA (0.24 g, 250 μ L, 1.8 mmol) and HOBt monohydrate (0.07 g, 0.5 mmol) dissolved in a small amount of dry DMF were added. Then, the solution was cooled down to 0°C in an ice water bath, TBTU (0.16 g, 0.5 mmol) was added and the reaction mixture was stirred for 30 min, before Tri-*tert*-butyl 10-(2-aminoethyl)-1,4,7,10-tetraazacyclododecane-1,4,7-tricarboxylate **4** (0.20 g, 0.4 mmol) was given to the reaction mixture in small portions. After 1 h of stirring at 40°C, the solvents were evaporated and the isolated crude product was purified by column chromatography on flash

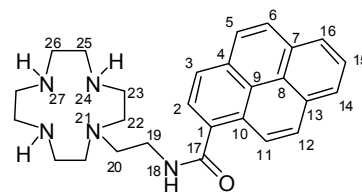
silica gel (EtOAc : PE = 7 : 3) yielding a slightly yellow, amorphous solid (0.27 g, 0.4 mmol, 94%).

MP: 121°C — **¹H-NMR** (400 MHz, CDCl₃, COSY, ROESY, HSQC, HMBC): δ [ppm] = 8.51 (d, ³J_{H,H} = 9.1 Hz, 1H, 11), 8.20 (d, ³J_{H,H} = 7.6 Hz, 2H, 14+16), 8.17-8.11 (m, 2H, 3+12), 8.11-8.05 (m, 2H, 6+12), 8.05-7.99 (m, 2H 5+15), 7.08 (s, 1H, 18), 3.74 (dt, ³J_{H,H} = 6.0 Hz, 5.4 Hz, 2H, 19), 3.44 (bs, 4H, 23), 3.37 (bs, 8H, 25+26), 2.99-2.80 (m, 2H, 20), 2.71 (bs, 4H, 22), 1.70-0.95 (m, 27H, 31+35) — **¹³C-NMR** (100 MHz, CDCl₃, COSY, ROESY, HSQC, HMBC): δ [ppm] = 170.5 (C_{quat.}, 1C, 17), 155.9 (C_{quat.}, 2C, 32), 155.4 (C_{quat.}, 1C, 28), 132.3 (C_{quat.}, 1C, 1), 131.1 (C_{quat.}, 2C, 4+7), 130.8 (C_{quat.}, 1C, 13), 128.6 (C_{quat.}, 1C, 10), 128.5 (+, 1C, 12), 128.4 (+, 1C, 6), 127.1 (+, 1C, 5), 126.2 (+, 1C, 15), 125.6 (+, 2C, 14+16), 124.8 (C_{quat.}, 1C, 9; +, 1C, 2), 124.6 (C_{quat.}, 1C, 11), 124.4 (+, 1C, 8), 124.3 (+, 1C, 3), 79.7 (C_{quat.}, 2C, 34), 79.5 (C_{quat.}, 1C, 30), 55.1 (–, 2C, 22), 52.5 (–, 1C, 20), 50.0 (–, 2C, 23), 48.2 (–, 4C, 25+26), 37.6 (–, 1C, 19), 28.5 (+, 6C, 35), 28.2 (+, 3C, 31) — **IR** (ATR) [cm^{–1}]: $\tilde{\nu}$ = 2973, 2931, 2816, 2357, 1682, 1527, 1456, 1413, 1364, 1153, 1105, 1030, 976, 848, 755, 633 — **UV** (MeCN) [nm]: λ (ε) = 339 (1900), 325 (1900) — **ESI-MS** (H₂O/MeOH + 10 mmol/L NH₄Ac): *m/z* (%) = 644.2 (2) [MH⁺ – Boc], 744.4 (100) [MH⁺], 766.3 (3) [MNa⁺] — **HR-MS** PI-LSI (MeOH/Glycerine): (C₄₂H₅₈N₅O₇) calc. 744.4336 [MH⁺], found 744.4326

Method B

Pyrene-1-carboxylic acid **3** (0.50 g, 2.0 mmol) was suspended in SOCl₂ (14.50 g, 121.8 mmol, 8.8 mL) and finally brought in solution by addition of a few drops of DMF. After stirring the reaction mixture for 2 h under reflux conditions, the solvents were removed to obtain the crude Pyrene-1-carboxylic acid chloride. The *in-situ* formed acid chloride was then dissolved under nitrogen atmosphere in dry DCM/DMF (50 mL; 9 : 1) and DMAP (0.03 g, 0.2 mmol) was added, followed by a solution of Tri-*tert*-butyl 10-(2-aminoethyl)-1,4,7,10-tetraazacyclo-dodecane-1,4,7-tricarboxylate **4** (0.84 g, 1.6 mmol) and DIPEA (0.53 g, 4.1 mmol, 0.56 mL) in dry DCM (5 mL). After 5 h stirring at reflux, the mixture was allowed to reach room temperature and water (50 mL) was added. The formed precipitate was filtered off and the layers were separated. In the following, the aqueous layer was extracted with DCM (3 x 50 mL) and the combined organic layers were washed with aqueous 1.25 M NaOH (3 x 30 mL). Finally, the combined aqueous layers were re-extracted with DCM (4 x 60 mL), dried over MgSO₄ and filtrated. Evaporation of the solvents gave the crude product, which was then purified by column chromatography on flash silica gel using a gradient of

MeOH in DCM (0% → 2%). The so obtained slightly yellowish foam was identified as the product (0.81 g, 67%) identical to that prepared by *Method A*.



***N*-[2-(1,4,7,10-Tetraazacyclododecan-1-yl)ethyl]pyrene-1-carboxamide**

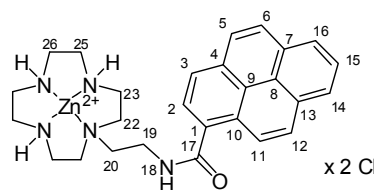
Tri-*tert*-butyl 10-[2-(pyrene-1-carboxamido)ethyl]-1,4,7,10-tetraazacyclododecane-1,4,7-tricarboxylate **6** (0.35 g, 0.47 mmol) was dissolved in 5 mL of DCM, cooled to 0°C in an ice water bath while stirring and then, HCl saturated Et₂O (9.41 mL) was added slowly. Reaching room temperature, the reaction mixture was stirred a further 16 h, while a precipitate was formed. After evaporation of the solvent under reduced pressure, the desired product was obtained as a yellowish, amorphous solid (0.27 g, 0.45 mmol, 97%).

MP: 188°C (decomp.) — **¹H-NMR** (400 MHz, D₂O, DEPT135): δ [ppm] = 7.89-7.29 (m, 9H, aryl-CH), 3.35 (m, 2H, 19), 3.05-2.71 (bs, 8H, 25+26), 2.71-2.56 (m, 6H, 20+22), 2.55-2.40 (bs, 4H, 23) — **¹³C-NMR** (100 MHz, D₂O, DEPT135): δ [ppm] = 171.1 (C_{quat.}, 1C, 17), 131.8 (C_{quat.}, 1C, 1), 129.9 (C_{quat.}, 1C, 4), 129.5 (C_{quat.}, 1C, 7), 128.9 (C_{quat.}, 1C, 13), 128.0 (+, 1C, 6), 127.7 (C_{quat.}, 1C, 10), 127.6 (+, 1C, 12), 126.5 (+, 1C, 5), 125.7 (+, 1C, 15), 125.2 (+, 2C, 14+16), 124.8 (+, 1C, 2), 124.3 (+, 1C, 11), 123.5 (+, 1C, 3), 123.2 (C_{quat.}, 1C, 9), 122.8 (C_{quat.}, 1C, 8), 50.7 (−, 1C, 20), 47.3 (−, 2C, 22), 43.8 (−, 2C, 26), 41.9 (−, 2C, 25), 41.3 (−, 2C, 23), 35.3 (−, 1C, 19) — **ES-MS** (MeCN/TFA): *m/z* (%) = 222.5 (56) [M + 2H⁺]²⁺, 444.1 (100) [MH⁺]

Ion exchange chromatography over a strong basic anion exchange resin (OH[−]-form) was used to obtain the free amine. A column was filled with ion exchanger (1.5 cm x 3 cm) and rinsed first with a mixture of H₂O/MeOH (1 : 1) then followed by pure H₂O. The ammonium salt was dissolved in a small amount of H₂O and eluted from the column to yield the free amine ligand.

¹H-NMR (400 MHz, CD₃OD, NOESY, HSQC, HMBC): δ [ppm] = 8.45 (d, ³*J*_{H,H} = 9.3 Hz, 1H, 11), 8.22-8.16 (m, 3H, 3+14+16), 8.15-8.11 (d, ³*J*_{H,H} = 9.3 Hz, 1H, 12), 8.11-8.07 (m, 2H, 2+6), 8.06-8.02 (m, 2H, 5+18), 8.00 (dd, ³*J*_{H,H} = 7.6 Hz, 7.7 Hz, 1H, 15), 3.59 (t, ³*J*_{H,H} = 6.6 Hz, 2H, 19), 2.75 (t, ³*J*_{H,H} = 6.6 Hz, 2H, 20), 2.57-2.47 (m, 12H, 22+23+25), 2.42-2.34

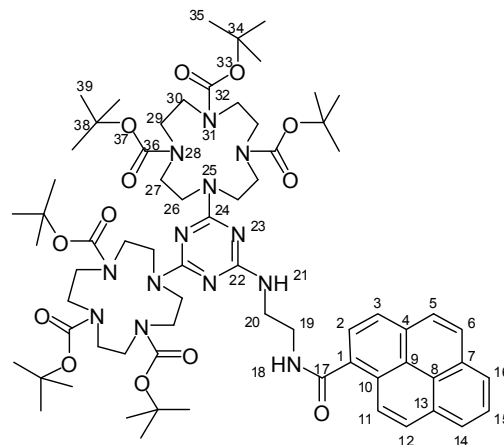
(m, 4H, 26) — $^{13}\text{C-NMR}$ (100 MHz, CD_3OD , NOESY, HSQC, HMBC): δ [ppm] = 172.6 ($\text{C}_{\text{quat.}}$, 1C, 17), 133.8 ($\text{C}_{\text{quat.}}$, 1C, 1), 132.5 ($\text{C}_{\text{quat.}}$, 1C, 4), 132.4 ($\text{C}_{\text{quat.}}$, 1C, 7), 132.0 ($\text{C}_{\text{quat.}}$, 1C, 13), 129.7 (+, 1C, 6), 129.6 ($\text{C}_{\text{quat.}}$, 1C, 10), 129.5 (+, 1C, 12), 128.2 (+, 1C, 5), 127.6 (+, 1C, 15), 127.0 (+, 1C, 16), 126.8 (+, 1C, 2), 125.7 ($\text{C}_{\text{quat.}}$, 1C, 9), 125.49 (+, 1C, 11), 125.48 ($\text{C}_{\text{quat.}}$, 1C, 8), 125.48 (+, 1C, 3), 54.7 (–, 2H, 20), 52.4 (–, 2C, 22), 47.0 (–, 2C, 26), 46.0 (–, 2C, 25), 45.2 (–, 2C, 23), 39.2 (–, 1C, 19)



Zinc(II)-{N-[2-(1,4,7,10-tetraazacyclododecan-1-yl)ethyl]pyrene-1-carboxamide} dichloride (1)

N-[2-(1,4,7,10-Tetraazacyclododecan-1-yl)ethyl]pyrene-1-carboxamide (157 mg, 0.35 mmol) was dissolved in 3 mL of MeOH and warmed up to 40°C. Then, ZnCl_2 (48 mg, 0.35 mmol; 193 μL , β = 250 mg/mL) as aqueous solution was added drop by drop while stirring and the mixture was heated 1 h to 60°C. In the following, MeOH was evaporated and water was removed by lyophilisation to get the crude product, which was precipitated with Et_2O from hot MeOH. The precipitate was isolated by centrifugation yielding a beige, amorphous solid (130 mg, 0.35 mmol, 99%).

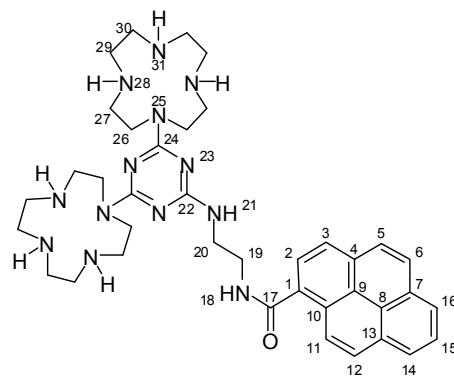
MP: 185°C (decomp.) — $^1\text{H-NMR}$ (400 MHz, D_2O , ROESY, HSQC, HMBC): δ [ppm] = 7.89-7.69 (m, 1H, pyrene-CH), 7.58-7.43 (m, 1H, pyrene-CH), 7.41-7.26 (m, 2H, pyrene-CH), 7.26-7.14 (m, 2H, pyrene-CH), 7.14-7.03 (m, 1H, pyrene-CH), 7.03-6.93 (m, 1H, pyrene-CH), 6.93-6.78 (m, 1H, pyrene-CH), 3.31 (bs, 2H, 19), 2.72 (bs, 2H, 20), 2.53 (bs, 2H, 25), 2.40 (bs, 4H, 23+26), 2.22 (bs, 2H, 22), 2.05 (bs, 2H, 25'), 2.47-2.30 (m, 4H, 22'+26'), 1.78 (bs, 2H, 23') — $^{13}\text{C-NMR}$ (100 MHz, D_2O , ROESY, HSQC, HMBC): δ [ppm] = 170.4 ($\text{C}_{\text{quat.}}$, 1C, 17), 131.7 ($\text{C}_{\text{quat.}}$, 1C, pyrene-C), 130.1 ($\text{C}_{\text{quat.}}$, 1C, pyrene-C), 129.7 ($\text{C}_{\text{quat.}}$, 1C, pyrene-C), 129.1 ($\text{C}_{\text{quat.}}$, 1C, pyrene-C), 127.7 ($\text{C}_{\text{quat.}}$, 1C, pyrene-C), 127.7 (+, 2C, pyrene-C), 126.7 (+, 1C, pyrene-C), 125.8 (+, 1C, pyrene-C), 125.2 (+, 2C, pyrene-C), 124.9 (+, 1C, pyrene-C), 124.3 (+, 1C, pyrene-C), 123.8 (+, 1C, pyrene-C), 123.3 ($\text{C}_{\text{quat.}}$, 1C, pyrene-C), 123.0 ($\text{C}_{\text{quat.}}$, 1C, pyrene-C), 51.2 (–, 1C, 20), 49.0 (–, 2C, 22), 44.1 (–, 2C, 26), 43.1 (–, 2C, 25), 41.9 (–, 2C, 23), 34.0 (–, 1C, 19) — **ES-MS** (MeCN/TFA): m/z (%) = 506.2 (100) [$\text{M}^{2+} - \text{H}^+$], 542.1 (10) [$\text{M}^{2+} + \text{Cl}^-$]



Pyrene-1-carboxylic acid {2-[4,6-bis-(1,4,7,10-tetraaza-cyclododec-1-yl)-[1,3,5]triazin-2-yl]-ethyl}-1,4,7-tricarboxylic acid tri-tert-butyl ester (7)

Pyrene-1-carboxylic acid **3** (0.15 g, 0.60 mmol), DIPEA (0.62 mL, 3.61 mmol), TBTU (0.21 g, 0.66 mmol), and HOBt (0.10 g, 0.66 mmol) were dissolved under nitrogen atmosphere in dry DMF (4 mL) under ice cooling and stirred for 1 h. Subsequently, amine **5** (0.50 g, 0.46 mmol) was added. The reaction was allowed to warm to room temperature and stirred 30 min, then a further 7 h at 40°C. The reaction progress was monitored by TLC (EtOAc : PE = 4 : 1). After completion of the reaction the solvent was removed and the crude product was purified by column chromatography on flash silica gel (EtOAc : PE = 3 : 2; R_f = 0.3) yielding compound **7** (0.34 g, 0.26 mmol, 57%) as a lightly yellow solid.

MP: 210°C. — **¹H-NMR** (600 MHz Cryo, CDCl₃, ROESY, HSQC, HMBC): δ [ppm] = 8.50-8.37 (m, 1H, 11), 8.16-8.10 (m, 2H, 14+16), 8.09-7.98 (m, 4H, 2+3+6+12), 7.98-7.93 (m, 2H, 5+15), 5.15 (bs, 1H, 18), 3.96-2.83 (m, 36H, 19+20+26+27+29+30), 1.35, 1.41 (s, 50H, boc-CH₃), 0.65 (bs, 4H, boc-CH₃) — **¹³C-NMR** (150 MHz Cryo, CDCl₃, ROESY, HSQC, HMBC): δ [ppm] = 170.6 (C_{quat.}, 1C, 17), 166.1 (C_{quat.}, 2C, 24), 165.1 (C_{quat.}, 1C, 22), 157.5-154.9 (C_{quat.}, 6C, 32+36), 132.0 (C_{quat.}, 2C, 1+4), 130.9 (C_{quat.}, 1C, 7), 130.6 (C_{quat.}, 1C, 13), 128.2 (C_{quat.}, 1C, 10), 128.1 (+, 2C, 6+12), 126.9 (+, 1C, 15), 126.0 (+, 1C, 5), 125.4 (+, 1C, 14/16), 125.3 (+, 1C, 16/14), 124.7 (+, 1C, 2), 124.5 (C_{quat.}, 1C, 9), 124.5 (+, 1C, 11), 124.3 (C_{quat.}, 1C, 8), 124.2 (+, 1C, 3), 79.9 (C_{quat.}, 2C, 34), 79.6 (C_{quat.}, 4C, 38), 50.1 (–, 16C, 26+27+29+30), 40.5 (–, 1C, 19/20), 40.0 (–, 1C, 20/19), 28.4 (+, 18C, 35+39) — **IR** (ATR) [cm^{–1}]: $\tilde{\nu}$ = 2976, 1686, 1539, 1496, 1474, 1410, 1364, 1246, 1161, 1109, 973, 851, 777, 759 — **UV** (CHCl₃) [nm]: λ (ϵ) = 343 (31200), 329 (22300), 278 (37300), 267 (23300), 242 (77600) — **ESI-MS** (DCM/MeOH + 10 mmol/L NH₄Ac): m/z (%) = 548.9 (20) [M – 2C₄H₈ – Boc + 2H⁺]²⁺, 577.0 (30) [M – C₄H₈ – Boc + 2H⁺]²⁺, 605.0 (15) [M – Boc + 2H⁺]²⁺, 627.0 (10) [M – C₄H₈ + 2H⁺]²⁺, 655.1 (14) [M + 2H⁺]²⁺, 1308.9 (100) [MH⁺]



Pyrene-1-carboxylic acid {2-[4,6-bis-(1,4,7,10-tetraaza-cyclododec-1-yl)-[1,3,5]triazin-2-ylamino]-ethyl}-amide

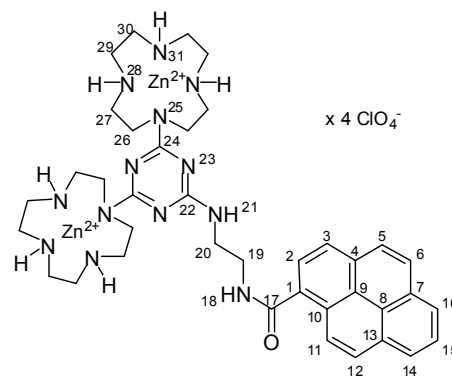
Compound **7** (150 mg, 0.12 mmol) was dissolved in DCM (4 mL) and cooled to 0°C. Subsequently, 4.6 mL HCl saturated Et₂O were added. The solution was stirred 15 min at 0°C and additionally 18 h at room temperature. The solvent was removed *in vacuo* yielding quantitatively a colorless solid.

¹H-NMR (400 MHz, CD₃OD): δ [ppm] = 8.56 (d, ³*J*_{H,H} = 8.7 Hz, 1H, 11), 8.38-8.19 (m, 5H, 2+3+4+16+18), 8.18-8.10 (m, 2H, 5+12), 8.07 (dd, ³*J*_{H,H} = 7.5 Hz, 7.5 Hz, 1H, 15), 4.00-2.67 (m, 36H, 19+20+26+27+29+30, solvent signal) — **¹³C-NMR** (100 MHz, CD₃OD): δ [ppm] = 173.0 (C_{quat.}, 1C, 17), 164.7 (C_{quat.}, 1C, 22), 156.8 (C_{quat.}, 2C, 24), 134.1 (C_{quat.}, 1C, 4), 132.6 (C_{quat.}, 1C, 7), 132.0 (C_{quat.}, 1C, 13), 131.9 (C_{quat.}, 1C, 1), 130.0 (+, 1C, 12), 129.9 (+, 1C, 6), 129.8 (C_{quat.}, 1C, 10), 128.4 (+, 1C, 5), 127.8 (+, 1C, 15), 127.3 (+, 1C, 16), 127.1 (+, 1C, 14), 126.8 (+, 1C, 2), 125.7 (C_{quat.}, 1C, 9), 125.7 (+, 2C, 3+11), 125.4 (C_{quat.}, 1C, 8), 47.0, 45.6, 44.9, 41.5, 40.3 (–, 18C, 19+20+26+27+29+30) — **ES-MS** (H₂O/MeOH + 10 mmol/L NH₄Ac): *m/z* (%) = 354.7 (100) [M + 2H²⁺]²⁺, 708.4 (10) [MH⁺], 822.5 (4) [MH⁺ + TFA]

To obtain the corresponding free base, a weak basic ion exchanger resin was swollen for 15 min in water and washed neutral with water. A column was charged with resin (805 mg, 40.0 mmol hydroxy equivalents at a given capacity of 5 mmol/g). The hydrochloride salt (115 mg, 0.12 mmol) was dissolved in water, put onto the column and eluted with water. The elution of the product was controlled by pH indicator paper (pH > 10) and was completed when pH again was neutral. The eluate was concentrated and lyophilised to yield (69 mg, 0.10 mmol, 83%) a lightly yellow solid.

MP: 192°C — **¹H-NMR** (600 MHz, CD₃CD : CDCl₃ = 1 : 1, COSY, ROESY, HSQC, HMBC): δ [ppm] = 8.39 (d, ³*J*_{H,H} = 9.2 Hz, 1H, 11), 8.20 (dd, ³*J*_{H,H} = 7.0 Hz, 7.2 Hz, 2H, 14+16), 8.15 (d, ³*J*_{H,H} = 7.9 Hz, 1H, 3), 8.11 (d, ³*J*_{H,H} = 9.0 Hz, 1H, 6), 8.09 (d, ³*J*_{H,H} = 6.5 Hz, 1H, 2), 8.07 (d, ³*J*_{H,H} = 8.0 Hz, 1H, 12), 8.04 (d, ³*J*_{H,H} = 8.7 Hz, 1H, 5), 8.02 (dd, ³*J*_{H,H} = 7.4

Hz, 7.5 Hz, 1H, 15), 4.20-3.49 (m, 12H, cyclen-CH₂, 19+20), 3.25-3.09 (m, 8H, cyclen-CH₂), 3.01 (bs, 6H, cyclen-CH₂), 2.97 (s, 2H, cyclen-CH₂), 2.93 (bs, 8H, cyclen-CH₂) — ¹³C-NMR (150 MHz, CD₃CD : CDCl₃ = 1 : 1, COSY, ROESY, HSQC, HMBC): δ [ppm] = 171.2 (C_{quat}, 1C, 17), 166.5 (C_{quat}, 1C, 24), 166.3 (C_{quat}, 1C, 24'), 165.5 (C_{quat}, 1C, 22), 132.0 (C_{quat}, 1C, 4), 130.6 (C_{quat}, 1C, 7), 129.94 (C_{quat}, 1C, 13), 129.92 (C_{quat}, 1C, 1), 128.1 (+, 1C, 6), 127.9 (+, 1C, 12), 127.7 (C_{quat}, 1C, 10), 126.4 (+, 1C, 5), 125.8 (+, 1C, 15), 125.4 (+, 1C, 16), 125.1 (+, 1C, 14), 124.3 (+, 1C, 2), 123.9 (C_{quat}, 1C, 9), 123.7 (+, 1C, 3), 123.6 (C_{quat}, 1C, 8), 123.4 (+, 1C, 11), 46.3 (–, 3C, cyclen-CH₂), 45.9 (–, 2C, cyclen-CH₂), 44.9 (–, 6C, cyclen-CH₂), 42.8 (–, 1C, cyclen-CH₂), 42.6 (–, 2C, cyclen-CH₂), 42.2 (–, 2C, cyclen-CH₂), 39.7 (–, 1C, 19), 39.1 (–, 1C, 20) — IR (ATR) [cm^{–1}]: $\tilde{\nu}$ = 3372, 3266, 2935, 2764, 2697, 1623, 1536, 1480, 1417, 1355, 1284, 1230, 1145, 1081, 972, 852 — UV (MeOH) [nm]: λ (ε) = 341 (12300) 327 (9400), 276 (15500), 266 (10000), 242 (28800), 227 (31700) — ESI-MS (EE/MeOH + 10 mmol/L NH₄Ac): m/z (%) = 354.7 (100) [M + 2H²⁺]²⁺, 708.4 (8) [MH⁺], 822.5 (4) [MH⁺ + TFA] — HR-MS PI-LSI (C₃₈H₅₄N₁₃O) calc. 708.4574 [MH⁺], found 708.4567



Bis-Zinc(II)(pyrene-1-carboxylic acid {2-[4,6-bis-(1,4,7,10-tetraaza-cyclododec-1-yl)-[1,3,5]triazin-2-ylamino]-ethyl}-amide) tetraperchlorate (2)

Pyrene-1-carboxylic acid {2-[4,6-bis-(1,4,7,10-tetraaza-cyclododec-1-yl)-[1,3,5]triazin-2-ylamino]-ethyl}-amide (58 mg, 0.08 mmol) was dissolved in 1 mL of MeOH and heated to 65°C to give a clear yellow solution. Subsequently, Zinc(II)perchlorate (64 mg, 0.17 mmol) dissolved in 1 ml of MeOH was added slowly. The reaction mixture was stirred for additional 20 h at 65°C. The solvent was removed *in vacuo* and the residue was redissolved in water and lyophilized. Bis-Zn²⁺-bis-cyclen pyrene **2** (101 mg, 0.08 mmol, 100%) was obtained as a colorless solid.

MP: 193°C — **¹H-NMR** (300 MHz, CD₃CN): δ [ppm] = 8.51-8.34 (m, 1H, 11), 8.33-7.99 (m, 7H, pyrene-CH), 7.95-7.68 (m, 1H, pyrene-CH), 7.39 (bs, 1H, 18), 7.06-5.63 (m, 7H, 28+30+21), 4.54-2.40 (m, 36 H, 19+20+26+27+29+30) — **IR** (ATR) [cm⁻¹]: $\tilde{\nu}$ = 3487, 3182, 1605, 1530, 1427, 1342, 1285, 1048, 975, 931, 858, 810, 775, 621 — **UV** (HEPES pH 7.4, 25 mM) [nm]: λ (ϵ) = 344 (15000), 330 (10900), 277 (16700), 267 (11200), 243 (27400), 230 (36400) — **ES-MS** (TFA/MeCN): m/z (%) = 447.2 (62) [$M^{4+} + CH_3COO^-$]³⁺, 476.7 (100) [$M^{4+} + 2CH_3COO^-$]²⁺

1.5 SUPPORTING INFORMATION

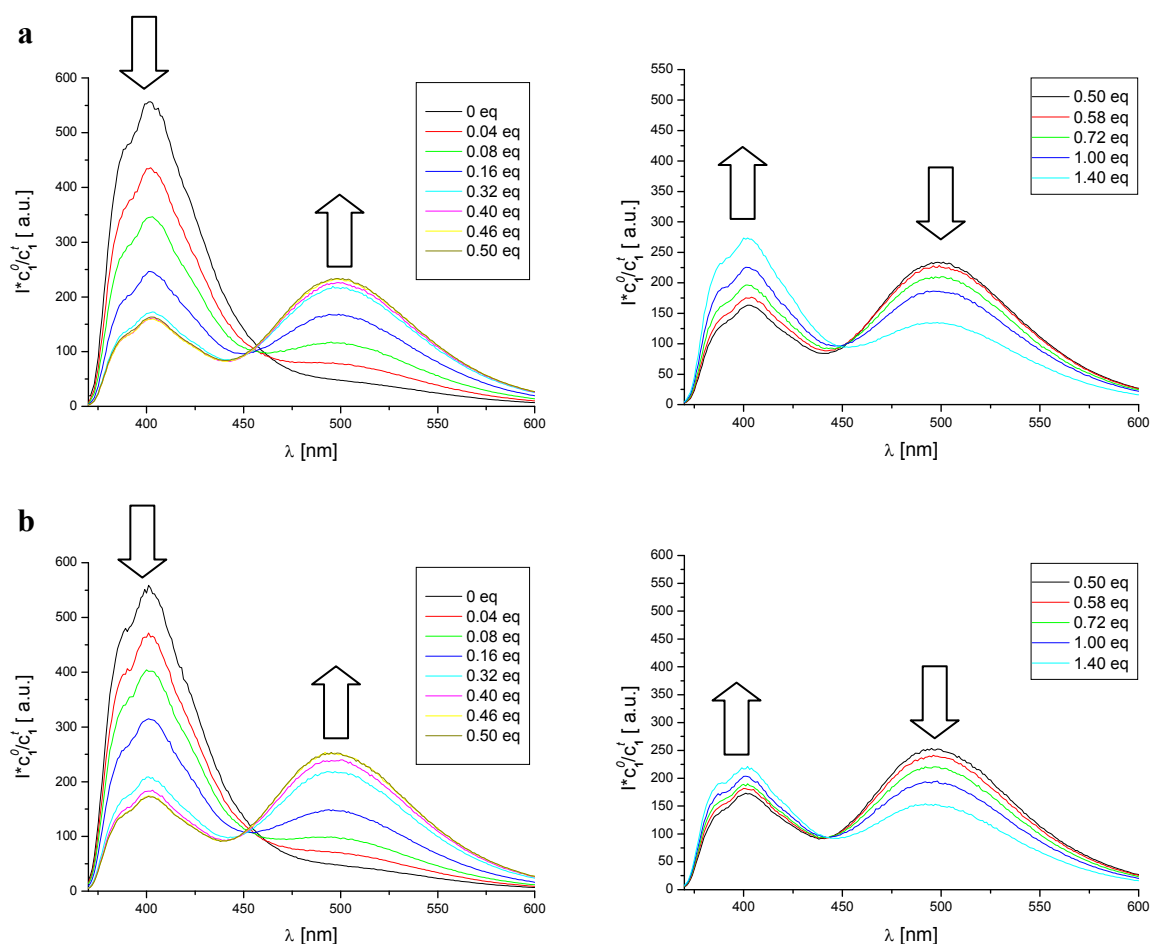


Figure S1: Emission spectra of compound 1 titrated with (a) UMP and (b) UDP, respectively. [1] = 0.5 mM, [UMP] = [UDP] = 1.0 mM; left side shows successive addition of up to 0.5 equiv. of nucleotide hence, formation of 2:1-aggregates indicated by arising excimer and decreasing monomer emission; right side displays disruption of 2:1 stoichiometry observable as increase in monomer emission, while excimer emission decreases

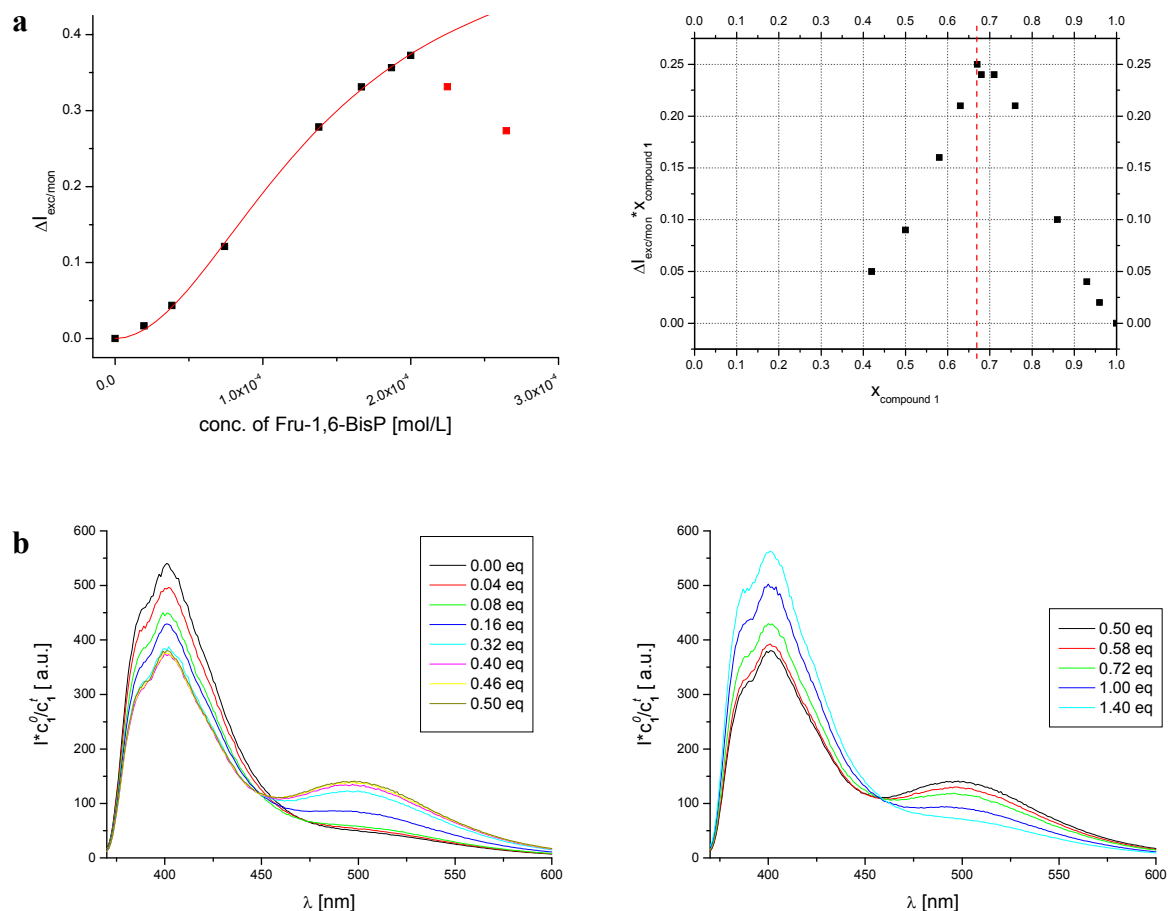


Figure S2: Titration of compound 1 with Fructose-1,6-bisphosphate. (a) Titration curve (left) and Job's plot analysis (right) for titration of $[1] = 0.5 \text{ mM}$ with $[\text{Fru-1,6-bisP}] = 1.0 \text{ mM}$ at pH 7.4 in HEPES buffered aqueous solution. (b) Obtained emission spectra show the typical behavior of successive formation (left) and disruption (right) of the corresponding ternary complex

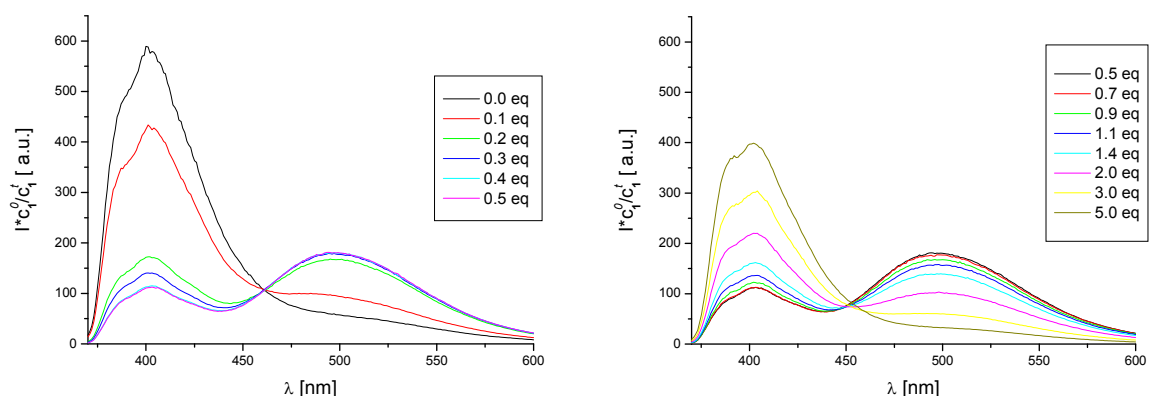


Figure S3: Emission spectra obtained for titration of compound 1 with TTP. Obtained emission spectra show the typical behavior of successive formation (left) and disruption (right) of the corresponding ternary complex; $[1] = 0.5 \text{ mM}$, $[\text{TTP}] = 5.0 \text{ mM}$

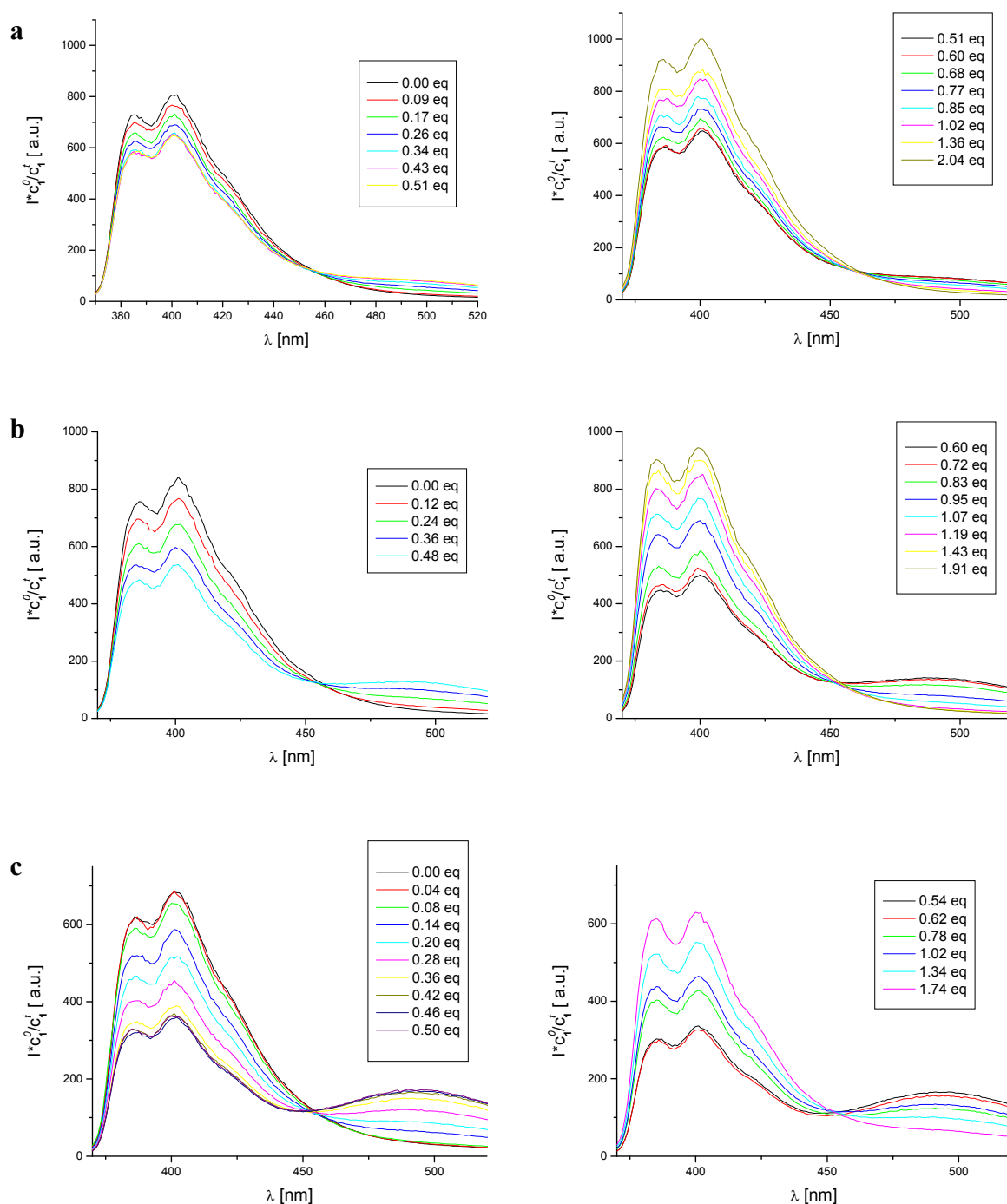


Figure S4: Emission spectra obtained for titration of compound 2 with IDP, ITP, UDP and UTP. Obtained emission spectra show the typical behavior of successive formation (left) and disruption (right) of the corresponding ternary complex; compound **2** (0.5 mM) was titrated with (a) IDP, (b) ITP, (c) UDP and (d) UTP (1.0 mM) in aqueous HEPES buffer at pH 7.4

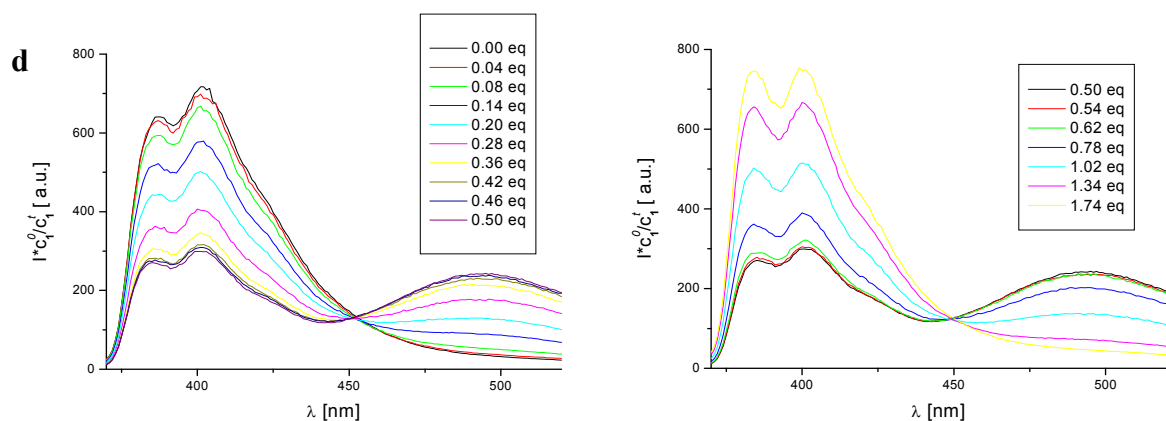


Figure S4 (cont.): Emission spectra obtained for titration of compound 2 with IDP, ITP, UDP and UTP. Obtained emission spectra show the typical behavior of successive formation (left) and disruption (right) of the corresponding ternary complex; compound **2** (0.5 mM) was titrated with (a) IDP, (b) ITP, (c) UDP and (d) UTP (1.0 mM) in aqueous HEPES buffer at pH 7.4

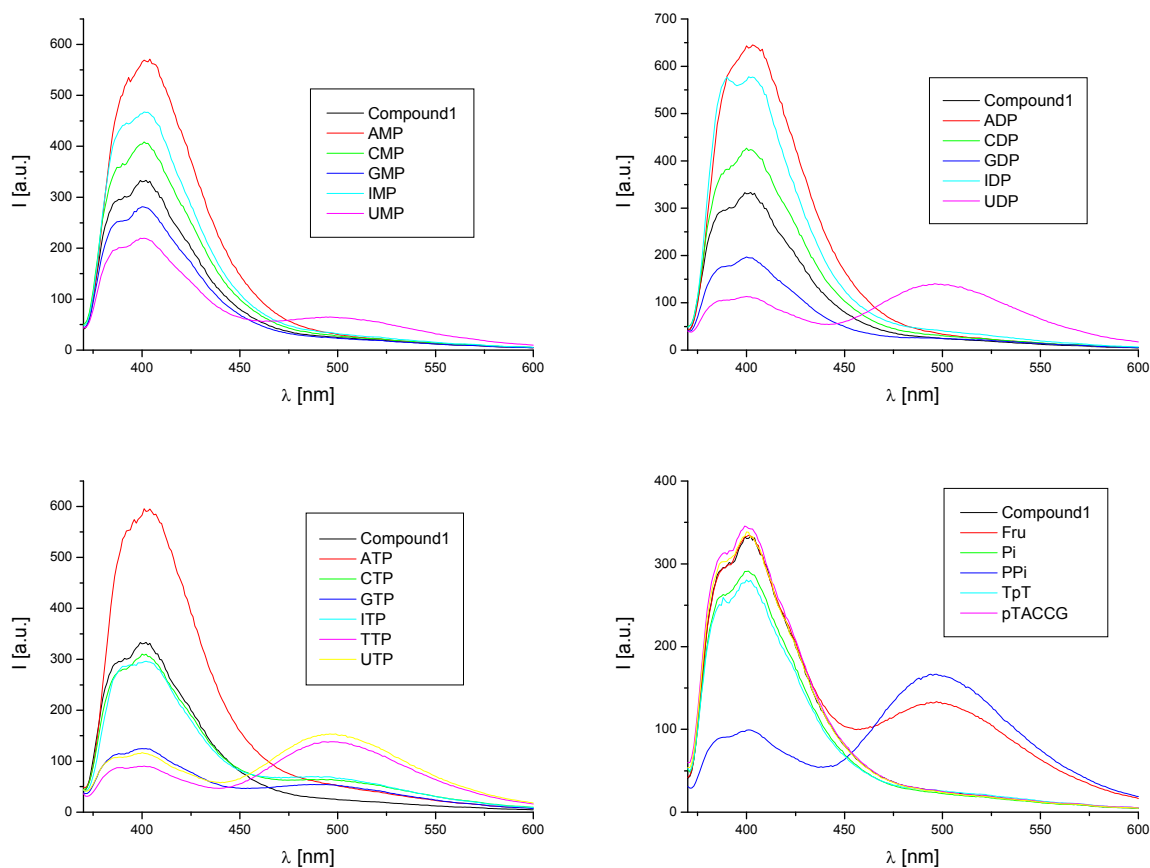


Figure S5: Emission spectra for analyte screening with compound 1 in HEPES buffered solution.

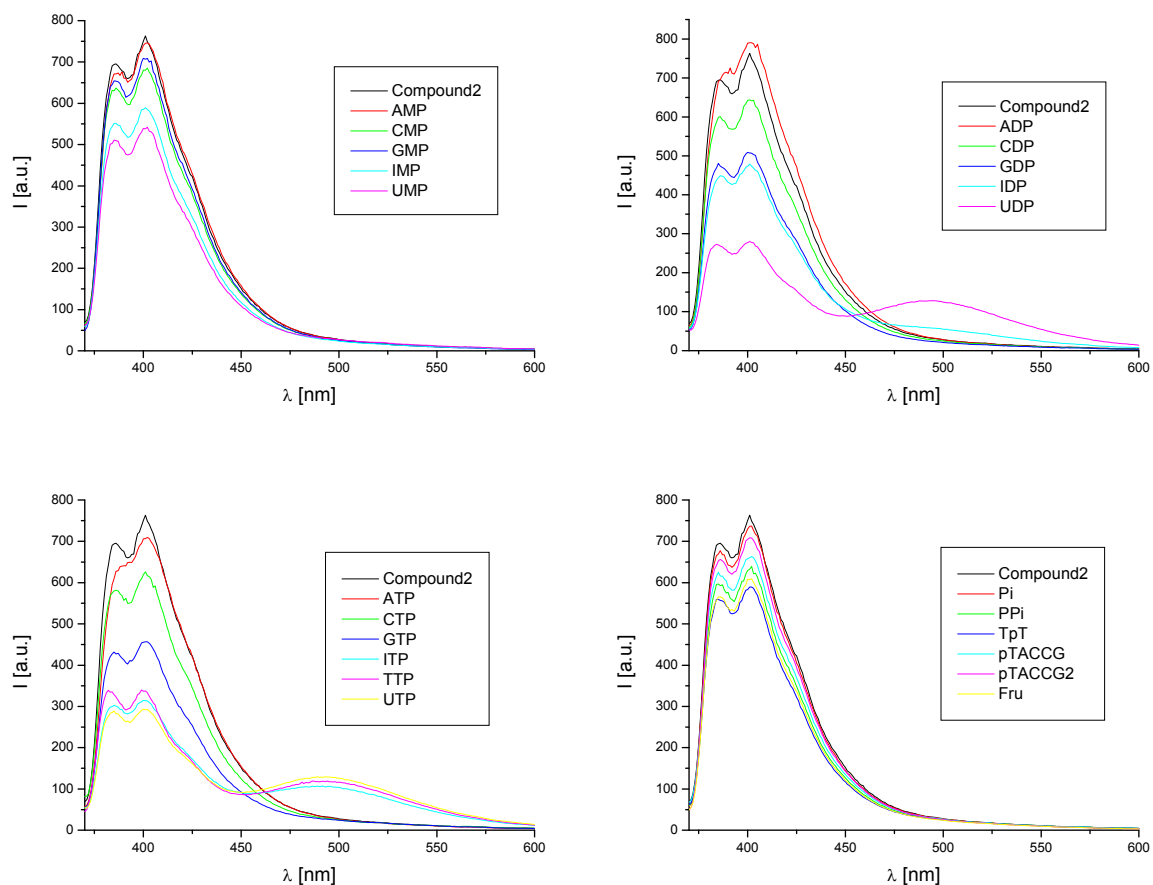


Figure S6: Emission spectra for analyte screening with compound 2 in HEPES buffered solution.

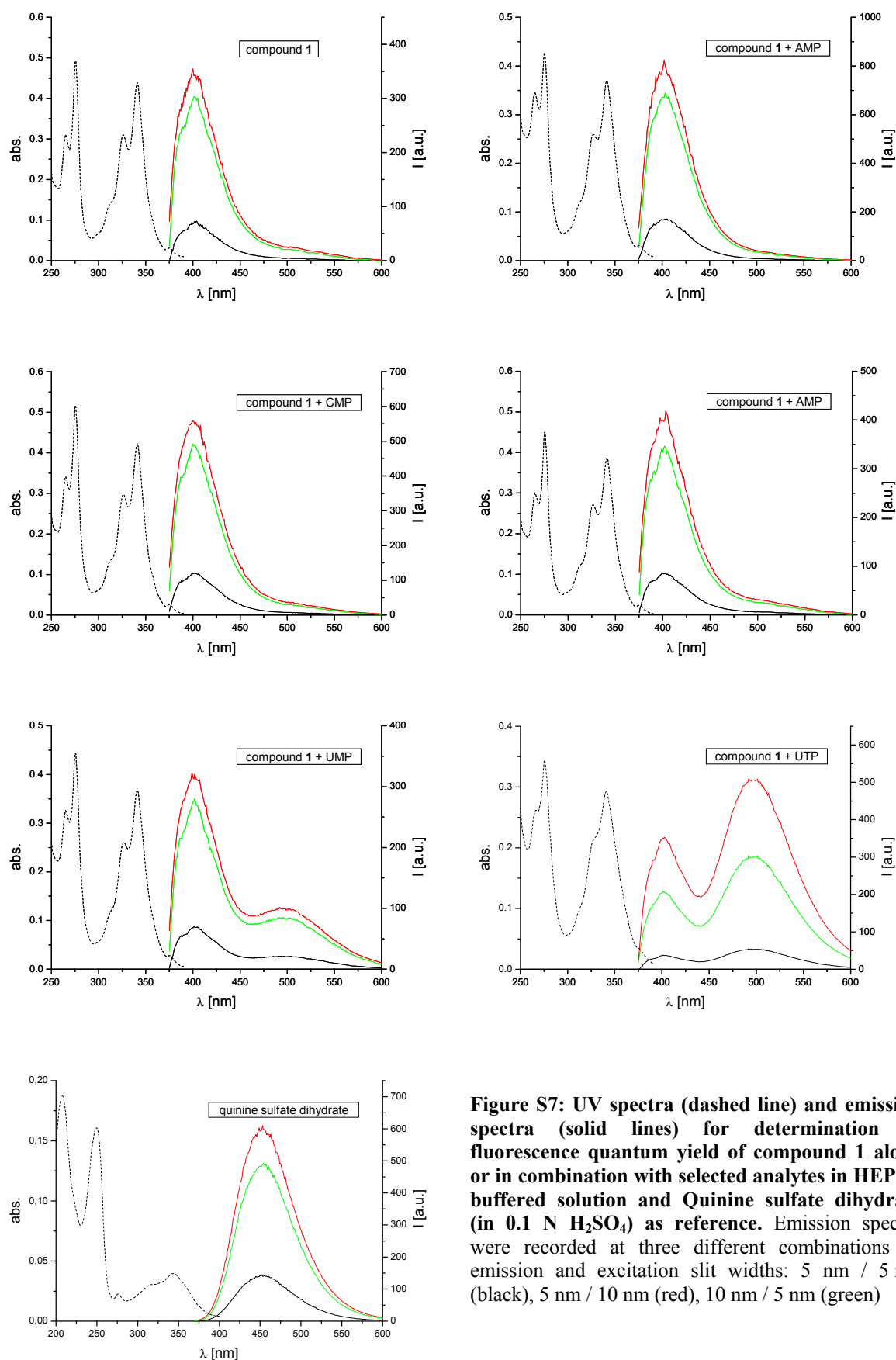


Figure S7: UV spectra (dashed line) and emission spectra (solid lines) for determination of fluorescence quantum yield of compound 1 alone or in combination with selected analytes in HEPES buffered solution and Quinine sulfate dihydrate (in 0.1 N H_2SO_4) as reference. Emission spectra were recorded at three different combinations of emission and excitation slit widths: 5 nm / 5 nm (black), 5 nm / 10 nm (red), 10 nm / 5 nm (green)

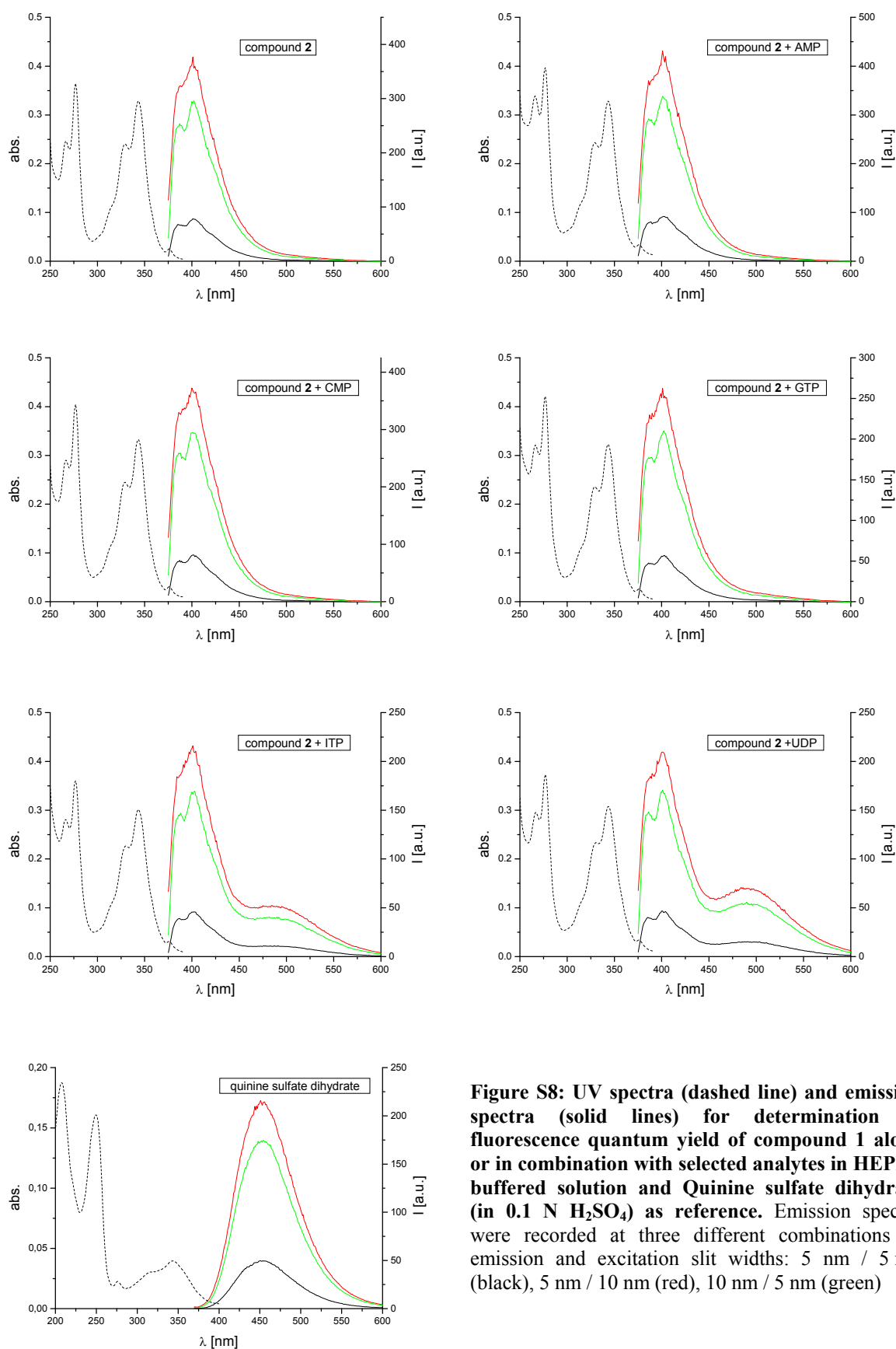


Figure S8: UV spectra (dashed line) and emission spectra (solid lines) for determination of fluorescence quantum yield of compound 1 alone or in combination with selected analytes in HEPES buffered solution and Quinine sulfate dihydrate (in 0.1 N H_2SO_4) as reference. Emission spectra were recorded at three different combinations of emission and excitation slit widths: 5 nm / 5 nm (black), 5 nm / 10 nm (red), 10 nm / 5 nm (green)

1.6 REFERENCES

- ¹ J. M. Berg, J. L. Tymoczko and L. Stryer, *Biochemistry*, W. H. Freeman & Company, 2002.
- ² W. H. Ko, S. M. Wilson and P. Y. D. Wong, *Br. J. Pharmacol.*, **1997**, *121*, 150-156.
- ³ D. Communi and J.-M. Boeynaems, *Trends Pharmacol. Sci.*, **1997**, *18*, 83-86.
- ⁴ E. Heilbronn, B. H. A. Knoblauch and C. E. Müller, *Neurochem. Res.*, **1997**, *22*, 1041-1050.
- ⁵ I. von Kügelgen, *Biotrend Reviews*, **2008**, *3*.
- ⁶ R. Czajkowski and J. Baranska, *Acta Biochim. Pol.*, **2002**, *49*, 877-889.
- ⁷ P. B. Dennis, A. Jaeschke, M. Saitoh, B. Fowler, S. C. Kozma and G. Thomas, *Science*, **2001**, *294*, 1102-1105.
- ⁸ S. Kato, M. Yoshida and Y. Kato-Yamada, *J. Biol. Chem.*, **2007**, *282*, 37618-37623.
- ⁹ I. Ruiz-Stewart, S. R. Tiyyagura, J. E. Lin, S. Kazerounian, G. M. Pitari, S. Schulz, E. Martin, F. Murad and S. A. Waldman, *Proc. Natl. Acad. Sci. USA*, **2004**, *101*, 37-42.
- ¹⁰ K. Inoue, M. Tsuda and H. Tozaki-Saitoh, *Purinergic Signalling*, **2007**, *3*, 311-316.
- ¹¹ H. Caohuy, M. Srivastava and H. B. Pollard, *Proc. Natl. Acad. Sci. USA*, **1996**, *93*, 10797-10802.
- ¹² G. Li, L. Han, T. C. Chou, Y. Fujita, L. Arunachalam, A. Xu, A. Wong, S. K. Chiew, Q. Wan, L. Wang and S. Sugita, *J. Neurosci.*, **2007**, *27*, 190-202.
- ¹³ *The Handbook: A Guide to Fluorescent Probes and Labeling Technologies*, Invitrogen, USA, 2005.
- ¹⁴ X. L. Zuo, S. P. Song, J. Zhang, D. Pan, L. H. Wang and C. H. Fan, *J. Am. Chem. Soc.*, **2007**, *129*, 1042-1043.
- ¹⁵ E. Llaudet, S. Hatz, M. Droniou and N. Dale, *Anal. Chem.*, **2005**, *77*, 3267-3273.
- ¹⁶ S. Migita, K. Ozasa, T. Tanaka and T. Haruyama, *Anal. Sci.*, **2007**, *23*, 45-48.
- ¹⁷ H. W. Rhee, C. R. Lee, S. H. Cho, M. R. Song, M. Cashel, H. E. Choy, Y. J. Seok and J. I. Hong, *J. Am. Chem. Soc.*, **2008**, *130*, 784-785.
- ¹⁸ M. Schaferling and O. S. Wolfbeis, *Chemistry*, **2007**, *13*, 4342-4349.
- ¹⁹ E. Kinoshita, E. Kinoshita-Kikuta, K. Takiyama and T. Koike, *Mol. Cell. Proteomics*, **2006**, *5*, 749-757.

- 20 S. Mizukami, T. Nagano, Y. Urano, A. Odani and K. Kikuchi, *J. Am. Chem. Soc.*, **2002**, *124*, 3920-3925.
- 21 A. Ojida, I. Takashima, T. Kohira, H. Nonaka and I. Hamachi, *J. Am. Chem. Soc.*, **2008**, *130*, 12095-12101.
- 22 C. Li, M. Numata, M. Takeuchi and S. Shinkai, *Angew. Chem., Int. Ed.*, **2005**, *44*, 6371-6374.
- 23 H. M. Wu, C. He, Z. H. Lin, Y. Liu and C. Y. Duan, *Inorg. Chem.*, **2009**, *48*, 408-410.
- 24 Z. Xu, N. J. Singh, J. Lim, J. Pan, H. N. Kim, S. Park, K. S. Kim and J. Yoon, *J. Am. Chem. Soc.*, **2009**, *131*, 15528-15533.
- 25 F. Sancenon, A. B. Descalzo, R. Martinez-Manez, M. A. Miranda and J. Soto, *Angew. Chem., Int. Ed.*, **2001**, *40*, 2640-2643.
- 26 S. Wang and Y. T. Chang, *J. Am. Chem. Soc.*, **2006**, *128*, 10380-10381.
- 27 J. Y. Kwon, N. J. Singh, H. N. Kim, S. K. Kim, K. S. Kim and J. Y. Yoon, *J. Am. Chem. Soc.*, **2004**, *126*, 8892-8893.
- 28 X. Q. Chen, M. J. Jou and J. Yoon, *Org. Lett.*, **2009**, *11*, 2181-2184.
- 29 M. Shionoya, T. Ikeda, E. Kimura and M. Shiro, *J. Am. Chem. Soc.*, **1994**, *116*, 3848-3859.
- 30 Z. Zeng and L. Spiccia, *Chemistry*, **2009**, *15*, 12941-12944.
- 31 T. H. Kwon, H. J. Kim and J. I. Hong, *Chemistry*, **2008**, *14*, 9613-9619.
- 32 S. Aoki and E. Kimura, *Rev. Mol. Biotechnol.*, **2002**, *90*, 129-155.
- 33 E. Kimura, S. Aoki, T. Koike and M. Shiro, *J. Am. Chem. Soc.*, **1997**, *119*, 3068-3076.
- 34 S. Aoki and E. Kimura, *J. Am. Chem. Soc.*, **2000**, *122*, 4542-4548.
- 35 R. Reichenbach-Klinke and B. König, *Dalton Trans.*, **2002**, 121-130.
- 36 M. Shionoya, E. Kimura and M. Shiro, *J. Am. Chem. Soc.*, **1993**, *115*, 6730-6737.
- 37 S. Aoki and E. Kimura, *Chem. Rev.*, **2004**, *104*, 769-788.
- 38 T. Koike and E. Kimura, *J. Am. Chem. Soc.*, **1991**, *113*, 8935-8941.
- 39 For both compounds **1** and **2** preliminary titrations with UTP revealed a 2:1 stoichiometry. Thus, 2:1 stoichiometry for both compounds was also suggested for the screening and was finally confirmed by titration of several analytes with **1** and **2**. These results indicated clearly that excimer formation was exclusively observed for the expected ternary complexes. Formation of quaternary or higher pyrene excimer emitting complexes could be excluded.
-

- ⁴⁰ S. Brandes, C. Gros, F. Denat, P. Pullumbi and R. Guillard, *Bull. Soc. Chim. Fr.*, **1996**, 133, 65-73.
- ⁴¹ R. Reichenbach-Klinke, M. Kruppa and B. König, *J. Am. Chem. Soc.*, **2002**, 124, 12999-13007.
- ⁴² A. Späth, *PhD Thesis*, **2010**, University of Regensburg.
- ⁴³ H. Vollmann, H. Becker, M. Corell and H. Streeck, *Liebigs Ann. Chem.*, **1937**, 531, 1-159.
- ⁴⁴ P. Babu, N. M. Sangeetha, P. Vijaykumar, U. Maitra, K. Rissanen and A. R. Raju, *Chem. Eur. J.*, **2003**, 9, 1922-1932.
- ⁴⁵ Traces of several chlorinated pyrenes were observed as byproducts in mass analysis when using Method B; however, from NMR spectra the purity could be determined to be at least 95% as no noteworthy additional signals referring to these impurities were observed. The small impurities could not be removed, but did not affect the following synthesis steps or fluorescence investigations.
- ⁴⁶ For compound **1** a 2-fold increase in pyrene monomer emission intensity was observed when adenine nucleotides were added; the effect was reported previously.²⁵ Addition of CMP, CDP and IMP increased pyrene monomer emission to a smaller extend, while the addition of guanine nucleotides decreased the monomer emission intensity to 45-65%.
- ⁴⁷ Addition of GDP or GTP to compound **2** lead to a decrease in monomer emission of about 35-40%; for CDP, CTP, PP_i and Fructose-1,6-bisphosphate of 15-20%. IMP and UMP quench the emission at 400 nm by about 25-30%, while excimer emission is barely increased. All observed weak changes in the spectra's excimer region are in accordance with previously published results.³⁶
- ⁴⁸ The preference of IDP and ITP induced excimer formation for compound **2** is presumably due to improved anion binding affinity with increasing number of Zn²⁺-cyclens known for phosphates.³³
- ⁴⁹ J. N. Wilson, Y. J. Cho, S. Tan, A. Cuppoletti and E. T. Kool, *ChemBioChem*, **2008**, 9, 279-285.
- ⁵⁰ P. Hobza, H. L. Selzle and E. W. Schlag, *J. Phys. Chem.*, **1996**, 100, 18790-18794.
-

2 DNA STAINING IN AGAROSE GELS WITH ZINC(II)CYCLEN-PYRENE



A pyrene-labelled Zn^{2+} -cyclen complex for the staining of DNA in agarose gels is reported. The metal chelate coordinates reversibly to the DNA phosphate backbone, which induces the formation of pyrene excimers. The typical pyrene excimer emission is used for the detection of the DNA. Staining is limited to agarose gels and less sensitive than Ethidium bromide, but DNA amounts down to 10 ng and short DNA strands (~300 bp) are detectable. Gel extraction as a standard technique in molecular biology was successfully performed after staining with Zn^{2+} -Cyclen-pyrene. Cytotoxicity tests on HeLa and V-79 cells reveal that the zinc-cyclen pyrene probe is significant less toxic compared to Ethidium bromide.

2.1 INTRODUCTION

DNA separation on agarose gels is a standard technique in molecular biology. Ethidium bromide is the most commonly used reagent for visualization of the separated fragments.^{1]} However, its genotoxic potential is controversially discussed. At physiologically relevant conditions, intercalation is the predominantly occurring binding mode of Ethidium bromide to DNA.²⁻³ Intercalation is very often associated with mutagenic potential as insertion of such intercalators between π -stacked base pairs results in local structural changes in DNA (e.g. unwinding and lengthening of the DNA double helix). Consequently, interaction with DNA polymerases and other DNA-related proteins is disrupted, thus DNA transcription is affected. Further, frameshift mutations are conceivable, since the widening of π -stacked base pairs especially in repetitive DNA sequences can lead to either leaving a single unpaired base or bulging several bases out of the helix. This propensity was indeed observed, however, only in bacteriophage and bacterial assays, but not in mammalian cells.⁴⁻⁶ In contrast, the Ames test reveals that only metabolites of Ethidium bromide are mutagenic in *Salmonella typhimurium*⁷ and a mutagenic potential of Ethidium bromide in *E. coli* was reported to depend on UV light exposure.⁸

Ethidium bromide should therefore be handled with care, generating additional costs in gel staining and imaging and disposal of waste.⁹⁻¹¹ To overcome drawbacks in DNA staining, a variety of alternative stains are available: SYBR Green I/II, SYBR Gold, SYBR Safe, PicoGreen, GelGreen, GelRed, Midori Green, RedSafe, OliGreen, BlueView are stated to be not genotoxic,¹² but the structure of the dyes, conditions of the mutagenicity tests and composition of the DMSO stock solutions is not always available.⁸ Furthermore, these reagents are often less stable than Ethidium bromide and therefore, are suggested not to be stored at room temperature. Nile Blue A and Methylene Blue are water-soluble DNA stains and suggested to be non-mutagenic. However, the sensitivity of Methylene Blue for DNA staining is significantly lower compared to Ethidium bromide.

We report now a water-soluble fluorescent DNA staining reagent Zn^{2+} -Cyclen-pyrene **1**. Coordination of the pyrene metal-chelate to DNA induces pyrene-pyrene excimer formation, which is easily detected. By this, staining down to 10 ng of DNA in agarose gels was achieved. Preliminary cytotoxicity studies on two different cell lines indicate that Zn^{2+} -Cyclen-pyrene **1** may have lower cytotoxicity compared to Ethidium bromide. Moreover, storage at special conditions is not necessary.

2.2 RESULTS & DISCUSSION

The ability of Zn^{2+} -cyclen complexes to bind phosphate anions and imide functional groups in aqueous solution is well known.¹³⁻¹⁹ Dye-labelled Zn^{2+} -cyclen complexes should therefore allow the staining of oligonucleotides in gels, as previously reported for phosphorylated proteins.²⁰⁻²² Figure 1 shows the Zn^{2+} -cyclen-dye conjugates used in this study. The pyrene-labelled compounds **1** and **2** are intended to signal the presence of an oligonucleotide by analyte induced excimer formation.

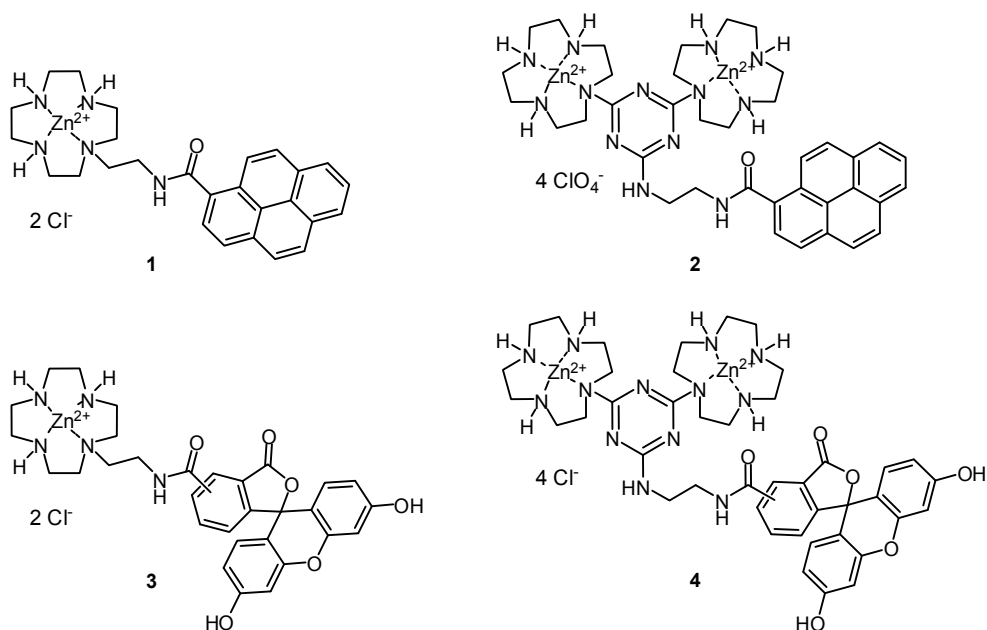


Figure 1: Dye-labelled Zn^{2+} -cyclen complexes used in gel staining. Compounds **1** and **2** were previously found to discriminate uridine-phosphates from other nucleotides by analyte induced excimer formation;²³ compound **4** was reported to be a phospho-protein staining reagent by emission increase upon binding to phosphate groups in proteins²¹

2.2.1 Staining of DNA with Zn^{2+} -Cyclen-pyrene

Plasmid DNA pMGFP was enzymatically cleaved by *NdeI* giving two linear strands of *dsDNA* (2241 bp, 2466 bp). This linear *dsDNA* and the circular plasmid were electrophoretically resolved on an agarose gel and stained by Zn^{2+} -Cyclen-pyrene **1** or Ethidium bromide. Both procedures yield identical staining patterns as shown in Figure 2. Compound **1** indicates the presence of the DNA by its enhanced excimer emission.

Compounds **2-4** were investigated likewise on their staining ability, but failed to identify DNA in the gel by a significant emission signal. All metal complexes **1-4** are expected to interact with the oligophosphate backbone of the DNA, and to a smaller extend, with thymine imide moieties. The experiments show, that the affinity of the complexes to the DNA analyte is under the experimental conditions not sufficient to achieve a non-covalent

labelling. Only in the case of **1**, presumably by stabilizing the DNA-complex aggregate by pyrene-pyrene interactions, a sufficient affinity is reached. (Figure 3)

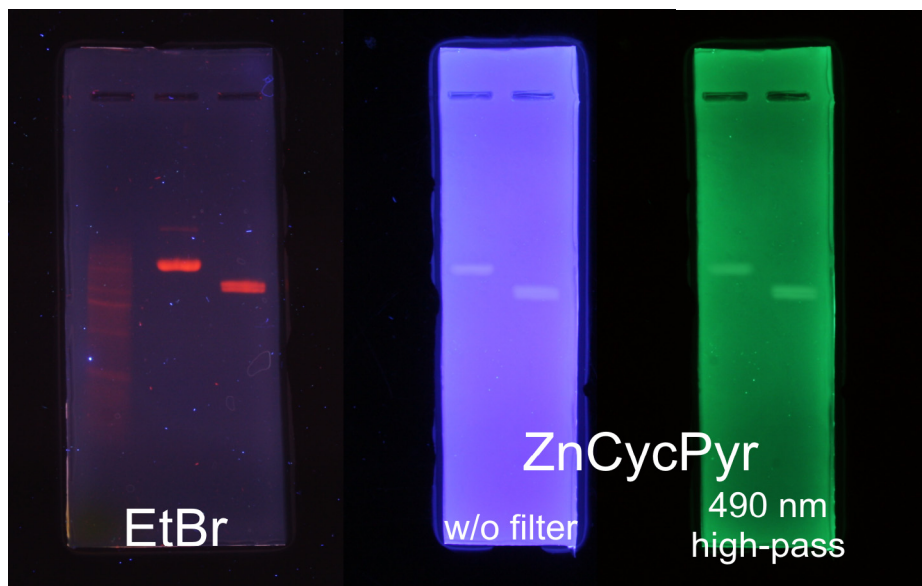


Figure 2: Staining of a linearized and a circular plasmid pHMGFP with Ethidium bromide or complex 1. Gel run of linearized (left lanes) and circular (right lanes) plasmid DNA on an agarose gel (0.8%) stained with either Zn^{2+} -Cyclen-pyrene **1** or Ethidium bromide; images were taken on a PeqLab Superbright UV table ($\lambda_{\text{max}} = 316 \text{ nm}$) with a Canon EOS 450D; using a high-pass filter (490 nm) bluish gel background emission appears in greenish color

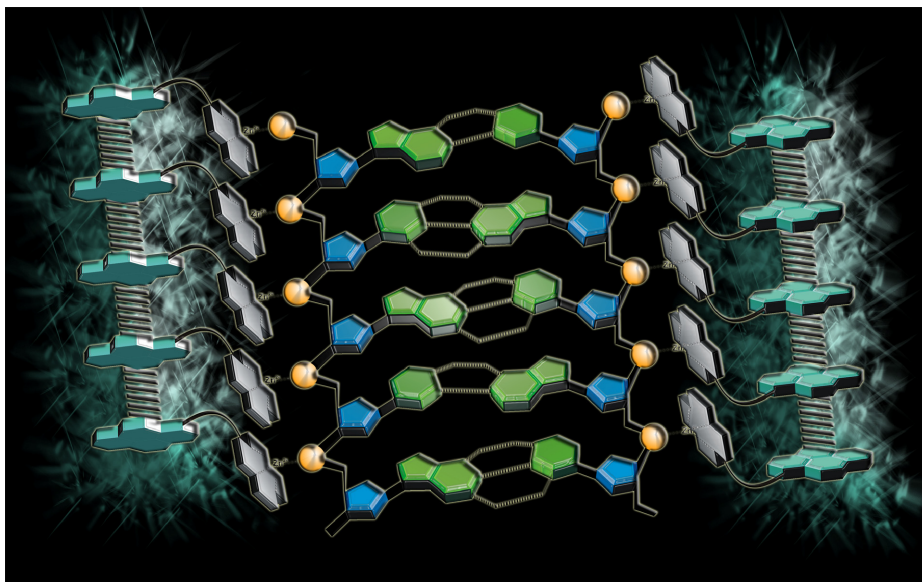


Figure 3: Proposed interaction of Zn^{2+} -Cyclen-pyrene with DNA and staining mechanism due to analyte induced pyrene excimer formation. Metal-chelates are suggested to bind to phosphodiester of the backbone while pyrene-pyrene interactions additionally stabilize the binding to DNA by π -stacking; due to formed pyrene-excimer upon irradiation, pyrene-emission is changed that finally allows the detection of lightened up DNA bands on the gel

Uridinemonophosphate (UMP), which is able to induce enhanced excimer emission of **1**,²³⁻²⁴ was used to investigate the response of the probes emission properties to gel matrices. Agarose and polyacrylamide gels containing UMP behave different when soaked in a solution of **1**: While the agarose gel develops quickly the typical turquoise excimer emission upon irradiation at 366 nm, no excimer emission is observed for Polyacrylamide.

To exclude the intercalation of the pyrene moiety into the *ds*DNA as binding motif, the staining ability of Zn^{2+} -Cyclen-pyrene **1** was compared to its non-complexed ligand. No staining was observed with the ligand (Figure 4) showing that the zinc(II)complex is essential for the staining ability of compound **1**.



Figure 4: Comparison of gel staining with complex **1 and the corresponding zinc-ion free ligand.** Gel runs of plasmid DNA pMGFP stained with either Zn^{2+} -Cyclen-pyrene **1** (left) or the non-complexed ligand (right) at comparable conditions; (left) distinct visualization of DNA band as pronounced fluorescent signal; (right) no staining of DNA could be observed when using the non-complexed, pyrene-labelled aza-macrocycle suggesting that 1. coordinative interactions are crucial for this staining method and 2. pyrene intercalation does not occur; this image was taken without using any filter and thus shows the total fluorescence of the stain upon irradiation

2.2.2 Sensitivity Comparison of Zn^{2+} -Cyclen-pyrene with Ethidium Bromide

To estimate the sensitivity of the staining reagent, dilution series ($m_{\text{DNA/lane}}$ [ng] \sim 700, 350, 175, 88, 44, 22, 11, 5) of plasmid pMGFP were transferred on two independent agarose gels and stained after the gel run with Zn^{2+} -Cyclen-pyrene **1** and Ethidium bromide, respectively, at comparable concentrations (\sim 1 mM). As deduced from the obtained images shown in Figure 5, compound **1** is not as sensitive as Ethidium bromide. However, DNA amounts of \sim 10 ng could be visualized with Zn^{2+} -Cyclen-pyrene.

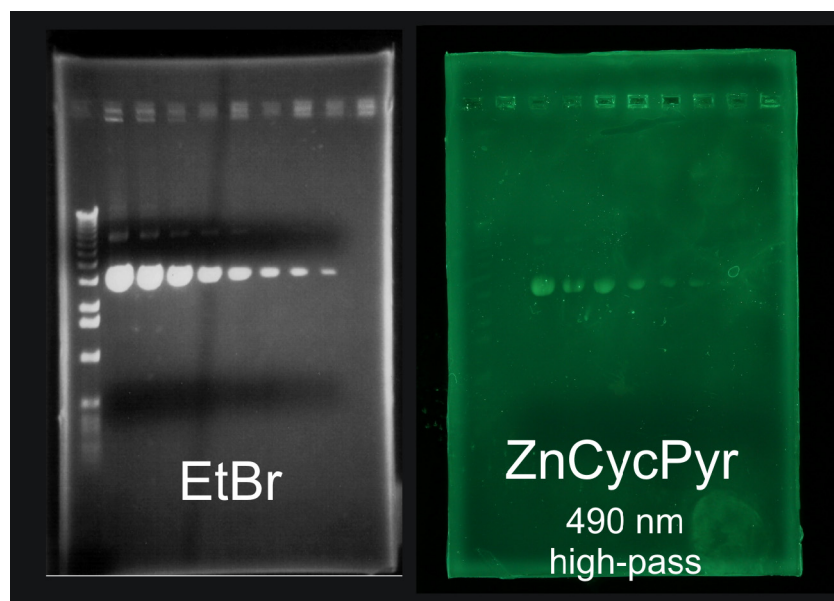


Figure 5: Sensitivity comparison of Zn^{2+} -Cyclen-pyrene and Ethidium bromide as staining reagents. Identical dilution rows (from left to right: $m_{\text{DNA/lane}}$ [ng] \sim 700, 350, 175, 88, 44, 22, 11, 5) were transferred in two separate gels followed by electrophoresis; staining with (left) Ethidium bromide (\sim 1 mM) and (right) compound **1** (\sim 1 mM) demonstrate the staining performance of both; in comparison, Ethidium bromide shows better sensitivity however, compound **1** is able to visualize concentrations of DNA of \sim 10 ng

2.2.3 Gel Extraction Experiments after Staining with Zn^{2+} -Cyclen-pyrene

Gel extraction experiments of the Zn^{2+} -Cyclen pyrene stained plasmid were performed. Gel extraction is a standard technique to isolate DNA from gels for further amplification or cloning. In addition, the experiment shows if compound **1** initiates major chemical modifications in the DNA (e.g. DNA cleavage) when bound to it. Plasmid pHMGFP was transferred on a gel and treated with compound **1** staining solution. The fluorescent DNA band was cut out and subsequently, extracted using a QIAquick Gel Extraction Kit. Afterwards, the recycled DNA was again electrophorized and then stained with Ethidium bromide. Comparison of re-extracted plasmid and a control sample of the plasmid confirmed that Zn^{2+} -Cyclen-pyrene **1** has not affected the plasmid pHMGFP since only one DNA band with comparable migration characteristics could be identified.

2.2.4 Staining of Short DNA Strands

The ability to stain short DNA strands (\sim 300 bp) was investigated comparing Zn^{2+} -Cyclen-pyrene **1** and Ethidium bromide. Staining of short strands (<150 bp) using Ethidium bromide generally results in cloudy, not well-defined bands. In this case, staining with compound **1** should be of advantage. In fact, direct comparison shows that for Zn^{2+} -Cyclen-pyrene **1** a better resolution of the band was observed, but with lower intensity. (Figure 6)

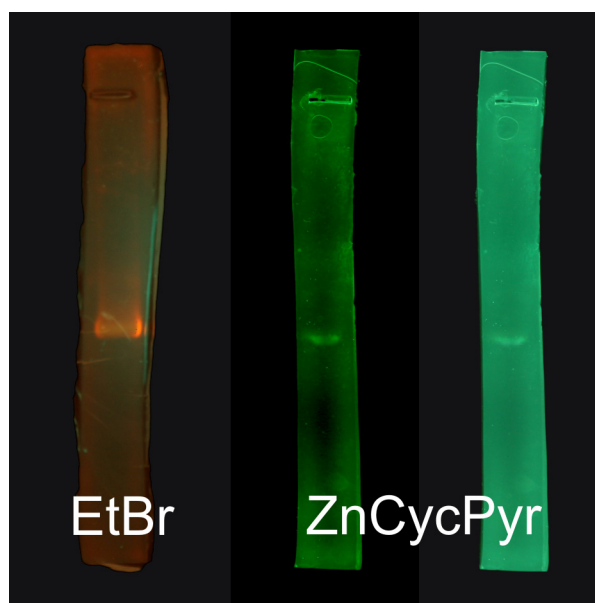


Figure 6: Short *ds*DNA (~300 bp) – comparison of staining ability of Ethidium bromide and Zn^{2+} -Cyclen-pyrene **1.** Two identical gels with *ds*DNA with a length of about 300 bp were stained in a solution of either Ethidium bromide or compound **1**; as generally known for Ethidium bromide, short DNA fragments (<150 bp) lead to cloudy and not well-defined bands as also demonstrated on the left side for this length; staining with Zn^{2+} -Cyclen-pyrene **1** leads obviously to DNA bands with improved resolution, however, intensity is lower compared to Ethidium bromide; in this case, Ethidium bromide stained gel was photographed in parallel with compound **1** stained gel on a PeqLab Superbright UV table ($\lambda_{\text{max}} = 316 \text{ nm}$) with a Canon EOS 450D and using a high-pass filter (490 nm)

2.2.5 Determination of Cytotoxicity

To compare the cytotoxic potential of complex **1** to Ethidium bromide, preliminary studies were performed. In a first series, HeLa cells were cultivated, transferred in a well-plate and treated in separate trials with Ethidium bromide and Zn^{2+} -Cyclen-pyrene **1**, respectively (100, 50, 25, 10, 1, 0.1 μM). Upon incubation for three days, 3-(4,5-Dimethylthiazol-2-yl)-2,5-diphenyltetrazolium bromide (MTT) was added, whose conversion into purple-colored Formazan is proportional to the cell viability rate.²⁵ Results obtained from fluorescence read out of the well-plates suggest that Zn^{2+} -Cyclen-pyrene **1** is less toxic compared to Ethidium bromide: While more than 60% of HeLa cells survived the treatment with 100 μM of compound **1**, the same concentration of Ethidium bromide caused complete cell mortality. (Figure 7) In a second series, V-79 cells were tested under comparable conditions for cytotoxic reaction in presence of compound **1**, Ethidium bromide and also the commercially available DNA staining reagent RedSafe, which is offered as stock solution in DMSO (20 000x) and described as very safe. Cell staining with Giemsa solution and counting of stained cell colonies surprisingly showed a significantly enhanced cytotoxic effect for

RedSafe and metabolites on this metabolizing cell line. Even the highest dilution (1:40 000 of a 20 000x stock solution) added to the cells lead to complete cell mortality in the culture solution. While metabolites of Ethidium bromide only lead to noticeable cell mortality at concentrations $>25\ \mu\text{M}$, Zn^{2+} -Cyclen-pyrene **1** and its metabolites seem not to affect the cells at all. (Figure 7)

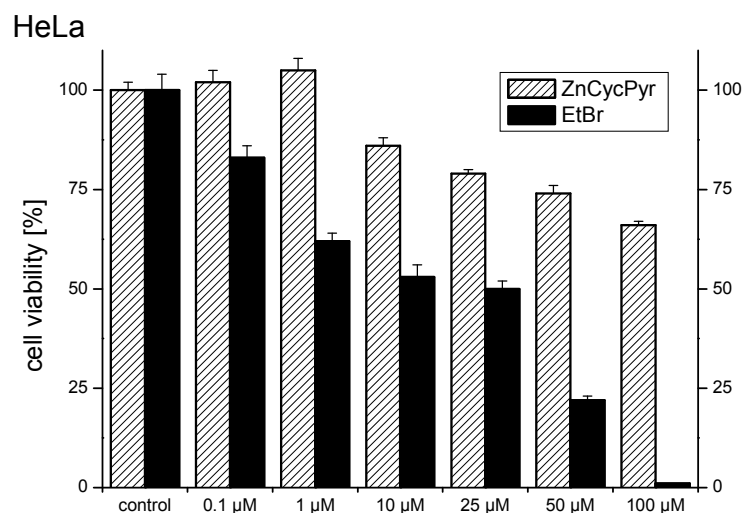


Figure 7: Results of preliminary cytotoxicity studies obtained for HeLa and V-79 cell lines. HeLa cells were incubated in a well-plate in independent trials for three days with Zn^{2+} -Cyclen-pyrene **1** and Ethidium bromide, respectively (100, 50, 25, 10, 1, 0.1 μM); V-79 cells were investigated under comparable conditions in Petri culture dishes in the presence of Zn^{2+} -Cyclen-pyrene **1**, Ethidium bromide (both at 100, 50, 25, 10, 1, 0.1 μM) and RedSafe (1:10 000, 1:20 000, 1:40 000 of a 20 000x stock solution in DMSO); fluorescence read out due to conversion of MTT into Formazan by surviving cells (HeLa) or counting intact cell colonies after Giemsa staining (V-79) represent cell viability that was finally plotted as columns (means \pm s.d.) against concentration of substances investigated; solvent control was set to 100%; Zn^{2+} -Cyclen-pyrene **1** was found to hardly influence non-metabolizing HeLa and to be affectless on metabolizing V-79 cells; in comparison, treatment of both cell lines with Ethidium bromide resulted in higher cell mortality, while RedSafe was found to show obviously dramatically increased cytotoxicity as shown on V-79 cells

V-79

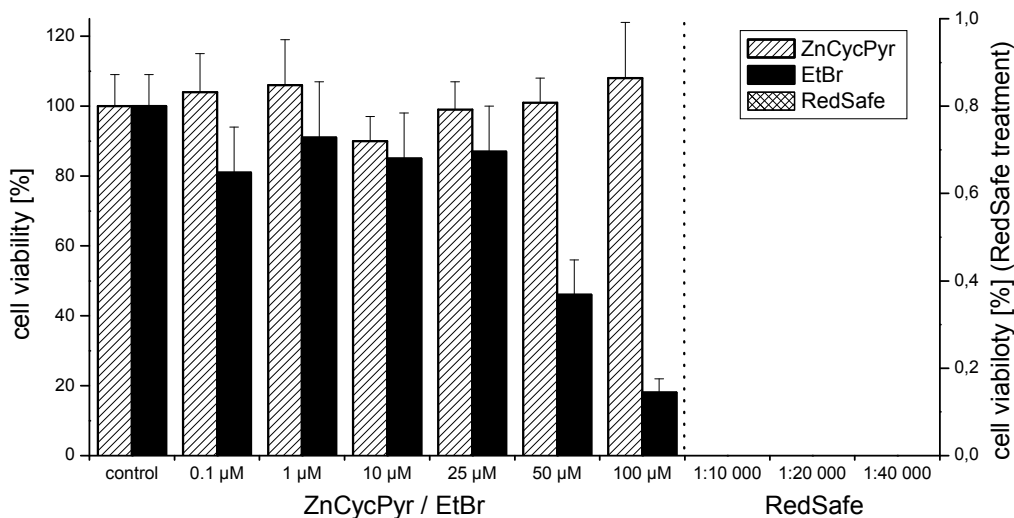


Figure 7 (cont.): Results of preliminary cytotoxicity studies obtained for HeLa and V-79 cell lines. HeLa cells were incubated in a well-plate in independent trials for three days with Zn^{2+} -Cyclen-pyrene **1** and Ethidium bromide, respectively (100, 50, 25, 10, 1, 0.1 μM); V-79 cells were investigated under comparable conditions in Petri culture dishes in the presence of Zn^{2+} -Cyclen-pyrene **1**, Ethidium bromide (both at 100, 50, 25, 10, 1, 0.1 μM) and RedSafe (1:10 000, 1:20 000, 1:40 000 of a 20 000x stock solution in DMSO); fluorescence read out due to conversion of MTT into Formazan by surviving cells (HeLa) or counting intact cell colonies after Giemsa staining (V-79) represent cell viability that was finally plotted as columns (means \pm s.d.) against concentration of substances investigated; solvent control was set to 100%; Zn^{2+} -Cyclen-pyrene **1** was found to hardly influence non-metabolizing HeLa and to be affectless on metabolizing V-79 cells; in comparison, treatment of both cell lines with Ethidium bromide resulted in higher cell mortality, while RedSafe was found to show obviously dramatically increased cytotoxicity as shown on V-79 cells

A likely reason for the increased cytotoxicity of RedSafe may be the presence of DMSO, which permeates cell membranes. Hence, the uptake of RedSafe in cells may be dramatically increased compared to the trials performed with aqueous solutions of either compound **1** or Ethidium bromide.

2.3 CONCLUDING REMARKS

Inhere, the application of Zn^{2+} -Cyclen-pyrene **1** as DNA staining reagent on agarose gels was demonstrated. Based on coordinative interactions between the metal-chelate and the phosphate backbone in DNA being additionally stabilized by pyrene-pyrene π -stacking interactions, irradiation results in formation of pyrene excimers. These excimers allowed the detection of DNA bands as brightened up, well resolved signals on gels. In contrast, intercalation of the pyrene moiety into DNA could be excluded. In comparison to Ethidium bromide as a standard staining reagent, compound **1** was found to be marginally less sensitive, but showed better resolution of short *ds*DNA fragments (~ 300 bp). However, this staining

method is limited to agarose gels. Nevertheless, important features of **1** are excellent water-solubility and a presumably low cytotoxic potential according to preliminary cell-based studies presented herein. Though, to further confirm its comparably low risks, a more comprehensive cytotoxicity profile has to be drawn and also mutagenicity studies would be of high interest.

2.4 ACKNOWLEDGEMENTS

We thank Petra Unger for kind support with V-79 cell viability tests.

2.5 CONFLICT OF INTEREST STATEMENT

All authors declare that there are no financial or commercial conflicts of interest.

2.6 MATERIALS & METHODS

2.6.1 General

Absorption spectroscopy. Absorption spectra were recorded on a Varian Cary BIO 50 UV/VIS/NIR Spectrometer by use of 1 cm quartz cuvettes (Hellma) and Uvasol solvents (Merck or Baker).

NMR spectra. Bruker Avance 400 (^1H : 400.1 MHz, ^{13}C : 100.6 MHz, $T = 300\text{ K}$). The chemical shifts are reported in δ [ppm] relative to internal standards (solvent residual peak). The spectra were analyzed by first order, the coupling constants are given in Hertz [Hz]. Characterization of the signals: s = singlet, d = doublet, t = triplet, m = multiplet, dd = double doublet, dt = double triplet. Integration is determined as the relative number of atoms. Assignment of signals in ^{13}C -spectra was determined with DEPT-technique (pulse angle: 135°) and given as (+) for CH_3 or CH , (–) for CH_2 and (C_{quat}) for quaternary C_{quat} . Error of reported values: chemical shift: 0.01 ppm for ^1H -NMR, 0.1 ppm for ^{13}C -NMR and 0.1 Hz for coupling constants. The solvent used is reported for each spectrum.

Mass spectra. MS analysis was performed on a Finnigan MAT 95 (LSI) and a Finnigan MAT TSQ 7000 (ESI).

IR spectra. IR spectra were recorded with a Bio-Rad FTS 2000 MX FT-IR.

Melting point. Melting points were determined on a Büchi SMP or a Lambda Photometrics OptiMelt MPA 100.

TLC analysis and column chromatography. Analytical TLC plates (silica gel 60 F254) and silica gel 60 (70-230 or 230-400 mesh) for column chromatography were purchased from Merck. Spots were visualized by UV light and/or staining with ninhydrine in EtOH.

Dry DMF was purchased from Fluka, dichloromethane (DCM) was dried by adsorption and stored over molecular sieves. All other solvents and chemicals were of reagent grade and used without further purification.

Electrophoresis of DNA on agarose gels. Plasmid DNA (circular and linearized) was electrophoretically resolved on 0.8% Agarose in TAE buffer (20 mM Tris/acetate, 1 mM EDTA) at a voltage of 100 V. The loading buffer consisted of 0.25% (w/v) Bromophenolblue, 0.25% (w/v) xlenecyanol and 40% (w/w) Sucrose. For short dsDNA fragments (~300 bp), agarose gels of 2% were prepared.

Zn²⁺-Cyclen-pyrene staining. Staining with Zn²⁺-Cyclen-pyrene **1** was done by soaking the gels in a solution of the fluorescent metal complex in deionized water at a probe concentration of 10⁻⁴ – 10⁻³ M. In general, incubating for 5-10 min was sufficient to fully resolve the DNA bands on the gels. Destaining in pure deionized water was not strictly necessary, but helpful when staining was performed in highly concentrated solutions of compound **1** to improve the contrast. To test the staining ability of the pyrene moiety itself, a highly concentrated solution of the metal-free ligand of compound **1** in MeOH was prepared and diluted with deionized water (~10⁻³ M). After soaking the gel in this staining bath for up to 1 h, destaining was performed in water.

Staining with compounds 2-4. Staining with fluorescent metal-chelates **2-4** was done according to the procedure for staining with compound **1** as described above.

Ethidium bromide staining. Staining with Ethidium bromide was performed according to standard procedures by treating the gels with an aqueous solution of Ethidium bromide (~1 mM when freshly prepared). Depending on the concentration of the staining bath, gels were soaked about 5-30 min. If necessary, gels were destained by washing with pure deionized water or an aqueous MgCl₂ (~mM) solution for up to 30 min.

Imaging. Zn²⁺-Cyclen-pyrene gels were placed on a PeqLab Superbright UV table (λ_{max} = 316 nm) and images were taken either by a Pentax K10D or a Canon EOS 450D. Ethidium bromide gels were imaged on either a standard UV table and photographed or as described for Zn²⁺-cyclen-pyrene gels.

Plasmid digestion. pHMGFP DNA (Monster Green[®] Fluorescent Protein pHMGFP vector Promega GmbH, Mannheim, Germany) was digested using *NdeI* restriction enzyme (CA/TATG) incubated in NEBuffer 4 (both New England Biolabs Inc., Frankfurt/Main, Germany) for 2 h at 37°C. By this, pHMGFP (4707 bp) is cut at position 387 and 2628.

Gel extraction. For gel extraction, a QIAquick Gel Extraction Kit (Qiagen GmbH, Hilden, Germany) was used. Gel extraction was performed according to manufacturer instructions.

2.6.2 Cytotoxicity Investigations

Cell lines and cell culture conditions. The human epithelial cervical cancer cell line HeLa [CCL-17, American Type Culture Collection (ATCC)] was cultured in MEM Earle's medium. 500 mL MEM were supplemented with 0.8 mL Amphotericin B (250 µg/mL), 5 mL Penicillin/Streptomycin (10 000 U/mL / 10 000 µg/mL), 5 mL L-Glutamine (200 mM), 5 mL NEA (100x) and 50 mL fetal bovine serum (all from Biochrom AG, Berlin, Germany). Cells were split in 1:6-ratio twice a week. Chinese hamster lung fibroblast cells V-79 (HGPRT+) (ATCC, Manassas VA, USA) were maintained in DMEM (PAN Biotech, Aidenbach, Germany) supplemented with 10 µg/mL Thioguanine (Sigma Aldrich, Taufkirchen, Germany) and 10% fetal calf serum (PAN Biotech, Aidenbach, Germany) and split in 1:5-ratio every seven days. All cells were cultured in a humidified incubator at 37°C in a 5% CO₂ atmosphere.

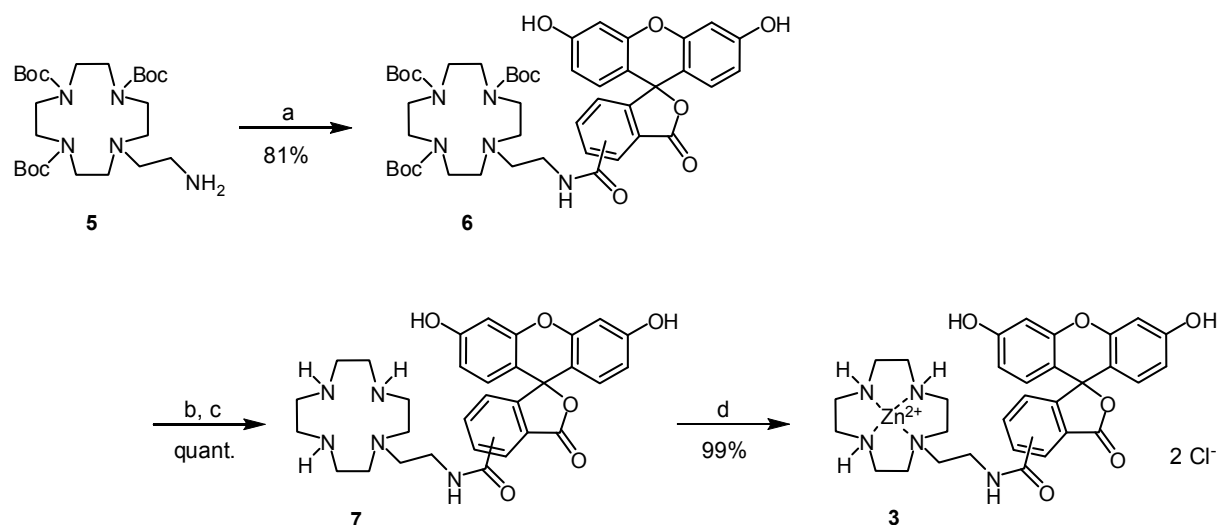
Determination of cytotoxicity. The cytotoxic effect of Zn²⁺-Cyclen-pyrene **1** and Ethidium bromide, respectively, was determined using two different cell lines, non-metabolizing HeLa (ATCC CCL-17) and metabolizing V-79 (HGPRT+).

For evaluation of cytotoxicity on HeLa cells, the colorimetric MTT (tetrazolium) assay was conducted as previously described by Mosmann²⁵ in a modified manner according to Heilmann *et al.*²⁶ In brief, following trypsinization, HeLa cells were counted and 11 250 cells/well were seeded into a 96 well plate (Techno Plastic Products AG, Trasadingen, Switzerland). Afterwards, cells were exposed to compound **1** or Ethidium bromide dissolved in 30% of EtOH (final concentrations: 0.1, 1, 10, 25, 50, 100 µM) for 72 h at 37°C and 5% CO₂. For quantification of viability, cells were incubated with 15 µL/well MTT (tetrazolium) solution (4 mg/mL) for 4 h, which was then converted into insoluble, violet Formazan. After removal of the supernatant, 150 µL SDS solution (10%) was added to dissolve the formazan crystals. The next day, absorption was measured at 560 nm using a SpectraFluorPlus microplate reader (Tecan GmbH, Crailsheim/Germany).

In a second cell culture based experiment according to *Lindl*,²⁷ V-79 cells were also tested on the cytotoxic potential of RedSafe (Intron Biotechnology Inc., Seongnam, South Korea) beyond Zn^{2+} -Cyclen-pyrene **1** and Ethidium bromide. In this assay format, approximately 200 V-79 cells were seeded into Petri dishes of 6 cm in diameter (Corning Incorporated, Corning NY, USA) and exposed to compound **1** and Ethidium bromide dissolved in H_2O at the same final concentrations described above; in the case of RedSafe, defined amounts of a commercially available 20 000x stock solution in DMSO were added to the cell medium to obtain the final concentrations (1:10 000, 1:20 000, 1:40 000). After 72 h of incubation at 37°C in 5% CO_2 atmosphere, cells were fixed (Methanol : Glacial acetic acid = 3 : 1), stained (Giemsa solution) and colonies were counted.

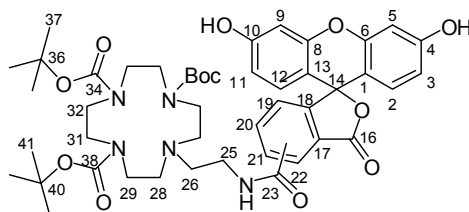
All tests were performed in quadruplicates and all experiments have been repeated two times. Solvent control was set to 100%. Results were plotted as bar graphs and are expressed as means \pm s.d. (range).

2.6.3 Synthesis



Scheme S1: Synthesis of carboxyfluorescein labelled Zn^{2+} -cyclen. a) 5/6-Carboxyfluorescein, TBTU, HOBT, DIPEA, DMF/DCM; b) $\text{HCl-Et}_2\text{O}$, DCM; c) strong basic anion exchange resin; d) ZnCl_2 , H_2O , pH 7-8

Following compounds were synthesized according to literature known procedures and determined to be consistent with analytical data derived from the corresponding published procedures: Zn^{2+} -Cyclen-pyrene **1**,²³ Bis- Zn^{2+} -bis-cyclen-pyrene **2**,²³ Bis- Zn^{2+} -bis-cyclen-carboxyfluorescein **4**,²¹ 3-Boc-cyclen,²⁸ Tri-tert-butyl 10-(2-aminoethyl)-1,4,7,10-tetraazacyclododecane-1,4,7-tricarboxylate **5**.²⁹



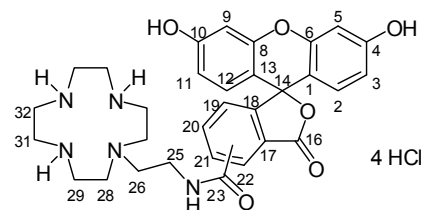
Regioisomeric Tri-tert-butyl 10-[2-(3',6'-dihydroxy-3-oxo-3H-spiroisobenzofuran-1,9'-xanthene]-5/6-ylcarboxamido)ethyl]-1,4,7,10-tetraazacyclododecane-1,4,7-tricarboxylate (6)

A regioisomeric mixture of 5/6-Carboxyfluorescein (0.10 g, 0.27 mmol) was filled in a nitrogen-flushed round bottom flask and dissolved in 5 ml of a 2:1-mixture of DCM and DMF. Then, DIPEA (0.15 g, 164 μ L, 1.20 mmol) and HOBt monohydrate (0.05 g, 0.32 mmol) were added and the mixture was cooled in an ice water bath to 0°C. After addition of TBTU (0.10 g, 0.32 mmol) and stirring for 30 min, Tri-tert-butyl 10-(2-aminoethyl)-1,4,7,10-tetraazacyclododecane-1,4,7-tricarboxylate (0.21 g, 0.40 mmol) was given to the reaction mixture in small portions while stirring.

In the following, the mixture was stirred for 2 h at 40°C then, the solvents were evaporated and finally, the crude product was purified by column chromatography on flash-silica-gel (CHCl_3 : MeOH = 11 : 1) to obtain the product as yellow, amorphous solid (0.19 g, 0.21 mmol, 81%).

MP: 214°C — **$^1\text{H-NMR}$** (400 MHz, CD_3OD , COSY, ROESY, HSQC, HMBC): δ [ppm] = 8.41 (s, 0.6H, 22a), 8.18 (dd, $^3J_{\text{H,H}} = 8.1$ Hz, $^4J_{\text{H,H}} = 1.5$ Hz, 0.6H, 20a), 8.11 (dd, $^3J_{\text{H,H}} = 8.0$ Hz, $^4J_{\text{H,H}} = 1.1$ Hz, 0.4H, 21b), 8.05 (d, $^3J_{\text{H,H}} = 8.0$ Hz, 0.4H, 22b), 7.59 (s, 0.4H, 19b), 7.28 (d, $^3J_{\text{H,H}} = 8.1$ Hz, 0.6H, 19a), 6.68 (d, $^3J_{\text{H,H}} = 2.2$ Hz, 2H, 2+12), 6.59 (dd, $^4J_{\text{H,H}} = 8.7$ Hz, $^5J_{\text{H,H}} = 4.8$ Hz, 2H, 5+9), 6.52 (dt, $^3J_{\text{H,H}} = 8.7$ Hz, $^4J_{\text{H,H}} = 1.7$ Hz, 2H, 3+11), 3.73-3.30 (m, 14H, 25a/b+29+31+32), 2.91 (t, $^3J_{\text{H,H}} = 6.6$ Hz, 1.2H, 26a), 2.82-2.64 (m, 4.8H, 26b+28), 1.49-1.37 (m, 27H, 37+42) — **$^{13}\text{C-NMR}$** (100 MHz, CD_3OD , COSY, ROESY, HSQC, HMBC): δ [ppm] = 170.5 (C_{quat} , 1C, 16a/b), 168.2 (C_{quat} , 0.6C, 23a), 168.0 (C_{quat} , 0.4C, 23b), 161.5 (C_{quat} , 2C, 4+10), 157.5 (C_{quat} , 2C, 38), 157.2 (C_{quat} , 1C, 34), 156.5 (C_{quat} , 0.6C, 18a), 154.6 (C_{quat} , 0.4C, 18b), 154.0 (C_{quat} , 2C, 6+8), 142.1 (C_{quat} , 0.4C, 20b), 137.7 (C_{quat} , 0.6C, 21a), 135.4 (+, 0.6C, 20a), 130.3 (+, 0.4C, 21b), 130.1 (+, 2C, 5+9), 128.7 (C_{quat} , 1C, 17a/b), 126.2 (+, 0.4C, 22b), 125.7 (+, 0.6C, 19a), 124.8 (+, 0.6C, 22a), 123.9 (+, 0.4C, 19b), 113.8 (+, 2C, 3+11), 110.7 (C_{quat} , 2C, 1+13), 103.6 (+, 2C, 2+12), 81.1 (C_{quat} , 2C, 40), 81.0 (C_{quat} , 1C, 36), 79.4 (C_{quat} , 1C, 14), 55.5 (–, 2C, 28), 50.4 (–, 1C, 26a/b), 48.6-48.2 (–, 6C, 29+31+32), 36.5 (–, 0.6C, 25a), 36.1 (–, 0.4C, 25b), 29.1 (+, 3C, 37), 28.8 (+, 6C, 41) —

IR (ATR) [cm^{-1}]: $\tilde{\nu}$ = 2976, 2935, 2830, 1760, 1657, 1611, 1456, 1417, 1365, 1246, 1155, 1109, 993, 849, 761, 664, 605 — **UV** (MeCN): λ (ϵ) = 454 (500), 480 (500) — **ESI-MS** ($\text{H}_2\text{O}/\text{MeOH} + 10 \text{ mmol/L NH}_4\text{Ac}$): m/z (%) = 874.5 (100) [MH^+], 774.4 (12) [$\text{MH}^+ - \text{Boc}$], 437.7 (32) [$\text{M} + 2\text{H}^+$], 287.6 (64) [$\text{M} + 2\text{H}^+ - 3\text{Boc}$] — **HR-MS** PI-LSI ($\text{MeOH}/\text{DCM}/\text{NBA}$): ($\text{C}_{46}\text{H}_{60}\text{N}_5\text{O}_{12}$) calc. 874.4238 [MH^+], found 874.4225

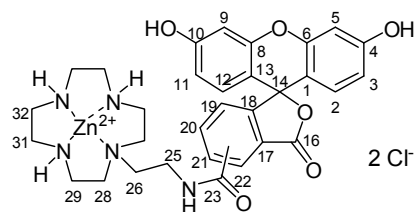


Regioisomeric *N*-[2-(1,4,7,10-Tetraazacyclododecan-1-yl)ethyl]-3',6'-dihydroxy-3-oxo-3H-spiro[isobenzofuran-1,9'-xanthene]-5/6-carboxamide tetrahydrochloride (7 · 4 HCl)

Compound **6** (0.12 g, 0.13 mmol) was dissolved in 2 mL of DCM and cooled to 0°C in an ice water bath, while stirring. After slow addition of HCl saturated Et_2O (2.65 mL), the mixture was allowed to reach room temperature and stirring continued a further 16 h, while a yellowish precipitate was formed. To get the desired product, the solvents were removed under reduced pressure yielding an orange amorphous solid (0.10 g, 0.13 mmol, quant.).

MP: 175°C (decomp.) — **$^1\text{H-NMR}$** (400 MHz, D_2O , DEPT135): δ [ppm] = 8.71-6.80 (m, 9H, aryl-CH), 3.73-2.75 (m, 21H, CH_2 + amide-NH) — **$^{13}\text{C-NMR}$** (100 MHz, D_2O , DEPT135): δ [ppm] = 132.0 (+, 2C, 5+9), 118.6 (+, 2C, 3+11), 102.5 (+, 2C, 2+12), 52.5 (−, 2C, 28), 48.1 (−, 1C, 26a), 47.9 (−, 1C, 26b), 44.2-41.5 (−, 6C, 29+31+32), 36.8 (−, 0.6C, 25a), 36.4 (−, 0.4C, 25b) *further signals could not be detected* — **ESI-MS** (MeCN/TFA): m/z (%) = 287.5 (100) [$\text{M} + 2\text{H}^+$], 574.2 (26) [MH^+]

A column was filled with a strong basic anion exchange resin (OH^- -form; 1.5 cm x 3 cm) and rinsed first with a mixture of water/MeOH (1 : 1) then followed by pure water. The above obtained compound was dissolved in a small amount of water and eluted from the column thus yielding quantitatively the salt-free ligand **7**.



Regioisomeric Zinc(II){N-[2-(1,4,7,10-tetraazacyclododecan-1-yl)ethyl]-3',6'-dihydroxy-3-oxo-3H-spiro[isobenzofuran-1,9'-xanthene]-5/6-carboxamid} dichloride (3)

The salt-free ligand **7** (92 mg, 0.16 mmol) was dissolved in 2 mL of warm water and Zinc(II)-chloride (23 mg, 0.17 mmol) was added. The mixture was heated up to reflux for 4 h while pH 7-8 was adjusted throughout the reaction by addition of aqueous LiOH solution (1 M) if necessary. In the following, the crude product was obtained after lyophilizing as an orange solid, which was then purified by precipitation from a mixture of 2-Propanol/MeOH with Et₂O. The resulting brown solid was pelletized by centrifugation, dissolved in water and freeze-dried again to gain the pure product (110 mg, 0.16 mmol, 99%) as an orange, amorphous solid.

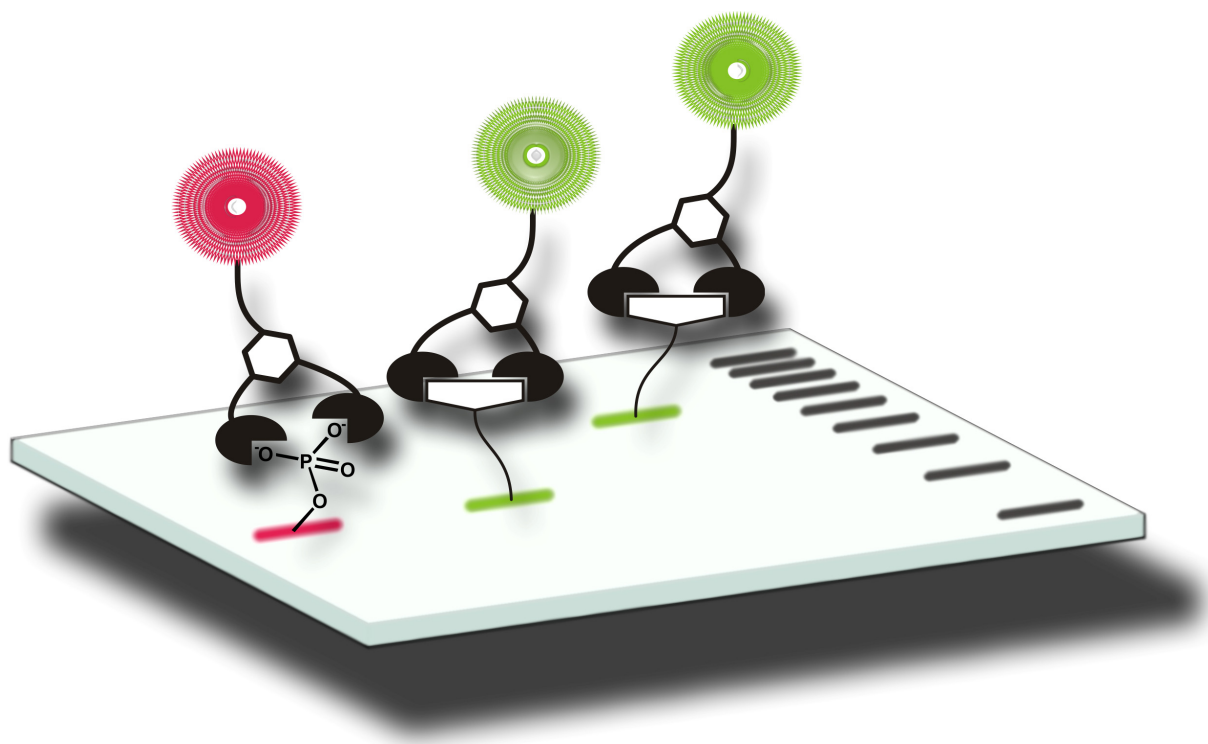
MP: 187°C — **¹H-NMR** (400 MHz, D₂O, HSQC): δ [ppm] = 8.43 (s, 0.6H, 22a), 8.20-7.98 (m, 1.4H, 20a+21b+22b), 7.59 (s, 0.4H, 19b), 7.28 (s, 0.6H, 19a), 6.88 (dd, ⁴J_{H,H} = 8.7 Hz, ⁵J_{H,H} = 4.8 Hz, 2H, 2+12), 6.76-6.47 (m, 4H, 3+5+9+11), 3.73-2.74 (m, 21H, CH₂ + amide-NH) — **¹³C-NMR** (100 MHz, D₂O, HSQC): δ [ppm] = 170.6 (C_{quat}, 1C, 16a/b), 168.5 (C_{quat}, 0.6C, 23a), 168.3 (C_{quat}, 0.4C, 23b), 165.0 (C_{quat}, 2C, 4+10), 163.9 (C_{quat}, 0.6C, 18a), 155.2 (C_{quat}, 0.4C, 18b), 154.7 (C_{quat}, 2C, 6+8), 145.5 (C_{quat}, 0.4C, 17a), 144.2 (C_{quat}, 0.6C, 17b), 138.1 (C_{quat}, 0.4C, 20b), 135.1 (C_{quat}, 0.6C, 21a), 132.2 (+, 0.6C, 20a), 130.7-130.5 (+, 2C, 2+12), 129.0 (+, 0.4C, 21b), 127.9 (+, 0.4C, 22b), 127.7 (+, 0.6C, 19a), 126.4 (+, 0.6C, 22a), 125.3 (+, 0.4C, 19b), 116.5-115.8 (+, 2C, 3+11), 112.5-112.1 (C_{quat}, 2C, 1+13), 102.8 (+, 2C, 5+9), 52.5-51.9 (–, 0.4C+0.6C, 25a/b), 48.1 (–, 0.6C, 26a), 47.9 (–, 0.4C, 26b), 46.7 (–, 2C, 28), 44.3-41.5 (–, 6C, 29+31+32), 36.8-36.5 (–, 0.4C+0.6C, 25'a/b) — **ESI-MS (M):** *m/z* (%) = 318.6 (100) [M²⁺], 636.2 (52) [M²⁺ – H⁺], 672.2 (35) [M²⁺ + Cl[–]]

2.7 REFERENCES

- ¹ C. Mühlhardt, *Der Experimentator - Molekularbiologie/Genomics*, Spektrum Akademischer Verlag, Heidelberg, 2006.
 - ² J. B. LePecq and C. Paoletti, *J. Mol. Biol.*, **1967**, 27, 87-106.
 - ³ M. J. Waring, *J. Mol. Biol.*, **1965**, 13, 269-282.
 - ⁴ G. Streisinger, Y. Okada, J. Emrich, J. Newton, A. Tsugita, E. Terzaghi and M. Inouye, *Cold Spring Harb. Symp. Quant. Biol.*, **1966**, 31, 77-84.
 - ⁵ L. S. Ripley, J. S. Dubins, J. G. deBoer, D. M. DeMarini, A. M. Bogerd and K. N. Kreuzer, *J. Mol. Biol.*, **1988**, 200, 665-680.
 - ⁶ W. A. Denny, P. M. Turner, G. J. Atwell, G. W. Rewcastle and L. R. Ferguson, *Mutat. Res.*, **1990**, 232, 233-241.
 - ⁷ J. McCann, E. Choi, E. Yamasaki and B. N. Ames, *Proc. Natl. Acad. Sci. USA*, **1975**, 72, 5135-5139.
 - ⁸ T. Ohta, S. Tokishita and H. Yamagata, *Mutat. Res.*, **2001**, 492, 91-97.
 - ⁹ O. Bensaude, *Trends Genet.*, **1988**, 4, 89-90.
 - ¹⁰ G. Lunn, *Trends Genet.*, **1990**, 6, 31-31.
 - ¹¹ G. Lunn and E. B. Sansone, *Anal. Biochem.*, **1987**, 162, 453-458.
 - ¹² As derived from substance data sheets provided by the manufacturers.
 - ¹³ E. Kikuta, T. Koike and E. Kimura, *J. Inorg. Biochem.*, **2000**, 79, 253-259.
 - ¹⁴ S. Aoki and E. Kimura, *J. Am. Chem. Soc.*, **2000**, 122, 4542-4548.
 - ¹⁵ S. Aoki and E. Kimura, *Rev. Mol. Biotechnol.*, **2002**, 90, 129-155.
 - ¹⁶ S. Aoki and E. Kimura, *Chem. Rev.*, **2004**, 104, 769-788.
 - ¹⁷ E. Kimura, S. Aoki, T. Koike and M. Shiro, *J. Am. Chem. Soc.*, **1997**, 119, 3068-3076.
 - ¹⁸ R. Reichenbach-Klinke and B. König, *Dalton Trans.*, **2002**, 121-130.
 - ¹⁹ M. Shionoya, E. Kimura and M. Shiro, *J. Am. Chem. Soc.*, **1993**, 115, 6730-6737.
 - ²⁰ B. Schulenberg, T. N. Goodman, R. Aggeler, R. A. Capaldi and W. F. Patton, *Electrophoresis*, **2004**, 25, 2526-2532.
 - ²¹ A. Riechers, F. Schmidt, S. Stadlbauer and B. König, *Bioconjug. Chem.*, **2009**, 20, 804-807.
-

- ²² A. Ojida, T. Kohira and I. Hamachi, *Chem. Lett.*, **2004**, 33, 1024-1025.
- ²³ F. Schmidt, S. Stadlbauer and B. König, *Dalton Trans.*, **2010**, *accepted*.
- ²⁴ Induction of excimer formation in homogeneous solution is restricted to UMP. ssDNA pentamer *pTACCG* does not lead to pyrene excimers if added to HEPES buffered solutions of **1**.
- ²⁵ T. Mosmann, *J. Immunol. Methods*, **1983**, 65, 55-63.
- ²⁶ J. Heilmann, M. R. Wasescha and T. J. Schmidt, *Bioorg. Med. Chem.*, **2001**, 9, 2189-2194.
- ²⁷ T. Lindl and G. Gstraunthaler, *Zell- und Gewebekultur - Von den Grundlagen zur Laborbank*, Spektrum Akademischer Verlag, Heidelberg, 2008.
- ²⁸ S. Brandes, C. Gros, F. Denat, P. Pullumbi and R. Guillard, *Bull. Soc. Chim. Fr.*, **1996**, 133, 65-73.
- ²⁹ R. Reichenbach-Klinke, M. Kruppa and B. König, *J. Am. Chem. Soc.*, **2002**, 124, 12999-13007.

3 DETECTION OF PROTEIN PHOSPHORYLATION ON SDS-PAGE USING PROBES WITH A PHOSPHATE-SENSITIVE EMISSION RESPONSE



Fluorescent probes for the detection of protein phosphorylation on SDS-PAGE are presented. The probes were designed using a dinuclear metal-chelate phosphate recognition unit and an environment-sensitive fluorophore. The specificity of the probes is determined by their binding site selectivity towards phosphate ions and the emission wavelength shift induced by the change in the electrostatic environment of the fluorophore upon binding to a phosphorylated amino acid residue. The staining is fully reversible due to the non-covalent binding of the probe. Gel bands with less than 100 μg of phosphorylated α -Casein are detectable with the new probes on a normal UV-table without specialized equipment like a laser-based gel scanner or a cooled camera detector.

3.1 INTRODUCTION

Staining of SDS gels is a standard technique in molecular biology. While silver- and Coomassie-staining are widely used for total protein staining, a number of stains selective for certain functional groups have emerged. Glycosylation,¹⁻² His-tags³ and phosphorylation⁴⁻⁵ are typical protein modifications targeted by selective gel stains reported so far. With respect to its biological importance, phosphorylation⁶⁻⁷ is widely regarded as the most significant post-translational modification. Phosphorylation plays an important part in signaling pathways and it is estimated that 30% of the entire proteome becomes phosphorylated at some point.⁸ While there are phospho-specific antibodies available,⁹⁻¹⁰ they require blotting of the proteins onto a polyvinylidene difluoride (PVDF) or nitrocellulose membrane and may also be specific for additional epitopes in proximity to the phosphorylation site. Alternatively, ³²P-labeling of the proteins provides a very sensitive tool for detection of phosphorylation,¹¹⁻¹² however, the handling and disposal of radioactive material are costly, potentially hazardous and increasingly regulated. When staining for sub-stoichiometric features such as phosphorylation, fluorescence detection is the method of choice due to its inherent sensitivity. The reported¹³ and commercially available⁴⁻⁵ fluorescent phospho-specific stains gain their sensitivity from their binding site specificity. While other fluorescent probes for phosphorylated amino acids have been reported,¹⁴ their selectivity has only been demonstrated for peptides without other metal-chelating amino acids like Histidine, Tryptophan or Cysteine.

Herein, we report two novel phospho-specific gel stains based on the interaction of a metal-chelate binding site and a covalently attached fluorophore. We have previously described the binding of a Bis-zinc(II)cyclen triazine to phosphorylated Serine and Histidine.¹⁵ Since these artificial receptors showed high affinity under physiological conditions, we set about using this interaction in molecular biology. Based on these findings and a previously reported mono-zinc(II)cyclen coumarin receptor,¹⁶ which changes its emission wavelength when bound to inorganic phosphate in solution, we designed fluorescently labeled bis-zinc(II)cyclen triazine complexes for staining of phosphorylated proteins in SDS gels. Bis-zinc(II)cyclen triazine was found to have a higher affinity towards phosphate than mononuclear zinc(II)cyclen complexes and was therefore used as the recognition moiety. As fluorophores, we selected the widely employed Carboxyfluorescein and 7-(Diethylamino) coumarin since a similar fluorophore has shown large solvatochromic emission shifts,¹⁷ which we associate to its sensitivity to the environment.¹⁸ The resulting

probes **1** and **2** are depicted in Figure 1 while the emission response concept is shown in Scheme 1.

3.2 RESULTS & DISCUSSION

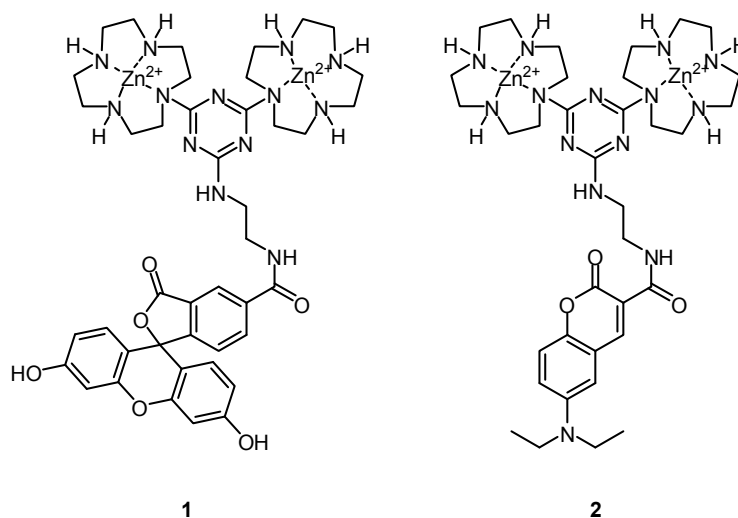
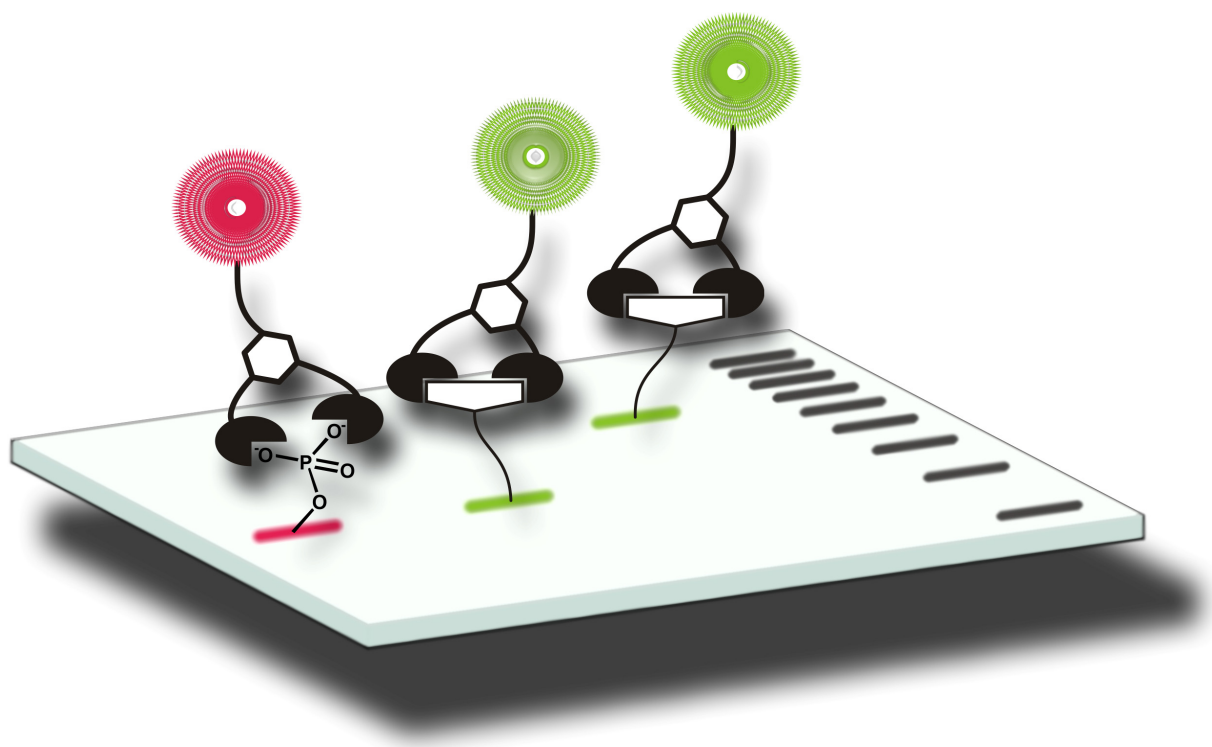


Figure 1: Probes 1 and 2 used for staining of phosphoproteins. Counterions are not shown.

To evaluate the phospho-staining selectivity and sensitivity of our probes, a dilution series of phosphorylated bovine α -Casein was electrophoretically resolved from the non-phosphorylated protein BSA. In addition, a sample of α -Casein was dephosphorylated using λ -PPase and used as a control to ensure the emission response would not depend on the amino acid composition of the protein. After fixation, the gels were stained and destained when necessary until little or no background was visible.



Scheme 1: Probes 1 and 2 discriminate phosphorylated from nonphosphorylated proteins on SDS gels via emission intensity and wavelength shift, respectively.

Probe **1** showed a distinct emission in the bands of phosphorylated α -Casein, whereas the bands of dephosphorylated α -Casein and BSA are barely visible (Figure 2). Bis-zinc(II)cyclen triazine complexes coordinate phosphate groups strongly, but we also expect an affinity of the probe to non-phosphorylated proteins due to the coordination of Histidine by the bis-zinc(II)cyclen triazine^{15, 19} or further unspecific interactions. However, these interactions do not interfere with the specific detection of phosphorylation: The emission of the probe is quenched, when bound to non-phosphorylated amino acid residues and the emission remains, when bound to phosphorylated amino acid residues. Similar emission quenching effects have been previously reported for the interaction of Riboflavin with a zinc(II)imidazole complex²⁰ and for zinc(II)porphyrin with Histidine.²¹ To prove that the observed effects originate from the coordination of the bis-zinc(II)cyclen triazine complex and not from the binding of the fluorophore itself, a control gel was prepared and treated with Carboxyfluorescein. No staining could be observed in this experiment.

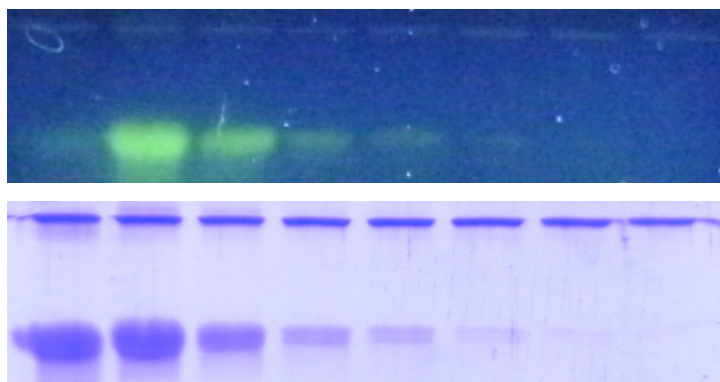


Figure 2: Gel stained with probe 1. Each lane contains 1 μ g BSA (66 kDa). From left to right: lane 1: 1 μ g α -Casein (23 kDa) dephosphorylated, lanes 2-8: 1 μ g, 500 ng, 250 ng, 125 ng, 62 ng, 31 ng, 15 ng α -Casein. Top image was taken on a UV table ($\lambda_{\text{ex}} = 316$ nm), lower image shows CBB R-250 total protein restain.

When bound to phosphorylated α -Casein, probe **2** showed a strong redshift in the emission compared to unphosphorylated α -Casein and BSA (Figure 3). We attribute this spectral change to the different electronic environments when the probe molecule is either unspecifically interacting with non-phosphorylated amino acid residues, such as Histidine (unphosphorylated α -Casein and BSA) or is coordinating a negatively charged phosphorylated amino acid residue (phosphorylated α -Casein). These findings are in agreement with the reported redshift in emission of a mono-zinc(II)cyclen coumarin complex upon coordination to inorganic phosphate ions.¹⁶ To quantify this change in emission, fluorescence spectra of the gel bands were obtained using a photonic multi-channel analyzer equipped with a fiber optic (Figure 4). As with probe **1**, a control gel was treated with the fluorophore itself, and again no staining was observed.

With both probes, the dilution series proved that 62 ng of phosphorylated α -Casein are still detectable on a normal UV-table by the unaided eye (which was protected from UV light) while imaging was performed with common digital cameras. Hence, even without the use of specialized equipment like laser-illuminated gel scanners or cooled camera detectors as described in the protocols of commercially available phosphoprotein gel stains our probes reach similar limits of detection.

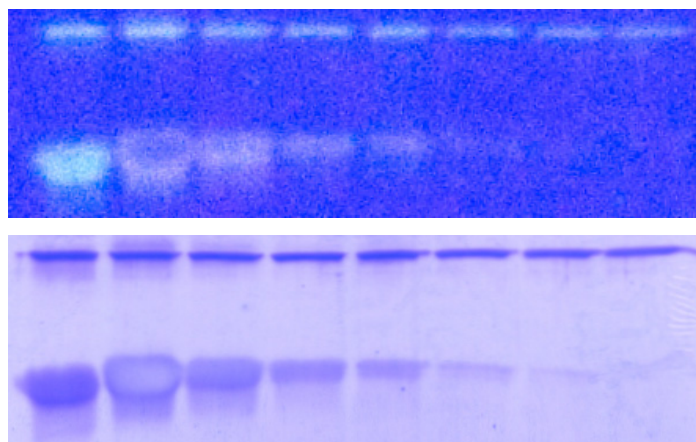


Figure 3: Gel stained with probe 2. Each lane contains 1 μg BSA (66 kDa). From left to right: lane 1: 1 μg α -Casein (23 kDa) dephosphorylated, lanes 2-8: 1 μg , 500 ng, 250 ng, 125 ng, 62 ng, 31 ng, 15 ng α -Casein. Top image was taken on a UV table ($\lambda_{\text{ex}} = 316 \text{ nm}$), lower image shows CBB R-250 total protein restain.

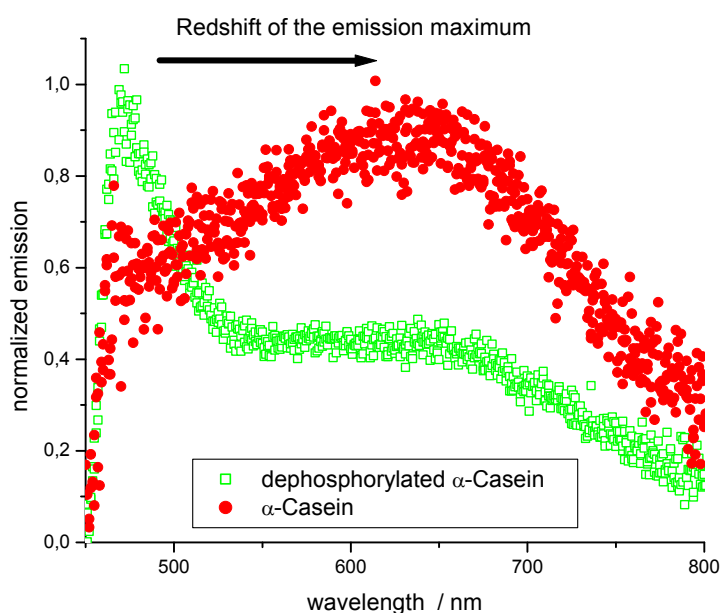


Figure 4: Normalized emission spectra of gel bands stained with probe 2 acquired through a 455 nm longpass filter ($\lambda_{\text{ex}} = 316 \text{ nm}$). BSA band showed the same spectrum as dephosphorylated α -Casein (data not shown).

3.3 CONCLUSIONS

We have demonstrated the application of two new non-covalent, reversible and fluorescent SDS-PAGE probes capable of indicating protein phosphorylation. The probes show different fluorescence responses discriminating phosphorylated from non-phosphorylated proteins. While probe **1** signals binding to a phosphorylated protein by a significant increase of emission intensity, probe **2** is the first phosphoprotein gel stain to change its emission spectrum upon binding to a phosphorylated protein. The probes achieve their selectivity through a combination of the specificity of the dinuclear metal chelate binding site towards phosphate oxoanions and a modulation of the chromophore emission due to the proximity of the phosphorylated amino acid. The environment-sensitive fluorophore allows a clear distinction between phosphorylated and non-phosphorylated proteins on SDS-PAGE and allow the detection of 62 ng of phosphorylated α -Casein on a normal UV-table. Evaluations of other metal chelate fluorophore conjugates and applications of the existing probes to monitor signaling pathways are currently under way.

3.4 ACKNOWLEDGEMENTS

We thank Lorenz Fischer for help with the Hamamatsu PMA-11 analyzer and Andreas Grauer for help with the imaging. We are grateful to Jennifer Schmidt, Silke Kuphal and Anja-Katrin Bosserhoff for valuable discussions.

3.5 MATERIALS & METHODS

3.5.1 General

All reactions were performed under an inert atmosphere of N₂ using standard Schlenk techniques if not otherwise stated. A Varian Cary BIO 50 UV/VIS/NIR Spectrometer was used. A 1 cm quartz cell was purchased from Hellma and Uvasol solvents from Merck or Baker. Absorption and emission maxima are given in nm, molar absorptivities (ϵ) are given in M⁻¹ cm⁻¹. IR spectra were recorded on a Bio-Rad FT-IR FTS 155 and a Bio-Rad FTS 2000 MX FT-IR using a Specac Golden Gate Mk II ATR accessory where stated. NMR spectrometers used were: Bruker Avance 600 (¹H: 600.1 MHz, ¹³C: 150.1 MHz, T = 300 K), Bruker Avance 400 (¹H: 400.1 MHz, ¹³C: 100.6 MHz, T = 300 K) and Bruker Avance 300 (¹H: 300.1 MHz, ¹³C: 75.5 MHz, T = 300 K). The chemical shifts are reported in δ [ppm] relative to internal standards (solvent residual peak). The spectra were analyzed by first order, the coupling constants are given in Hertz [Hz]. Characterization of the signals: s = singlet, d = doublet, t = triplet, q = quartet, m = multiplet, bs = broad singlet, dd = double doublet. Integration is determined as the relative number of atoms. Assignment of signals in ¹³C-spectra was determined with DEPT-technique (pulse angle: 135 °) and given as (+) for CH₃ or CH, (–) for CH₂ and (C_{quat}) for quaternary C. Error of reported values: chemical shift: 0.01 ppm for ¹H-NMR, 0.1 ppm for ¹³C-NMR and 0.1 Hz for coupling constants. The solvent used is reported for each spectrum. Mass spectra were recorded on Finnigan MAT TSQ 7000 (ESI). Melting Points were determined on a Büchi SMP-20 melting point apparatus and are uncorrected. TLC analyses were performed on silica gel 60 F-254 with a 0.2 mm layer thickness. Detection was via UV light at 254 nm / 366 nm or by staining with Ninhydrin in EtOH. For preparative column-chromatography, Merck Geduran SI 60 silica gel was used. Commercially available solvents of standard quality were used. Unless otherwise stated, purification and drying was done according to accepted general procedures. Compounds **3** and **5** were synthesized according to literature known procedures.²²⁻²³

Dephosphorylation by λ -PPase treatment. Bovine α -Casein (40 μ g, purchased from Sigma-Aldrich) was treated with 400 U of λ -PPase (purchased from New England Biolabs) in Tris-HCl (50 mM), NaCl (100 mM), Dithiothreitol (2 mM), MnCl₂ (2 mM), EGTA (0.1 mM), 0.01% Brij 35, pH 7.5 at 30°C for 6 h.

SDS-PAGE. Proteins were resolved on mini gels under denaturing and reducing Laemmli conditions on a PeqLab 45-1010-i apparatus. The gels consisted of a 4% Acrylamide (w/v), 120 mM Tris-HCl (pH 6.8), 0.1% SDS (w/v) stacking gel and a 15% Acrylamide (w/v), 375 mM Tris-HCl (pH 8.8), 0.1% SDS (w/v) running gel. A 25 mM Tris, 192 mM Glycine, 0.1% SDS (w/v) running buffer (pH 8.3) was used. Protein samples were heated to 70°C for 10 min with reducing and denaturing RotiLoad 1 sample buffer (purchased from Carl Roth, Germany) before being loaded onto the gel. The gels were run at 150 V until the proteins entered the running gel, then the voltage was increased to 250 V. Water cooling was used during the entire run. Fixation was accomplished by treating the gels with 50% MeOH / 10% AcOH twice, for 30 min and overnight, respectively.

Staining and imaging. The gels were soaked in deionized water (4 x 10 min) before being treated with a solution of probe **1** or **2** in deionized water for 1 h with a probe concentration of 10^{-7} M. We found destaining was not strictly necessary at this concentration, however, when the probes were used at higher concentrations, the gels could be destained by washing with deionized water until a nonfluorescent background was obtained. Due to their non-covalent binding mode,²⁴ the probes could be completely removed by repeated washing of the gel with water. Conveniently, removal of the probes was not necessary for Coomassie restaining.

The gels were wrapped in cling film to prevent them from drying out and placed on a PeqLab Superbright UV table ($\lambda_{\text{ex}} = 316$ nm). Images were taken using either a Pentax K10D or a Traveler DC 8500. Emission spectra of individual protein bands were obtained using the same UV table and a Hamamatsu PMA-11 photonic multi-channel analyzer. Data were acquired using the supplied PMA Optic software. A 455 nm longpass filter was placed on top of the gel to prevent the UV light saturating the detector. Longpass filters with a shorter cutoff proved unsuitable as they showed a strong fluorescence when subjected to the UV light.

After fluorescence imaging, a restain for total protein was accomplished with 0.1% Coomassie R-250, 50% MeOH, 10% AcOH for 1 h. Destaining was accomplished in 7% AcOH, 10% MeOH over night. The gels were again wrapped in cling film and scanned using an office scanner.

3.5.2 Synthesis of Probes 1 and 2

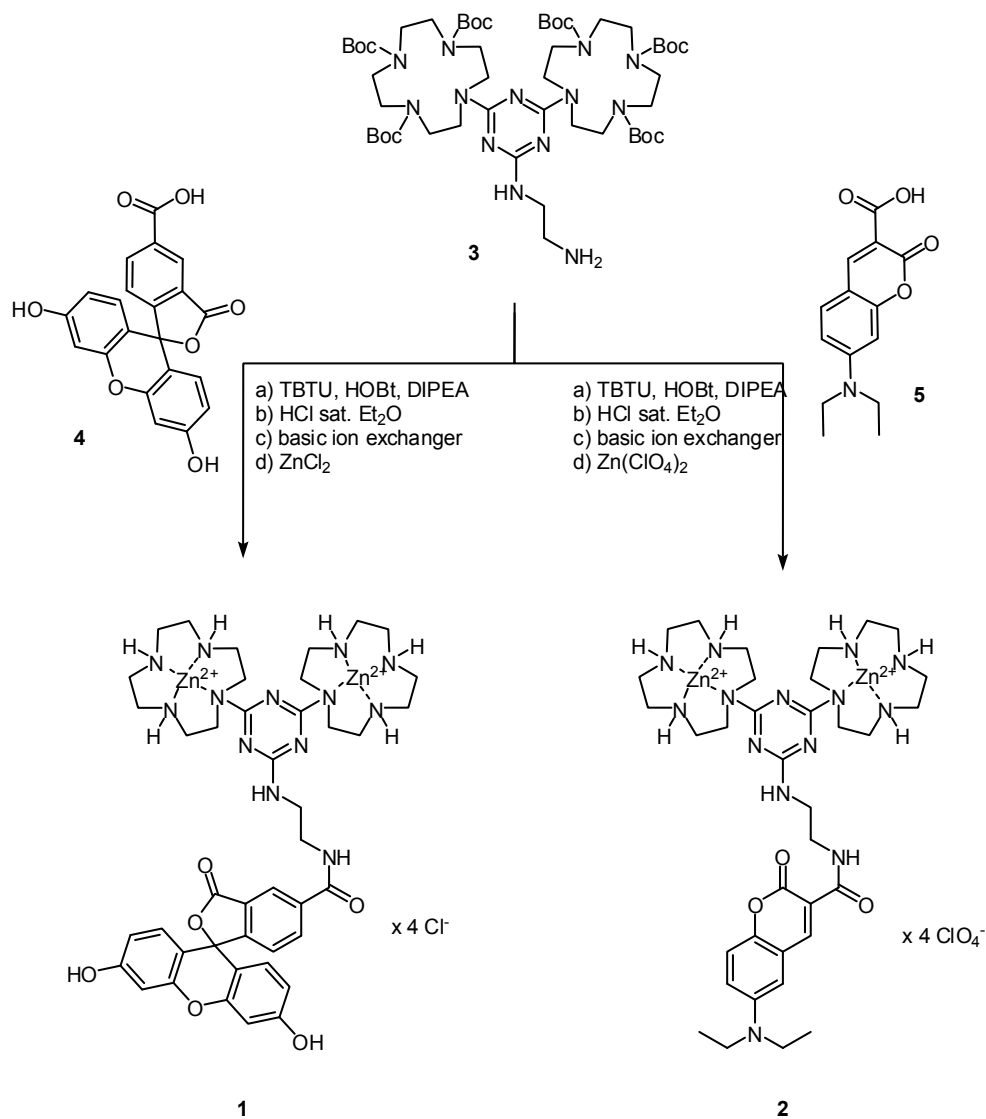
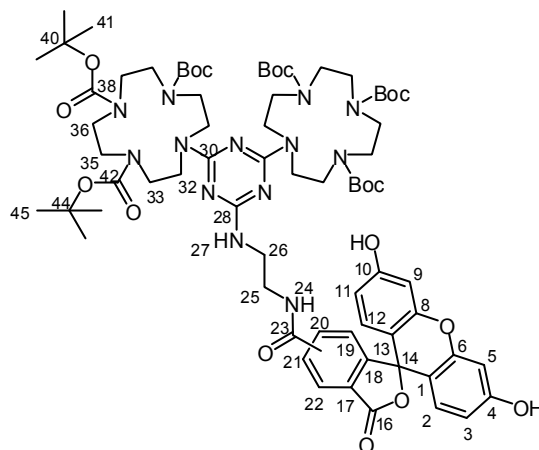


Figure S1: Preparation of probes 1 and 2

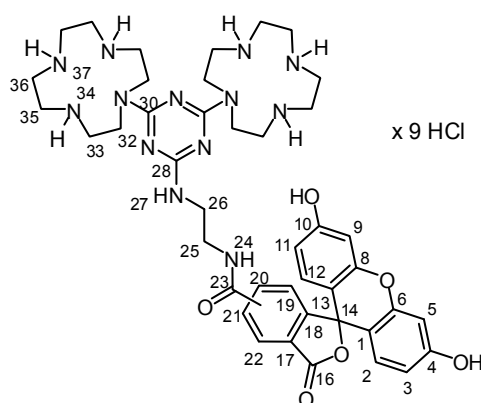


Regioisomeric 1,4,7-Tri-tert-butyl 10,10'-[6-[2-(3',6'-dihydroxy-3-oxo-3H-spiro[isobenzofuran-1,9'-xanthene]-5/6-ylcarboxamido)ethylamino]-1,3,5-triazine-2,4-diyl]bis(1,4,7,10-tetraazacyclododecane-1,4,7-tricarboxylate) (6)

In a nitrogen flushed round bottom flask, regioisomeric 5/6-Carboxyfluorescein (0.15 g, 0.40 mmol) was dissolved in 10 mL of a mixture of DCM and DMF (2:1), then DIPEA (0.17 g, 180 μ L, 1.32 mmol) and HOBt monohydrate (0.07 g, 0.48 mmol) were added. While stirring, the mixture was cooled to 0°C in an ice water bath to add TBTU (0.15 g, 0.48 mmol). After 30 min, 1,4,7-Tri-tert-butyl 10,10'-[6-(2-aminoethylamino)-1,3,5-triazine-2,4-diyl]bis(1,4,7,10-tetraazacyclo-dodecane-1,4,7-tricarboxylate) **3** (0.47 g, 0.44 mmol) was added in portions and the reaction mixture was heated to 40°C for 2 h. Subsequently, the solvents were evaporated and the crude product was purified by column chromatography (CHCl_3 : MeOH = 15 : 1) on flash-silica-gel yielding compound **6** as an orange amorphous solid (0.34 g, 0.23 mmol, 59%).

MP: 207°C — **$^1\text{H-NMR}$** (600 MHz, MeOD, COSY, ROESY, HSQC, HMBC): δ [ppm] = 8.36 (s, 0.7H, 22a), 8.13 (d, $^3J_{\text{H,H}} = 7.9$ Hz, 0.7H, 20a), 8.07 (d, $^3J_{\text{H,H}} = 8.1$ Hz, 0.3H, 21b), 8.03 (d, $^3J_{\text{H,H}} = 8.0$ Hz, 0.3H, 22b), 7.61 (s, 0.3H, 19b), 7.24 (d, $^3J_{\text{H,H}} = 8.0$ Hz, 0.7H, 19a), 6.68 (dd, $^3J_{\text{H,H}} = 1.8$ Hz, $^5J_{\text{H,H}} = 1.8$ Hz, 2H, 2+12), 6.57 (dd, $^4J_{\text{H,H}} = 8.7$ Hz, $^5J_{\text{H,H}} = 8.7$ Hz, 2H, 5+9), 6.52 (dd, $^3J_{\text{H,H}} = 8.7$ Hz, $^4J_{\text{H,H}} = 2.3$ Hz, 2H, 3+19), 3.99-3.20 (m, 36H, 25a/b, 26a/b, 32+33+35+36), 1.45-1.37 (m, 54H, 41+45) — **$^{13}\text{C-NMR}$** (150 MHz, MeOD, COSY, ROESY, HSQC, HMBC): δ [ppm] = 170.4 ($\text{C}_{\text{quat.}}$, 0.3C, 16b), 170.3 ($\text{C}_{\text{quat.}}$, 0.7C, 16a), 168.5 ($\text{C}_{\text{quat.}}$, 0.7C, 23a), 168.3 ($\text{C}_{\text{quat.}}$, 0.3C, 23b), 167.8 ($\text{C}_{\text{quat.}}$, 2C, 30), 167.5 ($\text{C}_{\text{quat.}}$, 0.7C, 28a), 167.3 ($\text{C}_{\text{quat.}}$, 0.3C, 28b), 161.3 ($\text{C}_{\text{quat.}}$, 2C, 4+10), 158.0 ($\text{C}_{\text{quat.}}$, 6C, 38+42), 156.7 ($\text{C}_{\text{quat.}}$, 0.7C, 18a), 154.4 ($\text{C}_{\text{quat.}}$, 0.3C, 18b), 153.9 ($\text{C}_{\text{quat.}}$, 2C, 6+8), 142.4 ($\text{C}_{\text{quat.}}$, 0.3C, 20b), 138.0 ($\text{C}_{\text{quat.}}$, 0.7C, 21a), 135.5 (+, 0.7C, 20a), 130.2 (+, 0.3C, 21b), 130.1 (+, 2C, 5+9), 128.5 ($\text{C}_{\text{quat.}}$,

1C, 17a/b), 126.1 (+, 0.3C, 22b), 125.6 (+, 0.7C, 19a), 124.8 (+, 0.7C, 22a), 124.0 (+, 0.3C, 19b), 113.7 (+, 2C, 3+11), 110.8 (C_{quat.}, 2C, 1+13), 103.7 (+, 2C, 2+12), 81.5 (C_{quat.}, 2C, 38), 81.4 (C_{quat.}, 4C, 42), 79.4 (C_{quat.}, 1C, 14), 51.4 (–, 16C, 32+33+35+36), 41.7 (–, 0.7C, 25a), 41.5 (–, 0.3C, 25b), 40.9 (–, 0.7C, 26a), 40.8 (–, 0.3C, 26b), 29.9 (+, 6C, 41), 28.8 (+, 12C, 45) — **IR** (ATR) [cm^{–1}]: $\tilde{\nu}$ = 3318, 2971, 2935, 1766, 1689, 1665, 1539, 1466, 1410, 1365, 1247, 1157, 1024, 852, 811, 751, 665 — **UV** (MeCN): λ (ϵ) = 454 (2200), 481 (1900) — **ESI-MS** (DCM/MeOH + 10 mmol/L NH₄Ac): m/z (%) = 720.0 (100) [M + 2H⁺], 1439.0 (5) [MH⁺]

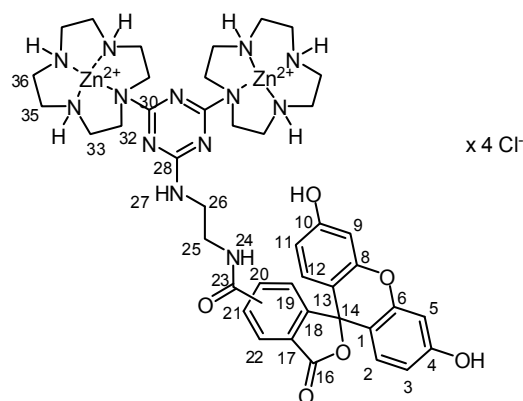


Regioisomeric *N*-{2-[4,6-di(1,4,7,10-Tetraazacyclododecan-1-yl)-1,3,5-triazin-2-ylamino]ethyl}-3',6'-dihydroxy-3-oxo-3*H*-spiro[isobenzofuran-1,9'-xanthene]-5/6-carboxamide nonahydrochloride (**7**)

Compound **6** (80 mg, 0.05 mmol) was dissolved in as little DCM as possible and cooled to 0°C before HCl saturated Et₂O (1.06 mL) was added slowly to this solution. Stirring was continued for 16 h while the reaction mixture was allowed to reach room temperature. Formation of a yellowish precipitate was observed. The desired product was obtained by evaporation of the solvent in vacuum as a red amorphous solid (50 mg, 0.05 mmol, quant.), which was deprotonated by ion exchange column on weakly basic anion exchanger resin.

¹H-NMR (600 MHz, D₂O, COSY, HSQC, HMBC): δ [ppm] = 8.43 (s, 2H, 24), 7.97 (s, 0.6H, 22a), 7.93-7.86 (d, $^3J_{H,H}$ = 7.4 Hz, 0.4H, 21b), 7.85-7.79 (d, $^3J_{H,H}$ = 7.4 Hz, 0.4H, 22b), 7.74 (bs, 0.6H, 20a), 7.44 (s, 0.4H, 19b), 7.02 (bs, 0.6H, 19a), 6.99-6.70 (m, 2H, 2+12), 6.61-6.41 (m, 2H, 3+11), 6.41-6.13 (m, 2H, 5+9), 3.87-3.39 (m, 12H, 25+26+36), 3.27-2.88 (m, 24H, 32+33+35) — **¹³C-NMR** (150 MHz, D₂O, COSY, HSQC, HMBC): δ [ppm] = 179.9 (C_{quat.},

2C, 30), 174.2 (C_{quat.}, 0.4C, 16b), 173.2 (C_{quat.}, 0.6C, 16a), 171.5 (C_{quat.}, 1C, 28), 170.1 (C_{quat.}, 0.4C, 23b), 169.5 (C_{quat.}, 0.6C, 23a), 167.2-166.3 (C_{quat.}, 2C, 4+10), 158.6-158.4 (C_{quat.}, 2C, 6+8), 157.9 (C_{quat.}, 0.6C, 18a), 157.2 (C_{quat.}, 0.4C, 18b), 143.7 (C_{quat.}, 0.4C, 20b), 140.7 (C_{quat.}, 0.6C, 21a), 135.6 (C_{quat.}, 0.4C, 17b), 135.2 (C_{quat.}, 0.6C, 17a), 131.9-131.5 (+, 2C, 2+12), 130.7 (+, 0.6C, 19a), 129.5 (+, 0.4C, 22b), 129.2 (+, 0.4C, 21b), 128.7 (+, 0.4C, 19b), 128.4 (+, 1.2C, 20a+22a), 123.3 (+, 2C, 3+11), 104.4 (+, 2C, 5+9), 46.5-45.2 (–, 12C, 33+35+36), 43.9 (–, 4C, 32), 40.8-40.6 (–, 1C, 25a/b), 39.9 (–, 1C, 26) — **ESI-MS** (H₂O/MeOH + 0.10% TFA): *m/z* (%) = 280.1 (100) [M + 3H⁺]³⁺, 419.8 (63) [M + 2H⁺]²⁺, 838.5 (4) [MH⁺], 874.4 (3) [MH⁺ + HCl]

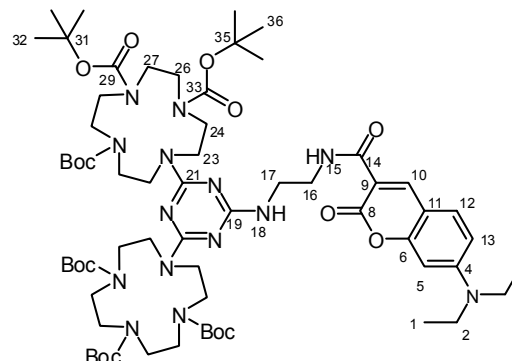


Bis-Zinc(II)(N-{2-[4,6-di(1,4,7,10-tetraazaacyclododecan-1-yl)-1,3,5-triazin-2-ylamino]ethyl}-3',6'-dihydroxy-3-oxo-3H-spiro[isobenzofuran-1,9'-xanthene]-5/6-carboxamide) tetrachloride (1)

Deprotonated compound **7** (48 mg, 0.06 mmol) was dissolved in 2 mL of warm water, then Zinc(II)chloride (16 mg, 0.12 mmol) was added. After pH-adjustment to 7-8 with saturated NaHCO_{3, aq.}, the mixture was heated to 100°C for 2 h while stirring. The desired product was isolated by lyophilisation of the reaction mixture as a dark orange, amorphous solid (48 mg, 0.04 mmol, 75%).

¹H-NMR (600 MHz, D₂O, COSY, HSQC, HMBC): δ [ppm] = 8.14-6.06 (m, 9H, *aryl*), 4.25-2.62 (m, 35H, *amide-NH+CH₂*) — **¹³C-NMR** (150 MHz, D₂O, COSY, HSQC, HMBC): δ [ppm] = 174.1-103.2 (C_{quat.} & –, 24C, 1-23+28+30), 46.3-38.7 (–, 18C, 25+26+32-36) — **UV** (40 mM TRIS-buffer, 10 mM MgCl₂, 2 mM DTE, pH 7.6): λ (ε) = 321 (6400), 497 (56300) — **Fluorescence** (40 mM TRIS-buffer, 10 mM MgCl₂, 2 mM DTE, pH 7.6): exc.

494 nm, emission max. 526 nm — **ESI-MS** ($\text{H}_2\text{O}/\text{MeOH} + 10 \text{ mmol/L } \text{NH}_4\text{Ac}$): m/z (%) = 481.8 (37) $[\text{M}^{4+} - 2\text{H}^+]^{2+}$, 511.4 (70) $[\text{M}^{4+} - \text{H}^+ + \text{CH}_3\text{COO}^-]^{2+}$

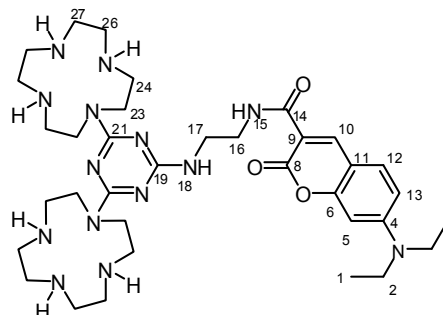


7-Diethylamino-2-oxo-2H-chromene-3-carboxylic acid {2-[4,6-bis-(1,4,7,10-tetraazacyclododec-1-yl)-[1,3,5]triazin-2-yl]-ethyl}-1,4,7-tricarboxylic acid tri-tert-butyl ester (8)

7-Diethylamino-2-oxo-2H-chromene-3-carboxylic acid (150 mg, 0.56 mmol), DIPEA (386 μL , 2.24 mmol), TBTU (203 mg, 0.63 mmol), and HOBt monohydrate (97 mg, 0.63 mmol) were dissolved under nitrogen atmosphere in dry DMF (4 mL) under ice cooling and stirred for 1 h. Subsequently amine **3** (635 mg, 0.59 mmol) dissolved in DMF (2 mL) was added drop wise. The reaction was allowed to warm to room temperature and was stirred 30 min at room temperature and 3 h at 40°C. The reaction progress was monitored by TLC ($\text{CHCl}_3 : \text{MeOH} = 97.5 : 2.5$). After completion of the reaction the solvent was removed and the crude product was purified by flash column chromatography on flash silica gel ($\text{CHCl}_3 : \text{MeOH} = 97.5 : 2.5$; $R_f \text{ EtOAc} = 0.60$) yielding compound **8** (684 mg, 0.52 mmol, 93%) as a yellow solid.

MP: 147°C — **$^1\text{H-NMR}$** (400 MHz, CDCl_3 , COSY, HSQC, HMBC): δ [ppm] = 8.90 (bs, 1H, 15), 8.65 (s, 1H, 10), 7.39 (d, $^3J_{\text{H,H}} = 8.9 \text{ Hz}$, 1H, 5), 6.82 (dd, $^3J_{\text{H,H}} = 8.9 \text{ Hz}$, $^4J_{\text{H,H}} = 2.4 \text{ Hz}$, 1H, 13), 6.46 (d, $^4J_{\text{H,H}} = 2.3 \text{ Hz}$, 1H, 12), 5.02 (bs, 1H, 18), 3.42 (q, $^3J_{\text{H,H}} = 7.1 \text{ Hz}$, 4H, 2), 3.76-3.11 (m, 36H, 16+17+23+24+26+27), 1.40 (s, 18H, 32), 1.42 (s, 36H, 36), 1.21 (t, $^3J_{\text{H,H}} = 7.1 \text{ Hz}$, 6H, 1) — **$^{13}\text{C-NMR}$** (100 MHz, CDCl_3 , COSY, HSQC, HMBC): δ [ppm] = 165.8 (C_{quat} , 3C, 19+21), 163.7 (C_{quat} , 1C, 14), 162.5 (C_{quat} , 1C, 8), 157.6 (C_{quat} , 1C, 6), 156.2 (C_{quat} , 6C, 29+33), 152.5 (C_{quat} , 1C, 4), 148.0 (+, 1C, 10), 131.1 (+, 1C, 5), 110.1 (C_{quat} , 1C, 9), 109.9 (+, 1C, 13), 108.3 (C_{quat} , 1C, 11), 96.5 (+, 1C, 12), 79.6 (C_{quat} , 6C, 31+35), 50.2 (–, 16C, 23+24+26+27), 45.0 (–, 2C, 2), 40.8 (–, 1C, 17), 39.6 (–, 1C, 16), 28.4, 28.5 (+, 18C, 32+36), 12.4 (+, 2C, 1) — **IR** (ATR) [cm^{-1}]: $\tilde{\nu} = 2974, 2933, 1686, 1619, 1584, 1532, 1512, 1466, 1409, 1364, 1246, 1158, 971, 751$ — **UV** (CHCl_3): λ (ϵ) = 419 (41000) — **ESI-MS**

(DCM/MeOH + 10 mmol/L NH₄Ac): m/z (%) = 362.2 (17) $[M + 2H^+ - 5Boc]^{2+}$, 412.3 (34) $[M + 2H^+ - 4Boc]^{2+}$, 462.3 (55) $[M + 2H^+ - 3Boc]^{2+}$, 512.4 (51) $[M + 2H^+ - 2Boc]^{2+}$, 562.5 (25) $[M + 2H^+ - Boc]^{2+}$, 612.5 (12) $[M + 2H^+]^{2+}$, 1324.0 (100) $[MH^+]$



7-Diethylamino-2-oxo-2H-chromene-3-carboxylic acid {2-[4,6-bis-(1,4,7,10-tetraaza-cyclododec-1-yl)-[1,3,5]triazin-2-ylamino]-ethyl}-amide (9)

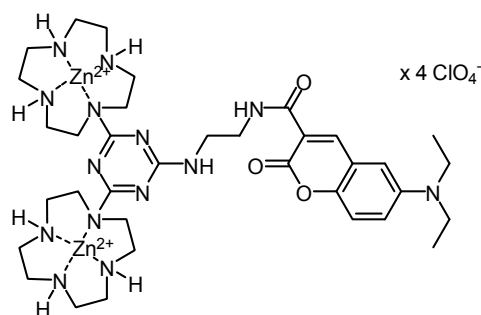
Compound **8** (275 mg, 0.21 mmol) was dissolved in DCM (4 mL) and cooled to 0°C. Subsequently, 4.5 mL of HCl saturated Et₂O were added. The solution was stirred 15 min at 0°C and an additional 20 h at room temperature. The solvent was removed *in vacuo*, the residue was redissolved in water and extracted with DCM (3x). Subsequently the combined organic layers were dried over MgSO₄ and the solvent was evaporated yielding the protonated hydrochloride of compound **9** as a yellow solid in quantitative yield (213 mg, 0.21 mmol).

¹H-NMR (400 MHz, CDCl₃, COSY, HSQC, HMBC): δ [ppm] = 8.72 (s, 1H, 10), 7.96 (d, $^3J_{H,H}$ = 8.4 Hz, 1H, 5), 7.56-7.37 (m, 2H, 12+13), 3.89 (bs, 8H, cyclen-CH₂), 3.75 (t, $^3J_{H,H}$ = 5.6 Hz, 2H, 17), 3.57-3.72 (m, 6 H, 2+16), 3.54-2.97 (m, 24H, cyclen-CH₂), 1.13 (t, $^3J_{H,H}$ = 7.3 Hz, 6H, 1) — **¹³C-NMR** (100 MHz, CDCl₃, COSY, HSQC, HMBC): δ [ppm] = 164.1 (C_{quat.}, 1C, 14), 163.6 (C_{quat.}, 1C, 21), 161.4 (C_{quat.}, 1C, 8), 155.8 (C_{quat.}, 1C, 19), 155.2 (C_{quat.}, 1C, 21'), 154.9 (C_{quat.}, 1C, 6), 147.6 (+, 1C, 10), 143.2 (C_{quat.}, 1C, 4), 132.5 (+, 1C, 5), 118.1 (+, 1C, 13), 117.9 (C_{quat.}, 1C, 9), 117.6 (C_{quat.}, 1C, 11), 108.8 (+, 1C, 12), 52.6 (–, 2C, 2), 48.3 (–, 2C, cyclen-CH₂), 47.7 (–, 2C, cyclen-CH₂), 46.1 (–, 4C, cyclen-CH₂), 44.3 (–, 6C, cyclen-CH₂), 44.0 (–, 2C, cyclen-CH₂), 39.9 (–, 1C, 17), 39.0 (–, 1C, 16), 10.1 (+, 2C, 1) — **ESI-MS** (MeCN/TFA): m/z (%) = 362.3 (100) $[M + 2H^+]^{2+}$, 723.5 (10) $[MH^+]$

To obtain the free base of compound **9** a weakly basic ion exchanger resin was swollen for 15 min in water and washed neutral with water. A column was charged with resin (473 mg, 40.0 mmol hydroxy equivalents at a given capacity of 5 mmol/g). The hydrochloride salt (60 mg, 59 μ mol) was dissolved in water, put onto the column and eluted with water. The

elution of the product was controlled by pH indicator paper ($\text{pH} > 10$) and was completed when pH was again neutral. The eluate was concentrated and lyophilised to yield (43 mg, 59 μmol , 100%) the free base **9** as a yellow solid.

MP: 169°C — **$^1\text{H-NMR}$** (600 MHz, D_2O , COSY, ROESY, HSQC, HMBC): δ [ppm] = 8.28 (bs, 1H, 15), 8.09 (s, $^4J_{\text{H,H}} = 1.8$ Hz, 1H, 10), 7.24 (d, $^3J_{\text{H,H}} = 9.2$ Hz, 1H, 12), 6.58 (d, $^3J_{\text{H,H}} = 9.0$ Hz, 1H, 13), 6.13 (d, $^4J_{\text{H,H}} = 1.8$ Hz, 1H, 5), 3.62 (bs, 8H, cyclen- CH_2), 3.48 (t, $^3J_{\text{H,H}} = 5.2$ Hz, 2H, 17), 3.38 (t, $^3J_{\text{H,H}} = 4.6$ Hz, 2H, 16), 3.27 (q, $^3J_{\text{H,H}} = 7.0$ Hz, 4H, 2), 3.12 (bs, 16H, cyclen- CH_2), 3.02 (bs, 8H, cyclen- CH_2), 1.04 (t, $^3J_{\text{H,H}} = 7.1$ Hz, 6H, 1) — **$^{13}\text{C-NMR}$** (150 MHz, D_2O , COSY, ROESY, HSQC, HMBC): δ [ppm] = 166.8 (C_{quat} , 2C, 21), 166.7 (C_{quat} , 1C, 19), 165.3 (C_{quat} , 1C, 8), 163.1 (C_{quat} , 1C, 14), 157.0 (C_{quat} , 1C, 6), 153.6 (C_{quat} , 1C, 4), 148.1 (+, 1C, 10), 131.7 (+, 1C, 12), 111.4 (+, 1C, 13), 107.6 (C_{quat} , 1C, 9), 106.0 (C_{quat} , 1C, 11), 95.5 (+, 1C, 5), 46.1 (–, 4C, cyclen- CH_2), 45.7 (–, 4C, cyclen- CH_2), 45.1 (–, 2C, 2), 44.7 (–, 4C, cyclen- CH_2), 42.8 (–, 2C, cyclen- CH_2), 42.4 (–, 2C, cyclen- CH_2), 40.1 (–, 1C, 16), 39.4 (–, 1C, 17), 11.8 (+, 2C, 1) — **IR** (ATR) [cm^{-1}]: $\tilde{\nu} = 3382, 3315, 2968, 2732, 1694, 1576, 1537, 1506, 1417, 1350, 1231, 1134, 1079, 809$ — **UV** (CHCl_3): λ (ϵ) = 260 nm (12500), 426 (43300) — **ESI-MS** (TFA/MeCN): m/z (%) = 241.7 (10) $[\text{M} + 3\text{H}^+]^{3+}$, 362.2 (100) $[\text{M} + 2\text{H}^+]^{2+}$, 723.5 (6) $[\text{MH}^+]$, 837.4 (3.0) $[\text{MH}^+ + \text{TFA}]$ — **HR-MS**: ($\text{C}_{35}\text{H}_{58}\text{N}_{14}\text{O}_3$) calc. 723.4895 $[\text{MH}^+]$, found 723.4915



Bis-Zinc(II)(7-Diethylamino-2-oxo-2H-chromene-3-carboxylic acid {2-[4,6-bis-(1,4,7,10-tetraaza-cyclo-dodec-1-yl)-[1,3,5]triazin-2-ylamino]-ethyl}-amide) tetraperchlorate (2)

Compound **9** (43 mg, 59 μmol) was dissolved in 1 mL of water and heated to 65°C to get a clear yellow solution. Subsequently Zinc(II)perchlorate (44 mg, 119 μmol) dissolved in 1 mL of water was added slowly. The reaction mixture was stirred for an additional 28 h at 65°C. The solvent was removed *in vacuo* and the residue was redissolved in water and lyophilized. Probe **2** (74 mg, 59 μmol , 100%) was obtained as a yellow solid.

MP: 166°C — **¹H-NMR** (300 MHz, CD₃CN): δ [ppm] = 9.23 (bs, 1H, NH), 8.72 (s, 1H, CH), 7.58 (d, ³J_{H,H} = 9.1 Hz, 1H, CH), 6.80 (d, ³J_{H,H} = 9.1 Hz, 1H, CH), 6.55 (s, 1H, CH), 5.35-6.65 (m, 6H, cyclen-NH), 4.50-3.71 (m, 8H, cyclen-CH₂), 3.49 (q, ³J_{H,H} = 7.0 Hz, 6H, ethyl-CH₂, ethylene diamine-CH₂), 3.37 (bs, 2H, ethylene diamine-CH₂), 3.26 (bs, 12H, cyclen-CH₂), 3.02 (bs, 8H, cyclen-CH₂), 2.45 (bs, 4H, cyclen-CH₂), 1.19 (t, ³J_{H,H} = 7.0 Hz, 6H, ethyl-CH₃) — **IR** (ATR) [cm⁻¹]: $\tilde{\nu}$ = 3246, 2938, 2864, 1558, 1457, 1421, 1342, 1287, 1083, 968, 793 — **UV** (HEPES pH 7.4, 25 mM): λ (ε) = 432 (25800) — **ESI-MS** (TFA/MeCN): m/z (%) = 425.1 (28) [M⁴⁺ - 2H⁺]²⁺, 455.7 (50) [M⁴⁺ - H⁺ + CH₃COO⁻]²⁺, 485.5 (100) [M⁴⁺ + 2CH₃COO⁻]²⁺

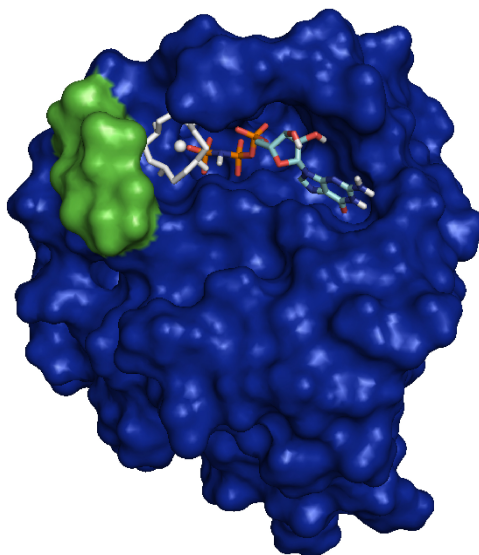
3.6 REFERENCES

- ¹ R. Pio, A. Martinez, E. J. Unsworth, J. A. Kowalak, J. A. Bengoechea, P. F. Zipfel, T. H. Elsasser and F. Cuttitta, *J. Biol. Chem.*, **2001**, 276, 12292-12300.
- ² T. M. Misenheimer, A. J. Hahr, A. C. Harms, D. S. Annis and D. F. Mosher, *J. Biol. Chem.*, **2001**, 276, 45882-45887.
- ³ N. K. Williams, P. Prosselkov, E. Liepinsh, I. Line, A. Sharipo, D. R. Littler, P. M. G. Curmi, G. Otting and N. E. Dixon, *J. Biol. Chem.*, **2002**, 277, 7790-7798.
- ⁴ B. Schulenberg, T. N. Goodman, R. Aggeler, R. A. Capaldi and W. F. Patton, *Electrophoresis*, **2004**, 25, 2526-2532.
- ⁵ E. Kinoshita, E. Kinoshita-Kikuta, K. Takiyama and T. Koike, *Mol. Cell. Proteomics*, **2006**, 5, 749-757.
- ⁶ T. Hunter, *Cell*, **1995**, 80, 225-236.
- ⁷ T. Hunter, *Cell*, **2000**, 100, 113-127.
- ⁸ G. Manning, D. B. Whyte, R. Martinez, T. Hunter and S. Sudarsanam, *Science*, **2002**, 298, 1912-1934.
- ⁹ A. R. Salomon, S. B. Ficarro, L. M. Brill, A. Brinker, Q. T. Phung, C. Ericson, K. Sauer, A. Brock, D. M. Horn, P. G. Schultz and E. C. Peters, *Proc. Natl. Acad. Sci. USA*, **2003**, 100, 443-448.
- ¹⁰ T. P. Conrads and T. D. Veenstra, *Nat. Biotechnol.*, **2005**, 23, 36-37.
- ¹¹ M. R. Larsen, G. L. Sorensen, S. J. Fey, P. M. Larsen and P. Roepstorff, *Proteomics*, **2001**, 1, 223-238.
- ¹² D. Immler, D. Gremm, D. Kirsch, B. Spengler, P. Presek and H. E. Meyer, *Electrophoresis*, **1998**, 19, 1015-1023.
- ¹³ A. Ojida, T. Kohira and I. Hamachi, *Chem. Lett.*, **2004**, 33, 1024-1025.
- ¹⁴ A. Ojida, Y. Mito-oka, M. Inoue and I. Hamachi, *J. Am. Chem. Soc.*, **2002**, 124, 6256-6258.
- ¹⁵ A. Grauer, A. Riechers, S. Ritter and B. Konig, *Chem. Eur. J.*, **2008**, 14, 8922-8927.
- ¹⁶ S. Mizukami, T. Nagano, Y. Urano, A. Odani and K. Kikuchi, *J. Am. Chem. Soc.*, **2002**, 124, 3920-3925.
- ¹⁷ O. S. Wolfbeis and G. Uray, *Monatsh. Chem.*, **1978**, 109, 123-136.
- ¹⁸ To assess the influence of the fluorophore further, we also prepared the same type of probe with pyrene and dansyl fluorophores. Neither of these probes exhibited any

distinction between phosphorylated and nonphosphorylated proteins (data not shown).

- ¹⁹ M. Kruppa, D. Frank, H. Leffler-Schuster and B. König, *Inorg. Chim. Acta*, **2006**, 359, 1159-1168.
- ²⁰ L. N. Lugina, N. K. Davidenko and S. P. Gavrish, *Theor. Exp. Chem.*, **1985**, 466-470.
- ²¹ V. P. Mocharla, B. Colasson, L. V. Lee, S. Roper, K. B. Sharpless, C. H. Wong and H. C. Kolb, *Angew. Chem., Int. Ed.*, **2004**, 44, 116-120.
- ²² A. Späth, *PhD Thesis*, **2010**, University of Regensburg.
- ²³ T. Berthelot, J. C. Talbot, G. Lain, G. Deleris and L. Latxague, *J. Pept. Sci.*, **2005**, 11, 153-160.
- ²⁴ M. Kruppa and B. König, *Chem. Rev.*, **2006**, 106, 3520-3560.

4 ZINC(II)CYCLEN PEPTIDE CONJUGATES INTERACTING WITH THE WEAK EFFECTOR BINDING STATES OF RAS



Zinc(II)cyclen-peptide hybrid compounds and bis-zinc(II)cyclen complexes are prepared as potential binders of the guanine nucleotide binding protein Ras, an important molecular switch in cellular signal transduction. The design of the compounds is based on the previous observation that zinc(II)cyclen complexes could serve as lead compounds for inhibitors of Ras-effector interaction and thus be able to interrupt Ras induced signal transduction. Zinc(II)cyclen selectively stabilizes conformational state 1 of active Ras, a conformational state with drastically decreased affinity to effector proteins like Raf-kinase. To achieve higher binding affinities of such Ras-Raf interaction inhibitors, zinc(II)cyclen conjugates with short peptides, derived from the sequence of the Ras-activator SOS, were prepared by solid phase synthesis protocols. Dinuclear bis-zinc(II)cyclen complexes were obtained from alkyne-azide cycloaddition reactions. NMR investigations of the prepared compounds revealed that the peptide conjugates do not lead to an increase in Ras binding affinity of the metal complex – peptide conjugates. The dinuclear zinc complexes lead to an immediate precipitation of the protein prohibiting spectroscopic investigations of their binding.

4.1 INTRODUCTION

The development of small molecules for the inhibition of protein-protein interactions is of high current interest due to possible implications in medicinal chemistry. However, achieving sufficient binding affinity and selectivity is still challenging.¹⁻³ A very common approach to improve the affinity and selectivity of a low affinity binder is the introduction of additional binding sites. Such bi- or multivalent ligands may lead to improved binding affinities by additive or even cooperative action of the different binding sites.⁴⁻⁶ There are two principal ways to inhibit protein-protein interactions by chemical inhibitors: They can either block the interface (competitive inhibition) or induce changes in the proteins conformation (allosteric inhibition) leading to an altered binding ability of the surface of the protein interface.¹

Ras protein, which is known for several years to play an important role in pathogenesis of certain human cancer types,⁷⁻⁹ exists in its active, GTP-bound form, in an equilibrium between at least two conformational states (state 1 and state 2).¹⁰ Ras variants, which exist predominately in conformational state 1 show a more than 20-fold decreased affinity to effector proteins.¹¹ This affinity is too low in order to transduce the signal at physiological concentrations. We could show, that the azamacrocyclic metal complex Zn^{2+} -1,4,7,10-Tetraazacyclododecane (Cyclen) selectively binds state 1,¹² and that it is able to shift the equilibrium totally towards that weak effector-binding conformation at higher concentration. Zn^{2+} -Cyclen shows affinity to phosphate ions¹³⁻¹⁵ and binds with millimolar affinity near the γ -phosphate at the active site of Ras stabilizing conformation of state 1. Ras in conformational state 2, which represents the strong effector binding mode, and thus is responsible for Ras-effector-protein complex formation in the cell, did not show significant interaction with Zn^{2+} -Cyclen. The same results are obtained for GDP-bound, inactive Ras, here again no indication for Zn^{2+} -cyclen binding could be obtained in the active site as studied by ^{31}P NMR spectroscopy. Therefore, Zn^{2+} -Cyclen can serve as lead for inhibitors of Ras-Raf interaction. In this work we used the GTP analogue GppNHp in order to resist GTPase activity of Ras. The mutant Ras(T35A) was chosen because it predominantly exists in the conformational state 1, which should be recognized by the ligand, and because for this mutant in contrast to wild-type Ras all resonances can be obtained in the $[\text{}^1\text{H}-\text{}^{15}\text{N}]$ -HSQC NMR experiments. As the formation of such Ras-effector-protein complexes induces certain cell signalling pathways leading to unregulated cell growth in tumour cells, its selective inhibition is of considerable interest.⁷ However, a 20-fold excess of Zn^{2+} -Cyclen is required to shift the equilibrium

completely towards state 1 due to the low binding affinity of the metal-complex to the active site of Ras.¹²

The structure of the metal-cyclen complex with Ras was solved recently¹⁶ where two Zn^{2+} -cyclen binding sites could be identified. To increase the binding affinity, two types of bidentate ligands based on the Zn^{2+} -cyclen binding motif were synthesized: 1. Heterotopic peptide-metal complex hybrid-ligands, as it was known that short peptides can interfere with the Ras-effector-protein interaction.¹⁷⁻¹⁹ 2. Bidentate bis(Zn^{2+} -cyclen) metal-complexes, as previous NMR-investigations showed that there is more than one binding site for Zn^{2+} -Cyclen on the protein surface of Ras.¹⁶

4.2 RESULTS & DISCUSSION

4.2.1 Ligand Design

Figure 1 shows the solution structure of the $\text{Ras}:\text{Mg}^{2+}:\text{GppNHp}$ complex in the conformational state that is only weakly interacting with effectors. This state is stabilised by Zn^{2+} -Cyclen bound to the γ -phosphate of GppNHp.¹⁶

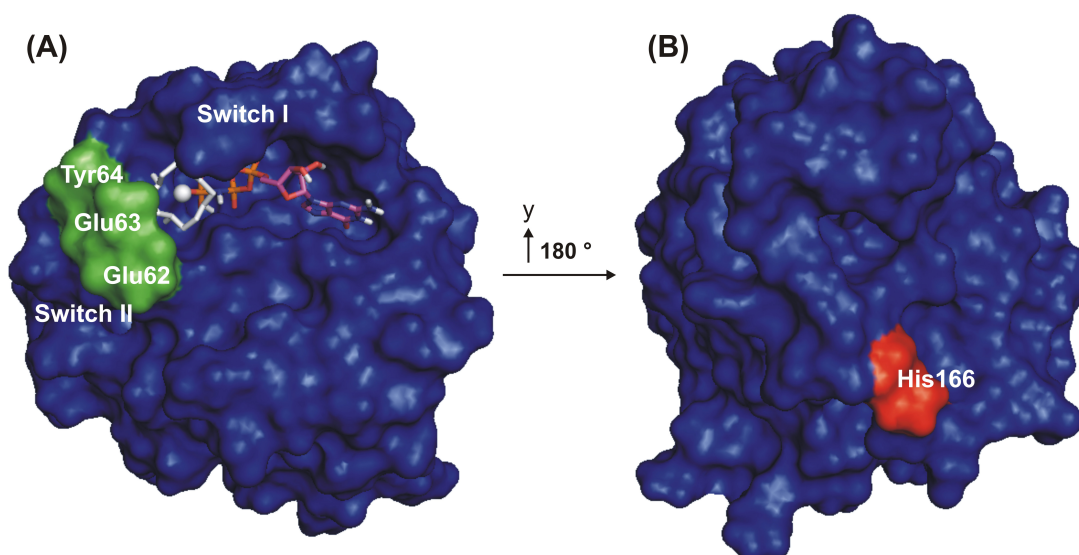


Figure 1: Solution structure of Zn^{2+} -Cyclen complexed to $\text{Ras}:\text{Mg}^{2+}:\text{GppNHp}$ in conformational state 1. The solution structure of Ras complexed with Zn^{2+} -cyclen was taken from *Rosnizeck et al.*¹⁶; Zn^{2+} -Cyclen is depicted in white; the second binding site of Zn^{2+} -Cyclen is indicated in red, the amino acids of Ras interacting in the crystal structure of the Ras-SOS complex with the SOS-pentapeptide from amino acid 822-826 (Leu-Lys-Met-Ile-Arg)¹⁸ are labelled in green

In the approach presented here Zn^{2+} -Cyclen bound to its site close to the γ -phosphate group of GppNHp should be linked with a second interacting group via a flexible linker. State 1 is assumed to be closely related to the conformation of Ras found in the complex with its nucleotide exchange factor SOS (son of sevenless).²⁰⁻²¹ Therefore, the crystal structure of the Ras-SOS complex¹⁸ was used to derive Zn^{2+} -cyclen – peptide ligands (Figure 2) containing a possible additional interacting site with Ras. The pentapeptide contains three amino acids (Leu822, Ile825, Arg826) from the sequence of the exchange factor SOS, which directly interact with Ras. The amino acids that do not contribute to the interaction with Ras have been replaced by glycines in order to allow for more flexibility. Next, the distance between the binding position of Zn^{2+} -Cyclen at the proteins active centre and the peptide was estimated and the peptide was tethered to Zn^{2+} -Cyclen by spacers of different lengths.

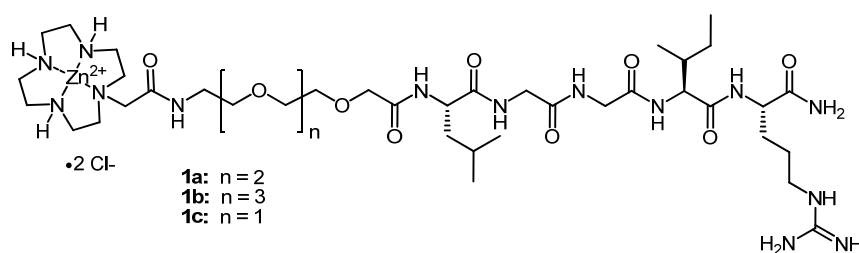


Figure 2: Zn^{2+} -Cyclen - peptide hybrid ligands 1 for Ras binding.

Two binding sites for Zn^{2+} -cyclen complexes had been identified on the surface of the Ras protein.¹⁶ One is located close to the γ -phosphate of the bound nucleotide, the other is located close to the C-terminus of Ras. In binding site 1 the Zn^{2+} ion is directly coordinated to the phosphate group, in binding site 2 to the imidazole nitrogen of His166 of Ras. Dinuclear bis(Zn^{2+} -cyclen) complexes that recognize the two binding sites should therefore show an increased affinity to Ras-GTP, if they act synergistically or even cooperatively. (Figure 4) However, if the PEG linker would be smaller than the distance between the Ras GTP binding site and the Zn^{2+} -Cyclen surface binding site, the compound should be able to cross-link the proteins. PEG-linked bis(Zn^{2+} -cyclen) complexes based on tri- and tetra(ethylene glycol) units should be suitable to probe the hypothesis.

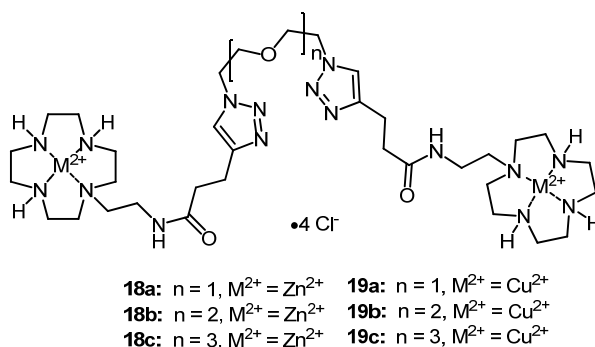
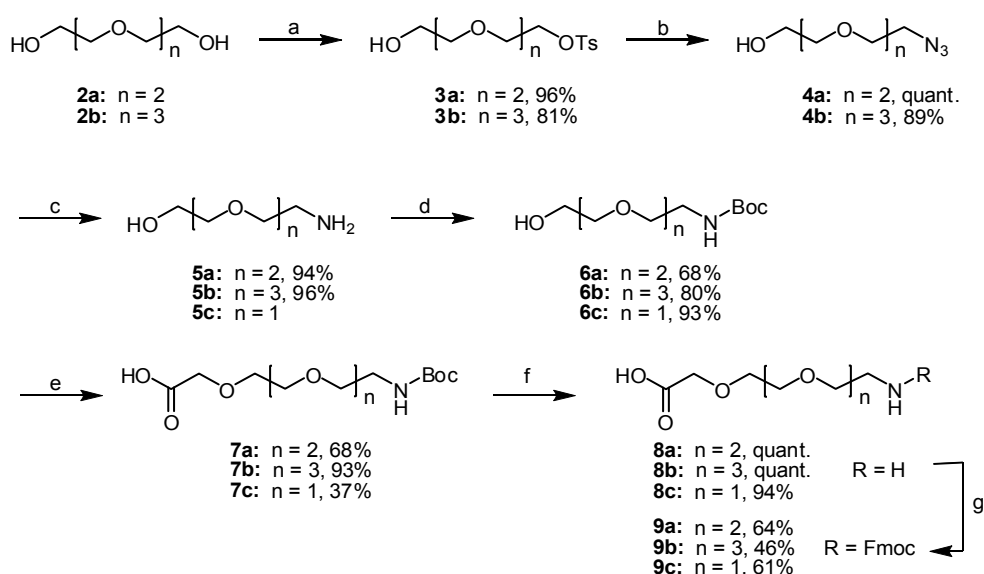


Figure 4: Bis(Zn^{2+} -cyclen) complexes **18** and bis(Cu^{2+} -cyclen) complexes **19**

4.2.2 Synthesis and Characterization of Zn^{2+} -Cyclen - peptide Hybrid Ligands

Solid phase peptide synthesis (SPPS) and Fmoc-strategy were used to prepare ligands **1** in analogy to our previously published protocols.²²⁻²³ The appropriate PEG spacers, assuring sufficient water solubility of the target molecules, were synthesized as shown in Scheme 1.

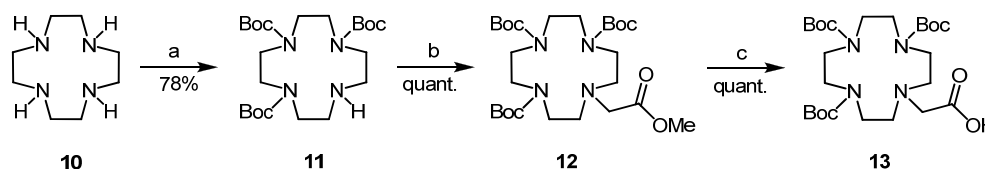


Scheme 1: Synthesis of Fmoc-protected amino-PEG-acid spacers **9**. a) TsCl , NaOH ; b) NaN_3 , DMF ; c) Pd/C , H_2 , THF ; d) Boc_2O , DCM ; e) 2-bromoacetic acid, NaOH , THF/toluene ; f) HCl_{aq} (~18%); g) Fmoc-succinimide, K_2CO_3 , water

Ethylene glycols were mono-tosylated according to literature known procedures giving compounds **3a** and **3b**.²⁴⁻²⁵ For the preparation of azides **4a** and **4b** two different reaction conditions have been reported.²⁵⁻²⁷ In our hands, the room temperature reactions gave higher

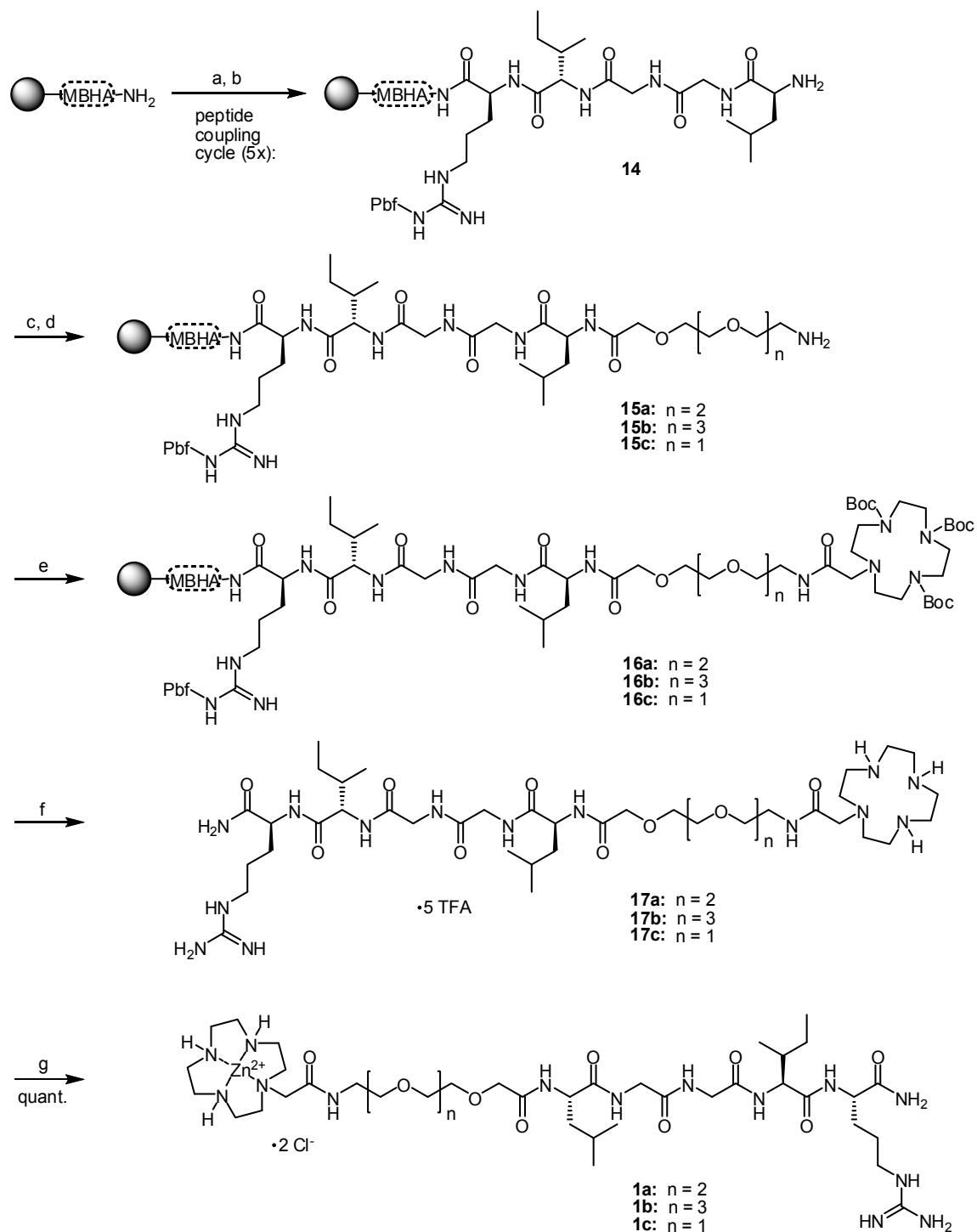
yields compared to heating to 80°C. The clean catalytic reduction of **4a** was performed analogously to the reported conversion of **4b**²⁷ and the amines were Boc protected to give **6a-c**.²⁸⁻²⁹ The subsequent alkylation step with 2-Bromoacetic acid in the presence of Sodium hydroxide provided the corresponding acids in moderate yields. Finally, the Boc-protection groups were replaced by Fmoc. The synthesis of compound **9c** was performed following an already published method.³⁰

An N-protected cyclen carboxylic acid was prepared for later use in the Fmoc SPPS protocol (Scheme 2). Compound **13**³¹ was obtained in almost quantitative overall yield starting from compound **11**, which was prepared according to a literature known procedure.³²



Scheme 2: Synthesis of cyclen carboxylic acid 13. a) Boc_2O , CHCl_3 ; b) Methyl bromoacetate, K_2CO_3 , MeCN ; c) LiOH , Acetone/water

The pentapeptide was synthesized by standard Fmoc-based SPPS protocols using an automated peptide synthesizer on Rink amide MBHA resin. Subsequent it was coupled to spacers **9** and finally, compound **13** was N-terminally added to yield the resin bound peptide-(3-Boc)cyclen conjugate **16** (Scheme 3). TFA treatment cleaved the peptide-(3-Boc)cyclen conjugate from the resin and removed cyclen and the arginine side-chain protecting groups. Compounds **17a** and **17b** were purified by HPLC; compound **17c** was directly reacted with Zinc(II)-chloride.



Scheme 3: SPPS synthesis of peptide-cyclen conjugates. a) Fmoc-AA, TBTU, HOBT, DIPEA (2x); b) Piperidine (40%); c) **9a/b/c**, TBTU, HOBT, DIPEA (2x); d) Piperidine (40%); e) **13**, TBTU, HOBT, DIPEA (2x); f) TFA/TIS/water (90 : 5 : 5); g) ZnCl₂, water, pH 7-8.

Compounds **1a** and **1b** were characterized by STD-experiments. All compounds show a positive STD effect and thus bind to Ras. As an example Figure 3 shows the results obtained for compound **1b**. Clearly the largest STD enhancement factor A_{STD} is observed for the cyclen moiety and a lower value for the peptide moiety. This suggests that Zn^{2+} -Cyclen is involved in a direct interaction, but that the linker is too short in compound **1b** to allow for a direct interaction of the peptide with Ras. In line with this observation, STD titration experiments show that the affinity of these compounds is not increased relative to Zn^{2+} -Cyclen alone.

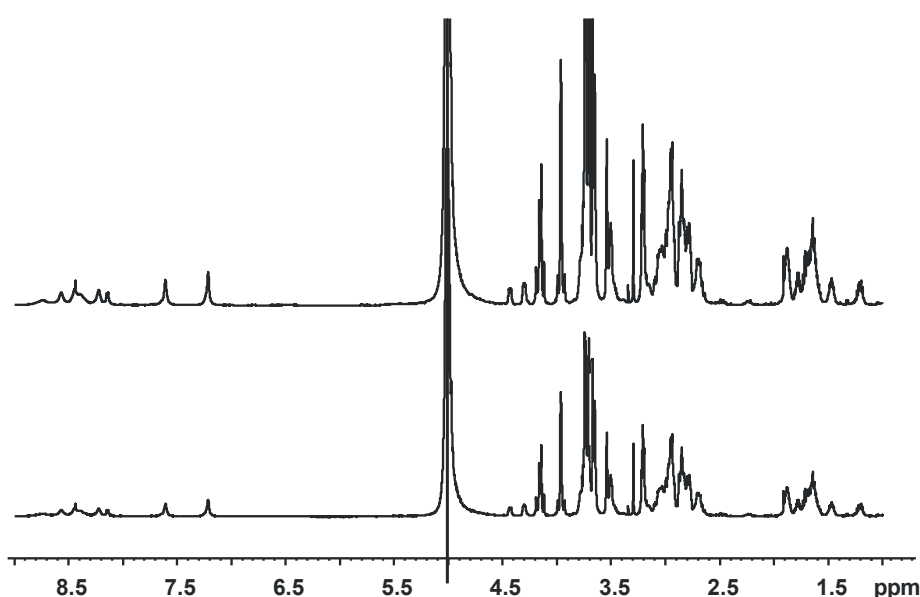
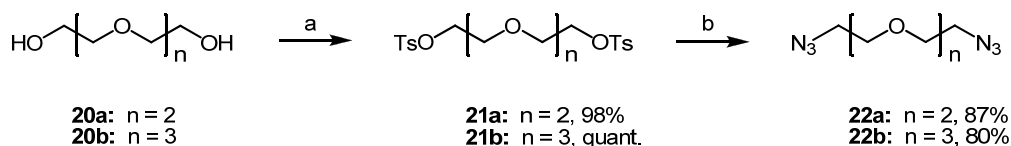


Figure 3: STD experiment with the Zn^{2+} -Cyclen hybrid ligand **1b in the presence of Ras.** Off-resonance spectrum (upper trace) and STD spectrum (lower trace) of a sample containing 50 μ M Ras(T35A)·GppNHp in 40 mM Tris/HCl pH 7.4 and 10 mM $MgCl_2$ and 4.84 mM compound **1b**

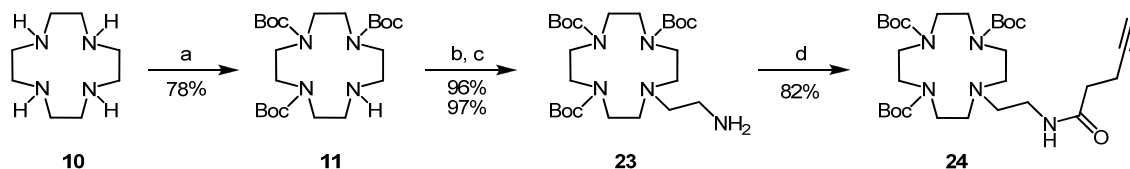
4.2.3 PEG-linked bis(Zn^{2+} -cyclen) Complexes

Ethylene glycol based spacers with corresponding lengths were azide functionalized on each terminus by substitution of a previously synthesized bis-tosylate with Sodium azide following a literature procedure.²⁶ (Scheme 4) Tri(ethylene glycol)-ditosylate **21a** and Tetra(ethylene glycol)-ditosylate **21b** were prepared adapting a published synthesis protocol for the corresponding mono-tosylates.²⁴



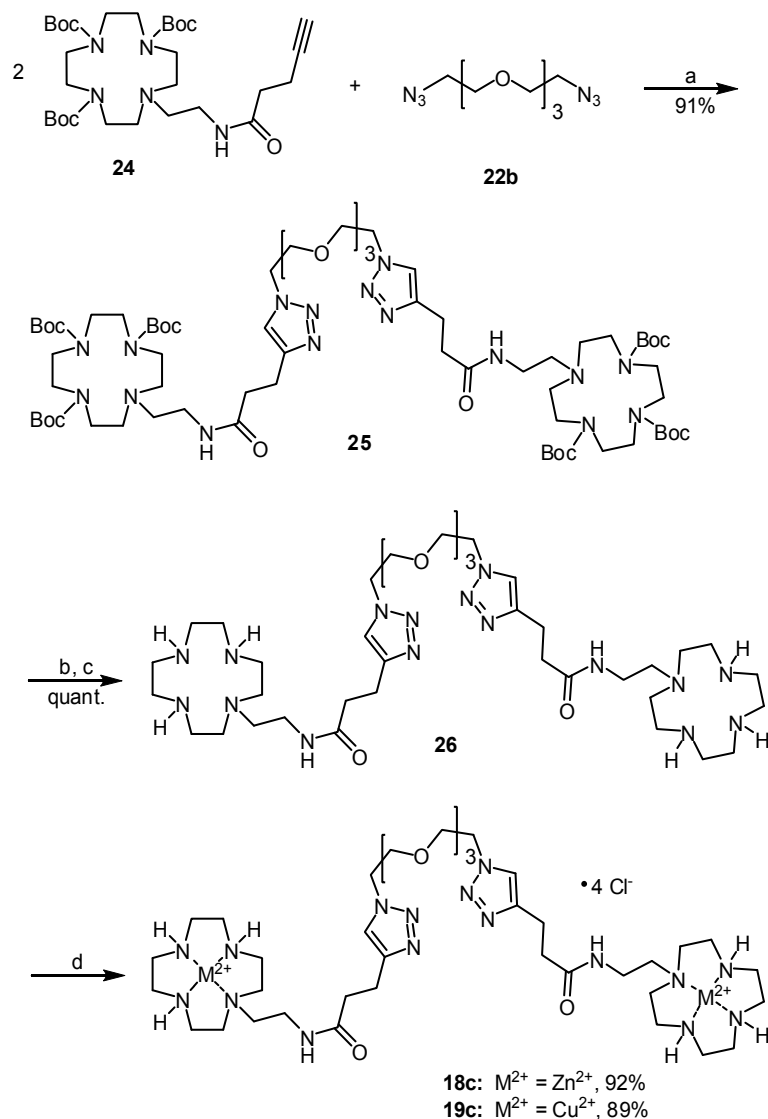
Scheme 4: Preparation of tri- and tetra(ethylene glycol)-diazides **22**. a) TsCl, KOH, THF; b) NaN₃, DMF

Alkyne cyclen **24** was prepared as reactant for a copper catalyzed alkyne – azide cycloaddition reaction³³⁻³⁴ with **22**. (Scheme 5) Therefore, N-2-Aminoethyl-3-Boc-cyclen (10-(2-Aminoethyl)-1,4,7,10-tetraazacyclododecan-1,4,7-tricarboxylic-acid-tri-*tert*-butylester) **23** was synthesized in three steps from threefold Boc protected Cyclen **11**.³² The free amino group was alkylated by Bromoacetonitrile and hydrogenated to the corresponding amine **23**.³⁵ Compound **23** was then reacted under peptide coupling conditions with 4-Pentynoic acid to give N-10-(2-Aminoethyl)-1,4,7,10-tetraazacyclododecan-1,4,7-tricarboxylicacid-tri-*tert*-butylester-pent-4-ynamide **24**.



Scheme 5: Synthesis of alkyne 3-Boc-cyclen **24**. a) Boc₂O, CHCl₃; b) Bromoacetonitrile, K₂CO₃, MeCN; c) Raney-Ni, H₂, EtOH(NH₃ sat.); d) 4-Pentynoic acid, EDC, HOBt, DIPEA

The twofold Cu(I)-catalyzed 1,3-dipolar cycloaddition of **22b** and **24** worked best using Copper(II)sulfate/Sodium ascorbate in aqueous methanolic solution providing **25** in sufficient purity and good yield after filtration over flash silica gel. Acidic cleavage of the Boc groups and complex formation under slightly basic conditions with Zinc(II)-chloride and Copper(II)-chloride, gave complexes **18c** and **19c**, respectively. Only the dinuclear complexes based on **22b** were prepared. (Scheme 6)



Scheme 6: Click-reaction yielding six-fold Boc protected metal chelator and synthesis of PEG-linked bis(M^{2+} -cyclen) complexes **18c and **19c**.** a) CuSO_4 , Sodium ascorbate, MeOH/water; b) $\text{HCl-Et}_2\text{O}$, DCM; c) basic anion exchanger; d) ZnCl_2 or CuCl_2 , water, pH 7-8

Addition of the PEG-linked bis(M^{2+} -Cyclen) complexes ($\text{M}^{2+} = \text{Zn}^{2+}$, Cu^{2+}) (compounds **18c** and **19c**) led to a immediate precipitation of Ras(T35A)-GppNHp present in a concentration of 50 μM). This effect is clearly due to a direct interaction with the protein, since compound **26** lacking the metal ions does not induce a precipitation, but also does not bind Ras as inferred from the missing STD.

4.3 CONCLUSIONS

We have reported two different types of artificial ligands for state 1, the low affinity state for effectors of active Ras based on the known Zn^{2+} -cyclen binding motif. It was the intention to strengthen the binding to the protein by additive or even cooperative effects due to the introduction of a second binding site for Ras. Hybrid peptide- $(\text{Zn}^{2+}$ -Cyclen) ligands were synthesized on solid-phase using Fmoc-based standard protocols for SPPS, whereas symmetrical PEG-linked bis($\text{Zn}^{2+}/\text{Cu}^{2+}$ -Cyclen) ligands were prepared in solution using a twofold “click”-reaction as the key step in the reaction sequence. Unfortunately, the peptide- $(\text{Zn}^{2+}$ -Cyclen) ligands did not show a significantly increased binding affinity to Ras compared to the parent compound Zn^{2+} -Cyclen. The PEG-linked bis($\text{Zn}^{2+}/\text{Cu}^{2+}$ -Cyclen) ligands precipitated the protein immediately, thus preventing any spectroscopic studies. Most probably this effect is due to a cross-linking of Ras proteins by the bivalent ligand. Overall, rationally designed bivalent ligands for Ras protein binding are synthetically accessible, but among the so far investigated examples no increase in binding affinity could be observed.

4.4 ACKNOWLEDGEMENTS

Financial support of the Volkswagen Foundation and the University of Regensburg is gratefully acknowledged.

4.5 EXPERIMENTAL SECTION

4.5.1 General

Absorption spectroscopy. Absorption spectra were recorded on a Varian Cary BIO 50 UV/VIS/NIR Spectrometer by use of 1 cm quartz cuvettes (Hellma) and Uvasol solvents (Merck or Baker).

NMR spectroscopy. Bruker Avance 600 (Cryo) (^1H : 600.1 MHz, ^{13}C : 150.1 MHz, T = 300 K), Bruker Avance 400 (^1H : 400.1 MHz, ^{13}C : 100.6 MHz, T = 300 K), Bruker Avance 300 (^1H : 300.1 MHz, ^{13}C : 75.5 MHz, T = 300 K). The chemical shifts are reported in δ [ppm] relative to internal standards (solvent residual peak). The spectra were analyzed by first order, the coupling constants are given in Hertz [Hz]. Characterization of the signals: s = singlet, d = doublet, t = triplet, q = quartet, m = multiplet, bs = broad singlet, dd = double doublet, ddd = double double doublet. Integration is determined as the relative number of atoms. Assignment of signals in ^{13}C -spectra was determined with DEPT-technique (pulse angle: 135°) and given as (+) for CH_3 or CH, (–) for CH_2 and (C_{quat}) for quaternary C_{quat} . Error of reported values: chemical shift: 0.01 ppm for ^1H -NMR, 0.1 ppm for ^{13}C -NMR and 0.1 Hz for coupling constants. The solvent used is reported for each spectrum. Molecular structures with atom numbers of the synthesized compounds are provided in the Supporting Information to facilitate the assignment traceability.

Mass spectrometry. Varian CH-5 (EI), Finnigan MAT 95 (CI), Finnigan MAT TSQ 7000 (ESI).

IR spectroscopy. Recorded with a Bio-Rad FTS 2000 MX FT-IR.

Melting point. Melting points were determined on Büchi SMP or a Lambda Photometrics OptiMelt MPA 100.

TLC analysis and column chromatography. Analytical TLC plates (silica gel 60 F254) and silica gel 60 (70-230 or 230-400 mesh) for column chromatography were purchased from Merck. Spots were visualized by UV light and/or staining with Ninhydrin in EtOH.

Dry DMF was purchased from Fluka, Dichloromethane (DCM) was dried by adsorption and stored over molecular sieves. Solvents for SPPS were all peptide grade. Petrol ether (PE) had a boiling range of 70-90°C. All other solvents and chemicals were of reagent grade and used without further purification.

4.5.2 Protein Preparation

The unlabeled C-terminal truncated T35A-mutant of human H-Ras (amino acids 1-166) was expressed in *Escherichia coli* and purified as described before.³⁶

Uniformly ¹⁵N-labeled protein was obtained by growing the bacteria in M9 minimal media containing 1 g L⁻¹ ¹⁵NH₄Cl as the sole nitrogen source.³⁷ The final purity of the proteins was > 95% as judged from the Sodium dodecyl sulfate-polyacrylamide gel electrophoresis. Nucleotide exchange from GDP to GppNHp was done using alkaline phosphatase treatment in the presence of low excess GppNHp analogous to *John et al.*³⁸ Free nucleotides were removed by size exclusion chromatography.

4.5.3 STD NMR Spectroscopy

NMR samples originally contained 50 μM c'Ras(T35A)·Mg²⁺·GppNHp in 40 mM Tris/HCl pH 7.4, 10 mM MgCl₂, 25% D₂O and 0.2 mM DSS as a reference standard. The spectra were recorded on a Bruker Avance 600 MHz spectrometer equipped with a 5 mm triple resonance cryo probe at 278 K. The ligands were dissolved in the sample buffer and titrated to the protein sample.

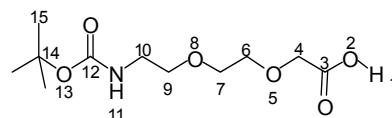
Saturation transfer difference (STD) NMR spectroscopy³⁹⁻⁴⁰ was used to detect the binding of the ligand to Ras. Compared to non-NMR methods STD is especially well-suited for the detection of the weak binding expected. The on-resonance irradiation frequency was set to a chemical shift value of -2 ppm with an attenuation of 40 dB in the titration with Zn²⁺-Cyclen and **1a** or 30 dB in the titration experiment with **1b**. Off-resonance irradiation was performed at +30 ppm. The protein was selectively saturated by a train of 40 Gauss-shaped 90° pulses of 50 ms length giving a total saturation time of 2 s. On- and off-resonance experiments have been performed in an interlaced fashion. Water suppression was achieved using a delay of 100 μs for binomial water suppression. Prior to acquisition a T_{1ρ}-filter consisting of a spinlock pulse with 50 ms length and an attenuation of 15 dB was implemented in order to suppress protein proton resonances, which eases data evaluation.⁴¹ 32k data points have been collected, zero-filled to 64k and multiplied by an exponential line broadening function of 0.3 Hz. After splitting the data into on- and off-resonance both spectra were processed and phased identically. Baseline correction was done automatically using a polynomial of 5th degree. Processing was performed using topspin 2.0 software (Bruker, Rheinstetten, Germany). The STD amplification factor A_{STD} ⁴⁰ is defined by

$$A_{STD} = \frac{I_0 - I}{I_0} ([L] - [P]) = \frac{\alpha_{STD} [L]}{[L] - K_d} \quad \text{Equation 1}$$

with [L] and [P] the total ligand and protein concentrations, respectively. I_0 is the line intensity with off-resonance irradiation, I the line intensity with saturation of the protein resonances (on-resonance), K_d the dissociation constant and α_{STD} the maximum value of A_{STD} .

4.5.4 Syntheses

Following compounds were synthesized according to literature known procedures and determined to be consistent with analytical data derived from the corresponding published syntheses: Toluene-4-sulfonic acid 2-[2-(2-hydroxy-ethoxy)-ethoxy]-ethyl ester **3a** and Toluene-4-sulfonic acid 2-{2-[2-(2-hydroxy-ethoxy)-ethoxy]-ethoxy}-ethyl ester **3b**,²⁴⁻²⁵ 2-[2-(2-Azido-ethoxy)-ethoxy]-ethanol **4a** and 2-{2-[2-(2-Azido-ethoxy)-ethoxy]-ethoxy}-ethanol **4b**,²⁵⁻²⁷ {2-[2-(2-Hydroxy-ethoxy)-ethoxy]-ethyl}-carbamic acid *tert*-butyl ester **6a**, (2-{2-[2-(2-Hydroxy-ethoxy)-ethoxy]-ethoxy}-ethyl)-carbamic acid *tert*-butyl ester **6b** and [2-(2-Hydroxy-ethoxy)-ethyl]-carbamic acid *tert*-butyl ester **6c**,²⁸⁻²⁹ {2-[2-(9H-Fluoren-9-yl-methoxycarbonylamino)-ethoxy]-ethoxy}-acetic acid **9c**,³⁰ 3-Boc-cyclen **11**,³² 1-Azido-2-[2-(2-azido-ethoxy)-ethoxy]-ethane **22a** and 1-(2-Azido-ethoxy)-2-[2-(2-azido-ethoxy)-ethoxy]-ethane **22b**,²⁶ 10-(2-Aminoethyl)-1,4,7,10-tetraazacyclododecan-1,4,7-tricarboxylic-acid-*tert*-butylester **23**.³⁵

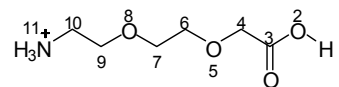


[2-(2-*tert*-Butoxycarbonylamino-ethoxy)-ethoxy]-acetic acid (**7c**)

[2-(2-Hydroxy-ethoxy)-ethyl]-carbamic acid *tert*-butyl ester **6c** (4.50 g, 21.9 mmol) was dissolved in 200 mL of THF/toluene (1 : 1), then Bromoacetic acid (9.06 g, 65.2 mmol) was added. After heating the reaction mixture to 45°C, powdered Sodium hydroxide (5.40 g, 135.0 mmol) was added and the mixture was stirred over night. Afterwards, THF was evaporated and water was added to the toluene layer. After separating the aqueous layer, the organic layer was extracted with aqueous Sodium hydroxide solution (5%; 3 x 70 mL) and the combined aqueous layers were washed with DCM (3 x 100 mL). Conc. HCl_{aq.} was added slowly to the aqueous layer until pH ~ 4 was reached while stirring. By extraction with DCM

(3 x 50 mL) excess of Bromoacetic acid could be removed. After further addition of conc. HCl_{aq} until pH ~ 2 , the product was isolated by again extracting with DCM (5 x 50 mL). The combined organic layers were dried over MgSO_4 , filtrated and the solvent was evaporated yielding a slightly yellow oil (2.07 g, 36%).

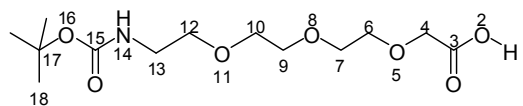
$^1\text{H-NMR}$ (400 MHz, CDCl_3 , COSY, HSQC): δ [ppm] = 8.61 (s, 1H, 1), 5.03 (s, 1H, 11), 4.16 (s, 2H, 4), 3.77-3.71 (m, 2H, 6), 3.68-3.61 (m, 2H, 7), 3.55 (t, $^3J_{\text{H,H}} = 4.9$ Hz, 2H, 9), 3.31 (bs, 2H, 10), 1.43 (s, 9H, 15) — **$^{13}\text{C-NMR}$** (100 MHz, CDCl_3 , COSY, HSQC): δ [ppm] = 173.2 ($\text{C}_{\text{quat.}}$, 1C, 3), 156.1 ($\text{C}_{\text{quat.}}$, 1C, 12), 79.5 ($\text{C}_{\text{quat.}}$, 1C, 14), 71.1 (–, 1C, 6), 70.4 (–, 1C, 7), 70.0 (–, 1C, 9), 68.5 (–, 1C, 4), 40.2 (–, 1C, 10), 28.3 (+, 3C, 15) — **IR** (ATR) [cm^{-1}]: $\tilde{\nu} = 3343$, 2975, 2933, 2883, 1700, 1529, 1456, 1394, 1367, 1255, 1149, 1117, 858 — **ESI-MS** (DCM/MeOH + 10 mmol/L NH_4Ac): m/z (%) = 264.0 (40) [MH^+], 281.1 (100) [MNH_4^+], 286.0 (27) [MNa^+], 544.3 (14) [$2\text{M} + \text{NH}_4^+$], 549.2 (15) [$2\text{M} + \text{Na}^+$] — **EA**: calc. (%) for $\text{C}_{11}\text{H}_{21}\text{NO}_6$ (263.29) + $\frac{1}{3} \text{H}_2\text{O}$: C 49.06, H 8.11, N 5.20; found: C 49.15, H 8.00, N 4.96



[2-(2-Amino-ethoxy)-ethoxy]-acetic acid hydrochloride (8c)

[2-(2-*tert*-Butoxycarbonylamino-ethoxy)-ethoxy]-acetic acid **7c** (3.72 g, 14.1 mmol) was diluted with 20 mL of DCM and HCl saturated Et_2O (80 mL) was added at 0°C while stirring. After stirring over night, the solvents were evaporated yielding the product as yellowish oil (2.64 mg, 94%).

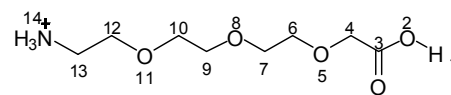
$^1\text{H-NMR}$ (400 MHz, D_2O): δ [ppm] = 4.18 (s, 2H, 4), 3.75-3.65 (m, 6H, 6+7+9), 3.16 (t, $^3J_{\text{H,H}} = 4.9$ Hz, 2H, 10) — **$^{13}\text{C-NMR}$** (100 MHz, D_2O): δ [ppm] = 174.3 ($\text{C}_{\text{quat.}}$, 1C, 3), 70.2, 69.5, 67.6, 66.4 (–, 4C, 4+6+7+9), 39.2 (–, 1C, 10) — **ESI-MS** ($\text{H}_2\text{O}/\text{MeOH}$ + 10 mmol/L NH_4Ac): m/z (%) = 164.1 (100) [MH^+], 327.2 (17) [$2\text{M} + \text{H}^+$]



{2-[2-(2-*tert*-Butoxycarbonylamino-ethoxy)-ethoxy]-ethoxy}-acetic acid (7a**)**

{2-[2-(2-Hydroxy-ethoxy)-ethoxy]-ethyl}-carbamic acid *tert*-butyl ester **6a** (4.68 g, 14.8 mmol) was dissolved in 40 mL of THF/Toluene (1 : 1) and Bromoacetic acid (6.16 g, 44.4 mmol) was added. After heating the reaction mixture to 45°C, powdered Sodium hydroxide (3.55 g, 88.7 mmol) was added and the mixture was stirred over night. THF was evaporated and water was added to the toluene layer. After separating the aqueous layer, the organic layer was extracted with aqueous Sodium hydroxide solution (5%; 3 x 40 mL) and the combined aqueous layers were washed with DCM (3 x 40 mL). Conc. HCl_{aq.} was added slowly to the aqueous layer until pH ~ 4 was reached while stirring. By extraction with DCM (3 x 50 mL) excess of bromoacetic acid could be removed. After further addition of conc. HCl_{aq.} until pH ~ 2, the product was isolated by again extracting with DCM (5 x 50 mL). The combined organic layers were dried over MgSO₄ and filtrated. Evaporation of the solvent gave a yellowish oil (3.10 g, 68%).

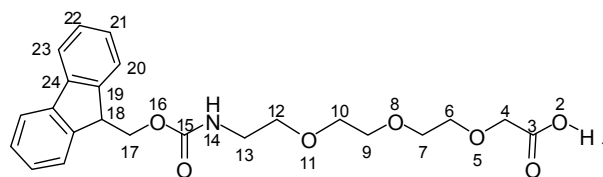
¹H-NMR (400 MHz, CDCl₃, COSY, HSQC): δ [ppm] = 8.68 (s, 1H, 1), 5.12 (s, 1H, 14), 4.15 (s, 2H, 4), 3.76-3.71 (m, 2H, 6), 3.71-3.63 (m, 4H, 7+9), 3.63-3.58 (m, 2H, 10), 3.52 (t, ³J_{H,H} = 5.2 Hz, 2H, 12), 3.35-3.19 (m, 2H, 13), 1.42 (s, 9H, 18) — **¹³C-NMR** (100 MHz, CDCl₃, COSY, HSQC): δ [ppm] = 172.8 (C_{quat.}, 1C, 3), 156.2 (C_{quat.}, 1C, 12), 79.3 (C_{quat.}, 1C, 17), 71.2 (–, 1C, 6), 70.4 (–, 1C, 9), 70.2 (–, 2C, 7+12), 70.0 (–, 1C, 10), 68.6 (–, 1C, 4), 40.3 (–, 1C, 13), 28.3 (+, 3C, 18) — **IR** (ATR) [cm^{–1}]: $\tilde{\nu}$ = 3468, 3346, 1722, 1625, 1532, 1478, 1449, 1378, 1345, 1263, 1211, 1161, 1080, 1009, 916, 833, 759, 737 — **ESI-MS** (DCM/MeOH + 10 mmol/L NH₄Ac): *m/z* (%) = 308.1 (44) [MH⁺], 330.1 (22) [MNa⁺], 352.2 (100) [MNH₄⁺] — **HR-MS** PI-EI (MeOH/Glycerine): (C₁₃H₂₆NO₇) calc. 308.1709 [MH⁺], found 308.1717 — **EA**: calc. (%) for C₁₃H₂₅NO₇ (307.34) + 4/5 H₂O: C 48.53, H 8.33, N 4.35; found: C 48.51, H 8.32, N 4.60



2-[2-(2-Amino-ethoxy)-ethoxy]-ethoxy}-acetic acid hydrochloride (8a)

{2-[2-(2-*tert*-Butoxycarbonylamino-ethoxy)-ethoxy]-ethoxy}-acetic acid **7a** (3.00 g, 9.8 mmol) was diluted with 10 mL of water, then half concentrated HCl_{aq.} (97.6 mmol) was added to the solution until CO₂ evolution was observed. After stirring for 1 h the reaction was complete as no gas bubbles were formed anymore. The solvent was removed by lyophilizing the aqueous solution to obtain the product as highly viscous, yellowish oil (2.40 g, quant.).

¹H-NMR (400 MHz, D₂O): δ [ppm] = 4.28 (s, 2H, 4), 3.84-3.75 (m, 10H, 6+7+9+10+12+14), 3.27 (t, ³J_{H,H} = 5.0 Hz, 2H, 13) — ¹³C-NMR (100 MHz, D₂O): δ [ppm] = 174.3 (C_{quat.}, 1C, 3), 71.1, 69.7, 69.6, 69.5, 67.6, 66.4 (–, 6C, 4+6+7+9+10+12), 39.2 (–, 1C, 13) — ES-MS (MeCN/TFA): *m/z* (%) = 207.9 (100) [MH⁺], 229.9 (17) [MNa⁺]

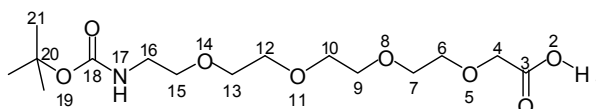


(2-[2-[2-(9H-Fluoren-9-ylmethoxycarbonylamino)-ethoxy]-ethoxy]-ethoxy)-acetic acid (9a)

2-[2-(2-Amino-ethoxy)-ethoxy]-ethoxy}-acetic acid hydrochloride **8a** (2.45 g, 10.1 mmol) was diluted with 5 mL of water and Potassium carbonate (4.17 g, 30.2 mmol) was added. After 15 min stirring at room temperature, N-(9H-Fluoren-2-ylmethoxycarbonyloxy)-succinimide (5.09 g, 15.1 mmol) was added in portions over 30 min and stirring was continued for 16 h. The solution was adjusted to pH 9 by adding aqueous Sodium hydroxide solution (2 M) and the aqueous layer was washed with DCM (3 x 200 mL). Conc. HCl_{aq.} was added while stirring to reach pH ~ 2 and the crude product was extracted with DCM (5 x 100 mL). After drying of the organic phase over MgSO₄, filtration and evaporation of the solvent, the product was isolated by flash column chromatography (DCM → DCM : MeOH = 95 : 5 → DCM : MeOH = 9 : 1; *R*_fDCM : MeOH = 8 : 2 = 0.23) as a greenish-yellow solid (2.76 g, 64%).

MP: 46°C — ¹H-NMR (600 MHz Cryo, CDCl₃, COSY, HSQC, HMBC): δ [ppm] = 7.72 (d, ³J_{H,H} = 7.5 Hz, 2H, 23), 7.59 (d, ³J_{H,H} = 7.3 Hz, 2H, 20), 7.36 (dd, ³J_{H,H} = 7.4 Hz, 7.5 Hz, 2H,

22), 7.28 (dd, $^3J_{H,H} = 7.4$ Hz, 7.5 Hz, 2H, 21), 5.97 (bs, 1H, 14), 4.46-4.31 (m, 2H, 17), 4.19 (t, $^3J_{H,H} = 6.8$, 1H, 18), 3.99 (s, 2H, 4), 3.74-3.53 (m, 8H, 6+7+9+10), 3.53-3.47 (m, 2H, 12), 3.39-3.29 (m, 2H, 13) — $^{13}\text{C-NMR}$ (150 MHz Cryo, CDCl_3 , COSY, HSQC, HMBC): δ [ppm] = 174.7 ($\text{C}_{\text{quat.}}$, 1C, 3), 156.7 ($\text{C}_{\text{quat.}}$, 1C, 15), 144.0 ($\text{C}_{\text{quat.}}$, 1C, 19), 141.2 ($\text{C}_{\text{quat.}}$, 1C, 24), 127.6 (+, 2C, 22), 127.0 (+, 2C, 21), 125.1 (+, 2C, 20), 119.9 (+, 2C, 23), 70.1-69.8 (–, 6C, 4+6+7+9+10+12), 66.5 (–, 1C, 17), 47.2 (+, 1C, 18), 40.6 (–, 1C, 13) — **IR** (ATR) [cm^{-1}]: $\tilde{\nu} = 3057, 2880, 1706, 1608, 1531, 1449, 1247, 1089, 1023, 740$ — **UV** (MeOH) [nm]: λ (ϵ) = 265 (7552), 269 (10944), 272 (11312), 289 (4040), 300 (4912) — **ESI-MS** (DCM/MeOH + 10 mmol/L NH_4Ac): m/z (%) = 430.2 (100) [MH^+], 447.3 (12) [MNH_4^+], 452.2 (50) [MNa^+] — **HR-MS** PI-LSI (MeOH/Glycerine): ($\text{C}_{23}\text{H}_{28}\text{NO}_7$) calc. 430.1866 [MH^+], found 430.1865

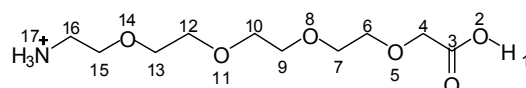


(2-{2-[2-(2-*tert*-Butoxycarbonylamino-ethoxy)-ethoxy]-ethoxy}-ethoxy)-acetic acid (7b)

(2-{2-[2-(2-Hydroxy-ethoxy)-ethoxy]-ethoxy}-ethyl)-carbamic acid *tert*-butyl ester **6b** (0.46 g, 1.6 mmol) was dissolved in 5 mL of THF/Toluene (1 : 1), then Bromoacetic acid (0.66 g, 4.8 mmol) was added. After heating the reaction mixture to 45°C, powdered sodium hydroxide (0.38 mg, 9.5 mmol) was added and the mixture was stirred over night. THF was evaporated and water (10 mL) was added to the toluene layer. After separating the aqueous layer, the organic layer was extracted with aqueous Sodium hydroxide solution (5%; 3 x 15 mL) and the combined aqueous layers were washed with DCM (3 x 30 mL). Conc. $\text{HCl}_{\text{aq.}}$ was added slowly to the aqueous layer while stirring until pH ~ 4 was reached, and was then washed with DCM (3 x 50 mL). After further addition of conc. $\text{HCl}_{\text{aq.}}$ until pH ~ 2 was reached, the product was isolated by extraction with DCM (5 x 50 mL). Drying over MgSO_4 , filtration and evaporation of the solvent yielded a slightly yellow oil with high viscosity (0.52 g, 93%).

$^1\text{H-NMR}$ (600 MHz Cryo, CDCl_3 , COSY, HSQC, HMBC): δ [ppm] = 4.15 (s, 2H, 4), 3.81-3.73 (m, 2H, 6), 3.73-3.59 (m, 10H, 7+9+10+12+13), 3.55 (t, $^3J_{H,H} = 5.1$ Hz, 2H, 11), 3.31 (t, $^3J_{H,H} = 4.8$ Hz, 2H, 12), 1.43 (s, 9H, 15) — $^{13}\text{C-NMR}$ (150 MHz Cryo, CDCl_3 , COSY, HSQC, HMBC): δ [ppm] = 172.5 ($\text{C}_{\text{quat.}}$, 1C, 3), 156.1 ($\text{C}_{\text{quat.}}$, 1C, 18), 79.2 ($\text{C}_{\text{quat.}}$, 1C, 20), 71.1 (–, 1C, 6), 70.5-69.8 (–, 6C, 7+9+10+12+13+15), 68.7 (–, 1C, 4), 40.2 (–, 1C, 16), 28.3

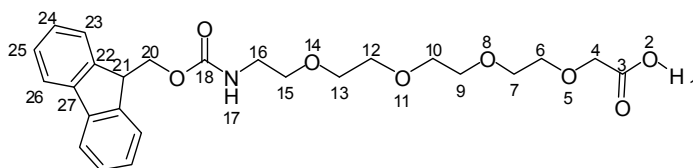
(+, 3C, 21) — **IR** (ATR) [cm^{-1}]: $\tilde{\nu}$ = 3346, 2972, 2927, 2870, 1712, 1521, 1454, 1366, 1277, 1251, 1122, 631, 535, 499, 408 — **ESI-MS** (DCM/MeOH + 10 mmol/L NH_4Ac): m/z (%) = 251.9 (57) [$\text{MH}^+ - \text{Boc}$], 259.9 (20) [$\text{MH}^+ - \text{C}_4\text{H}_8$], 352.0 (76) [MH^+], 369.1 (100) [MNH_4^+], 374.0 (12) [MNa^+] — **HR-MS** PI-EI (MeOH/Glycerine): ($\text{C}_{15}\text{H}_{29}\text{NO}_8$) calc. 352.1966 [MH^+], found 352.1969 — **EA**: calc. (%) for $\text{C}_{15}\text{H}_{29}\text{NO}_8$ (351.40) + 3/5 H_2O : C 49.74, H 8.40, N 3.87; found: C 49.76, H 8.10, N 4.64



(2-{2-[2-(2-Amino-ethoxy)-ethoxy]-ethoxy}-ethoxy)-acetic acid hydrochloride (8b)

(2-{2-[2-(2-*tert*-Butoxycarbonylamino-ethoxy)-ethoxy]-ethoxy}-ethoxy)-acetic acid **7b** (3.00 g, 8.5 mmol) was diluted with 10 mL of water, then half concentrated HCl_{aq} (14.2 mL, 85.3 mmol) was added until formation of CO_2 was observed. After stirring for 1 h the reaction was complete. The solvent was removed by lyophilization of the aqueous solution to obtain the product as highly viscous, yellowish oil (2.50 g, quant.).

$^1\text{H-NMR}$ (400 MHz, D_2O): δ [ppm] = 4.28 (s, 2H, 4), 3.84-3.75 (m, 14H, 6+7+9+10+12+13+15), 3.28 (t, $^3J_{\text{H,H}}$ = 5.0 Hz, 2H, 16) — **$^{13}\text{C-NMR}$** (100 MHz, D_2O): δ [ppm] = 174.4 ($\text{C}_{\text{quat.}}$, 1C, 3), 70.1, 69.7, 69.6, 69.5, 67.7, 66.4 (—, 8C, 4+6+7+9+10+12+13+15), 39.2 (—, 1C, 16) — **ESI-MS** ($\text{H}_2\text{O}/\text{MeOH}$ + 10 mmol/L NH_4Ac): m/z (%) = 252.0 (100) [MH^+], 274.0 (9) [MNa^+]

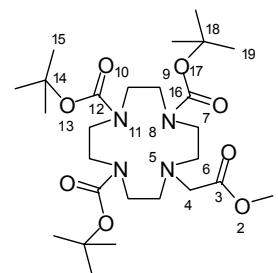


[2-(2-{2-[2-(9H-Fluoren-9-yl-methoxycarbonylamino)-ethoxy]-ethoxy}-ethoxy)-ethoxy]-acetic acid (9b)

2-{2-[2-(2-Amino-ethoxy)-ethoxy]-ethoxy}-ethoxy)-acetic acid hydrochloride **8b** (2.25 g, 7.8 mmol) was diluted in 5 mL of water, then Potassium carbonate (3.24 g, 23.5 mmol) was added and deprotonation was observed as gas formation occurred. After 15 min stirring at room temperature, N-(9H-Fluoren-2-ylmethoxycarbonyloxy)succinimide (3.96 g, 11.7 mmol)

was added in portions over 30 min and stirring was continued for 16 h. The solution was adjusted to pH 9 by adding aqueous Sodium hydroxide solution (2 M) and the aqueous layer was washed with DCM (3 x 200 mL). Conc. HCl_{aq.} was added while stirring to reach pH ~ 2 and the crude product was extracted with DCM (5 x 100 mL). After drying of the organic layer over MgSO₄, filtration and evaporation, the product was purified by flash column chromatography (DCM → DCM : MeOH = 95 : 5 → DCM : MeOH = 9 : 1; $R_{f,DCM : MeOH : TFA} = 9 : 0.5 : 0.5 = 0.22$) to obtain a greenish-yellow, hygroscopic solid (1.70 g, 46%).

MP: 51°C — **¹H-NMR** (400 MHz, CDCl₃, COSY, NOESY, HSQC, HMBC): δ [ppm] = 7.73 (d, $^3J_{H,H} = 7.5$ Hz, 2H, 26), 7.60 (d, $^3J_{H,H} = 7.3$, 2H, 23), 7.37 (dd, $^3J_{H,H} = 7.4$ Hz, 7.4 Hz, 2H, 25), 7.29 (ddd, $^3J_{H,H} = 7.4$ Hz, 7.4 Hz, $^4J_{H,H} = 1.1$ Hz, 2H, 24), 5.90 (bs, 1H, 17), 4.37 (d, $^3J_{H,H} = 6.9$, 2H, 20), 4.20 (t, $^3J_{H,H} = 6.8$, 1H, 21), 3.98 (s, 2H, 4), 3.68-3.47 (m, 14H, 6+7+9+10+12+13+15), 3.42-3.29 (m, 2H, 16) — **¹³C-NMR** (100 MHz, CDCl₃, COSY, NOESY, HSQC, HMBC): δ [ppm] = 174.6 (C_{quat.}, 1C, 3), 156.7 (C_{quat.}, 1C, 18), 144.0 (C_{quat.}, 2C, 22), 141.2 (C_{quat.}, 2C, 27), 127.6 (+, 2C, 25), 127.0 (+, 2C, 24), 125.1 (+, 2C, 23), 119.8 (+, 2C, 26), 70.1 (–, 1C, 15), 70.0-69.8 (–, 6C, 6+7+9+10+12+13), 69.6 (–, 1C, 4), 66.5 (–, 1C, 20), 47.2 (+, 1C, 21), 40.7 (–, 1C, 16) — **IR** (ATR) [cm^{–1}]: $\tilde{\nu} = 3049, 2874, 1710, 1607, 1538, 1449, 1349, 1246, 1092, 1030, 945, 858, 760, 740$ — **UV** (MeOH) [nm]: λ (ε) = 269 (12664), 272 (12784), 288 (4672), 300 (5344) — **ESI-MS** (DCM/MeOH + 10 mmol/L NH₄Ac): m/z (%) = 474.2 (100) [MH⁺], 491.3 (15) [MNH₄⁺], 496.2 (45) [MNa⁺] — **HR-MS** PI-LSI (MeOH/Glycerine): (C₂₅H₃₂NO₈) calc. 474.2128 [MH⁺], found 474.2136

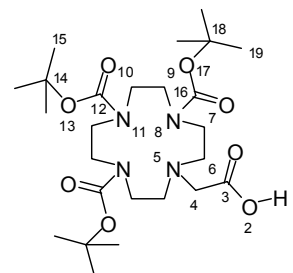


10-Methoxycarbonylmethyl-1,4,7,10-tetraaza-cyclododecane-1,4,7-tricarboxylic acid tri-tert-butyl ester (12)

3-Boc-cyclen **11** (1.00 g, 2.1 mmol) was dissolved in 20 mL of MeCN, then Potassium carbonate (0.35 g, 2.6 mmol) and Methyl bromoacetate (0.36 g, 2.4 mmol) were added. The mixture was stirred over night at 50°C, then solids were filtered off and the solvent was

evaporated to obtain the crude product, which was purified by column chromatography (EtOAc : PE = 1 : 1; $R_{f\text{EtOAc : PE}} = 7 : 3 = 0.63$) yielding a pale yellow solid (1.16 g, quant.).

MP: 69°C — **¹H-NMR** (600 MHz, CDCl₃, NOESY, HSQC, HMBC): δ [ppm] = 3.66 (s, 3H, 1), 3.60-3.11 (m, 14H, 4+7+9+10), 2.99-2.75 (m, 4H, 6), 1.45 (s, 9H, 15), 1.42 (s, 18H, 19) — **¹³C-NMR** (150 MHz, CDCl₃, NOESY, HSQC, HMBC): δ [ppm] = 171.1 (C_{quat.}, 1C, 3), 156.1, 155.7, 155.3 (C_{quat.}, 3C, 12+16+16'), 79.7 (C_{quat.}, 1C, 18), 79.5 (C_{quat.}, 1C, 18'), 79.2 (C_{quat.}, 1C, 14), 54.9 (–, 1C, 6), 53.6 (–, 1C, 6'), 51.2 (+, 1C, 1), 50.9 (–, 1C, 4), 50.0 (–, 2C, 9+9'), 47.7 (–, 2C, 7+7'), 47.3 (–, 1C, 10), 47.0 (–, 1C, 10'), 28.7 (+, 3C, 15), 28.4 (+, 6C, 19) — **IR** (ATR) [cm^{–1}]: $\tilde{\nu}$ = 2974, 2933, 2874, 1739, 1692, 1456, 1413, 1364, 1246, 1180, 978, 859, 772 — **ESI-MS** (DCM/MeOH + 10 mmol/L NH₄Ac): m/z (%) = 345.2 (10) [MH⁺ – 2Boc], 389.2 (10) [MH⁺ – Boc – C₄H₈], 445.3 (38) [MH⁺ – Boc], 489.3 (7) [MH⁺ – C₄H₈], 545.4 (100) [MH⁺] — **EA:** calc. (%) for C₂₆H₄₈N₄O₈ (544.69): C 57.33, H 8.88, N 10.29; found: C 57.04, H 8.83, N 10.05



10-Carboxymethyl-1,4,7,10-tetraaza-cyclododecane-1,4,7-tricarboxylic acid tri-tert-butyl ester (13)

10-Methoxycarbonylmethyl-1,4,7,10-tetraaza-cyclododecane-1,4,7-tricarboxylic acid tri-*tert*-butyl ester **12** (1.26 g, 2.3 mmol) was dissolved in 30 mL of Acetone/water (3 : 1), Lithium hydroxide monohydrate (0.29 g, 6.9 mmol) was added and the mixture was stirred over night at 50°C. Afterwards, Acetone was evaporated and the aqueous layer was acidified with aqueous KHSO₄ (5%). The product was extracted with EtOAc and isolated after drying over MgSO₄, filtration and evaporation of the solvent as yellowish solid (1.10 g, quant.).

MP: 138°C — **¹H-NMR** (600 MHz, CDCl₃, NOESY, HSQC, HMBC): δ [ppm] = 3.61-3.21 (m, 14H, 4+7+9+10), 2.85 (bs, 4H, 6), 1.45 (s, 9H, 15), 1.43 (s, 18H, 19) — **¹³C-NMR** (150 MHz, CDCl₃, NOESY, HSQC, HMBC): δ [ppm] = 173.4 (C_{quat.}, 1C, 3), 156.2 (C_{quat.}, 2C, 16), 155.5 (C_{quat.}, 1C, 12), 80.1 (C_{quat.}, 2C, 18), 79.7 (C_{quat.}, 1C, 14), 54.3 (–, 2C, 6), 52.4

(–, 1C, 4), 49.9 (–, 2C, 9), 47.5 (–, 4C, 7+10), 28.6 (+, 3C, 15), 28.4 (+, 6C, 19) — **ESI-MS** (DCM/MeOH + 10 mM NH₄OAc): m/z (%) = 431.3 (52) [MH⁺ – Boc], 475.3 (10) [MH⁺ – C₄H₈], 531.4 (100) [MH⁺]

Solid-phase peptide-cyclen conjugate synthesis (17a and 17b)

The peptides were synthesized on an Advanced Chemtech 496 MOS synthesizer. Rink Amide MBHA resin and Fmoc protecting group strategy were used. Coupling was achieved by TBTU/HOBt/DIPEA. HOBt was used as a 0.45 M solution, TBTU as a 0.44 M solution and DIPEA as a 1.2 M solution, all in DMF. The Fmoc-protected amino acids as well as the Fmoc-protected amino-PEG-acid spacer and also the cyclen building block were dissolved in NMP as 0.4 M solutions. The syntheses were carried out in a 96 well reactor block where wells were left empty in between used ones due to the danger of resin being blown across the block, thus contaminating other wells. The peptides were synthesized on 50 mg resin. The lot of the resin used had a loading of 0.72 mmol/g (manufacturer's claims). Before each synthesis the resin was allowed to preswell in DMF for 30 min. Each coupling was done twice using a 5-fold excess of HOBt and slightly less than 5-fold excess of TBTU. DIPEA was used in 10-fold excess. Fmoc deprotection was done by shaking the resin with 40% Piperidine in DMF for 3 min, subsequent washing and addition of 20% Piperidine in DMF followed by shaking for 10 min. After completion, the resin was washed with MeOH, DCM and Et₂O (5 x 2 mL each). Cleavage from the resin was afforded by shaking the resin for 3 h after addition of 1.5 mL of TFA/TIS/water (90 : 5 : 5). After filtering off the resin, the TFA solution was reduced in volume to about 0.5 mL. It was then transferred to a Falcon tube and precipitated with cold Et₂O. The precipitate was centrifuged at –4°C for 10 min. The solution was then carefully decanted off and the precipitate resuspended in cold Et₂O before being centrifuged again. This resuspending/centrifuging step was repeated five times. Finally, Et₂O was decanted off again and the peptide dried under vacuum. The peptides were analysed by ESI-MS and LC-MS or HPLC or both and purified by preparative HPLC.

Peptide-cyclen conjugate **17a**: **ESI-MS**: m/z (%) = 305.8 (100) [M + 3H⁺]³⁺, 458.3 (74) [M + 2H⁺]²⁺, 573.6 (4) [M + 2H⁺ + TFA]²⁺, 915.7 (1) [MH⁺]

Peptide-cyclen conjugate **17b**: **ESI-MS**: m/z (%) = 480.3 (100) [M + 2H⁺]²⁺, 1073.9 (9) [MH⁺ + TFA]

General procedure hybrid-ligands 1a and 1b

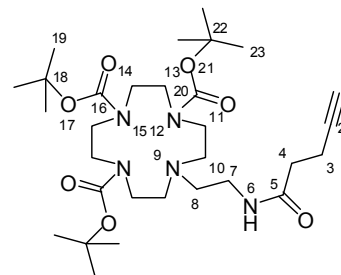
Hybrid-ligand precursors were dissolved in a small amount of water and pH 8 was adjusted by addition of LiOH (1 M) or NaHCO₃ (10% w/v). Then, 1 eq of ZnCl₂ was added as 1 M aqueous solution, which was prepared in advance. After heating the mixtures to reflux for 2 h, the products were obtained by lyophilization as colorless, amorphous solids in sufficient purities and with quantitative yields.

Hybrid-ligand **1a**: **ESI-MS** (MeOH + 10 mmol/L NH₄Ac): m/z (%) = 489.4 (100) [M²⁺], 519.4 (74) [M²⁺ + CH₃COOH], 546.4 (20) [M²⁺ + TFA], 977.8 (1.2) [M²⁺ – H⁺]

Hybrid-ligand **1b**: **ESI-MS** (H₂O/MeOH + 10 mmol/L NH₄Ac): m/z (%) = 511.3 (100) [M²⁺]²⁺, 541.3 (12) [M²⁺ + CH₃COOH]²⁺, 568.3 (8) [M²⁺ + TFA]²⁺, 1021.5 (0.3) [M²⁺ – H⁺], 1035.6 (0.1) [M²⁺ – H⁺ + TFA], 1057.6 (0.2) [M²⁺ + Cl[–]]

2-{2-[2-(2-{[(4-Methylphenyl)sulfonyl]oxy}ethoxy)ethoxy]ethoxy}ethyl-4-methyl-benzene sulfonate (tetra(ethylene glycol)-ditosylate) (21b)

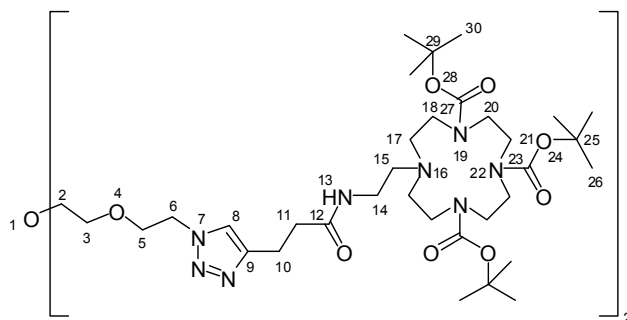
Tetra(ethylene glycol) **20b** (5.00 g, 4.40 mL, 25.7 mmol) and 4-Methylbenzene-1-sulfonyl chloride (14.7 g, 77.2 mmol) were dissolved in about 100 mL of THF and cooled to 0°C in an ice-bath. Then, Potassium hydroxide (10.1 g, 180.2 mmol) dissolved in 25 mL of water was added dropwise (~1 h). After additional 2 h of stirring at room temperature the mixture was poured into water/Et₂O (50 mL/150 mL). The organic layer was separated and the aqueous layer was re-extracted three times with Et₂O. The combined organic layers were washed with saturated NH₄Cl-solution and water and were dried over MgSO₄ before evaporating the solvent. The clean product was obtained by column-chromatography (EtOAc : MeOH = 95 : 5; R_f EtOAc : MeOH = 9 : 1 ~ 0,6) as a orange-brown, viscous oil (12.9 g, quant.) identical in every aspect to that prepared by the literature procedure.⁴²



***N*-10-(2-Aminoethyl)-1,4,7,10-tetraazacyclododecan-1,4,7-tricarboxylic acid-tri-*tert*-butyl ester-pent-4-ynamide (**23**)**

4-Pentynoic-acid (0.04 g, 0.4 mmol) was dissolved in a mixture of DCM and DMF in a nitrogen flushed round bottom flask, then DIPEA (0.24 g, 250 μ L, 1.8 mmol) and HOBT monohydrate (0.08 g, 0.5 mmol) were added. When the mixture was cooled to 0°C, EDC (0.08 g, 87 μ L, 0.5 mmol) and 10-(2-Aminoethyl)-1,4,7,10-tetraazacyclododecan-1,4,7-tricarboxylic-acid-tri-*tert*-butylester **23** (0.32 g, 0.6 mmol) – in portions – were added. After 12 h of stirring at room temperature, the mixture was quenched with water. Then, the organic layer was separated and the aqueous layer was extracted with DCM. The combined organic layers were washed with Citric acid solution (10%), dried over MgSO₄ and the solvent was evaporated. The crude product was purified by flash chromatography (EtOAc : MeOH = 95 : 5, R_f = 0.4) to obtain a colorless solid (0.20 g, 82%).

MP: 66-68°C — **¹H-NMR** (600 MHz, CDCl₃, COSY, HSQC, HMBC): δ [ppm] = 6.76 (bs, 1H, NH), 3.44 (s, 4H, 13), 3.32 (s, 4H, 14), 3.29-3.15 (m, 6H, 7+11), 2.73-2.43 (m, 6H, 8+10), 2.43-2.39 (m, 2H, 3), 2.35 (t, $^3J_{H,H}$ = 7.1 Hz, 2H, 4), 1.90 (t, $^3J_{H,H}$ = 2.5 Hz, 1H, 1), 1.38 (s, 9H, 19), 1.36 (s, 18H, 23) — **¹³C-NMR** (150 MHz, CDCl₃, COSY, HSQC, HMBC): δ [ppm] = 172.9 (C_{quat.}, 1C, 5), 155.8 (C_{quat.}, 2C, 20), 155.4 (C_{quat.}, 1C, 16), 83.0 (C_{quat.}, 1C, 2), 79.6 (C_{quat.}, 3C, 18+22), 69.0 (+, 1C, 1), 55.0 (–, 2C, 10), 52.3 (–, 1C, 8), 49.8 (–, 2C, 14), 48.5 (–, 2C, 13), 47.9 (–, 2C, 11), 36.4 (–, 1C, 7), 35.0 (–, 1C, 4), 28.4 (+, 9C, 19+23), 14.8 (–, 1C, 3) — **IR** (ATR) [cm^{–1}]: $\tilde{\nu}$ = 2975, 2927, 1763, 1543, 1458, 1413, 1364, 1246, 1152, 1039, 975, 858, 773 — **ESI-MS** (DCM/MeOH + 10 mmol/L NH₄Ac): m/z (%) = 596.4 (100) [MH⁺] — **HR-MS** PI-EI: (C₃₀H₅₃N₅O₇) calc. 595.3945 [MH⁺], found 595.3937

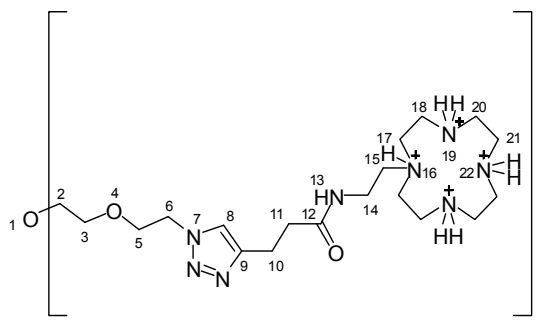


Boc-N-[2-(1,4,7,10-Tetraazacyclododec-1-yl)-ethyl]-3-{1-[2-(2-{2-[2-(4-{2-[2(1,4,7,10-tetraazacyclododec-1-yl)-ethylcarbamoyl]-ethyl}-[1,2,3]triazol-1-yl)ethoxy]-ethoxy}-ethoxy)-ethyl]-1H-[1,2,3]triazol-4-yl}-propionamide (25)

N-10-(2-Aminoethyl)-1,4,7,10-tetraazacyclododecan-1,4,7-tricarboxylic acid-tri-*tert*-butyl ester-pent-4-ynamide **24** (0.50 g, 0.84 mmol) was dissolved in 20 mL of MeOH. Then, Copper(II)sulfate hexahydrate (0.03 g, 0.13 mmol) and Sodium ascorbic acid (0.05 g, 0.25 mmol) were dissolved in a small amount of water – resulting in a dark brown solution, which turned slowly into beige – and poured into the reaction flask while stirring. When the reaction solution's color turns from beige to light blue within the first minute's further sodium ascorbic acid was added. The mixture was then warmed to 40°C and stirred for 20 min followed by the addition of 1-{2-[2-(2-Azidoethoxy)ethoxy]ethoxy}-2-azido-ethane **22b** (0.10 g, 0.42 mmol). Reaction was complete after stirring at 50°C for 30 min. Subsequently, MeOH was evaporated and a brown, viscous residue was left, insoluble in water. After addition of water (15 mL) and Chloroform (20 mL), the organic layer was separated and the aqueous solution was extracted with Chloroform (3 x 20 mL). The combined organic layers were dried over MgSO₄, filtered and evaporated. The resulting residue was cleaned by a short column filtration using flash silica gel (1.5 cm x 4 cm; EtOAc : EtOH = 95 : 5 → 7 : 3) to gain a colorless, resin-like solid (0.55 g, 91%).

MP: 89°C — **¹H-NMR** (400 MHz, CDCl₃, COSY, HSQC, HMBC): δ [ppm] = 7.45 (s, 2H, 8), 6.76 (bs, 2H, NH), 4.40 (t, ³J_{H,H} = 5.1 Hz, 4H, 6), 3.77 (t, ³J_{H,H} = 5.1 Hz, 4H, 5), 3.55-3.39 (m, 16H, 2+3+20), 3.38-3.10 (m, 20H, 14+18+21), 2.93 (t, ³J_{H,H} = 7.4 Hz, 4H, 10), 2.74-2.33 (m, 16H, 11+15+17), 1.38 (s, 18H, 26), 1.36 (s, 36H, 30) — **¹³C-NMR** (100 MHz, CDCl₃, COSY, HSQC, HMBC): δ [ppm] = 172.9 (C_{quat.}, 2C, 12), 155.8 (C_{quat.}, 4C, 27), 155.3 (C_{quat.}, 2C, 23), 146.4 (C_{quat.}, 2C, 9), 122.2 (C_{quat.}, 2C, 8), 79.5 (C_{quat.}, 4C, 29), 79.3 (C_{quat.}, 2C, 25), 70.3 (–, 4C, 2+3), 69.3 (–, 2C, 5), 55.6-53.7 (–, 4C, 17), 51.8 (–, 2C, 15), 49.9 (–, 2C, 6), 49.7 (–, 4C, 21), 48.2 (–, 4C, 20), 47.8 (–, 4C, 18), 35.8 (–, 2C, 14), 35.3 (–, 2C, 11), 28.5 (+, 6C, 26), 28.3 (+, 12C, 30), 21.3 (–, 2C, 10) — **IR** (ATR) [cm^{–1}]: $\tilde{\nu}$ = 2972, 2931, 1681, 1543,

1459, 1414, 1364, 1247, 1153, 1107, 1050, 976, 858, 773 — **UV** (MeCN) [nm]: λ (ϵ) = 215 (4821) — **ESI-MS** (DCM/MeOH + 10 mmol/L NH₄Ac): m/z (%) = 718.7 (100) [$M + 2H^+$]²⁺, 1436.2 (13) [MH^+], 1458.3 (4) [MNa^+] — **EA**: calc. (%) for C₆₈H₁₂₂N₁₆O₁₇ (1435.83) + 4 H₂O: C 54.16, H 8.69, N 14.86; found: C 54.11, H 8.50, N 14.70

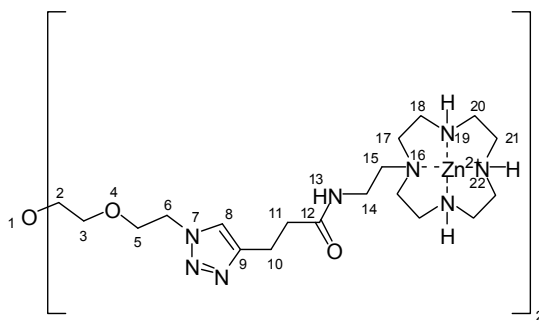


***N*-[2-(1,4,7,10-Tetraaza-cyclododec-1-yl)-ethyl]-3-{1-[2-(2-{2-[2-(4-{2-[2(1,4,7,10-tetraaza-cyclododec-1-yl)-ethylcarbamoyl]-ethyl}-[1,2,3]triazol-1-yl)ethoxy]ethoxy}-ethoxy)-ethyl]-H-[1,2,3]triazol-4-yl}-propionamide octahydrochloride (26 · 8 HCl)**

Boc-protected *N*-[2-(1,4,7,10-Tetraaza-cyclododec-1-yl)-ethyl]-3-{1-[2-(2-{2-[2-(4-{2-[2(1,4,7,10-tetraaza-cyclododec-1-yl)-ethylcarbamoyl]-ethyl}-[1,2,3]triazol-1-yl)ethoxy]ethoxy}-ethoxy)-ethyl]-1H-[1,2,3]triazol-4-yl}-propionamide **25** (0.10 g, 0.07 mmol) was dissolved in a small amount of DCM and cooled down to 0°C. While stirring rapidly, HCl saturated Et₂O (2.7 mL) was dropped into the reaction mixture. After 12 h of stirring at room temperature, the solvent was evaporated *in vacuo* to dryness to obtain the product (0.07 g, 99%) as a greenish-yellow solid.

MP: 85°C — **¹H-NMR** (600 MHz, D₂O, COSY, HSQC, HMBC): δ [ppm] = 8.10 (s, 2H, 8), 4.55 (t, ³ $J_{H,H}$ = 4.9 Hz, 4H, 6), 3.80 (t, ³ $J_{H,H}$ = 4.9 Hz, 4H, 5), 3.46-3.42 (m, 4H, 2), 3.41-3.35 (m, 4H, 3), 3.18 (t, ³ $J_{H,H}$ = 6.5 Hz, 14), 3.13 (t, ³ $J_{H,H}$ = 5.0 Hz, 8H, 19), 3.10-3.05 (m, 8H, 18), 3.10-3.05 (m, 8H, 20), 2.93 (³ $J_{H,H}$ = 7.3 Hz, 4H, 10), 2.86 (³ $J_{H,H}$ = 4.7 Hz, 8H, 17), 2.64 (t, ³ $J_{H,H}$ = 6.4 Hz, 4H, 15), 2.51 (t, ³ $J_{H,H}$ = 6.4 Hz, 4H, 11) — **¹³C-NMR** (150 MHz, D₂O, COSY, HSQC, HMBC): δ [ppm] = 174.0 (C_{quat.}, 2C, 12), 143.2 (C_{quat.}, 2C, 9), 126.5 (C_{quat.}, 2C, 8), 69.5 (–, 2C, 2), 69.3 (–, 2C, 3), 67.8 (–, 2C, 5), 52.3 (–, 2C, 6), 51.9 (–, 2C, 15), 48.2 (–, 4C, 17), 43.4 (–, 4C, 20), 42.4 (–, 4C, 18), 41.8 (–, 4C, 21), 35.1 (–, 2C, 11), 33.6 (–, 2C, 14), 19.2 (–, 2C, 10) — **ESI-MS** (DCM/MeOH + 10 mmol/L NH₄Ac): m/z (%) = 279.2 (100) [$M + 3H^+$]³⁺, 418.7 (96) [$M + 2H^+$]²⁺, 835.7 (5) [MH^+]

A column was filled with a strong basic anion exchange resin (OH⁻-form; 1.5 cm x 3 cm) and rinsed first with a mixture of water/MeOH (1 : 1) then followed by pure water. The above obtained compound was dissolved in a small amount of water and eluted from the column thus yielding the salt-free ligand **26** (0.05 g, quant.).



Bis-Zinc(II){N-[2-(1,4,7,10-Tetraaza-Cyclododec-1-yl)-ethyl]-3-{1-[2-(2-{2-[2-(4-{2-[2(1,4,7,10-tetraaza-cyclododec-1-yl)-ethylcarbamoyl]-ethyl}-[1,2,3]triazol-1-yl)ethoxy]ethoxy}-ethoxy)-ethyl]-1H-[1,2,3]triazol-4-yl}-propionamide} tetrachloride (18c)

N-[2-(1,4,7,10-Tetraaza-cyclododec-1-yl)-ethyl]-3-{1-[2-(2-{2-[2-(4-{2-[2(1,4,7,10-tetraaza-cyclododec-1-yl)-ethylcarbamoyl]-ethyl}-[1,2,3]triazol-1-yl) ethoxy]ethoxy}-ethoxy)-ethyl]-1H-[1,2,3]triazol-4-yl}-propionamide **26** (60.0 mg, 0.07 mmol) and Zinc(II)chloride (19.6 mg, 0.14 mmol) were dissolved separately in a small amount of water and then dropped simultaneously in 2 mL of warm water while stirring. The pH was adjusted to 7-8 with aqueous Lithium hydroxide (1 M). After 7 h of reflux, the mixture was cooled down to ~5°C in the fridge. As no precipitation occurred, also when MeOH or EtOH were added, the solvent was evaporated and subsequently lyophilized to obtain the product (62 mg, 92%) as a light brown solid.

MP: 109°C — **¹H-NMR** (400 MHz, D₂O, COSY, HSQC, HMBC): δ [ppm] = 7.88 (s, 2H, 8), 4.64 (dd, ³J_{H,H} = 4.9 Hz, 5.2 Hz, 4H, 6), 3.99 (dd, ³J_{H,H} = 4.9 Hz, 5.2 Hz, 4H, 5), 3.93-3.85 (m, 2H, 13), 3.68-3.63 (m, 4H, 2), 3.62-3.56 (m, 4H, 3), 3.18 (dd, ³J_{H,H} = 6.9 Hz, 7.3 Hz, 14), 3.13-2.78 (m, 40H, 10+15+17+16+20+21), 2.65 (dd, ³J_{H,H} = 7.2 Hz, 7.3 Hz, 4H, 11) — **¹³C-NMR** (100 MHz, D₂O, COSY, HSQC, HMBC): δ [ppm] = 175.0 (C_{quat.}, 2C, 12), 146.4 (C_{quat.}, 2C, 9), 123.7 (C_{quat.}, 2C, 8), 69.7 (–, 2C, 2), 69.5 (–, 2C, 3), 67.8 (–, 2C, 5), 51.3 (–, 2C, 15), 50.0 (–, 2C, 6), 49.5 (–, 4C, 17), 44.4 (–, 4C, 21), 43.5 (–, 4C, 20), 42.2 (–, 4C, 18), 35.2 (–, 2C, 11), 33.6 (–, 2C, 14), 21.0 (–, 2C, 10) — **ESI-MS** (H₂O/MeOH + 10 mmol/L

NH₄Ac): m/z (%) = 480.4 (70) $[M + 2H^+]^{2+}$, 498.4 (17) $[M + 3H^+ + Cl^-]^{2+}$, 517.4 (23) $[M + 4H^+ + 2Cl^-]^{2+}$

Bis-Copper(II){N-[2-(1,4,7,10-Tetraaza-cyclododec-1-yl)-ethyl]-3-{1-[2-(2-{2-[2-(4-{2-[2(1,4,7,10-tetraaza-cyclododec-1-yl)-ethylcarbamoyl]-ethyl}-[1,2,3]triazol-1-yl)ethoxy]ethoxy}-ethoxy)-ethyl]-1H-[1,2,3]triazol-4-yl]-propionamide} tetrachloride (19c)

N-[2-(1,4,7,10-Tetraaza-cyclododec-1-yl)-ethyl]-3-{1-[2-(2-{2-[2-(4-{2-[2(1,4,7,10-tetraaza-cyclododec-1-yl)-ethylcarbamoyl]-ethyl}-[1,2,3]triazol-1-yl) ethoxy]ethoxy}-ethoxy)-ethyl]-1H-[1,2,3]triazol-4-yl}-propionamide **26** (68.0 mg, 0.07 mmol) and Copper(II)chloride (18.6 mg, 0.14 mmol) were dissolved separately in a small amount of water and then dropped simultaneously in 2 mL of warm water while stirring resulting in a deep blue solution. The pH was adjusted to 7-8 with aqueous Lithium hydroxide (1 M). After 7 h of reflux, the mixture was cooled down to ~5°C in the fridge. The solvent was evaporated and subsequently lyophilized to obtain the product (68 mg, 89%) as a dark green solid.

MP: 126°C — **ESI-MS** (H₂O/MeOH + 10 mmol/L NH₄Ac): m/z (%) = 479.3 (95) $[M + 2H^+]^{2+}$, 497.3 (35) $[M + 3H^+ + Cl^-]^{2+}$, 516.3 (19) $[M + 4H^+ + 2Cl^-]^{2+}$

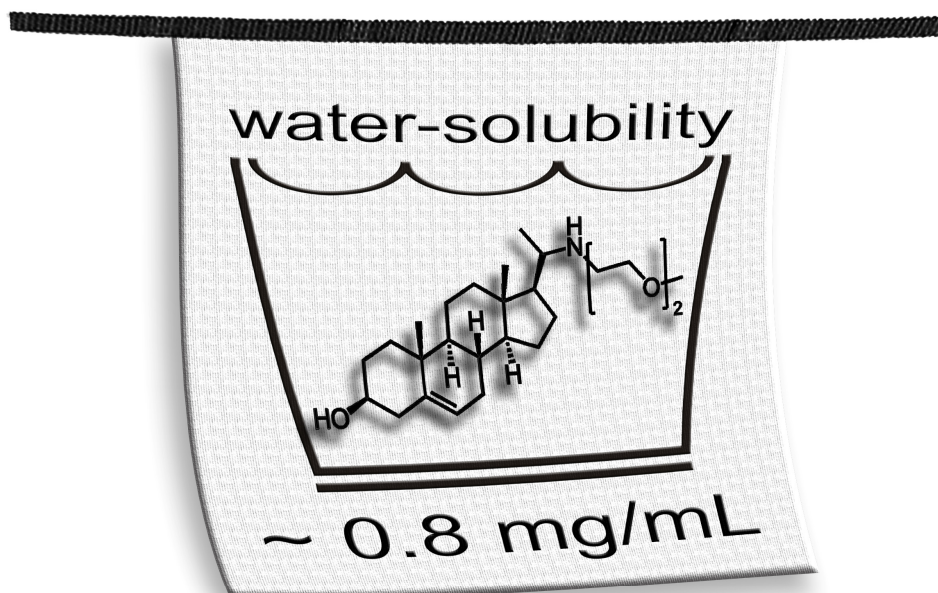
4.7 REFERENCES

- ¹ M. R. Arkin and J. A. Wells, *Nat. Rev. Drug Discovery*, **2004**, *3*, 301-317.
 - ² A. J. Wilson, *Chem. Soc. Rev.*, **2009**, *38*, 3289-3300.
 - ³ A. Bach, C. N. Chi, G. F. Pang, L. Olsen, A. S. Kristensen, P. Jemth and K. Strømgaard, *Angew. Chem., Int. Ed.*, **2009**, *121*, 9865-9869.
 - ⁴ A. Mulder, J. Huskens and D. N. Reinhoudt, *Org. Biomol. Chem.*, **2004**, *2*, 3409-3424.
 - ⁵ C. A. Hunter and H. L. Anderson, *Angew. Chem., Int. Ed.*, **2009**, *48*, 7488-7499.
 - ⁶ J. D. Badjic, A. Nelson, S. J. Cantrill, W. B. Turnbull and J. F. Stoddart, *Acc. Chem. Res.*, **2005**, *38*, 723-732.
 - ⁷ M. Malumbres and A. Pellicer, *Front. Biosci.*, **1998**, *3*, d887-912.
 - ⁸ A. Wittinghofer and N. Nassar, *Trends Biochem. Sci.*, **1996**, *21*, 488-491.
 - ⁹ A. Wittinghofer and H. Waldmann, *Angew. Chem., Int. Ed.*, **2000**, *39*, 4192-4214.
 - ¹⁰ M. Geyer, T. Schweins, C. Herrmann, T. Prisner, A. Wittinghofer and H. R. Kalbitzer, *Biochemistry*, **1996**, *35*, 10308-10320.
 - ¹¹ M. Spoerner, C. Herrmann, I. R. Vetter, H. R. Kalbitzer and A. Wittinghofer, *Proc. Natl. Acad. Sci. USA*, **2001**, *98*, 4944-4949.
 - ¹² M. Spoerner, T. Graf, B. König and H. R. Kalbitzer, *Biochem. Biophys. Res. Comm.*, **2005**, *334*, 709-713.
 - ¹³ S. Aoki and E. Kimura, *Rev. Mol. Biotechnol.*, **2002**, *90*, 129-155.
 - ¹⁴ S. Aoki and E. Kimura, *Chem. Rev.*, **2004**, *104*, 769-788.
 - ¹⁵ M. Kruppa, D. Frank, H. Leffler-Schuster and B. König, *Inorg. Chim. Acta*, **2006**, *359*, 1159-1168.
 - ¹⁶ I. C. Rosnizeck, T. Graf, M. Spoerner, J. Tränkle, D. Filchtinski, C. Herrmann, L. Gremer, I. R. Vetter, A. Wittinghofer, B. König and H. R. Kalbitzer, *Angew. Chem.*, **2010**, *accepted*.
 - ¹⁷ D. Barnard, H. Y. Sun, L. Baker and M. S. Marshall, *Biochem. Biophys. Res. Comm.*, **1998**, *247*, 176-180.
 - ¹⁸ P. A. Boriack-Sjodin, S. M. Margarit, D. Bar-Sagi and J. Kuriyan, *Nature*, **1998**, *394*, 337-343.
 - ¹⁹ G. J. Clark, J. K. Drugan, R. S. Terrell, C. Bradham, C. J. Der, R. M. Bell and S. Campbell, *Proc. Natl. Acad. Sci. USA*, **1996**, *93*, 1577-1581.
-

- ²⁰ B. Ford, K. Skowronek, S. Boykevisch, D. B. Bar-Sagi and N. Nassar, *J. Biol. Chem.*, **2005**, *280*, 25697-25705.
- ²¹ H. R. Kalbitzer, M. Spoerner, P. Ganser, C. Hozsa and W. Kremer, *J. Am. Chem. Soc.*, **2009**, *131*, 16714-16719.
- ²² G. Dirscherl, R. Knape, P. Hanson and B. König, *Tetrahedron*, **2007**, *63*, 4918-4928.
- ²³ G. Dirscherl and B. König, *Eur. J. Org. Chem.*, **2008**, 597-634.
- ²⁴ P. R. Ashton, J. Huff, S. Menzer, I. W. Parsons, J. A. Preece, J. F. Stoddart, M. S. Tolley, A. J. P. White and D. J. Williams, *Chem. Eur. J.*, **1996**, *2*, 31-44.
- ²⁵ M. Goncalves, K. Estieu-Gionnet, T. Berthelot, G. Lain, M. Bayle, X. Canon, N. Betz, A. Bikfalvi and G. Deleris, *Pharm. Res.*, **2005**, *22*, 1411-1421.
- ²⁶ A. R. Katritzky, S. K. Singh, N. K. Meher, J. Doskocz, K. Suzuki, R. Jiang, G. L. Sommen, D. A. Ciaramitaro and P. J. Steel, *ARKIVOC*, **2006**, 43-62.
- ²⁷ F. J. Dekker, N. J. de Mol, J. van Ameijde, M. J. E. Fischer, R. Ruijtenbeek, F. A. M. Redegeld and R. M. J. Liskamp, *ChemBioChem*, **2002**, *3*, 238-242.
- ²⁸ Y.-S. Kim, K. M. Kim, R. Song, M. J. Jun and Y. S. Sohn, *J. Inorg. Biochem.*, **2001**, *87*, 157-163.
- ²⁹ L. Lebeau, P. Oudet and C. Mioskowski, *Helv. Chim. Acta*, **1991**, *74*, 1697-1706.
- ³⁰ C. Visintin, A. E. Aliev, D. Riddall, D. Baker, M. Okuyama, P. M. Hoi, R. Hiley and D. L. Selwood, *Org. Lett.*, **2005**, *7*, 1699-1702.
- ³¹ J. W. Jeon, S. J. Son, C. E. Yoo, I. S. Hong, J. B. Song and J. Suh, *Org. Lett.*, **2002**, *4*, 4155-4158.
- ³² S. Brandes, C. Gros, F. Denat, P. Pullumbi and R. Guillard, *Bull. Soc. Chim. Fr.*, **1996**, *133*, 65-73.
- ³³ V. V. Rostovtsev, L. G. Green, V. V. Fokin and K. B. Sharpless, *Angew. Chem., Int. Ed.*, **2002**, *41*, 2596-2599.
- ³⁴ C. W. Tornøe, C. Christensen and M. Meldal, *J. Org. Chem.*, **2002**, *67*, 3057-3064.
- ³⁵ R. Reichenbach-Klinke, M. Kruppa and B. König, *J. Am. Chem. Soc.*, **2002**, *124*, 12999-13007.
- ³⁶ J. Tucker, G. Sczakiel, J. Feuerstein, J. John, R. S. Goody and A. Wittinghofer, *Embo J.*, **1986**, *5*, 1351-1358.
- ³⁷ F. C. Neidhardt, B. L. Bloch and D. F. Smith, *J. Bacteriol.*, **1975**, *119*, 736-747.
- ³⁸ J. John, R. Sohmén, J. Feuerstein, R. Linke, A. Wittinghofer and R. S. Goody, *Biochemistry*, **1990**, *29*, 6058-6065.
-

- ³⁹ J. Klein, R. Meinecke, M. Mayer and B. Meyer, *J. Am. Chem. Soc.*, **1999**, *121*, 5336-5337.
- ⁴⁰ M. Mayer and B. Meyer, *Angew. Chem., Int. Ed.*, **1999**, *38*, 1784-1788.
- ⁴¹ T. Scherf and J. Anglister, *Biophys. J.*, **1993**, *64*, 754-761.
- ⁴² X. Jiang, X. Yang, C. Zhao and L. Sun, *J. Phys. Org. Chem.*, **2009**, *22*, 1-8.

5 SYNTHESIS OF NEW WATER-SOLUBLE CHOLESTEROL DERIVATIVES



Water-soluble cholesterol derivatives for studies investigating the role of Cholesterol in mammalian cells under physiological conditions are rare. Therefore, efficient syntheses for new cholesterol derivatives with enhanced water-solubility have been developed. Either substitution at C(3)-OH of Cholesterol with ethylene glycols or reductive amination at the keto group of Pregnenolone yielded steroids with significantly increased water-solubility. The solubility of the cholesterol derivatives in water was determined by ^1H -NMR spectroscopy in D_2O with DSS as reference to be 1 to 6 mg/mL at room temperature. The comparison of resonance signal line width in water and chloroform solution showed little aggregation for compound **4** and **5**, while broader resonance signals indicate micelle formation for compound **9**.

5.1 INTRODUCTION

Cholesterol is an essential lipid, which plays an important role as structural and functional component regulating membrane fluidity over the range of physiological temperatures and permeability of the plasma membrane of mammalian cells. In cells, Cholesterol is the molecular precursor for steroid hormones (e.g. Testosterone, Progesterone, etc.) and bile acids, which are both compounds of biological importance. Moreover, Cholesterol was suggested to show antioxidative effects¹ and to be connected with biosynthesis of heart beneficial glycosides (cardiotonic steroids),²⁻⁷ which were furthermore reported to possess anticancer activity.⁸⁻¹¹

Due to insolubility in water, transport of Cholesterol via the bloodstream is accomplished by incorporation in lipoproteins. Among those, particularly low-density lipoproteins (LDL) and high-density lipoproteins (HDL) and their levels in the bloodstream are generally accepted to play an important role in pathogenesis of Atherosclerosis and Coronary heart disease. In the gallbladder, changes in the composition of bile can lead to formation of gallstones, which consist mainly of Cholesterol. In the last decades, Cholesterol was discussed in connection with the pathogenesis of Alzheimer disease, as it is assumed to promote the formation of plaques, which finally intercept the synaptical transmission in neurons.¹²⁻¹⁶

Investigations under physiological conditions and thus, in aqueous solution would be useful to further understand the role of Cholesterol and its derivatives in mammalian cells. Binding studies of Cholesterol towards several proteins will benefit dramatically from derivatives that show enhanced water-solubility. However, only a small number of water-soluble cholesterol derivatives have been published or are commercially available so far. Several working groups have introduced cholesterols with enhanced polarity due to attachment of polar residues to the C(3)-OH group via ester bond formation.¹⁷⁻²⁰ However, beyond physiological conditions this linkage is pH sensitive. While *Wang et al.* reported water-soluble lipopolymers for gene delivery, which were obtained by grafting Cholesterol onto branched Poly(ethyleneimine) of 1800 and 10,000 Da, respectively,²¹⁻²³ hydrophilicity of Cholesterol can also be enhanced by formation of a host - guest complex in presence of Methyl- β -cyclodextrin. Preparations of the latter kind are commercially available. However, the low content (4%) and the stability of this complex are limitations that reduce drastically the presence of free Cholesterol as such in aqueous solution. Therefore, its usage for binding studies as well as investigations with NMR spectroscopic methods is not possible. More

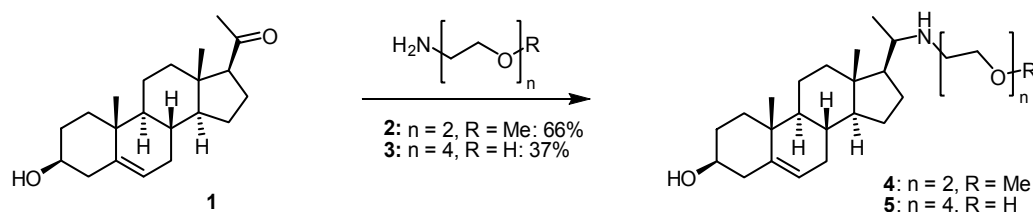
conveniently, *Roelen et al.*²⁴ synthesized water-soluble derivatives by attachment of ethylene glycol phosphorothioate monogalactosides to C(3)-OH of Cholesterol via an ether bond. However, these cholesterol derivatives were reported to form micelles and hence, investigations of their behaviour as single molecules are hampered.

We report the synthesis of two different types of cholesterol derivatives with enhanced water-solubility. Attachment of hydrophilic ethylene glycol to mediate solubility was performed by either ether-bond formation at the cholesteryl-hydroxy group or reductive amination of Pregnenolone using the corresponding mono-amino functionalized ethylene glycols. The solubility and aggregation behaviour of these cholesterol derivatives in buffered aqueous solution was investigated by ¹H-NMR.

5.2 RESULTS & DISCUSSION

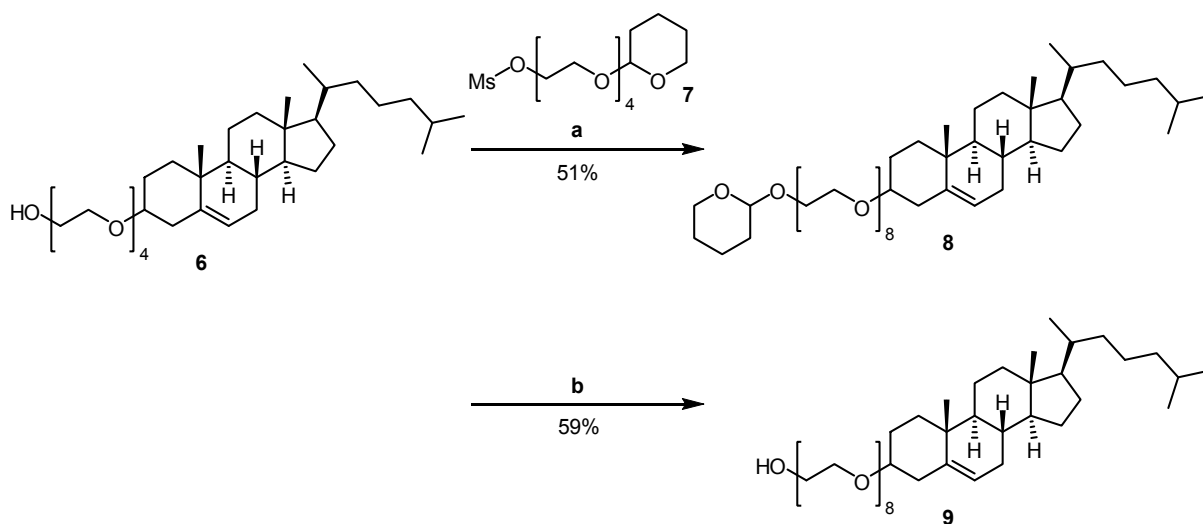
5.2.1 Design of Water-Soluble Cholesterol Derivatives & Synthesis Strategy

In order to enhance the water-solubility of Cholesterol, derivatives **4**, **5** and **9** were synthesized using two different approaches: In a first approach, the hydrophobic aliphatic side chain was replaced by hydrophilic ethylene glycol to increase the water-solubility. The starting material Pregnenolone **1** is a natural product obtained by enzymatic cleavage of the aliphatic steroid chain. The keto group was derivatized by reductive amination under mild conditions yielding 3 β -Hydroxy-20-aza-(8-N-2,5-dioxaoctan)-pregnane **4** or 3 β -Hydroxy-20-aza-(12-N-3,6,9-trioxaundecan-1-ol)-pregnane **5**. Similar to reported procedures,²⁵ primary aminoethylene glycols **2** or **3** were reacted with **1** in the presence of Sodium cyanoborohydride at pH 6 to give the cholesterol derivatives **4** and **5** in moderate to good yield. (Scheme 1) The aminoethylene glycols **2** and **3** were synthesized as previously reported in literature.²⁶⁻³⁰



Scheme 1: Synthesis of pregnenolone-derived cholesterol derivatives with enhanced water-solubility by reductive amination. Reagents and conditions: $\text{Na}(\text{CN})\text{BH}_3$, $\text{MeOH}_{\text{abs.}}$, $\text{THF}_{\text{abs.}}$, AcOH (pH 6), reflux, 12 h

In a second approach, the ethylene glycol chain was introduced by substitution of the hydroxy group of Cholesterol and thus, without changing the steroid scaffold. The log P values for such cholesterol derivatives were calculated (ACD/Labs, Advanced Chemistry Developments, Toronto, Ontario/Canada) to estimate an appropriate length of the ethylene glycol chain; for comparison the log P values of compound **4** (4.90 ± 0.52) and **5** (3.95 ± 0.60) were calculated. Octaethylene glycol substituted Cholesterol (8.15 ± 0.75) was selected for synthesis, as further extension of the glycol chain lengths changed calculated log P values only marginal. To synthesize compound **9**, freshly recrystallised Cholesterol was tosylated to obtain Cholest-5-en-3 β -ol-*p*-toluenesulfonate as previously reported.³¹ Subsequently, Tetra(ethylene) glycol and Cholest-5-en-3 β -ol-*p*-toluenesulfonate were reacted according to a published method in a Williamson type ether synthesis to give 11-(5-Cholesten-3 β -yloxy)-3,6,9-trioxaundecan-1-ol (**6**) in good yield.²⁴ Tetra(ethylene) glycol was first mono-THP-protected and the remaining alcohol functionality was transformed into the corresponding mesylate to give 11-(2H-Tetrahydropyran-2-yloxy)-trioxaundecan-1-ol **7** in moderate overall yield.³²⁻³³ Compound **6** was converted into 11-(5-Cholesten-3 β -yloxy)-1-(2H-tetrahydropyran-2-yloxy)-3,6,9,12,15,18-hepta oxatricosan **8** by ether formation with **7**. Finally, acidic cleavage of the THP protecting group by adding *para*-Toluenesulfonic acid gave 11-(5-Cholesten-3 β -yloxy)-3,6,9,12,15,18-hepta oxatricosan-1-ol **9** (OEG-Chol). (Scheme 2)



Scheme 2: Synthesis of OEG-cholesterol 9. Reagents and conditions: a) NaH, THF_{abs.}, 60°C, 24 h; b) *p*-TsOH, MeOH, rt, 12 h

5.2.2 Determination of Water Solubility of Compounds **4**, **5** and **9** by NMR

The new cholesterol derivatives **4**, **5** and **9** were investigated on their water-solubility and aggregation by ^1H -NMR. Therefore, from each compound a saturated solution in D_2O was prepared, which was spiked by a defined amount of DSS (2,2-Dimethyl-2-silapentane-5-sulfonic acid) as reference. Comparison of the integral of DSS (9H at 0.00 ppm) with that of the methyl group *Me-18*³⁴ (3H at ~0.5-0.8 ppm) of the steroid scaffold allowed to determine the concentration of cholesterol derivatives **4** and **5** in the investigated aqueous solution. For compound **9**, the DSS signal was compared with the integral of its octa-ethylene glycol chain.³⁵ Numerical values for water solubility are summarized in Table 1 and were calculated by Equation 1.

$$c_{\text{Chol.}} = \frac{I_{\text{DSS, theor.}}}{I_{\text{DSS, exp.}}} \cdot \frac{I_{\text{Chol., exp.}}}{I_{\text{Chol., theor.}}} \cdot c_{\text{DSS}} \quad \text{Equation 1}$$

^1H -NMR spectra of saturated solutions in D_2O of compounds **5** and **9** resulted in line-broadening of the resonance signals, which indicates the presence of aggregates. In contrast, compound **4** showed a small line width, which is similar to that in corresponding ^1H -NMR resonance signals of **4** in CDCl_3 (see Supporting Information for spectra). Therefore, the water solubility of compound **4** was deduced directly from this spectrum, while the solutions of compounds **5** and **9** were diluted for recording of further ^1H -NMR spectra.

Upon 1:12.5 dilution of compound **5** with D_2O / DSS (0.2 mM), a narrow line width indicated the absence of aggregates and thus, the solubility of **5** as single molecules was calculated from this spectrum (see Supporting Information for spectrum); further dilution steps did not change the line width. Moreover, the ^1H -NMR spectra of compound **5** in D_2O (1:12.5) and CD_3OD , respectively, were in good agreement (see Supporting Information) and showed similar line width.

In contrast, aggregation of compound **9** could not be reduced perceptibly by dilution. The 1:5 dilution did not cause decreasing line widths.³⁶ Line-broadening in D_2O was only found for the signals assigned to the steroid scaffold, but not for those of the ethylene glycol residue. Therefore for compound **9** only the concentration of the saturated solution likely containing aggregates was determined from the octa-ethylene glycol resonance signal. According to the aggregation characteristics of a similar cholesterol derivative published by *Roelen et al.*,²⁴ compound **9** is assumed to form micelles.

Compound	DSS		Solubility of 4, 5, 9 in D ₂ O ³⁷			log P _{calc.}
	c _{DSS} [mM]	int.-DSS, exp.	int.-Chol., exp.	c _{Chol.} [mM]	β _{Chol.} [mg/mL]	
4	0.05	0.92	3.00 ^(a)	2.0 ^(a)	0.8 ^(a)	4.90 ± 0.52
5	0.20	0.63	3.00 ^(b)	2.8 ^(b)	1.4 ^(b)	3.95 ± 0.60
9	0.20	0.29	32 ^(c,d)	6.2 ^(c,d)	6.2 ^(c,d)	8.15 ± 0.75
Cholesterol	0.05	9.00	— ^(e)	— ^(e)	3·10 ⁻⁵ ^(f) 38	9.62 ± 0.28
Pregnenolone	— ^(g)	— ^(g)	— ^(g)	— ^(g)	— ^(g)	4.60 ± 0.28

Table 1: Numerical values determined for water-solubility of cholesterol derivatives 4, 5 and 9.

$I_{DSS, \text{theoret.}} = 9$, $I_{Chol., \text{theoret.}} = 3$; (a) spectra of saturated solutions of **4** did not show any aggregation effects, therefore, water-solubility of **4** was calculated from those integrals; (b) at high concentrations, **5** was found to form aggregates and hence, a saturated solution of **5** was diluted (1:12.5) to obtain spectra from that water-solubility of single molecules could be determined; (c) aggregates of **9** could not be disrupted by dilution (1:5), consequently, maximum concentration of aggregates of **9** in aqueous solution was determined from a saturated solution; (d) due to strong line-broadening in the steroid range of the obtained spectra for **9**, the overall integral for the ethylene glycol chain was used for calculation, since this signal group was found to be hardly affected by aggregation; (e) no cholesterol derived signals were detected in spectra obtained for saturated solution of Cholesterol; (f) literature derived value determined at 30°C; (g) not investigated

5.3 CONCLUSIONS

We presented three new cholesterol derivatives with enhanced solubility in water, which were obtained by attaching ethylene glycol chains to the steroid scaffold. These compounds may offer new possibilities for spectroscopic investigations of cholesterol binding to proteins at physiological conditions. With regard to the length of the attached ethylene glycols, replacement of the non-polar aliphatic side-chain of Cholesterol (compounds **4** and **5**) was more efficient than substitution of the hydroxyl group (compound **9**). ¹H-NMR studies revealed that solubility of **4** and **5** in water is about 1 mg/mL and thus, drastically enhanced compared to Cholesterol (3 x 10⁻⁵ mg/mL).³⁸ In contrast, the high aggregation tendency of compound **9** interfered with solubility calculations. In particular compound **4** is a suitable compound to probe cholesterol – protein interactions in aqueous solutions by spectroscopic studies, as it has sufficient water solubility and a low tendency to form aggregates.

5.4 EXPERIMENTAL SECTION

5.4.1 General

NMR spectroscopy. Bruker Avance 600 (Cryo) (^1H : 600.1 MHz, ^{13}C : 150.1 MHz, $T = 300\text{ K}$), Bruker Avance 400 (^1H : 400.1 MHz, ^{13}C : 100.6 MHz, $T = 300\text{ K}$), Bruker Avance 300 (^1H : 300.1 MHz, ^{13}C : 75.5 MHz, $T = 300\text{ K}$). The chemical shifts are reported in δ [ppm] relative to internal standards (solvent residual peak). The spectra were analyzed by first order, the coupling constants are given in Hertz [Hz]. Characterization of the signals: s = singlet, d = doublet, t = triplet, q = quartet, m = multiplet, bs = broad singlet, dd = double doublet, ddd = double double doublet. Integration is determined as the relative number of atoms. If not stated otherwise, assignment of signals in ^{13}C -spectra was determined with DEPT-technique (pulse angle: 135°) and given as (+) for CH_3 or CH , (–) for CH_2 and (C_{quat}) for quaternary C_{quat} . Error of reported values: chemical shift: 0.01 ppm for ^1H -NMR, 0.1 ppm for ^{13}C -NMR and 0.1 Hz for coupling constants. The solvent used is reported for each spectrum.

Mass spectrometry. Finnigan MAT 95 (LSI), Finnigan MAT TSQ 7000 (ESI).

IR spectrometry. Recorded with a Bio-Rad FTS 2000 MX FT-IR equipped with a Specac Golden Gate Mk II ATR

Optical rotation. Perkin-Elmer PE 241 at 589 nm and room temperature. Cuvette length was 1 dm and data is presented as $[\alpha]_{\text{D}}^{20}$ in $[\text{mL} \cdot \text{g}^{-1} \cdot \text{dm}^{-1}]$

Melting point. Melting points were determined on Büchi SMP.

TLC analysis and column chromatography. Analytical TLC plates (silica gel 60 F254) and silica gel 60 (70-230 or 230-400 mesh) for column chromatography were purchased from Merck. Spots were visualized by staining with ninhydrine in EtOH or anisaldehyde in EtOH/AcOH/ H_2SO_4 .

Methanol (MeOH) was dried by distillation from Mg, tetrahydrofuran (THF) by adsorption. Both were stored over molecular sieves. All other solvents and chemicals were of reagent grade and used without further purification.

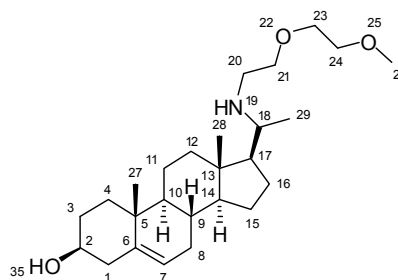
5.4.2 NMR Studies in Aqueous Solution

Saturated solutions of cholesterol were prepared by dissolving them in excess in 99% D_2O containing 50 μM (compound **4**) or 200 μM (compound **5** and **9**), DSS (2,2-Dimethyl-2-silapentane-5-sulfonic acid) for direct referencing. Subsequently, insoluble particles were pelletized by centrifugation and the so obtained saturated supernatant was transferred in a

NMR tube. ^1H NMR measurements were performed at 293 K on a Bruker AVANCE-600 spectrometer equipped with a 5 mm TXI cryo probe operating at a resonance frequency of 600.13 MHz. 90° pulses were applied with a repetition time of 9 s. Water suppression was achieved by applying presaturation or WATERGATE sequence,³⁹ respectively.

5.4.3 Syntheses

The following compounds were synthesized according to literature known procedures and determined to be consistent with analytical data derived from the corresponding published syntheses: 8-N-2,5-Dioxaoctan **2**,²⁶⁻³⁰ 12-N-3,6,9-Trioxaundecan-1-ol **3**,²⁶⁻³⁰ Cholest-5-en-3 β -ol-*p*-toluenesulfonate,³¹ 11-(5-Cholesten-3 β -yloxy)-3,6,9-trioxaundecan-1-ol **6**,²⁴ 11-(2H-Tetrahydropyran-2-yloxy)-trioxaundecan-1-ol **7**.^{32,33}

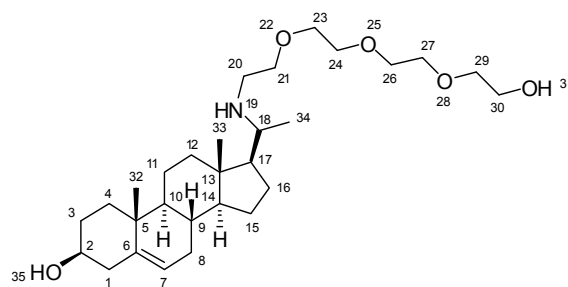


3 β -Hydroxy-20-aza-(8-N-2,5-dioxaoctan)-pregnane (4)

In a nitrogen flushed round bottom flask Pregnenolone **1** (50 mg, 0.16 mmol) was dissolved in 2.5 mL of MeOH_{abs} and 8-N-2,5-Dioxaoctan **2** (223 mg, 0.95 mmol) was added. The pH of the solution was adjusted to ~ 6 by adding Glacial acetic acid. Then, Sodium cyanoborohydride (11 mg, 0.17 mmol) was dissolved in 1 mL of MeOH_{abs} , mixed with 2.5 mL of THF_{abs} and added to the reaction mixture, which was finally stirred over night under reflux. After evaporation of the solvent, the obtained residue was resuspended in 2.5 mL of H_2O and the pH was adjusted to ~ 8 . The solution was extracted with CHCl_3 (3 x 10 mL) and the combined organic layers were washed with water and dried over MgSO_4 . After filtration, the solvent was evaporated yielding a yellow, viscous oil. After flash chromatography (CHCl_3 : EtOH = 6 : 4) the clean product (44 mg, 0.10 mmol, 66%) was obtained as a slightly yellow oil, turning into a colorless solid after several days under reduced pressure (1.0×10^{-3} mbar).

MP: 95°C — ^1H -NMR (600 MHz, CDCl_3 , COSY, HSQC, HMBC): δ [ppm] = 5.38-5.30 (m, 1H, 7), 3.76-3.67 (m, 2H, 21), 3.66-3.59 (m, 2H, 23), 3.56-3.49 (m, 3H, 2+24), 3.37 (s, 3H, 26), 3.09-3.02 (m, 1H, 20), 2.83-2.73 (m, 2H, 18+20'), 2.29 (dd, $^2J_{\text{H,H}} = 12.9$ Hz, $^3J_{\text{H,H}} =$

3.3 Hz, 1H, 1), 2.22 (m, 1H, 1'), 2.02-1.91 (m, 2H, 8+12), 1.87-1.74 (m, 3H, 3+4+16), 1.67-1.61 (m, 1H, 15), 1.61-1.36 (m, 7H, 3'+8'+9+11+12'+16'+17), 1.35-1.16 (m, 2H, 11'+15'), 1.12 (d, $^3J_{H,H} = 6.1$ Hz, 3H, 29), 1.10-1.05 (m, 2H, 4'+14), 1.00 (s, 3H, 27), 0.96 (dt, $^2J_{H,H} = 11.7$ Hz, $^3J_{H,H} = 4.7$ Hz, 1H, 10), 0.74 (s, 3H, 28) — **$^{13}\text{C-NMR}$** (150 MHz, CDCl_3 , HSQC, HMBC): δ [ppm] = 140.1 ($\text{C}_{\text{quat.}}$, 1C, 6), 121.4 (+, 1C, 7), 71.7 (–, 1C, 24), 71.6 (+, 1C, 2), 70.3 (–, 1C, 23), 68.6 (–, 1C, 21), 59.0 (+, 1C, 26), 56.2 (+, 1C, 18), 56.1 (+, 1C, 14), 54.9 (+, 1C, 17), 49.8 (+, 1C, 10), 45.8 (–, 1C, 20), 42.2 (–, 1C, 1), 42.0 ($\text{C}_{\text{quat.}}$, 1C, 13), 39.7 (–, 1C, 12), 37.2 (–, 1C, 4), 36.4 ($\text{C}_{\text{quat.}}$, 1C, 5), 31.7 (+, 1C, 9), 31.7 (–, 1C, 8), 31.6 (–, 1C, 3), 26.4 (–, 1C, 16), 24.1 (–, 1C, 15), 21.0 (–, 1C, 11), 19.4 (+, 1C, 27), 17.8 (+, 1C, 29), 12.3 (+, 1C, 28) — **IR** (ATR) [cm^{-1}]: $\tilde{\nu} = 3342, 2934, 2884, 1681, 1454, 1379, 1106, 1061, 1024, 951, 849, 808$ — **ESI-MS** (DCM/MeOH + 10 mmol/L NH_4Ac): m/z (%) = 420.3 (100) [MH^+] — **HR-MS** PI-LSI (DCM/MeOH/Glycerine): ($\text{C}_{26}\text{H}_{46}\text{NO}_3$) calc. 420.3478 [MH^+], found 420.3473 — **optical rotation**: $[\alpha]_{\text{D}}^{20} = -39.4^\circ$

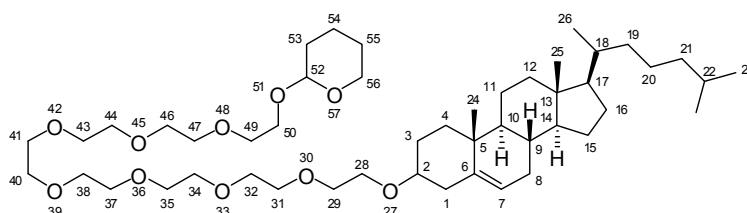


3 β -Hydroxy-20-aza-(12-N-3,6,9-trioxaundecan-1-ol)-pregnane (5)

In a nitrogen flushed round bottom flask Pregnenolone **1** (127 mg, 0.40 mmol) was dissolved in 2.5 mL of $\text{MeOH}_{\text{abs.}}$ and 12-N-3,6,9-Trioxaundecan-1-ol **3** (155 mg, 0.80 mmol) was added. The pH of the solution was maintained to ~ 6 by addition of Glacial acetic acid, a mixture of 2.5 mL of $\text{THF}_{\text{abs.}}$ and Sodium cyanoborohydride (28 mg, 0.44 mmol) dissolved in 1.5 mL of $\text{MeOH}_{\text{abs.}}$ was added. The reaction mixture was stirred over night under reflux. After addition of further reducing agent (28 mg, 0.44 mmol), reflux continued for additional 12 h. Then, solvents were evaporated and the remaining residue was resuspended in 2.5 mL H_2O . In the following, the pH was set to ~ 8 and the solution was extracted with CHCl_3 (3 x 10 mL). The combined organic layers were washed with water and dried over MgSO_4 . After filtration and subsequent evaporation of the solvent, the crude product was purified by flash

chromatography ($\text{CHCl}_3 : \text{EtOH} = 2 : 1 \rightarrow \text{EtOH } 100\%$) to obtain the pure target compound as an orange-brown oil (70 mg, 0.14 mmol, 37%).

$^1\text{H-NMR}$ (600 MHz, CD_3OD , COSY, HSQC, HMBC): δ [ppm] = 5.37-5.31 (m, 1H, 7), 3.75-3.70 (m, 1H, 21), 3.68-3.63 (m, 10H, 23+24+26+27+30), 3.62-3.59 (m, 1H, 21'), 3.57-3.53 (m, 2H, 29), 3.43-3.38 (m, 1H, 2), 3.06-3.01 (m, 1H, 20), 3.00-2.92 (m, 1H, 18), 2.92-2.83 (m, 1H, 20'), 2.28-2.16 (m, 2H, 1+1'), 2.03-1.98 (m, 1H, 12), 1.98-1.94 (m, 1H, 8), 1.86 (dt, $^2J_{\text{H,H}} = 13.3$ Hz, $^3J_{\text{H,H}} = 3.4$ Hz, 1H, 4), 1.84-1.76 (m, 2H, 3+16), 1.73-1.65 (m, 1H, 15), 1.65-1.60 (m, 1H, 11), 1.60-1.40 (m, 5H, 3'+8'+9+11'+17), 1.44-1.37 (m, 1H, 16'), 1.34 (dt, $^2J_{\text{H,H}} = 12.7$ Hz, $^3J_{\text{H,H}} = 4.2$ Hz, 1H, 12'), 1.22-1.15 (m, 1H, 15'), 1.15-1.05 (m, 5H, 4'+14+34), 1.03 (s, 3H, 32), 0.99 (dt, $^2J_{\text{H,H}} = 12.1$ Hz, $^3J_{\text{H,H}} = 4.8$ Hz, 1H, 10), 0.78 (s, 3H, 33) — **$^{13}\text{C-NMR}$** (150 MHz, CD_3OD , HSQC, HMBC): δ [ppm] = 142.2 (C_{quat} , 1C, 6), 122.3 (+, 1C, 7), 73.6 (–, 1C, 29), 72.3 (+, 1C, 2), 71.58 (–, 1C, 26), 71.54 (–, 1C, 27), 71.33 (–, 1C, 24), 71.30 (–, 1C, 23), 68.7 (–, 1C, 21), 62.2 (–, 1C, 30), 57.6 (+, 1C, 14), 56.4 (+, 1C, 18), 55.8 (+, 1C, 17), 51.6 (+, 1C, 10), 46.3 (–, 1C, 20), 43.2 (C_{quat} , 1C, 13), 43.0 (–, 1C, 1), 40.5 (–, 1C, 12), 38.6 (–, 1C, 4), 37.7 (C_{quat} , 1C, 5), 33.1 (+, 1C, 9), 32.9 (–, 1C, 8), 32.3 (–, 1C, 3), 26.8 (–, 1C, 16), 25.1 (–, 1C, 15), 22.2 (–, 1C, 11), 19.9 (+, 1C, 32), 17.5 (+, 1C, 34), 12.7 (+, 1C, 33) — **IR** (ATR) [cm^{-1}]: $\tilde{\nu} = 3343, 2928, 2867, 2111, 1711, 1606, 1461, 1375, 1101, 1069, 963, 841$ — **ESI-MS** (DCM/MeOH + 10 mmol/L NH_4Ac): m/z (%) = 494.5 (100) [MH^+], 496.5 (5) [MNa^+], 528.4 (35) [MCl^-], 552.5 (100) [MCH_3COO^-] — **HR-MS** PI-LSI (MeOH/Glycerine): ($\text{C}_{29}\text{H}_{52}\text{NO}_5$) calc. 494.3845 [MH^+], found 494.3846 — **optical rotation**: $[\alpha]_{\text{D}}^{20} = -41.9^\circ$

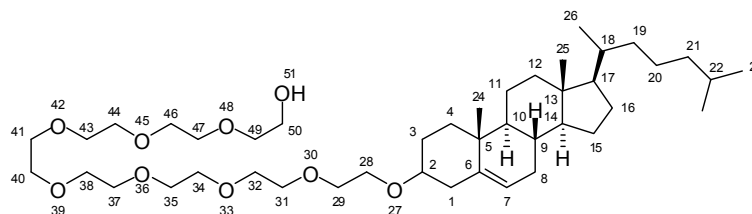


11-(5-Cholesten-3 β -yloxy)-1-(2H-tetrahydropyran-2-yloxy)-3,6,9,12,15,18-heptaooxatricosan (8)

In a nitrogen flushed round bottom flask 11-(5-Cholesten-3 β -yloxy)-3,6,9-trioxaundecan-1-ol **6** (190 mg, 0.34 mmol) and Sodium hydride (0.03 g, 1.13 mmol) in THF_{abs} (2 mL) were stirred for 10-15 min, then 11-(2H-Tetrahydropyran-2-yloxy)-trioxaundecan-1-ol **7** (181 mg, 0.51 mmol) in 1 mL of THF_{abs} was added dropwise. Subsequently, the mixture was stirred

24 h at 60°C. Excess of Sodium hydride was carefully destroyed with MeOH, the solvent was evaporated and the solid partitioned between EtOAc and H₂O (1:1). The aqueous layer was extracted with EtOAc, the combined organic layers were dried over MgSO₄, filtered and evaporated. The clean product (144 mg, 0.17 mmol, 51%) could be isolated after column chromatography on flash silica gel (EtOAc → EtOAc : EtOH = 8 : 2, R_{f, EtOAc} = 0.10) as a slightly yellow oil.

¹H-NMR (600 MHz, CDCl₃, COSY, HSQC, HMBC): δ [ppm] = 5.34-5.29 (m, 1H, 7), 4.64-4.58 (t, ³J_{H,H} = 3.6 Hz, 1H, 52), 3.88-3.82 (m, 2H, 50+56), 3.76-3.70 (m, 1H, 49), 3.67-3.58 (m, 30H, 49'+50'+28^(c)-47^(c)), 3.51-3.46 (m, 1H, 56'), 3.21-3.11 (m, 1H, 2), 2.38-2.31 (ddd, ²J_{H,H} = 13.2 Hz, ³J_{H,H} = 4.6 Hz, ⁴J_{H,H} = 2.3 Hz, 1H, 1), 2.22-2.16 (m, 1H, 1'), 2.02-1.99 (m, 1H, 12), 1.99-1.92 (m, 2H, 8+12'), 1.91-1.86 (m, 1H, 3), 1.85-1.75 (m, 3H, 4+16+54), 1.72-1.67 (m, 1H, 53), 1.62-1.58 (m, 1H, 53'), 1.58-1.54 (m, 2H, 15+55), 1.54-1.45 (m, 6H, 8'+20+20'+22+54'+55'), 1.45-1.41 (m, 2H, 3'+9), 1.38-1.34 (m, 1H, 18), 1.34-1.30 (m, 2H, 11+19), 1.28-1.23 (m, 1H, 16), 1.18-1.10 (m, 3H, 11'+21^(c)), 1.10-1.05 (m, 2H, 15'+17), 1.05-1.01 (m, 1H, 4'), 1.01-0.95 (m, 5H, 14+19'+24), 0.94-0.87 (m, 4H, 10+26), 0.85 (d, ³J_{H,H} = 2.7 Hz, 3H, 23), 0.84 (d, ³J_{H,H} = 2.7 Hz, 3H, 23'), 0.66 (s, 3H, 25) — **¹³C-NMR** (150 MHz, CDCl₃, HSQC, HMBC): δ [ppm] = 140.9 (C_{quat}, 1C, 6), 121.5 (+, 1C, 7), 98.9 (+, 1C, 52), 79.4 (+, 1C, 2), 70.8 (–, 1C, 49), 70.6-70.2 (–, 12C, 31-47), 67.2 (–, 1C, 28), 66.9 (–, 1C, 50), 62.2 (–, 1C, 56), 56.7 (+, 1C, 14), 56.1 (+, 1C, 17), 50.1 (+, 1C, 10), 42.3 (C_{quat}, 1C, 13), 39.7 (–, 1C, 12), 39.5 (–, 1C, 21), 39.0 (–, 1C, 1), 37.2 (–, 1C, 4), 36.8 (C_{quat}, 1C, 5), 36.1 (–, 1C, 19), 35.7 (+, 1C, 18), 31.9 (+, 1C, 9), 31.8 (–, 1C, 8), 30.5 (–, 1C, 53), 28.3 (–, 1C, 3), 28.2 (–, 1C, 16), 28.0 (+, 1C, 22), 25.4 (–, 1C, 55), 24.2 (–, 1C, 15), 23.8 (–, 1C, 11), 22.8 (+, 1C, 23), 22.5 (+, 1C, 23'), 21.0 (–, 1C, 20), 19.4 (–, 1C, 54), 19.3 (+, 1C, 24), 18.7 (+, 1C, 26), 11.8 (+, 1C, 25) — **IR** (ATR) [cm^{–1}]: $\tilde{\nu}$ = 2931, 2866, 1462, 1530, 1251, 1109, 1503, 988, 872 — **ESI-MS** (DCM/MeOH + 10 mmol/L NH₄Ac): *m/z* (%) = 840.7 (100) [MNH₄⁺] — **optical rotation**: [α]_D²⁰ = –11.7°

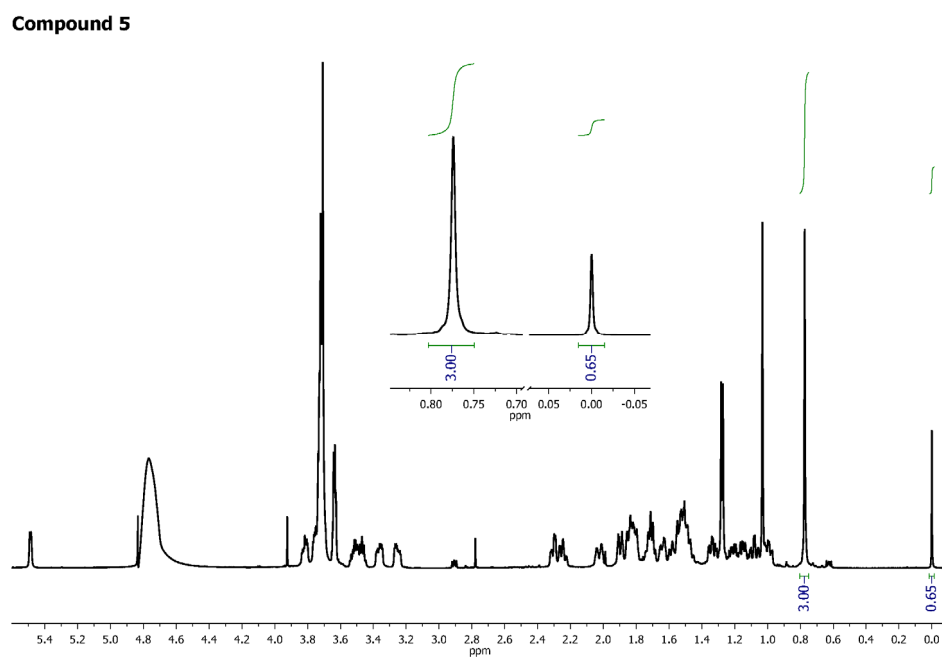
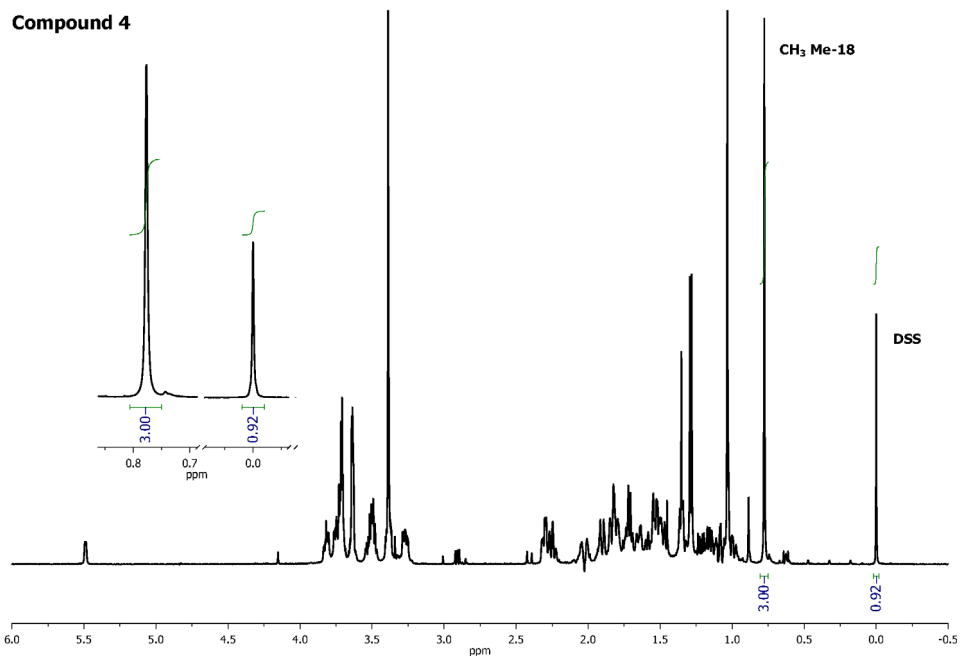


11-(5-Cholesten-3 β -yloxy)-3,6,9,12,15,18-heptaotricosan-1-ol (9)

A solution of 11-(5-Cholesten-3 β -yloxy)-1-(2H-tetrahydropyran-2-yloxy)-3,6,9,12,15,18-heptaotricosan **8** in MeOH was acidified with *p*-Toluene sulfonic acid and left stirring over night at room temperature. Afterwards, water was added and MeOH was evaporated, followed by extracting the aqueous layer with DCM. After drying the combined organic layers over MgSO₄, filtration and evaporation of the solvent, the product (22 mg, 0.03 mmol, 59%) could be isolated by column chromatography on flash silica gel (EtOAc : EtOH = 8 : 2, R_f = 0.15) as an almost colorless oil.

¹H-NMR (600 MHz, CDCl₃): δ [ppm] = 5.38-5.30 (m, 1H, 7), 3.73-3.71 (m, 2H, 50), 3.67-3.59 (m, 30H, 28^(c)-49^(c)), 3.21-3.13 (m, 1H, 2), 2.38-2.34 (ddd, ²*J*_{H,H} = 13.2 Hz, ³*J*_{H,H} = 4.6 Hz, ⁴*J*_{H,H} = 2.3 Hz, 1H, 1), 2.23-2.18 (m, 1H, 1'), 2.02-1.76 (m, 6H, 3+4+8+12^(c)+16), 1.59-1.40 (m, 7H, 3'+9+8'+15+20+20'+22), 1.38-1.23 (m, 4H, 11+16+18+19), 1.17-0.82 (m, 24H, 4'+10+11'+14+15'+17+19'+21^(c)+23^(c)+24+26), 0.66 (s, 3H, 25) — **¹³C-NMR** (150 MHz, CDCl₃): δ [ppm] = 141.0 (C_{quat.}, 1C, 6), 121.5 (+, 1C, 7), 79.5 (+, 1C, 2), 72.6 (–, 1C, 49), 70.8 (–, 1C, 29), 70.6-70.2 (–, 12C, 31-47), 67.3 (–, 1C, 28), 61.6 (–, 1C, 50), 56.8 (+, 1C, 14), 56.2 (+, 1C, 17), 50.2 (+, 1C, 10), 42.3 (C_{quat.}, 1C, 13), 39.8 (–, 1C, 12), 39.5 (–, 1C, 21), 39.0 (–, 1C, 1), 37.2 (–, 1C, 4), 36.9 (C_{quat.}, 1C, 5), 36.2 (–, 1C, 19), 35.8 (+, 1C, 18), 32.0 (+, C, 9), 31.9 (–, 1C, 8), 28.3 (–, 1C, 3), 28.2 (–, 1C, 16), 28.0 (+, 1C, 22), 24.3 (–, 1C, 15), 23.8 (–, 1C, 11), 22.8 (+, 1C, 23), 22.5 (+, 1C, 23'), 21.1 (–, 1C, 20), 19.4 (–, 1C, 24), 18.7 (+, 1C, 26), 11.8 (+, 1C, 25)

5.5 SUPPORTING INFORMATION



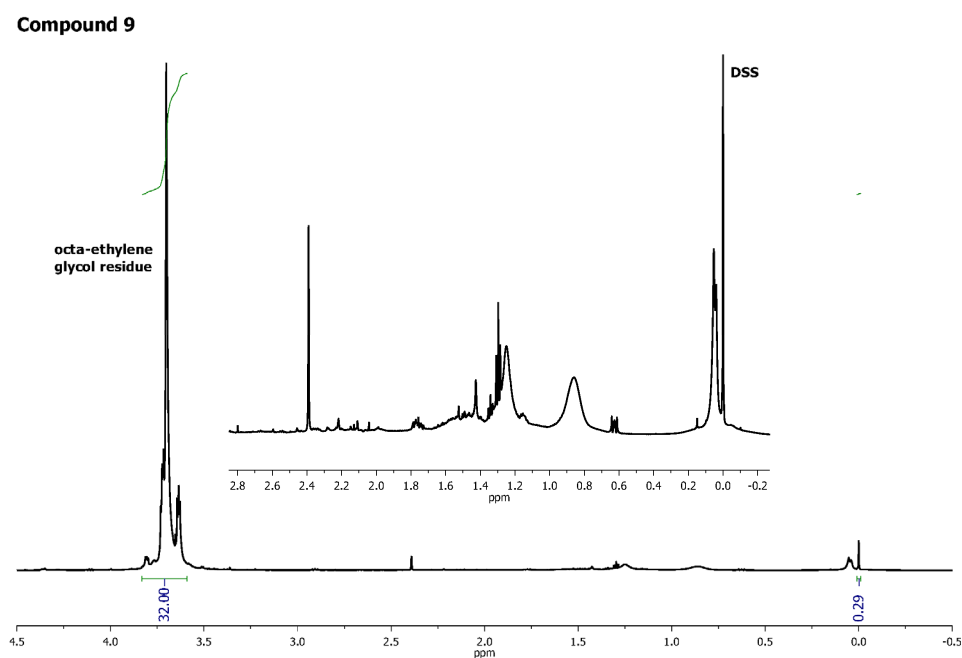
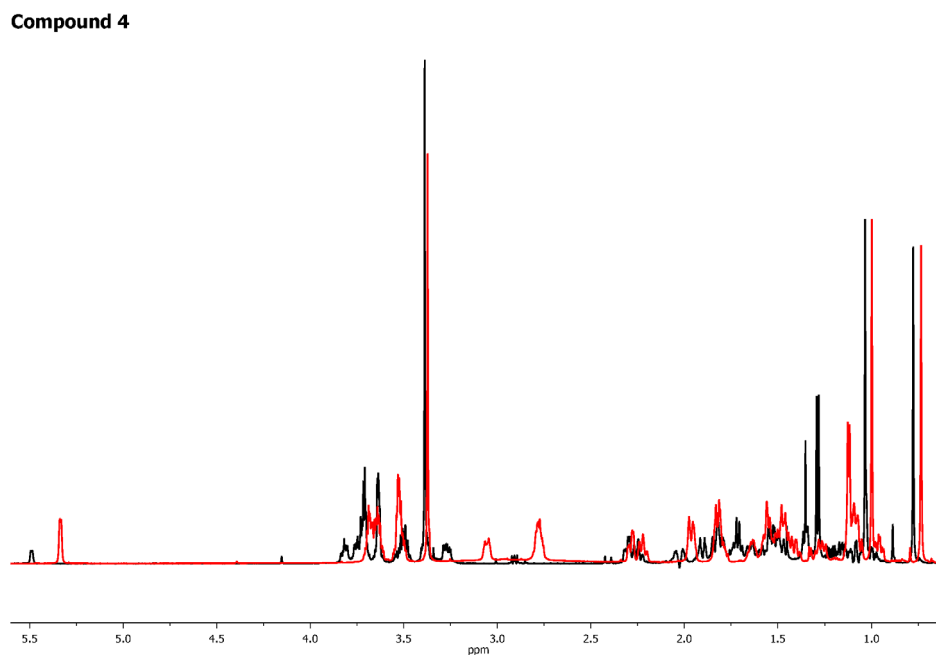


Figure S1: Final ^1H -NMR spectra of solutions of compounds 4, 5 and 9 in D_2O / DSS (0.2 mM) for determination of water-solubility. Saturated solutions of compound 4, 5 and 9 in D_2O were prepared, centrifuged and in the following, the supernatants were investigated by ^1H -NMR; due to regular line width, the amount of dissolved compound 4 in D_2O was directly calculated from the integrals of DSS and CH_3 (Me-18); spectra for compound 5 and 9 show broadened signals indicating formation of aggregates; consequently, solutions of 5 and 9 were diluted for further solubility studies; upon 1:12.5 dilution of a saturated solution of 5 in D_2O , aggregates could be broken up and water-solubility could be calculated; line width of 9 could not be decreased and therefore, only the maximum concentration of aggregated 9 in solution was estimated from the spectrum shown above; H_2O signals were suppressed by WATERGATE (compounds 4 and 9) or presaturation (compound 5)



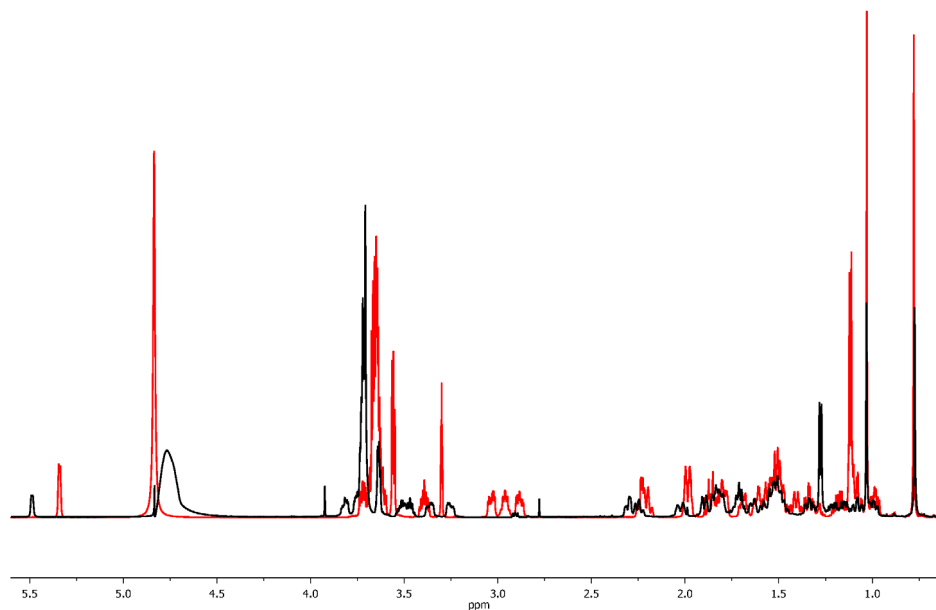
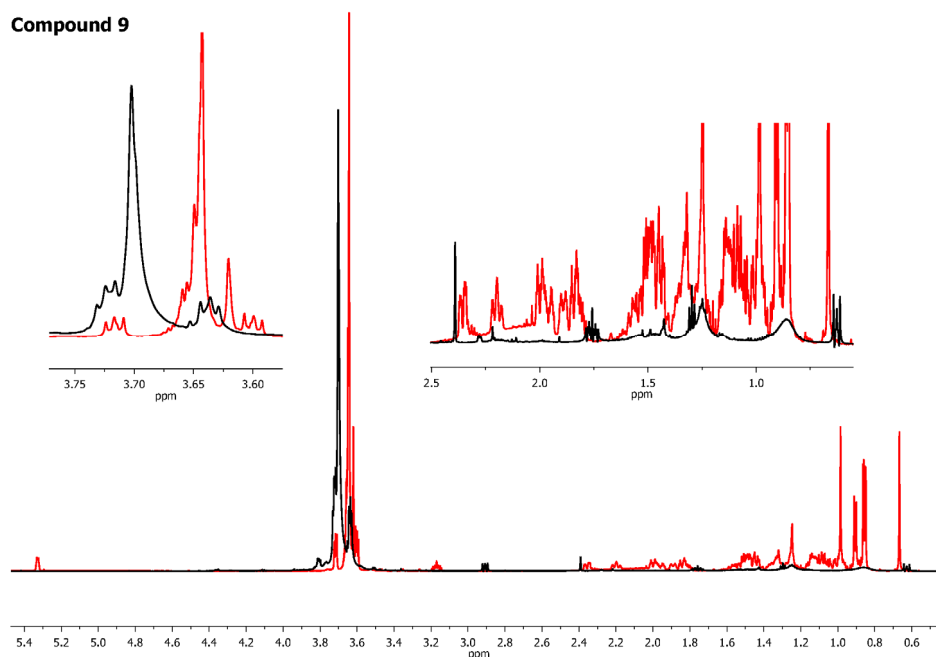
Compound 5**Compound 9**

Figure S2: Overlaying ^1H -NMR spectra of compounds 4, 5 and 9 in D_2O and organic solvent, respectively. For compound 4 and 5, signals obtained in D_2O (4: saturated solution; 5: 1:12.5 dilution of saturated solution) are in good agreement with those in organic solvents (4: 22 mg / 0.7 mL CDCl_3 ; 5: 60 mg / 0.9 mL CD_3OD); in contrast, spectra for compound 9 (D_2O : 1:5 dilution of saturated solution; org.: 20 mg / 0.8 mL CDCl_3) are only consistent in the range of signals that were assigned to the ethylene glycol chain, while the steroid scaffold signals are flattened; D_2O spectra are depicted in black, spectra in organic solvents in red; H_2O signals were suppressed either by WATERGATE (compound 4 and 9) or presaturation (compound 5)

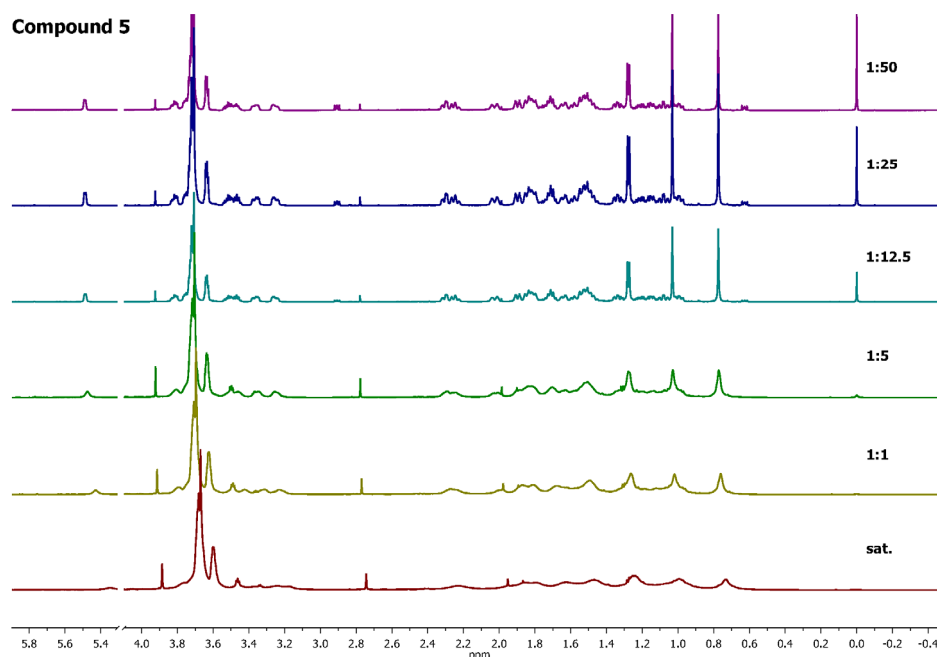


Figure S3: Stacked plot of the ^1H -NMR spectra for dilution of a saturated solution of compound 5 in D_2O / DSS (0.2 mM). By successive dilution of a saturated starting solution of compound 5 with D_2O / DSS (0.2 mM) line width could be decreased; no further improvement was obtained by dilutions higher than 1:12.5, already indicating the presence of monomers of compound 5 in solution; moreover, at higher concentrations, line-broadening was almost exclusively found for protons of the steroid scaffold, but not for those assigned to the ethylene glycol chain, which is in accordance with results for compound 9; H_2O signals were suppressed by presaturation

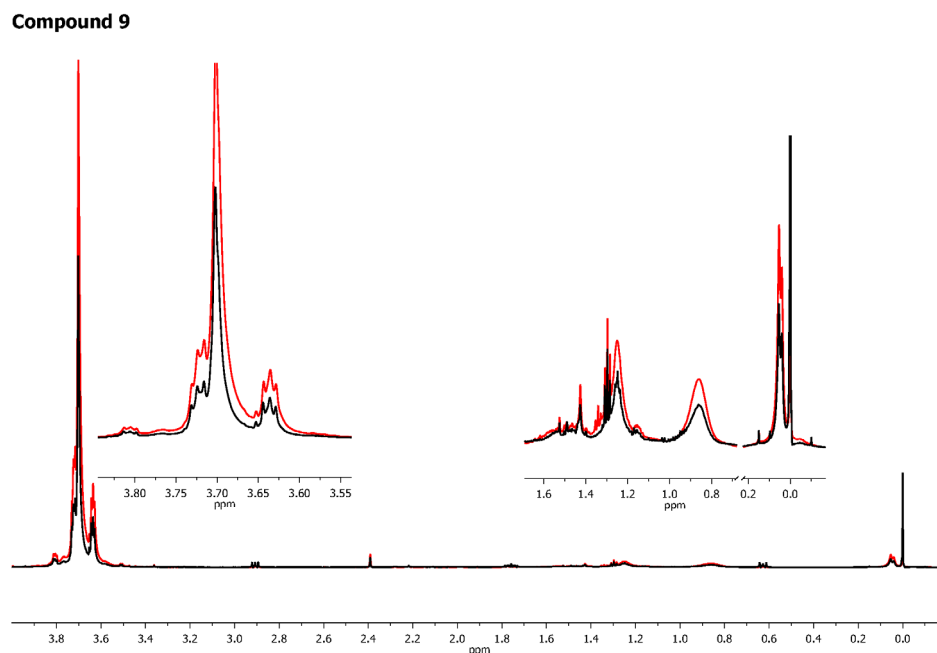


Figure S4: Overlaying ^1H -NMR spectra for dilution of a saturated solution of compound 9 in D_2O / DSS (0.2 mM). By 1:5 dilution (black) of a saturated solution (red) of compound 9 with D_2O / DSS (0.2 mM), line width was not found to decrease; integrals changed in accordance with the dilution ratio; hence, aggregates were not broken up, only their concentration in solution was reduced; H_2O signals were suppressed by WATERGATE

5.6 REFERENCES

- ¹ L. L. Smith, *Free Radic. Biol. Med.*, **1991**, *11*, 47-61.
 - ² J. M. Hamlyn, Z. R. Lu, P. Manunta, J. H. Ludens, K. Kimura, J. R. Shah, J. Laredo, J. P. Hamilton, M. J. Hamilton and B. P. Hamilton, *Clin. Exp. Hypertens.*, **1998**, *20*, 523-533.
 - ³ Y. Komiyama, N. Nishimura, M. Munakata, T. Mori, K. Okuda, N. Nishino, S. Hirose, C. Kosaka, M. Masuda and H. Takahashi, *J. Hypertens.*, **2001**, *19*, 229-236.
 - ⁴ A. Perrin, B. Brasmes, E. M. Chambaz and G. Defaye, *Mol. Cell. Endocrinol.*, **1997**, *126*, 7-15.
 - ⁵ D. Lichtstein, M. Steinitz, I. Gati, S. Samuelov, J. Deutsch and J. Orly, *Life Sci.*, **1998**, *62*, 2109-2126.
 - ⁶ H. M. Qazzaz, Z. Cao, D. D. Bolanowski, B.J. Clark and R. Valdes, Jr., *Clin. Chem.*, **2004**, *50*, 612-620.
 - ⁷ R. I. Dmitrieva, A. Y. Bagrov, E. Lalli, P. Sassone-Corsi, D. M. Stocco and P. A. Doris, *Hypertension*, **2000**, *36*, 442-448.
 - ⁸ Y. Jing, H. Ohizumi, N. Kawazoe, S. Hashimoto, Y. Masuda, S. Nakajo, T. Yoshida, Y. Kuroiwa and K. Nakaya, *Jpn. J. Cancer Res.*, **1994**, *85*, 645-651.
 - ⁹ N. Kawazoe, T. Aiuchi, Y. Masuda, S. Nakajo and K. Nakaya, *J. Biochem.*, **1999**, *126*, 278-286.
 - ¹⁰ Y. Masuda, N. Kawazoe, S. Nakajo, T. Yoshida, Y. Kuroiwa and K. Nakaya, *Leuk. Res.*, **1995**, *19*, 549-556.
 - ¹¹ Y. Sreenivasan, P. B. Raghavendra and S. K. Manna, *J. Clin. Immunol.*, **2006**, *26*, 308-322.
 - ¹² K. Fassbender, M. Simons, C. Bergmann, M. Stroick, D. Lutjohann, P. Keller, H. Runz, S. Kuhl, T. Bertsch, K. von Bergmann, M. Hennerici, K. Beyreuther and T. Hartmann, *Proc. Natl. Acad. Sci. USA*, **2001**, *98*, 5856-5861.
 - ¹³ R. W. Haley and J. M. Dietschy, *Arch. Neurol.*, **2000**, *57*, 1410-1412.
 - ¹⁴ L. M. Refolo, B. Malester, J. LaFrancois, T. Bryant-Thomas, R. Wang, G. S. Tint, K. Sambamurti, K. Duff and M. A. Pappolla, *Neurobiol. Dis.*, **2000**, *7*, 321-331.
 - ¹⁵ M. Simons, P. Keller, B. De Strooper, K. Beyreuther, C. G. Dotti and K. Simons, *Proc. Natl. Acad. Sci. USA*, **1998**, *95*, 6460-6464.
 - ¹⁶ M. Simons, P. Keller, J. Dichgans and J. B. Schulz, *Neurology*, **2001**, *57*, 1089-1093.
 - ¹⁷ K. Chandrasekar and G. Baskar, *Biomacromolecules*, **2007**, *8*, 1665-1675.
-

- ¹⁸ D. V. Ioffe, A. N. Klimov, O. A. Mal'tseva and V. B. Nekrasova, *Khim. Prir. Soedin.*, **1980**, *5*, 655-657.
- ¹⁹ B. Klein, N. B. Kleinman and J. A. Foreman, *Clin. Chem.*, **1974**, *20*, 482-485.
- ²⁰ G. J. Proksch and D. P. Bonderman, *Clin. Chem.*, **1978**, *24*, 1924-1926.
- ²¹ D. A. Wang, A. S. Narang, M. Kotb, A. O. Gaber, D. D. Miller, S. W. Kim and R. I. Mahato, *Biomacromolecules*, **2002**, *3*, 1197-1207.
- ²² M. Lee, J. Rentz, M. Bikram, S. Han, D. A. Bull and S. W. Kim, *Gene Ther.*, **2003**, *10*, 1535-1542.
- ²³ M. Lee, J. Rentz, S. O. Han, D. A. Bull and S. W. Kim, *Gene Ther.*, **2003**, *10*, 585-593.
- ²⁴ H. C. P. F. Roelen, M. K. Bijsterbosch, H. F. Bakkeren, T. J. C. Van Berkel, H. J. M. Kempen, M. Buytenhek, G. A. Van der Marel and J. H. Van Boom, *J. Med. Chem.*, **1991**, *34*, 1036-1042.
- ²⁵ W. Xie, H. R. Peng, D. I. Kim, M. Kunkel, G. Powis and L. H. Zalkow, *Bioorg. Med. Chem.*, **2001**, *9*, 1073-1083.
- ²⁶ P. R. Ashton, J. Huff, S. Menzer, I. W. Parsons, J. A. Preece, J. F. Stoddart, M. S. Tolley, A. J. P. White and D. J. Williams, *Chem. Eur. J.*, **1996**, *2*, 31-44.
- ²⁷ F. J. Dekker, N. J. de Mol, J. van Ameijde, M. J. E. Fischer, R. Ruijtenbeek, F. A. M. Redegeld and R. M. J. Liskamp, *ChemBioChem*, **2002**, *3*, 238-242.
- ²⁸ M. Goncalves, K. Estieu-Gionnet, T. Berthelot, G. Lain, M. Bayle, X. Canron, N. Betz, A. Bikfalvi and G. Deleris, *Pharm. Res.*, **2005**, *22*, 1411-1421.
- ²⁹ A. R. Katritzky, S. K. Singh, N. K. Meher, J. Doskocz, K. Suzuki, R. Jiang, G. L. Sommen, D. A. Ciaramitaro and P. J. Steel, *ARKIVOC*, **2006**, 43-62.
- ³⁰ C. Yanıç, M. W. Bredenkamp, E. P. Jacobs and P. Swart, *Bioorg. Med. Chem. Lett.*, **2003**, *13*, 1381-1384.
- ³¹ V. Barragan-Montero, J. Y. Winum, J. P. Moles, J. Emmanuelle, C. Clavel and J. L. Montero, *Eur. J. Med. Chem.*, **2005**, *40*, 1022-1029.
- ³² F. A. Loiseau, K. K. Hii and A. M. Hill, *J. Org. Chem.*, **2004**, *69*, 639-647.
- ³³ J. Barluenga, A. de Prado, J. Santamaria and M. Tomas, *Organometallics*, **2005**, *24*, 3614-3617.
- ³⁴ Methyl group #18 according to *IUPAC* recommendations for nomenclature of steroids.
- ³⁵ As shown later on, ¹H signals of the steroid scaffold of **9** showed enormous line-broadening, while ¹H signals of the octa-ethylene glycol did not.
-

- ³⁶ For comparison, 1:5 dilution of a saturated solution of compound **5** resulted indeed in improved linewidths.
- ³⁷ For compound **4** and **5**, solubility was determined by comparison of the intergral of DSS at 0.00 ppm (9H) with that of Me-18 (3H).
- ³⁸ H. Y. Saad and W. I. Higuchi, *J. Pharm. Sci.*, **1965**, *54*, 1205-1206.
- ³⁹ M. L. Liu, X. A. Mao, C. H. Ye, H. Huang, J. K. Nicholson and J. C. Lindon, *J. Magn. Reson.*, **1998**, *132*, 125-129.

6 SUMMARY

Chapter 1 of this work deals with pyrene-excimer signalled analyte recognition of small biomolecules. Therefore, pyrene labelled Zn^{2+} -cyclen and bis- Zn^{2+} -bis-cyclen complexes were synthesized. The reversible coordination at physiological pH of Zn^{2+} -cyclens to phosphate anions and to imide moieties, as present in thymine and uracil nucleotides, is well known. In the presence of analytes bearing a phosphate and an imide or two phosphate groups the formation of a ternary complex consisting of two pyrene-labelled metal complexes and the analyte molecule, was observed. The close proximity of the pyrene labels in the complex induced pyrene excimer emission, which was observable by the unarmoured eye. By this, the presence of UMP, UDP, UTP and TTP in buffered aqueous solution was signalled, while other nucleotides were not able to induce excimer emission. In the same way, Zn^{2+} -Cyclen-pyrene acted as luminescent chemosensor for PP_i and Fructose-1,6-bisphosphate in aqueous buffer. In contrast, Bis- Zn^{2+} -bis-cyclen-pyrene was found to be not as selective as the mono-nuclear complex since IDP and ITP also lead to formation of ternary complexes; moreover, UMP, PP_i and Fructose-1,6-bisphosphate did not result in excimer formation.

Chapter 2 demonstrates the ability of pyrene labelled Zn^{2+} -cyclen, which was already introduced in Chapter 1 to be a staining reagent for DNA in agarose gels. The metal chelate was found to coordinate reversibly to the DNA phosphate backbone inducing the formation of pyrene excimers. The typical pyrene excimer emission was used for the detection of the DNA. Staining was limited to agarose gels and less sensitive than Ethidium bromide, but DNA amounts down to 10 ng and short DNA strands (~300 bp) were detectable. Moreover, gel extraction as a standard technique in molecular biology was successfully performed after staining with Zn^{2+} -Cyclen-pyrene. Finally, cytotoxicity tests on HeLa and V-79 cells reveal that the zinc-cyclen pyrene probe is significant less toxic compared to Ethidium bromide.

In Chapter 3, fluorescent probes for the detection of protein phosphorylation on SDS-PAGE are presented. The probes were designed using bis- Zn^{2+} -bis-cyclen as a dinuclear metal-chelate phosphate recognition unit equipped with an environment-sensitive fluorophore. The specificity of the probes is determined by their binding site selectivity towards phosphate ions and the emission wavelength shift induced by the change in the electrostatic environment of the fluorophore upon binding to a phosphorylated amino acid residue. The staining is fully

reversible due to the non-covalent binding of the probe. Gel bands with less than 100 μg of phosphorylated α -Casein were detectable with these new probes on a normal UV-table without specialized equipment like a laser-based gel scanner or a cooled camera detector.

In Chapter 4, the preparation of Zn^{2+} -cyclen-peptide hybrid compounds and bis- Zn^{2+} -cyclen complexes is described as potential binders of the guanine nucleotide binding protein Ras, an important molecular switch in cellular signal transduction. The design of the compounds is based on the previous observation that Zn^{2+} -cyclen complexes could serve as lead compounds for inhibitors of Ras-effector interaction and thus be able to interrupt Ras induced signal transduction. Zn^{2+} -Cyclen selectively stabilizes conformational state 1 of active Ras, a conformational state with drastically decreased affinity to effector proteins like Raf-kinase. To achieve higher binding affinities of such Ras-Raf interaction inhibitors, Zn^{2+} -cyclen conjugates with short peptides, derived from the sequence of the Ras-activator SOS, were prepared by solid phase synthesis protocols. Dinuclear bis- Zn^{2+} -cyclen complexes were obtained from alkyne-azide cycloaddition reactions. NMR investigations of the prepared compounds revealed that the peptide conjugates do not lead to an increase in Ras binding affinity of the metal complex – peptide conjugates. The dinuclear zinc complexes lead to an immediate precipitation of the protein prohibiting spectroscopic investigations of their binding.

Chapter 5 shows the synthesis of three new cholesterol derivatives with enhanced water-solubility. Water-soluble cholesterol derivatives for studies investigating the role of Cholesterol in mammalian cells under physiological conditions are rare so far. Therefore, efficient syntheses for new cholesterol derivatives with enhanced water-solubility have been developed. Either substitution at C(3)-OH of Cholesterol with ethylene glycols or reductive amination at the keto group of Pregnenolone yielded steroids with significantly increased water-solubility. The solubility of the cholesterol derivatives in water was determined by ^1H -NMR spectroscopy in D_2O with DSS as reference to be 1 to 6 mg/mL at room temperature. The comparison of resonance signal line width in water and chloroform solution showed little aggregation for compound **4** and **5**, while broader resonance signals indicate micelle formation for compound **9**.

7 ZUSAMMENFASSUNG

In Kapitel 1 dieser Arbeit wird die molekulare Unterscheidung von kleinen Biomolekülen mittels Analyt-induzierter Pyren-Excimer-Fluoreszenz gezeigt. Die reversible Koordination von Zn^{2+} -Cyclenen an Phosphatanionen und Imide unter physiologischen Bedingungen ist literaturbekannt. Diese Eigenschaft von Zn^{2+} -Cyclen Komplexen in Kombination mit Pyren als Fluorophor führte im Fall von Thymin- und Uracil-Nukleotiden, zur Bildung ternärer Komplexe, die aus zwei Pyren-tragenden Metall-Komplexen und einem Analytmolekül bestehen. Auch andere Analyten mit zwei entsprechenden Bindungsstellen zeigten dieses Verhalten. Die somit erzwungene räumliche Nähe der beiden Pyren-Einheiten führte schließlich bei Anregung zur Bildung eines Pyren-Excimers, dessen Emission sich deutlich von der eines Pyren-Monomers unterscheidet. Dieser Unterschied war auch mit dem bloßen Auge erkennbar. Durch dieses Prinzip konnten in gepufferter, wässriger Lösung UMP, UDP, UTP und TTP nachgewiesen werden, während andere Nukleotide ohne Imid-Einheit als weitere Bindungsstelle für den Zn^{2+} -Cyclen Komplex keine Excimer-Emission induzierten und lediglich Pyren-Monomer Fluoreszenz zeigten. In gleicher Weise fungierte Zn^{2+} -Cyclen-pyren als Chemosensor für PP_i und Fructose-1,6-bis-Phosphat. Im Gegensatz dazu erwies sich der zweikernige Bis- Zn^{2+} -bis-cyclen Komplex als weniger selektiv für Thymin- und Uracil-Nucleotide, da er neben diesen auch in Gegenwart von IDP und ITP ternäre Komplexe bildete. Darüber hinaus wurde bei dieser Verbindung keine induzierte Excimer-Emission mit den Analyten UMP, PP_i und Fructose-1,6-bis-Phosphat beobachtet.

Kapitel 2 zeigt eine weitere interessante Eigenschaft des bereits in Kapitel 1 vorgestellten Zn^{2+} -Cyclen-pyren auf – es kann als DNA-Färbereagens eingesetzt werden. Die reversible Wechselwirkung des Pyren-markierten Metall-Komplexes mit dem Phosphatrückgrat der DNA induzierte bei Anregung im UV-Bereich – ähnlich wie in Kapitel 1 beschrieben – Pyren-Excimer Emission was zu sichtbaren Gelbanden führte. Zwar ist dieses Färbeverfahren auf Agarose-Gele beschränkt und auch die Sensitivität reicht nicht an die von Ethidiumbromid heran, jedoch konnten bis zu 10 ng DNA nachgewiesen sowie auch kurze DNA Stränge sichtbar gemacht werden. Darüber hinaus wurde durch Gelextraktion der mit Zn^{2+} -Cyclen-pyren angefärbten DNA-Banden und anschließender erneuter Gelelektrophorese gezeigt, dass dieses Färbeverfahren in DNA offensichtlich keine größeren Schäden (z. B. Strangbruch) hervorgerufen hatte. Aus einer abschließenden Cytotoxizitätsstudie auf HeLa-

und V-79-Zellen ging hervor, dass Zn^{2+} -Cyclen-pyren verglichen mit Ethidiumbromid wesentlich weniger toxisch ist.

In Kapitel 3 werden Fluoreszenzsonden vorgestellt, die als Färbereagentien in der Lage sind Proteinphosphorylierung nach der Durchführung von SDS-PAGE anzuzeigen. Hierfür wurden zweikernige, an Phosphatgruppen bindende Bis- Zn^{2+} -bis-cyclen Komplexe mit Coumarin und Carboxyfluorescein als umgebungsabhängige Fluorophore synthetisiert. Die Spezifität der Verbindung ist begründet durch die Selektivität der zweikernigen Metall-Komplexer für Phosphat-Gruppen und die durch die Bindungswechselwirkung dieser Metall-Komplexer mit Seitenketten-phosphorylierten Aminosäuren bewirkte Änderung der elektronischen Struktur des Fluorophors. Diese führt schließlich zur Verschiebung der Emissionsbande. Durch nicht-kovalente Bindungswechselwirkung zwischen Fluoreszenzsonde und Phosphat-Gruppe ist der Färbeprozess reversibel. Somit konnten auf einem gängigen UV-Tisch Gelbanden mit weniger als 100 μg phosphoryliertes α -Casein detektiert werden.

Kapitel 4 behandelt die Synthese von Zn^{2+} -Cyclen-Peptid Hybrid-Liganden und zweikernigen Bis- Zn^{2+} -cyclen Komplexen. Diese Verbindungen sollten an das Guanin-Nukleotid bindende Protein Ras binden, um dessen Funktion als wichtiger molekularer Schalter zellulärer Signaltransduktion zu beeinflussen. Da frühere Ergebnisse zeigten, dass Zn^{2+} -Cyclen in der Lage ist gezielt den Effektorprotein schwach bindenden Zustand 1 von Ras zu stabilisieren, wurde Zn^{2+} -Cyclen als Lead-Struktur zur Synthese neuer potentieller Inhibitoren der Ras-Raf Wechselwirkung herangezogen. Um Inhibitoren mit höheren Bindungsaffinitäten zu erhalten, wurden Zn^{2+} -Cyclen-Peptid Konjugate mittels Festphasenpeptidsynthese dargestellt, deren Peptid-Sequenz vom Ras-aktivierenden Protein SOS abgeleitet wurden. Darüber hinaus wurden auch zweikernige Bis- Zn^{2+} -cyclen Komplexe mittels 1,3-dipolarer Alkin-Azid Cycloaddition synthetisiert. NMR-Spektroskopische Untersuchungen zeigten jedoch, dass die Zn^{2+} -Cyclen-Peptid Konjugate keine verstärkte Bindungswechselwirkung mit Ras aufweisen. Die Bindungseigenschaften der zweikernigen Zink Komplexe konnten hingegen nicht mittels NMR-Techniken untersucht werden, da deren Zugabe zur Protein-Lösung eine Fällungsreaktion zur Folge hatte.

Kapitel 5 zeigt die Synthese von neuen Cholesterinderivaten mit erhöhter Wasserlöslichkeit. Bislang existieren kaum wasserlösliche Cholesterinderivate an Hand derer man die Rolle, die Cholesterin in Säugerzellen spielt unter physiologischen Bedingungen genauer untersuchen

könnte. Aus diesem Grund wurden effiziente Synthesen zur Herstellung solcher Cholesterine entwickelt. So wurden Steroide mit gesteigerter Wasserlöslichkeit erhalten indem man entweder die C(3)-OH Gruppe des Cholesterins mit Ethylenglykolen substituierte oder unter Verwendung von Ethylenglykolaminen eine reduktive Aminierung an der Keto-Funktion von Pregnenolon durchführte. Mittels ^1H -NMR Spektren der erhaltenen Verbindungen in D_2O mit DSS als Referenz konnte schließlich die Wasserlöslichkeit bestimmt werden (1-6 mg/mL bei Raumtemperatur). Aus den Spektren erkennbare Unterschiede der Linienbreiten wiesen des Weiteren darauf hin, dass Substanzen **4** und **5** nur sehr geringen Tendenz zur Aggregation aufweisen. Für Verbindung **9** hingegen wurde eine deutliche Verbreiterung der Resonanzlinien festgestellt, die auf Mizellenbildung zurückzuführen sein könnte.

8 ABBREVIATIONS

AA	amino acid
abs	absolute
AcOH	Acetic acid
ADP	Adenosine diphosphate
AMP	Adenosine monophosphate
aq	aqueous
Arg	Arginine
ATP	Adenosine triphosphate
Boc	<i>tert</i> -Butyloxycarbonyl
c	concentration
calc	calculated
Cbz	Benzyloxycarbonyl
CDP	Cytidine diphosphate
CHCl ₃	Chloroform
CMP	Cytidine monophosphate
COSY	correlated spectroscopy
CTP	Cytidine triphosphate
d	days
DCM	Dichloromethane
decomp	decomposition
DIPEA	Diisopropylethylamine
DMAP	4-(Dimethylamino)-pyridine
DMF	Dimethylformamide
DMSO	Dimethylsulfoxide
DNA	Deoxyribonucleic acid
EA	elemental analysis
ED	Ethylene diamine
EDC	1-(3-Dimethylaminopropyl)-3-ethylcarbodiimide
EI	electron impact
eq/equiv	equivalents
ESI	electronic spray ionisation

Et	ethyl
Et ₂ O	Diethylether
EtOAc	Ethylacetate
EtOH	Ethanol
Fmoc	Fluorenylmethyloxycarbonyl
FRET	fluorescence resonance energy transfer
GDP	Guanine diphosphate
GMP	Guanine monophosphate
GppNHp	GTP analog
GTP	Guanine triphosphate
h	hour
HBTU	2-(1H-Benzotriazole-1-yl)-1,1,3,3-tetramethyl-uronium hexafluorophosphate
HCl	Hydrochloric acid
HEPES	4-(2-Hydroxyethyl)-piperazine-1-ethane sulfonic acid
HOBt	1-Hydroxybenzotriazole
HPLC	high performance liquid chromatographie
HR	high resolution
HMBC	heteronuclear multiple bond correlation
HSQC	heteronuclear single quantum coherence
I/int.	fluorescence intensity; integral
IDP	Inosine diphosphate
Ile	Isoleucine
IMP	Inosine monophosphate
IR	infrared spectroscopy
ITP	Inosine triphosphate
J	coupling constant
Log P	partition coefficient between n-octanol and water
Leu	Leucine
Lys	Lysine
M	molecule
Me	methyl
MeCN	Acetonitrile
MeOH	Methanol

Met	methionine
min	minutes
MP	Melting point
MS	mass spectrometry
NEt ₃	Triethylamine
NMR	nuclear magnetic resonance
NOE	nuclear overhauser effect
NOESY	nuclear overhauser enhancement spectroscopy
Ph	phenyl
P _i	Orthophosphate
PP _i	Pyrophosphate
R _f	retention factor
ROESY	rotating frame NOE spectroscopy
rt	room temperature
Raf	Rat fibrosarcoma (Ras-effector)
Ras	Rat sarcoma (G-protein)
sat	saturated
SDS-PAGE	Sodium dodecyl sulphate polyacrylamide gel electrophoresis
SOS	Son of Sevenless (Ras-activator)
SPPS	Solid phase peptide synthesis
TBTU	2-(1H-benzotriazole-1-yl)-1,1,3,3-tetramethyl uranium tetrafluoroborate
THF	Tetrahydrofuran
THP	Tetrahydropyranyl
TLC	thin layer chromatography
Tos	toluenylsulfonyl
TRIS	Tris(hydroxymethyl)-aminomethane
TTP	Thymidine triphosphate
UDP	Uridine diphosphate
UMP	Uridine monophosphate
UTP	Uridine triphosphate
UV	ultraviolet, UV-Vis spectroscopy
Vis	visible
x	mole fraction

9 APPENDIX

9.1 Publications

F. Schmidt, S. Stadlbauer, B. König

“Induced pyrene excimer formation indicates UTP, TTP, Pyrophosphate and Fructose-1,6-bisphosphate”, *Dalton Trans.* **2010**, *accepted*.

A. Riechers, F. Schmidt, S. Stadlbauer, B. König

“Detection of protein phosphorylation on SDS-PAGE using probes with a phosphate-sensitive emission response”, *Bioconjug. Chem.* **2009**, *20*, 804-807.

F. Schmidt, I. C. Rosnizeck, M. Spoerner, H. R. Kalbitzer, B. König

“Zinc(II)cyclen peptide conjugates as potential inhibitors of the Ras mediated signal transduction”, *Inorg. Chim. Acta* **2010**, *submitted*.

F. Schmidt, J. Schmidt, A. Riechers, S. Haase, A.-K. Bosserhoff, J. Heilmann, B. König

“DNA Staining in Agarose Gels with Zn^{2+} -Cyclen pyrene”, *Electrophoresis* **2010**, *submitted*.

F. Schmidt, M. Spoerner, H. R. Kalbitzer, B. König

“Synthesis of new water soluble cholesterol derivatives”, *Synth. Commun.* **2010**, *submitted*.

9.2 Patent

A. Riechers, F. Schmidt, S. Stadlbauer, B. König **2009**, EPC 09155910.4 – 2117

9.3 Poster Presentation & Conferences

F. Schmidt, A. Riechers, H. R. Kalbitzer, C. Herrmann, B. König

“New inhibitors for oncogenic Ras – Zn²⁺-cyclen based peptide hybrid ligands for Ras-GppNHp” (Poster), 5th Status Symposium “Interplay between Molecular Conformations and Biological Function” (Volkswagen Stiftung), Bad Kissingen/Germany, **2008**.

4th Summer School “Medicinal Chemistry” (Graduiertenkolleg GRK 760), Regensburg/Germany, **2008**.

9.4 Curriculum Vitae

Personal Details

Name:	Florian Schmidt
Date of Birth:	02/02/1981
Place of Birth:	Grieskirchen/Oberösterreich
Nationality:	German/Austrian
Status:	married

Tertiary Education

01/2007 – 05/2010	PhD in Organic Chemistry under Prof. Dr. Burkhard König at the University of Regensburg.
01/2006 – 12/2006	Diploma-Thesis in Organic Chemistry under Prof. Dr. Burkhard König at the University of Regensburg, “Design and Synthesis of an Inhibitor of Protein-Protein-Interaction at the Example of RNA Polymerase II”
10/2001 – 09/2005	Chemistry studies at the University of Regensburg.

Civilian Service

09/2000 – 07/2001	Heilpädagogisches Zentrum “Die Burg“, Burglengenfeld
-------------------	--

School Education

05/2000	Abitur (A-levels), majors in Chemistry and French
09/1991 – 07/2000	Johann-Michael-Fischer Gymnasium (grammar school), Burglengenfeld
09/1987 – 07/1991	Grundschule (primary school), Pirkensee

Internships

03/2004	Practical course “Chemical Engineering II“, “Karl-Winnacker-Institut der DECHEMA e.V.“, Frankfurt am Main, Germany
10/2003	Practical course “Chemical Engineering I“, “Karl-Winnacker-Institut der DECHEMA e.V.“, Frankfurt am Main, Germany
09/1998	Student trainee, Siemens AG, Toulouse, France
08/1998	Student trainee, Siemens AG, Regensburg, Germany